Scuola Internazionale Superiore di Studi Avanzati - Trieste

Statistical Physics Group

Academic Year 2012/2013

A study on non-equilibrium dynamics in classical and quantum systems

October 30th, 2013

Thesis submitted for the degree of
Doctor Philosophiae
in Statistical Physics

Candidate
Marcuzzi Matteo

Advisor
Dr. Gambassi Andrea

SISSA - Via Bonomea 265 - 34136 TRIESTE - ITALY

SISSA

Scuola Internazionale Superiore di Studi Avanzati

International School for Advanced Studies

Statistical Physics Group

Academic Year 2012/2013

A study on non-equilibrium dynamics in classical and quantum systems

October 30th, 2013

Thesis submitted for the degree of
Doctor Philosophiae
in Statistical Physics

Candidate
Marcuzzi Matteo

Advisor
Dr. Gambassi Andrea

Contents

1 Overview of the thesis

The theory of statistical mechanics provides a powerful conceptual framework within which the relevant (macroscopic) features of systems at equilibrium can be described. As there is currently no equivalent capable of encompassing the much richer class of non-equilibrium phenomena, research in this direction proceeds mainly on an instance-by-instance basis. The aim of this Thesis is to describe in some detail three such attempts, which involve different dynamical aspects of classical and quantum systems. As summarised below, each of the last three Chapters of this document delves into one of these different topics, while Chapter 2 provides a brief introduction on the study of non-equilibrium dynamics.

In Chapter 3 we investigate the purely relaxational dynamics of *classical* critical ferromagnetic systems in the proximity of surfaces, paying particular attention to the effects that the latter induce on the early stages of the evolution following an abrupt change in the temperature of the sample. When the latter ends close enough to the critical value which separates the paramagnetic from the ferromagnetic phase, it effectively introduces a temporal boundary which can be treated as if it were a surface. Within this picture, we highlight the emergence of novel effects near the effective edge formed by the intersection of the two spatial and temporal boundaries. Our findings are apparently in disagreement with previous predictions which were based on the assumption that the presence of such an edge would not affect the scaling behaviour of observables; in order to explain this discrepancy, we propose an alternative for the original power-counting argument which, at least, correctly predicts the emergence of novel field-theoretical divergences in our one-loop calculations. We show that said singularities are associated with the scaling at the edge. Moreover, by encoding our findings in a boundary renormalisation group framework, we argue that the new predicted behaviour represents a universal feature associated to the short-distance expansion of the order parameter of the transition near the edge; we also calculate explicitly its anomalous dimension at the first-order in a dimensional expansion. As a qualitative feature, this anomalous dimension depends on the type of phase transition occurring at the surface. We exploit this fact in order to provide numerical support to our predictions via Monte Carlo simulations of the dynamical behaviour of a three-dimensional Ising model. The main results reported in Chap. 3 have appeared in Ref. [1].

In Chapter 4 we revisit the Euclidean mapping to imaginary times which has been recently proposed [2, 3] as an alternative for approaching the problem of *quantum dynamics* following a quench. This is expected to allow one to reformulate the original problem as a static one confined in a film geometry. We show that this interpretation actually holds only if the initial state of the dynamics is pure. Statistical mixtures, instead, intertwine the effects due to the two boundaries, which therefore cannot be regarded as being independent. We emphasize that, although the afore-

mentioned reinterpretation as a confined static problem fails, one is still able, in principle, to write down and solve the corresponding equations. We also discuss in some detail the relation between this approach and the real-time field-theoretical one which makes use of the two-time Keldysh contour. For this purpose, we study the analytical structure of relevant observables — such as correlation functions — in the complex plane of times, identifying a subdivision of this domain into several sectors which depend on the ordering of the imaginary parts of the involved time coordinates. Within each of these subdomains, the analytic continuation to the real axis provides in principle a different result. This feature allows one to reconstruct from the Euclidean formalism all possible non-time-ordered functions, which in particular include all those which can be calculated via the Keldysh two-time formalism. Moreover, we give a prescription on how to retrieve response functions, discussing some simple examples and rationalising some recent numerical data obtained for one of these observables in a one-dimensional quantum Ising chain [4]. We also highlight the emergence of a light-cone effect fairly similar to the one previously found for correlation functions [2], which therefore provides further confirmation to the fact that information travels across the system in the form of the entanglement of quasi-particles produced by the quenching procedure. We have reported part of this analysis in Ref. [5].

Chapter 5 presents part of our recent work on effective relaxation in *quantum* systems following a quench and on the observed prethermalisation. We analyse the effects caused by the introduction of a long-range integrability-breaking interaction in the early stages of the dynamics of an otherwise integrable quantum spin chain following a quench in the magnetic field. By employing a suitable transformation, we redefine the theory in terms of a fully-connected model of hard-core bosons, which allows us to exploit the (generically) low density of excitations for rendering our model exactly solvable (in a numerical sense, i.e., by numerically diagonalising an exact matrix). We verify that, indeed, as long as the parameters of the quench are not too close to the critical point, the low-density approximation captures the dynamical features of the elementary operators, highlighting the appearance of marked plateaux in their dynamics, which we reinterpret as the emergence of a prethermal regime in the original model. As expected, the latter behaviour is reflected also on extensive observables which can be constructed as appropriate combinations of the mode populations. For these quantities, the typical approach to the quasi-stationary value is algebraic with exponent $\alpha \approx 3$, independently of the size of the system, the strength of the interaction and the amplitude of the magnetic field (as long as it is kept far from the critical point). The plateaux mentioned above last until a recurrence time — which can be approximately identified with $t_R \approx N/2$ for single modes and $t'_R \approx N/4$ for extensive quantities — after which quantum oscillations due to the finite size of the chain reappear. Our procedure allows us to shed some light over prethermal features without having to considerably limit the size of the system, which we can choose to be quite large, as we discuss in Ref. [6].

2 Introduction to non-equilibrium dynamics

The description of the physics of many-body systems is unavoidably complicated by the huge number of degrees of freedom they display. This issue is typically averted by introducing the concept of statistical ensembles, which leads to encoding the relevant information on macroscopic quantities within a suitable, small set of random variables. This, however, requires that the system be at equilibrium. Outside of this condition, we generically lack a comprehensive framework for approaching the problem, as the aforementioned interpretation is no longer valid. As time enters into the picture, in fact, it may happen that a system becomes unable to probe all equivalent configurations corresponding to a given macroscopic state; consequently, the uniform distribution dictated by equipartition cannot but fail to capture its physical features. Both from a conceptual and a practical point of view, a simple and widely-employed method to affect a macroscopic system is to vary some external control parameter T, such as the temperature or the magnetic field. The effects of this procedure will then depend upon the interplay between two time scales: the one governing the aforementioned variation $\tau_v \sim T/\dot{T}$ and the typical relaxation time of the sample τ_r. For $\tau_v \gg \tau_r$ the system is given enough time to adapt to the altered conditions and can be thought to be almost at equilibrium at every moment; such a reversible transformation, referred to as "adiabatic", can be fully studied within a thermodynamical framework. Novel, non-trivial effects appear instead for $\tau_v \lesssim \tau_r$, i.e., when the changes are happening so fast that the system is unable to cope with them and lags behind. In the latter case, the dynamics becomes non-trivial and the system is driven out of equilibrium. If the focus lies in the inherent dynamical features, rather than in the stationary state emerging as a consequence of the external driving, it may be convenient to employ a variation limited on a time frame Δt, after which the system is let evolve freely. In particular, if $\tau_v \ll \tau_r$ and $\Delta t \ll \tau_r$, the change may be effectively thought to be instantaneous, since, with good approximation, the system's properties are not modified while it is being carried out; a protocol of this kind, which is conceptually the simplest possible, is named *quench*. Moreover, in order to actually capture the dynamics, one must be able to resolve events on time scales τ_O smaller than τ_r. Thus, we can conclude that, quite generally, the observation of non-equilibrium conditions requires either the ability to modify the external parameters and to observe the system quickly, or the choice of materials which exhibit a slow relaxation. An outstanding example among the latter is provided by glasses [7–9], but long relaxation rates are not just a prerogative of random media: a particularly relevant context in which they naturally occur is provided by continuous phase transitions. At equilibrium, it is a well-known theoretical and experimental fact that, upon approaching a critical point (e.g., by tuning the temperature to a specific value $T \to T_c$), the correlation length ξ of the

thermal fluctuations diverges algebraically as $\xi \sim |T - T_c|^{-\nu}$ with $\nu > 0$ [10–12]. This has some fundamental implications: from a formal point of view, the system loses the only inherent mesoscopic length-scale, thereby becoming self-similar under dilatations; of course, for real samples this represents an approximate statement, as microscopic scales such as the lattice spacing a and macroscopic ones such as the typical linear dimension L inevitably persist, granting it validity only within the range $a \ll \xi \ll L$, which can nonetheless encompass several orders of magnitude. Because of this, the system's behaviour becomes dominated by collective effects which only depend on features that can be read off at any scale, such as the range and symmetries of the underlying interaction, the global dimensionality or the presence or absence of disorder. In turn, since in general many microscopically different systems may be found sharing those properties, this gives rise to *universality*. In other words, all quantities which do not explicitly depend on the scale chosen for the description, such as the well-known *critical exponents* and *scaling functions*, are found to be the same in many different instances, which form the so-called *universality class* of the transition.

In a dynamical setting, not only length scales, but also time scales must be taken into account; near criticality ($T \approx T_c$), the typical relaxation rate τ_r of a system scales as $\tau_r \sim \xi^z \sim |T - T_c|^{-z\nu}$, where z is called *dynamical exponent* and measures the anisotropy between spatial and temporal coordinates under scaling [11, 13]. The divergence of this characteristic time at the critical point, also known as *critical slowing down*, reflects the fact that, as collective behaviours take over in the system, external changes must be able to affect larger and larger domains, each tending to react as a whole rather than as a collection of parts, which makes them slower and slower at adapting. Conceptually, this implies that no transformation can be carried out adiabatically across a phase transition, as there will always be a range of values of the control parameter T for which $\tau_r \gtrsim \tau_v$ (see Ref. [14] for some experimental consequences of this fact). Critical systems constitute therefore a suitable choice for studying non-equilibrium dynamics, be it in an experimental [15], numerical [16, 17] or analytical [18–22] fashion; furthermore, any transformation which ends up close enough to the critical point can be conveniently approximated by a quench. As a relevant implication, the early-time dynamics which follows does not strongly depend upon the details of the protocol, but just on its starting and ending points; in this time frame, novel universal features emerge [23], as will be further detailed in Chapter 3, which are related to the initial state's properties and, interestingly enough, have been highlighted by treating the quench as if it were a temporal surface. As a matter of fact, every change which is sufficiently abrupt to preserve, with good approximation, the system's configuration can be regarded as being instantaneous. This very instant constitutes a boundary separating the equilibrium and non-equilibrium regimes, exactly as a surface separates the inside of a sample from the outside. This identification, which has been proved to hold in systems subject to stochastic dynamics, allows one to make use of the available knowledge on critical, static systems with boundaries [24, 25] for describing dynamical features and has led to understanding that typical observables $\mathscr{O}(t)$ display a crossover from an early-time algebraic behaviour $t^{\theta_{\mathscr{O}}}$ to the usual power-law decay found at equilibrium $t^{-\frac{x_{\mathscr{O}}}{z}}$, where $x_{\mathscr{O}}$ denotes the scaling dimension of $\mathscr{O}$. The universal exponent $\theta_{\mathscr{O}}$ depends on the gross features of the quench, which can be encoded in effective boundary (initial) conditions for the order parameter. A typical example is illustrated by Fig. 2.1, where this initial regime is clearly highlighted.

In the case of *quantum* many-body systems, an additional, relevant time scale has to be taken into account, which is the typical decoherence time τ_D. The latter measures how long pure quan-

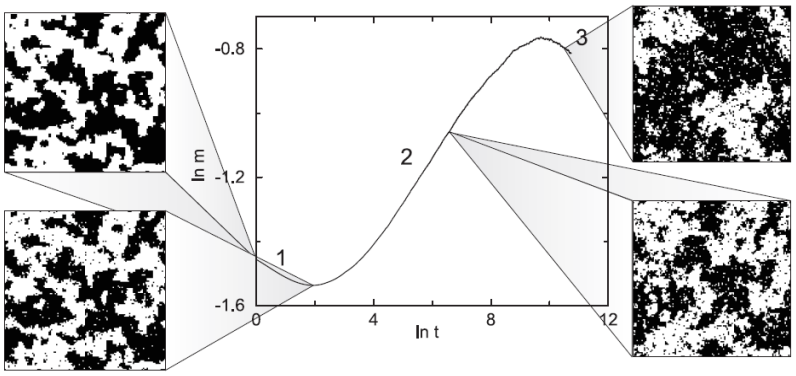

Figure 2.1: Monte Carlo simulation of the order parameter's early-time dynamics in a two-dimensional random field Ising model. Here the magnetisation m is reported as a function of time t in a double-logarithmic scale. The initial, non-algebraic, behaviour is due to microscopic, non-universal effects. The subsequent algebraic increase corresponds to the early-time universal regime discussed in the main text. On the right, the beginning of the crossover to the relaxation decay shows up. The four boxes at the sides represent snapshots of the spin configuration (white corresponding to spin up, whereas black to spin down) taken at different times. This figure has been adapted from Ref. [26].

tum effects (e.g., linear superposition of states, unitarity of the evolution, entanglement) can last before being affected and, more often than not, destroyed, by interaction with the environment. Although the advances in experimental techniques have progressively increased this scale to higher and higher values (see, e.g., Fig. 3 of Ref. [27]), it still remains much smaller than the typical relaxation rate τ_r [28]. Thereby, as it can hardly rely on the intrinsic slowness of systems, the study of quantum non-equilibrium dynamics generically requires fast changes and quick measurements. As a matter of fact, only very recently it became possible to experimentally probe the quantum evolution of many-body systems, mainly thanks to the improved capabilities in manipulating ultracold gases. Cold atoms trapped in optical lattices provide the means to investigate many relevant aspects of quantum many-body physics [29]: on the one hand, via Feshbach resonances [30], external magnetic fields allow to finely tune the strength of the interaction between particles; on the other, the substantial control over lasing emission grants great freedom in shaping the optical trap, opening the path to the realisation of effectively low-dimensional systems, while providing also a way to tune the interaction range to some extent. As a consequence, in the past years it has become possible to actually realise and study in the laboratory many important models of condensed matter [31–34]. Seminal works conducted in a dynamical framework have highlighted the presence of quantum revival effects in Bose-Einstein condensates [27] and of periodic recurrence in one-dimensional gases of interacting bosons [35], which reflect the unitarity of quantum evolution. Figure 2.2(a) shows a clear example of resonance effects, as the corresponding system has been engineered in such a way that its energy levels, which also represent the relevant frequency modes, are in rational proportion and, thus, a well-defined period can be extracted from the smallest of their

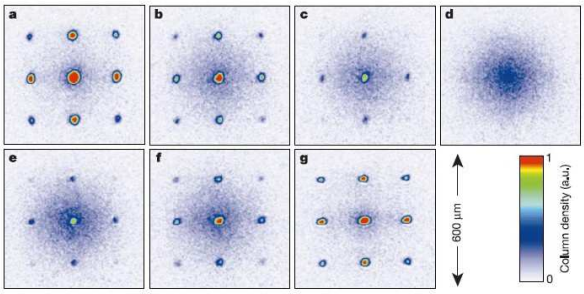

(a)

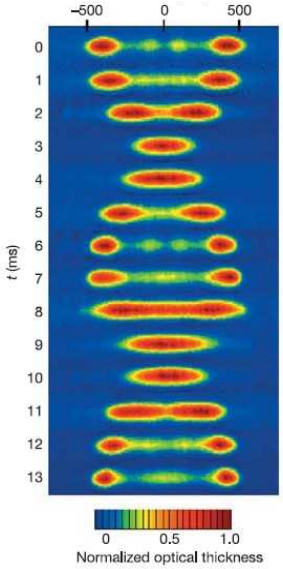

(b)

Figure 2.2: Experimental observation of long-lasting quantum dynamics. (a) Collapse and revival of the density configuration in a three-dimensional Bose-Einstein condensate after quenching the depth of the optical potential; the different boxes correspond, in alphabetical order, to 0, 100, 150, 250, 350, 400 and 550μs elapsed since the quench. An almost periodic behaviour clearly emerges, as the original pattern (panel (a)) is approximately recovered at the end of the sequence (panel (g)). (b) Oscillations of two quasi-one-dimensional clouds of interacting bosons. Despite the scattering processes happening when they meet, no significant relaxation is highlighted on the time-scales of the experiment. These figures have been adapted from Refs. [27, 35].

ratios. Another intriguing non-equilibrium feature consists in the fact that, despite the intrinsically non-local nature of quantum mechanics, the velocity v at which information can travel across a system is always finite, as theoretically determined 40 years ago by Lieb and Robinson [36] on systems defined on a lattice. Clearly, any local perturbation will propagate at most at such a maximal value v and it will thus take some time for it to affect every part of the system. However, this property emerges also in the case of global, uniform perturbations which do not break translational invariance, as most quenches are chosen to be. In this case, a light-cone effect may be in principle highlighted in correlation functions at different points (say, at a distance r), which will be affected by the quench only after waiting a time $t > r/v$, whereas for $t < r/v$ their behaviour will remain substantially unaltered with respect to the initial one. Recently, this feature has been identified in several analytical studies on integrable systems [2, 3, 37, 38] and a physical interpretation has been given in terms of quasi-particles [2, 3]: while driving the system out of equilibrium, the quench is injecting energy into it, which corresponds to the production of excitations; clearly, the latter will appear uniformly throughout the system. On the other hand, they will turn out to be entangled (and thus, correlated) only on typical length scales of the order of the initial state's correlation length ξ_0. After the quench, they will start propagating with a group velocity v effectively dictated

by the dispersion relation, i.e., by the spectral properties, building up correlations in their paths. Very recently, these light-cone effects have been observed experimentally in the correlations of a Bose-Hubbard chain [39], as reported in Fig. 2.3.

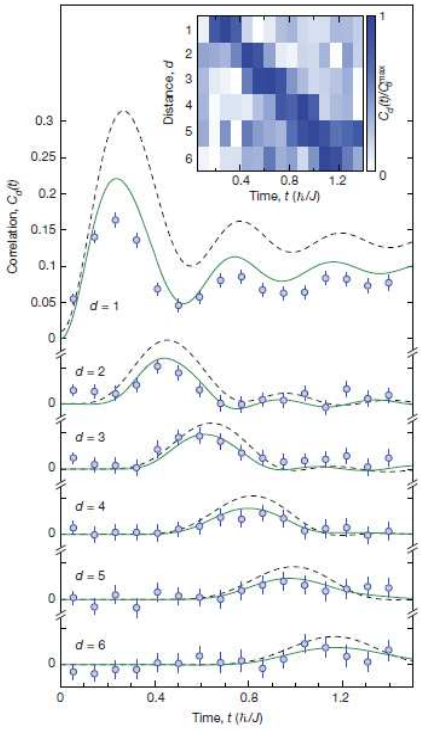

Figure 2.3: Light-cone effect in a Bose-Hubbard chain for the parity $\widehat{s}_j = \mathrm{e}^{i\pi\widehat{n}_j}$ of the occupancy $\widehat{n}_j$ of the j-th site of the optical lattice. The plot shows the two-point parity correlation $C_d(t)$ as a function of time for different distances d after a quench in the depth of the optical potential. Blue symbols represent experimental data, whereas green solid and black dashed lines stand for numerical and analytical predictions, respectively. In the inset, experimental data for C_d is used in a color map in order to highlight the light-cone structure. This figure has been adapted from Ref. [39].

The strong constraints posed by the unitarity of the evolution make the problem of quantum relaxation even more subtle than its classical counterpart, as actual thermalisation cannot really occur in closed systems [40]: this is readily understood by considering the dynamics of a system governed by a Hamiltonian H starting from a generic pure state $\rho_i = |\psi\rangle\langle\psi|$ with average energy $E = \langle\psi|H|\psi\rangle$: clearly, the unitary transformation $U_t = \mathrm{e}^{-iHt}$ (with $\hbar = 1$) — associated with the quantum evolution — can never turn ρ_i into a thermal distribution $\rho_f = \mathrm{e}^{-\beta(E)H}/Z$, as the latter is a statistical mixture with $\mathrm{tr}\{\rho_f^2\} < 1$ (for $\beta^{-1} \neq 0$), whereas the identity

$$1 = \mathrm{tr}\left\{\rho_i^2\right\} = \mathrm{tr}\left\{\rho_i^2 U_t^\dagger U_t\right\} = \lim_{t\to+\infty} \mathrm{tr}\left\{U_t \rho_i^2 U_t^\dagger\right\} = \mathrm{tr}\left\{\rho_f^2\right\}$$

always holds. Therefore, one may look for signs of thermalisation only in an effective sense [41], which involves focusing on a suitable set of macroscopic observables whose expectations, in the

long-time limit, are equivalently captured by the thermal distribution, its temperature determined by the energy set by the initial state [41, 42]. On the other hand, this picture is not universally valid: from the point of view of statistical inference, one can think of the thermal ensemble as being the best estimate that can be given for a system's properties by relying only on the knowledge of the internal energy. However, there are systems displaying non-trivial conservation laws which increase the amount of information that cannot be lost during the course of the evolution. In particular, *integrable* systems are characterised by having an extensive amount of independent integrals of motion, which are sufficient to completely solve the related models. Accounting for them, one can construct the corresponding highest entropy state [43], which is usually referred to as *generalised Gibbs ensemble* (GGE).

As a matter of fact, evidence has been found of a significant interplay between integrability and effective relaxation in quantum systems. Figure 2.2(b) represents a recent experimental confirmation: the system, which consists of two bosonic clouds with different momenta trapped in an harmonic potential, shows no clear sign of energy redistribution among the modes even after many scattering events. This behaviour hints at the presence of conservation laws far more stringent than the ones on total energy and momentum. The current understanding is that effective

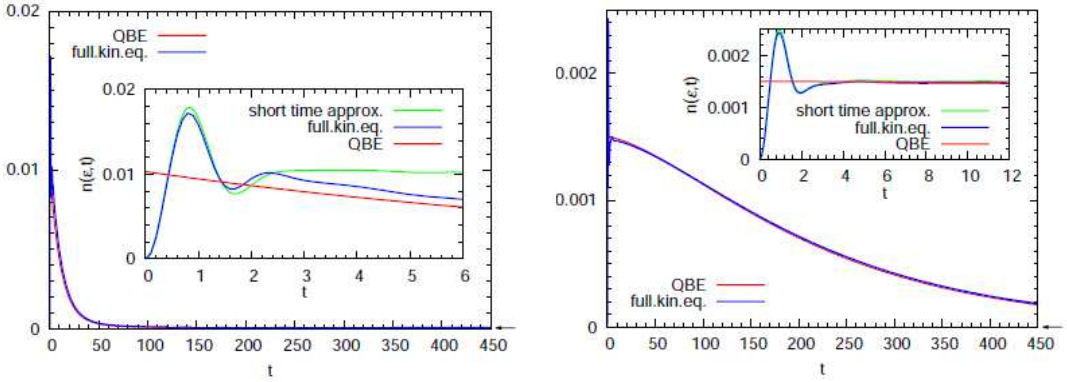

Figure 2.4: Long-time (main plots) and early-time (insets) evolution of the momentum distribution $n(\varepsilon,t)$ in an infinitely-dimensional Fermi-Hubbard model for fixed value of the energy $\varepsilon = 1.486$. Green lines correspond to analytical calculations in a short-time expansion, blue ones to a numerical, non-perturbative solution of the quantum Boltzmann equations and red ones to the solution of said equation in a long-time approximation. The tiny arrows on the right of each plot indicate the final, thermal values. (a) Strong integrability breaking: prethermalisation is absent, because the system equilibrates too fast. (b) Weak integrability breaking: a prethermal plateau is clearly highlighted in the inset, which is subsequently left while the system proceeds towards thermalisation (reached for $t \approx 1500$). This figure has been adapted from Ref. [44].

thermalisation may be observed only in non-integrable systems [45–48], whilst integrable ones are expected to display a GGE-like behaviour in the long-time limit [41, 48–50]. In the presence of a weak integrability-breaking interaction, though, a richer structure is bound to appear, as illustrated in Fig. 2.4; it is in fact reasonable to assume that the initial phase of the dynamics will still

be dominated by the integrable part of the Hamiltonian; as a consequence, a two-stage relaxation emerges [51]: first, the system is brought close to the GGE corresponding to the integrable part, which thus represents an intermediate, metastable state; then, on time scales which depend on the strength of the interaction, scattering between the quasi-particles becomes relevant enough to drive it away from its neighbourhood and towards thermalisation. The first half of this process has been called "prethermalisation" and has very recently been observed in both experimental [52] and theoretical/numerical [44] studies.

3 Surface critical dynamics

Our general understanding of the thermodynamic properties of real materials has been primarily built upon translationally-invariant descriptions of their bulk behaviour, which is effectively described by means of infinitely-extended models. As a matter of fact, although any real sample is necessarily finite, its bulk features can still be captured within such a framework, as long as the system is large enough and the focus is kept far from the surfaces; the latter introduce indeed corrections in the picture, which however can typically be neglected: intuitively, in a system with N constituents (e.g., atoms or molecules), the size of the portion in the proximity of the boundaries scales as $N^{\frac{2}{3}}$, and is therefore subdominant with respect to the bulk features ($\propto N$) in the thermodynamic limit $N \gg 1$. On the other hand, as miniaturisation techniques advance, making us capable of crafting increasingly smaller devices, boundary effects become progressively more and more important. As a consequence, the physics of surfaces and interfaces has attracted in the past decades an increasing interest, concerning systems at equilibrium [24, 53] as well as non-equilibrium dynamical processes [23], since applications may generally involve changes in the external control parameters. Describing these features requires in principle the knowledge of many microscopic details and specific material properties which vary widely from system to system. However, as we have already mentioned in the Introduction, circumstances may be found in which collective phenomena emerge, making only few coarse-grained, mesoscopic properties relevant. As a matter of fact, it is now well-established, both theoretically and experimentally, that the behaviour of statistical systems close to continuous phase transitions can be characterised by just a limited set of quantities, such as exponents and scaling functions, which depend only on the range and symmetries of the underlying interaction and on the dimensionality of the space. All the microscopically different systems sharing these same gross features form the so-called *universality class* of the transition. Universality also provides a powerful prescription for investigating continuous phase transitions, since it is sufficient to study just one representative system in order to gain information on the whole class it belongs to. Moreover, the various thermodynamic and structural properties are known to show, in the neighbourhood of the critical point, leading algebraic behaviours characterised by common exponents, which can be therefore considered the hallmark of the transition. In turn, upon approaching it and provided it is not of topological nature [54–56], the relevant contribution to the various thermodynamic quantities is effectively determined by the fluctuations of the so-called order parameter φ (e.g., the local magnetisation for an Ising ferromagnet). The behaviour of the latter highlights a phenomenon known as *spontaneous symmetry breaking*, as it typically vanishes in one phase and takes one among multiple, equivalent (non-vanishing) values in the other [10].

The emergence of universality is currently understood within the framework of the renormalisation group (RG) [10, 11, 57], which stands among the most important theoretical achievements of the past fifty years. RG transformations effectively act upon the scale at which a system is described, ideally providing a connection between the interactions among the microscopic constituents and the effective theories based on coarse-grained properties which emerge at a mesoscopic level. In the proximity of a continuous phase transition, scale invariance ensues due to the divergence of the correlation length ξ of the fluctuations of the order parameter; not too far from the critical point, ξ is much larger than the microscopic scales and typically constitutes the only mesoscopic length-scale present. In such a context the RG reaches a fixed point, since, upon changing the scale, it cannot but map the original model onto itself. Hence, the behaviour the system displays at space and time scales larger than the microscopic ones must be dictated by features which are not specific to the scale chosen, such as the ones mentioned above. These features constrain the form of the free-energy

$$F = F(u_1, u_2, u_3 \ldots) \approx V f_{bulk}(u_1, u_2, u_3 \ldots), \tag{3.1}$$

which generically encodes all the relevant thermodynamic information. In the expression above V stands for the volume of the system, $f_{bulk} = \lim_{V\to\infty} F/V$ is the free-energy density and each u_i denotes a control parameter — e.g., the temperature or the magnetic field for a ferromagnet— or, more commonly, the distance from its critical value. The phase transition corresponds to a point of non-analyticity for F; because of the self-similarity discussed above, its singular part F_{sing} must display homogeneity under dilatations; therefore, by rescaling the system by a factor b close to a phase transition, the identity

$$F_{sing}(u_1, u_2, u_3 \ldots) = b^{-d} F_{sing}(u_1 b^{y_1}, u_2 b^{y_2}, u_3 b^{y_3} \ldots) \tag{3.2}$$

must hold, where $y_i \equiv u_i$ is called the *scaling dimension* of the corresponding parameter (or *scaling field*) u_i. Among the latter, only those with $y_i > 0$ can cause the breakdown of this picture, as the transformation above brings them further away from their critical values; for this reason they are referred to as *relevant*, whereas those with negative dimension $y_i < 0$ are called *irrelevant* and the ones with $y_i = 0$ *marginal*. This reflects the fact that typically, at mesoscopic scales, the leading behaviour displayed by observables is determined by the first ones, which are therefore the only "relevant" ones for the description of the system. The non-analytic behaviour of F_{sing} is unavoidably reflected on all the physical observables which can be obtained by deriving it. For example, ferromagnetic systems, which are generically characterised by having only two relevant parameters, i.e., the temperature $u_1 = t \equiv T - T_c$ and the magnetic field $u_2 = h$, display a well-known algebraic singularity $\chi \sim t^{-\gamma}$ in the magnetic susceptibility when the critical temperature is approached ($t \to 0$). This emerges quite naturally in this picture because χ is defined as

$$\chi = \left(\partial_h^2 F(t,h)\right)|_{h=0} \approx b^{-d} \left(\partial_h^2 F_{sing}(tb^{y_t}, hb^{y_h})\right)|_{h=0} = b^{-d+2y_h} F''_{sing}(tb^{y_t}, 0). \tag{3.3}$$

Now, by fixing $b = t^{-1/y_t}$ one finds that indeed $\chi \sim t^{-\gamma}$ with an exponent

$$\gamma = \frac{2y_h - d}{y_t}. \tag{3.4}$$

In an analogous fashion, one can extract the algebraic dependence of other relevant observables on t and h, therefore re-expressing the corresponding *critical exponents* in terms of y_t, y_h and of the dimensionality d. In particular, this means that in this specific case there are only two independent universal exponents. Typically, in addition to γ, one introduces the set of exponents β, ν, α and δ which enter the scaling laws [10, 11]

$$\begin{aligned} m \sim t^{\beta}, \qquad & \xi \sim t^{-\nu}, \qquad c_V \sim t^{-\alpha} \qquad (h=0, t\to 0), \\ & m \sim h^{1/\delta} \qquad (h\to 0, t=0), \end{aligned} \tag{3.5}$$

for the magnetisation m, the correlation length ξ and the specific heat c_V as functions of the temperature, and the magnetisation as a function of the magnetic field, respectively. They correspond to

$$\beta = \frac{d-y_h}{y_t}, \quad \nu = \frac{1}{y_t}, \quad \alpha = 2-\frac{d}{y_t}, \quad \delta = \frac{y_h}{d-y_h} \tag{3.6}$$

and one can easily reconstruct *(hyper-)scaling relations* between them such as

$$2-\alpha = d\nu = 2\beta+\gamma = \beta(\delta+1). \tag{3.7}$$

At mesoscopic scales, the underlying discrete structure of the lattice becomes inconsequential, and an effective description in terms of fields on a space-time continuum can be adopted; in such a field-theoretical context, the divergences mentioned above are associated to the short-distance (ultraviolet, UV) singularities appearing when evaluating expectations at the same point in space [11], e.g.,

$$G(x,y)\,|_{x\to y} = \langle \varphi(x)\varphi(y)\rangle\,|_{x\to y} \propto (x-y)^{-(d-2+\eta)}, \tag{3.8}$$

where η is called the *anomalous dimension* of the field — as it measures how much its scaling dimension deviates from the mean-field (or "naive") one — and is related to other critical exponents by scaling laws such as

$$2\frac{\beta}{\nu} = d-2+\eta, \quad \text{and} \quad 2-\eta = \frac{\gamma}{\nu}. \tag{3.9}$$

In the opposite limit, i.e., for large distances, one finds instead an exponential decay

$$G(x,y) \propto \mathrm{e}^{-\frac{|x-y|}{\xi}} \tag{3.10}$$

which is commonly employed as a definition of the correlation length ξ. When $\xi\to\infty$ the algebraic behaviour in Eq. (3.8) extends to the whole space; thus, one can relate the emerging infrared (IR) singularities associated to the phase transition to the UV ones introduced above. For this reason, the field-theoretical approach primarily developed in the context of elementary particle physics can be conveniently employed for the study of critical phenomena [11].

In the following, in Sec. 3.1 we briefly recall the main concepts behind the extension of the renormalisation group to systems with boundaries, both of spatial and temporal nature. In Sec. 3.2 we introduce our model, which displays breaking of both space- and time-translational invariance; we discuss our analytical predictions and our numerical findings. Finally, in Sec. 3.3 we summarise our main results.

3.1 Critical phenomena at boundaries

Being originally devised for describing the behaviour of unbounded, uniform systems, the renormalisation group has been subsequently generalised in order to account for the finiteness any real sample displays, which enforces an upper bound upon the correlation length [58] and smooths the typical algebraic singularities one would otherwise encounter. Furthermore, it has been extended to capture the features which emerge in the proximity of flat surfaces [24, 53]. We wish to remark that such an approach is conceptually different from the study of finite-size effects: this last case, in fact, depicts a situation in which the correlation length ξ becomes comparable with the size of the system L; critical surface effects, instead, are localized in a region of the system which lies within a distance from one of the boundaries smaller than ξ, which is in turn kept much smaller than L. In such a context the breaking of translational invariance plays a fundamental role, leading to the appearance of novel universal features, as we will explain in Sec. 3.1.1. On a different note, since this choice implies that the effects of the other boundaries are negligible, the system can be effectively treated as if it were infinitely-extended along all directions running parallel to the considered surface.

Within the RG approach, a new set of relevant parameters has to be introduced in order to account for the gross features of the boundary, such as local magnetic fields and variations in the boundary interaction strength with respect to the bulk. Accordingly, subleading terms depending on them must be included in the free energy (3.1), which becomes

$$F = V f_{bulk}(t,h) + S f_{surf}(t,h,u_1^s,u_2^s,\ldots), \tag{3.11}$$

where S is the area of the surface and u_i^s denotes one of the new scaling fields. As a result, novel singularities might emerge upon approaching the boundary, which split the original universality class in surface subclasses characterised by a set of boundary exponents and scaling functions associated, e.g., with the algebraic behaviour of the correlation functions in its proximity [24, 53]. In general, these exponents cannot be inferred from the bulk ones. A number of analytical [59–61], numerical [62, 63] and experimental (see, e.g., Ref. [64]) studies investigated primarily semi-infinite and film geometries, whereas wedges, edges [65, 66], as well as curved and irregular surfaces [25, 53] were studied to a lesser extent. In Sec. 3.1.1 we will briefly summarize the basic concepts used in the field-theoretical approach to semi-infinite systems. Universal features emerge also in the dynamic behaviour at equilibrium (both in infinite and finite systems) [67] and out of equilibrium [23]; in this context the universality class is further split depending on the gross features of the dynamics, such as the possible global conservation of the order parameter [68, 69]. In Sec. 3.1.2 we shall recall the relationship existing between this dynamical framework and the static one in the presence of boundaries.

3.1.1 Spatial surfaces

It is a well-known fact that the phase transition belonging to the so-called $O(n)$ universality class, which effectively describes the collective properties of ferromagnetic materials, is described in the continuum by a φ^4 theory with Landau-Ginzburg effective free-energy density [10, 11]

$$\mathscr{H}[\varphi] = \frac{1}{2}\left(\vec{\nabla}\varphi\right)^2 + \frac{r}{2}\varphi^2 + \frac{g}{4!}\left(\varphi^2\right)^2, \tag{3.12}$$

where φ is a vector composed of n scalar fields φ_i, $g > 0$ and $r \propto T - T_c$. Note that, despite its name, this function does not coincide with the *actual* free-energy (3.1); the latter can be however obtained from the former by integrating over the possible configurations of the fields, as depicted by Eq. (3.13) below. For the φ^4 model, the *upper critical dimension*, above which mean-field theory becomes exact, is $d = 4$. In its proximity, no terms of higher degree in φ are needed since their scaling dimensions are negative. This is readily proved by taking into account that the effective action $S = \int \mathrm{d}^d x \mathscr{H}[\varphi]$ is scale invariant, which implies that the scaling dimension of the field is $[\varphi] = (d-2)/2$, so that the coupling of a generic term $c_{2n}\varphi^{2n}$ has dimension $[c_{2n}] = d - n(d-2)$, which for $d \approx 4$ is positive only for $n \leq 2$.

In the case of semi-infinite systems, the partition function in general takes the form

$$Z \equiv \mathrm{e}^{-\frac{F}{k_B T}} = \int \mathscr{D}\varphi \; exp\left\{ -\int \mathrm{d}^{d-1}x \int_0^\infty \mathrm{d}x_\perp \, \mathscr{H}[\varphi(\vec{r}, x_\perp)] - \int \mathrm{d}^{d-1}x \, \mathscr{H}_1[\varphi(\vec{r}, 0)] \right\}, \tag{3.13}$$

where $x_\perp$ is the coordinate orthogonal to the surface and the second addend at the exponent is a boundary term responsible for the breaking of translational invariance along it. The latter gives also rise to the surface part f_{surf} of the free-energy (3.11). Taking the functional derivative of the total action with respect to the components of the bulk field $\varphi_i(\vec{r}, x_\perp)$ and of the boundary one $\varphi_i(\vec{r}, 0)$ one obtains the equations of motion

$$\left(-\nabla^2 + r + \frac{g}{6}\phi^2 \right) \varphi_i = 0 \tag{3.14}$$

and

$$\partial_{x_\perp} \varphi_i \mid_{x_\perp = 0} = \frac{\delta}{\delta \varphi_i(x_\perp = 0)} \int \mathrm{d}^{d-1}x \, \mathscr{H}_1, \tag{3.15}$$

respectively, the l.h.s. of Eq. (3.15) coming from integration by parts of the Laplacian in Eq. (3.12). This highlights the fact that the properties of the surface are effectively encoded in the typical behaviour the order parameter shows in the proximity of the boundary; within a mean-field description, this is entirely captured by suitable boundary conditions such as Eq. (3.15). By applying the same arguments used above for $\mathscr{H}$ one can show that the only relevant terms compatible with the $\mathbb{Z}_2$ symmetry $\varphi \to -\varphi$ which can appear in $\mathscr{H}_1$ are $c_0\varphi^2/2$ and $c_1 \varphi \partial_{x_\perp} \varphi$; thus, the boundary conditions become

$$\partial_z \varphi_i \mid_{x_\perp = 0} = c_0 \varphi_i(x_\perp = 0) + c_1 \partial_{x_\perp} \varphi_i \mid_{x_\perp = 0}, \tag{3.16}$$

which can be rewritten as

$$\partial_{x_\perp} \varphi_i \mid_{x_\perp = 0} = \frac{c_0}{1 - c_1} \varphi_i(x_\perp = 0), \tag{3.17}$$

thereby showing that the effect of the term proportional to c_1 amounts just to a suitable renormalisation of c_0 and can effectively be disregarded. This argument, which is based on a mean-field description, can be generalised to every order in a standard perturbative expansion by applying it at the external legs of any given Feynman diagram [59]. Consequently, the boundary term $\mathscr{H}_1$ can be conveniently restricted to the form

$$\mathscr{H}_1[\varphi] = \frac{1}{2} c_0 \varphi^2. \tag{3.18}$$

Despite its simplicity, non-trivial consequences emerge because of its presence. In a mean-field approximation, one recovers the phase diagram qualitatively represented in Fig. 3.1, which exhibits a richer structure than the one found for infinite systems. In addition to the usual phases in which

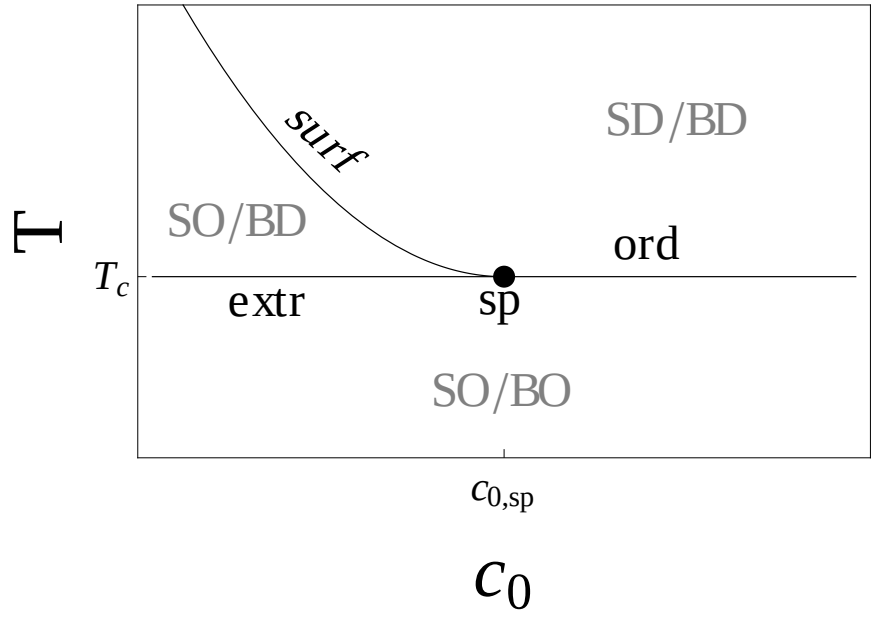

Figure 3.1: Qualitative temperature-surface enhancement phase diagram of the $O(1)$ model. Here S stands for "surface", B for "bulk", O for "ordered" and D for "disordered". The point $c_{0,sp}$ denotes the tri-critical special transition. For $c_0 > c_{0,sp}$ one identifies only the ordinary transition (ord), whereas for $c_0 > c_{0,sp}$ the surface undergoes ordering at a higher temperature T_{cs} than the bulk, identified by the critical line denoted as "surf", while the bulk still becomes critical at $T = T_c$ (extr). For $n > 1$ this picture is valid only in dimension $d > 3$, as continuous symmetries cannot undergo spontaneous breaking for $d \leq 2$, thus no surface transition can occur [70].

the system is ordered (O) or disordered (D) as a whole, a third one appears which displays a magnetised surface (SO) and a paramagnetic bulk (BD); the latter emerges when the coefficient c_0, often referred to as *surface enhancement*, as it accounts for the difference of the interaction between the surface and the bulk, is smaller than a threshold value $c_{0,sp}$. Four different phase transitions can thus be encountered by varying the temperature. For $c_0 > c_{0,sp}$ the interaction at the surface is not sufficiently strong to let it acquire an ordered configuration at a higher temperature than the bulk. Thus, the boundary becomes critical when the bulk does, as long-range correlations at the surface build up as a consequence of the ones emerging inside the sample; this transition is referred to as *ordinary*. Under RG transformations c_0 flows to $+\infty$, which, when applied to Eq. (3.16), produces Dirichlet conditions

$$\varphi(x_\perp = 0) = 0 \tag{3.19}$$

for the order parameter. For the ordinary transition, the critical point $c_0 = +\infty$ remains the same at every order in the perturbative expansion; therefore, even when fluctuations are accounted for, the

boundary condition (3.19) holds. For $c_0 < c_{0,sp}$, instead, the surface becomes critical at a temperature $T_{cs} > T_c$; the corresponding *surface transition* reflects the properties of a bulk transition in a $(d-1)$-dimensional system, which can be understood by taking the limit of vanishing interactions in the bulk, therefore making the boundary a truly independent system. Note that, for the surface transition to be observed, it is necessary that $d > d_{lc} + 1$, d_{lc} being the lower critical dimension below which no transition can occur. In particular, the Mermin-Wagner theorem [70] forbids the existence of spontaneous breaking of continuous symmetries for $d \leq 2$; as a consequence, the surface transition can be present in $O(n)$ models only in $d \geq 4$, with the exception of $n = 1$ (the Ising universality class, which corresponds to a $\mathbb{Z}_2$ discrete symmetry) which admits it also for $d = 3$. Lowering the temperature down to T_c, the bulk is then subject to ordering in the presence of an already magnetised surface, giving rise to the so-called *extraordinary transition*. The latter has also been proved to be equivalent [71] to the *normal transition* which takes place for $c_0 > c_{0,sp}$ in the presence of a strong magnetic field h_1 localised at the surface. Finally, the intersection of the critical lines identifies a tri-critical point $c_0 = c_{0,sp}$ and a corresponding *special transition*. Within a mean-field description, $c_{0,sp} = 0$ gives rise to Neumann conditions

$$\partial_{x_\perp} \varphi \,|_{x_\perp = 0} = 0. \tag{3.20}$$

One has however to take care of the fact that this critical point is not known to all orders in perturbation theory, as in the case of the ordinary transition [53]. Still, one can apply Eq. (3.20) to any regularised (bare) function. In this case c_0 flows to a renormalised value c_{sp}^R which generically depends on the chosen regularisation; in particular, within a dimensional regularisation scheme (such as the one employed in the following Sections) it vanishes at every order. In real systems, in general, sharp conditions such as the ones in Eqs. (3.19) and (3.20) above will not be observed, as in the very proximity of the surface the microscopic structure of the system, such as the configuration of the lattice, ceases to be inconsequential. On the other hand, since they are associated to microscopic scales, these effects are typically sufficiently small not to spoil the entire discussion and their effect can be understood in terms of a shift from the ordinary ($c_0 = +\infty$) or special ($c_0 = 0$) fixed point to λ^{-1}, where λ is usually referred to as *extrapolation length* [24]. The implications of imposing an effective condition

$$\partial_{x_\perp} \varphi \,|_{x_\perp = 0} = \frac{1}{\lambda} \varphi(x_\perp = 0) \tag{3.21}$$

may be inferred from Fig. 3.2: the magnetisation profile is slightly modified near the surface, while it remains substantially the same in the bulk. Its tangent at $x_\perp = 0$ identifies the extrapolation length on the horizontal axis. Note that, in the ordinary case, this approximately corresponds to moving the Dirichlet condition from $x_\perp = 0$ to an effective distance $x_\perp = -\lambda$ outside of the sample. We remark that, according to Eq. (3.21), the extrapolation length also provides a description of the "distance" of c_0 from the actual critical point and can thus constitute a mesoscopic length scale [24, 53].

The discussion above highlights a typical example of the aforementioned subdivision of a universality class; as a matter of fact, the critical behaviour of bulk observables is the same in every subclass, whereas surface quantities, such as the magnetisation m_1 at the surface or the associated susceptibility χ_1, show distinctively different algebraic laws depending on the boundary transition

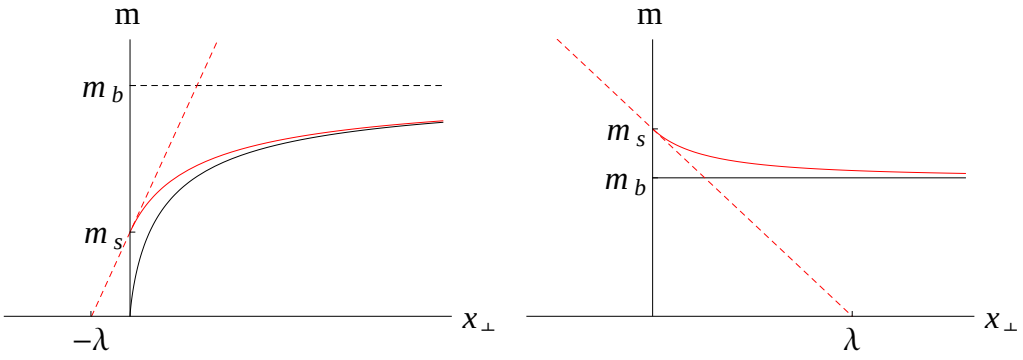

Figure 3.2: Qualitative representation of typical magnetisation m profiles as functions of the distance $x_\perp$ from the surface expected in real materials for (a) the ordinary and (b) the special transition. The black solid lines exactly obey Dirichlet and Neumann boundary conditions, respectively. The red ones sketch the deviation from the theoretically-expected profiles. The red, dashed lines highlight the slope of the solid ones of the same colour at the origin and identify the extrapolation length on the horizontal axis. Here m_b denotes the magnetisation in the bulk and m_s the one at the surface.

considered. Moreover, corresponding observables in the bulk and at the surface do not typically share the same critical exponents: for example, for the Ising ($n = 1$) ordinary ($c_0 \to +\infty$) transition in two dimensions one can find analytically

$$\begin{cases} m \sim (T_c - T)^{\beta} & \text{with} \quad \beta = \frac{1}{8} \\ m_1 \sim (T_c - T)^{\beta_1} & \text{with} \quad \beta_1 = \frac{1}{2}. \end{cases} \tag{3.22}$$

This difference is usually understood in terms of a *short-distance expansion* (SDE) [53, 61] of the corresponding operator, which is conceptually not too different from the operator product expansion (OPE) which has been introduced in scale-invariant field theories [72–74]: considering the whole class of surface operators $\{\mathscr{O}_i^s\}_i$, a generic bulk field $\phi(\vec{r}, x_\perp)$ can be rewritten, when approaching the boundary (i.e., for $x_\perp \to 0$), as a linear combination

$$\phi(\vec{r}, x_\perp) = \sum_i B_i(x_\perp)\mathscr{O}_i^s(\vec{r}), \tag{3.23}$$

where the coefficients B_i entirely enclose the asymptotic dependence on $x_\perp$. In particular, since every term of the series on the r.h.s. must have the same scaling dimension $[\phi]$ as the l.h.s., we find that

$$[B_i(x_\perp)] = [\phi] - [\mathscr{O}_i^s]. \tag{3.24}$$

At the critical point $\xi \to \infty$; consequently, the only length-scale entering the definitions of the B_is is the distance $x_\perp$ from the surface, which implies that

$$B_i(x_\perp) = b_i\, x_\perp^{[\mathscr{O}_i^s] - [\phi]}, \tag{3.25}$$

where each b_i has now vanishing scaling dimension. For example, in a mean-field approach Eq. (3.23) corresponds to the Taylor expansion

$$\phi(\vec{r},x_\perp) = \sum_{i=0}^{\infty} b_i \, x_\perp^i \, (\partial_{x_\perp})^i \phi(\vec{r},x_\perp) \mid_{x_\perp=0}, \tag{3.26}$$

where however the constants b_i have to be fixed according to the specific boundary conditions, e.g., $b_0 = 0$ for Dirichlet (ordinary) ones and $b_1 = 0$ for Neumann (special) ones. This expansion is meant to be valid when performed inside any average and is clearly dominated by the non-vanishing term corresponding to the surface operator ϕ_1 with the highest scaling dimension. In the same mean-field setting as above, that would be $\phi(\vec{r},0)$ in the special case and its normal derivative $\partial_{x_\perp}\phi(\vec{r},x_\perp) \mid_{x_\perp=0}$ in the ordinary one. Once the bulk features are known, one can also make use of the SDE to retrieve the boundary critical exponents from the asymptotic behaviour of the corresponding observables. For example, for the magnetisation in Eq. (3.22) one would find

$$\langle \varphi(x_\perp) \rangle \approx x_\perp^{\frac{\beta_1-\beta}{\nu}} \langle \varphi_1 \rangle \qquad (x_\perp \to 0); \tag{3.27}$$

knowing both bulk exponents β and ν one can easily retrieve β_1 by studying the power-law behaviour of $\langle \varphi(x_\perp) \rangle$ upon approaching the surface, which is described by the formula above.

In order to understand how new divergences can be generated at the surface, we need to proceed beyond the mean-field level (see also Ref. [53]). We shall consider for simplicity the first non-trivial order in a perturbative expansion of the φ^4 theory (3.12), i.e., the "tadpole" Feynman diagram in Fig. 3.3, although the following considerations are valid in general. We shall also

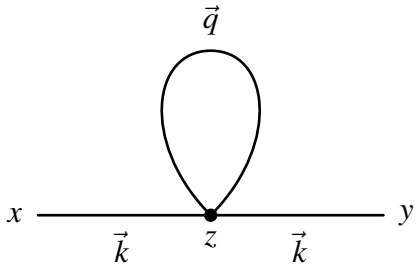

Figure 3.3: Tadpole diagram, corresponding to a graphical representation of the convolution (3.31). Each line stands for an unperturbed propagator $G^{(0)}$, each vertex for a set of coordinates.

restrict ourselves to the vicinity of the upper critical dimension $d = 4$. First of all, we wish to calculate the 0-th order two-point function, i.e., the free propagator

$$G^{(0)}(\vec{r}_1,x;\vec{r}_2,y) = \widehat{G}^{(0)}(\vec{r}_1-\vec{r}_2;x,y) = \langle \varphi(\vec{r}_1,x)\varphi(\vec{r}_2,y) \rangle_{g=0}, \tag{3.28}$$

where x and y denote the distances from the surface. $G^{(0)}$ obeys the equations of motion (3.14) and (3.15) with $g = 0$ and is more conveniently written in a mixed momentum-space representation $(\vec{k},x_\perp)$ which keeps in coordinate space only the direction orthogonal to the surface [53, 59, 60]:

$$\widetilde{G}^{(0)}(\vec{k};x,y) = \frac{1}{2\omega_k}\left[\mathrm{e}^{-\omega_k|x-y|} + \frac{\omega_k - c_0}{\omega_k + c_0} \mathrm{e}^{-\omega_k(x+y)} \right] = \widetilde{G}_b^{(0)}(\vec{k};x-y) + \frac{\omega_k - c_0}{\omega_k + c_0} \widetilde{G}_b^{(0)}(\vec{k};x+y), \tag{3.29}$$

where we introduced the notation $\omega_k = \sqrt{k^2 + r}$. Note that indeed, for $c_0 \to +\infty$ and $c_0 = 0$ one recovers the structure $G_b^{(0)}(x-y) \mp G_b^{(0)}(x+y)$ dictated by the method of image charges for Dirichlet and Neumann boundary conditions, respectively, where the "bulk propagator" $G_b^{(0)}$ reproduces the two-point function for infinite systems. As we have mentioned above, we are mainly interested here in the short-distance (ultraviolet) singularities of this function, which emerge for $\left|\vec{k}\right| = k \to \infty$. In this limit, the factor $(\omega_k - c_0)/(\omega_k + c_0)$ asymptotically reaches 1 and its dependence on k can thus be neglected. Thereby, we can rewrite

$$\widehat{G}^{(0)}(\vec{r}_1 - \vec{r}_2; x, y) \sim \widehat{G}_b^{(0)}(\vec{r}_1 - \vec{r}_2; x-y) + \widehat{G}_b^{(0)}(\vec{r}_1 - \vec{r}_2; x+y), \tag{3.30}$$

separating the "bulk" from the "surface" contribution. Upon integrating over the three-dimensional vector $\vec{k}$, $G_b^{(0)}(x-y)$ displays a singularity for every $x = y$, whereas $G_b^{(0)}(x+y)$ requires the more stringent condition $x = y = 0$, i.e., both points must be located at the boundary. Introducing a momentum cutoff Λ to such an integral, it is easy to see that both divergences are of order Λ^2, which is consistent with Eq. (3.8) (here $\eta = 0$ since at this level we are considering the non-interacting theory). Now, consider the tadpole contribution to the propagator depicted in Fig. (3.3), which is proportional to the convolution

$$\widehat{G}^{(1)}(\vec{r}_1 - \vec{r}_2; x, y) \propto \int_0^\infty \mathrm{d}z \int \frac{\mathrm{d}^{d-1} r}{(2\pi)^{d-1}} \widehat{G}^{(0)}(\vec{r}_1 - \vec{r}; x, z)\, \widetilde{G}^{(0)}(0; z, z)\, \widetilde{G}^{(0)}(\vec{r} - \vec{r}_2; z, y). \tag{3.31}$$

Separating the central part, i.e., the bubble in Fig. 3.3, into its "bulk" and "surface" contributions, one can see that the first produces the usual Λ^2 divergence which renormalises the parameter r (often referred to as "mass", in analogy with a particle physics context). The second, instead, is regular for any $z > 0$ and therefore does not receive any divergent contribution from the integration over this coordinate; as a consequence, its degree of divergence is generally lowered by 1, i.e., it is of order Λ and can be reabsorbed as a renormalisation of the surface enhancement c_0. On the other hand, if we move one of the external points to the surface (e.g., $x = 0$), the corresponding external leg becomes singular too for $z = 0$ and can in principle contribute an additional singularity. In order to estimate its degree of divergence, we consider that cutting the corresponding external leg should recover the one found above, i.e., Λ [53]; this operation corresponds to removing the intrinsic singularity of the two-point function $\propto 1/k^2$, which increases it by 2, and removing the relevant integrations (excluding the one in the orthogonal direction, which does not contribute), which decreases it by 3. Thus, the degree of divergence is further lowered to 0, i.e., a logarithmic singularity is found which corresponds to a renormalisation of the boundary field $\varphi_1 \to Z_1^{\frac{1}{2}} \varphi_1$. Actually, since in general also the bulk field is subject to a renormalisation, the typically-employed convention corresponds to

$$\varphi \to Z^{\frac{1}{2}} \varphi, \qquad \varphi_1 \to Z^{\frac{1}{2}} Z_1^{\frac{1}{2}} \varphi_1, \tag{3.32}$$

which distinguishes between the two effects. The surface order parameter exponents have been calculated in a dimensional expansion $d = 4 - \varepsilon$ around $\varepsilon = 0$ for both the ordinary [60] and the

special [59] transitions up to the second order, and found out to be

$$\beta_{1,ord} = 1 - \frac{3}{2(n+8)}\varepsilon - \frac{3(n+2)(12-n)}{8(n+8)^3}\varepsilon^2 + O\left(\varepsilon^3\right), \tag{3.33a}$$

$$\beta_{1,sp} = \frac{1}{2} - \frac{1}{4}\varepsilon - n\frac{(n+2)}{8(n+8)^2}\varepsilon^2 + O\left(\varepsilon^3\right). \tag{3.33b}$$

It has to be noted that the introduction of boundaries produces another non-trivial consequence: due to the breaking of translational invariance, the one-particle-irreducible (1PI) formalism is not sufficient anymore to completely renormalise the theory [53, 59]. Consider in fact, neglecting for simplicity the directions parallel to the surface, a non-1PI contribution $A(x_1,\dots x_n, y_1,\dots y_m)$ to a $(n+m)$-point function; by definition, A can be written as

$$A(x_1,\dots x_n, y_1,\dots y_m) = B(x_1,\dots x_n) * G^{(0)}(x_n, y_1) * C(y_1,\dots y_m), \tag{3.34}$$

where $*$ denotes convolution. Equation (3.34) corresponds to the graphical representation in Fig. 3.4. Clearly, if translational invariance holds, the expression above can be rewritten as

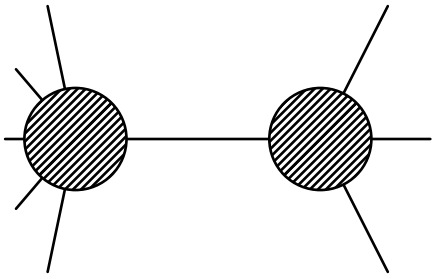

Figure 3.4: Example of a non-1PI diagram, representing expression (3.34) for $n = 6$, $m = 4$. Cutting the line in the middle disconnects the graph.

$$A = B(x_2 - x_n,\dots x_{n-1} - x_n) * G^{(0)}(x_n - y_1) * C(y_2 - y_1,\dots y_m - y_1), \tag{3.35}$$

and, upon performing a Fourier transformation, the convolution becomes a product; therefore, as long as the divergences of the terms B and C are separately cured, A remains regular. In a non-translationally-invariant framework, instead, this argument does not hold.

3.1.2 Temporal boundaries

A quench of the system's temperature (or any other control parameter) breaks time-translational invariance — a characteristic symmetry of stationary states — in the same way as a surface breaks space-translational invariance; as a matter of fact, as long as the change can be considered instantaneous, it effectively introduces a sharp temporal boundary for the evolution [23, 75]. The subsequent non-equilibrium dynamics is typically affected by the memory of the initial state and, in certain circumstances, it is also responsible for the later occurrence of ageing phenomena [20, 23, 75]. Within this framework, the "early-time" dynamics becomes akin to the behaviour of equilibrium

quantities close to a spatial surface; therefore, it is natural to pose the question whether it is possible to apply the same RG techniques briefly reviewed in Sec. 3.1.1 to the present case. For simplicity, also in this Section we shall focus on the ferromagnetic $O(n)$ models, whose thermal stochastic dynamics can be described by a Langevin formalism [68] such as

$$\frac{\partial \varphi_i}{\partial t} = -\Omega \frac{\delta \mathscr{H}}{\delta \varphi_i} + \eta_i, \tag{3.36}$$

where Ω acts as a diffusion constant, $\eta_i(\vec{r},t)$ is an n-component white Gaussian noise with zero mean and variance

$$\left\langle \eta_i(\vec{x},t)\eta_j(\vec{y},s)\right\rangle = 2\delta_{ij}\,\Omega\, k_B T\,\delta\left(\vec{x}-\vec{y}\right)\delta\left(t-s\right) \tag{3.37}$$

which accounts for the thermal fluctuations induced on the system by an external bath at fixed temperature T, and $\mathscr{H}$ is the Ginzburg-Landau energy density (3.12). For simplicity, below we will set $k_B T = 1$. Equation (3.36), which corresponds to "model A" according to the classification of Ref. [68], describes an evolution which does not preserve the order parameter φ. Other dynamical prescriptions include conserved order parameters (model B), coupling to conserved fields (model C) and more elaborated ones, such as the description of the universal behaviour of gas-fluid mixtures (model H), superfluid helium (model F) or Heisenberg antiferromagnets (model G).

It is now well-established that a Langevin equation can be recast in a path-integral formalism by a suitable transformation [19, 76–78], which we review shortly in App. 3.B. This requires the introduction of an auxiliary n-component field $\widetilde{\varphi}_i$ and produces for our choice a generating functional of correlations

$$Z[J,\widetilde{J}] = \int \mathscr{D}\varphi \mathscr{D}\widetilde{\varphi}\; \mathrm{e}^{-S[\varphi,\widetilde{\varphi}]-J\cdot\varphi-\widetilde{J}\cdot\widetilde{\varphi}}\,\mathscr{P}_{t_0}[\varphi] \tag{3.38}$$

where $\mathscr{P}_{t_0}$ is the probability distribution of the field φ at time $t = t_0$ and J, $\widetilde{J}$ are external sources, while the shorthand notation $J\cdot\varphi$ stands for

$$J\cdot\varphi = \int_{t_0}^{\infty} \mathrm{d}t \int \mathrm{d}^d x\, J(\vec{x},t)\,\varphi(\vec{x},t). \tag{3.39}$$

In Eq. (3.38) the effective action S is given by

$$S[\varphi,\widetilde{\varphi}] = \int_{t_0}^{\infty}\mathrm{d}t \int \mathrm{d}^d x \left\{ \widetilde{\varphi}_i \left[\dot{\varphi}_i + \Omega\left(r-\nabla^2\right)\varphi_i + \Omega\frac{g}{6}\varphi^2\varphi_i \right] - \Omega\widetilde{\varphi}^2 \right\}, \tag{3.40}$$

where the sum over repeated indices is understood. This expression can be slightly simplified by rescaling time according to $t \to t/\Omega$. Note that, by doing this, we are actually intermingling the renormalisation of Ω with that of time scales; however, since we are primarily interested in the behaviour at boundaries, we can safely relinquish the distinction between these two effects. This rescaling yields

$$S[\varphi,\widetilde{\varphi}] = \int_{t_0\Omega}^{\infty}\mathrm{d}t \int \mathrm{d}^d x \left\{ \widetilde{\varphi}_i \left[\dot{\varphi}_i + \left(r-\nabla^2\right)\varphi_i + \frac{g}{6}\varphi^2\varphi_i \right] - \widetilde{\varphi}^2 \right\}. \tag{3.41}$$

By introducing a source term $h_i\varphi_i$ in the free-energy density (3.12), it is not difficult to see that it is mapped into $h_i\widetilde{\varphi}_i$ in the action (3.41). This means that obtaining the linear response of a certain observable $\langle \varphi_{j_1}(t_1)\dots\varphi_{j_n}(t_n)\rangle$ to an external perturbation $h_i(s)$ amounts to calculating

$$\frac{\delta}{\delta h_i(s)}\langle \varphi_{j_1}(t_1)\dots\varphi_{j_n}(t_n)\rangle = \langle \varphi_{j_1}(t_1)\dots\varphi_{j_n}(t_n)\widetilde{\varphi}_i(s)\rangle, \tag{3.42}$$

which justifies the name of *response field* attributed to $\widetilde{\varphi}$. Moreover, causality requires that no response be observed before a perturbation is applied; therefore, a generic expectation

$$\langle \varphi_{j_1}(t_1)\dots\varphi_{j_n}(t_n)\widetilde{\varphi}_{i_1}(s_1)\dots\widetilde{\varphi}_{i_m}(s_m)\rangle \tag{3.43}$$

identically vanishes whenever $\max_j\{t_j\} < \max_i\{s_i\}$. In particular, out of three different two-point functions which can be constructed with two commuting fields, only two are not identically 0, namely the correlation function $C(\vec{x};t,s) = \langle\varphi(\vec{x},t)\varphi(0,s)\rangle$ and the response function $R(\vec{x};t,s) = \langle\varphi(\vec{x},t)\widetilde{\varphi}(0,s)\rangle$.

If one is interested in the asymptotic stationary state, the limit $t_0 \to -\infty$ can be taken and $\mathscr{P}_{t_0}$ disregarded, as the relaxational dynamics will erase any memory of the initial state in the long-time limit. Our interest here is focused instead on the evolution close to the initial point, which in the following we will conventionally set to $t_0 = 0$. In order to highlight universal features, we shall consider a quench to the critical temperature T_c, which can be effectively obtained in dimensional regularisation by setting $r = 0$ in Eq. (3.41) [11]. From expression (3.41) one realises that the scaling dimension of time differs from the one of spatial coordinates (typically taken as reference, i.e., -1); in particular, the mean-field dynamical exponent is $z = 2$ [23]. Consequently, the naive dimensions

$$[\varphi] = \frac{d-2}{2}, \qquad [\widetilde{\varphi}] = \frac{d+2}{2} \tag{3.44}$$

for the order parameter and the response field can be derived. The initial distribution $\mathscr{P}_{t_0}$ is in general a complicated function of its argument, but one can employ RG arguments similar to the ones used in the previous Section to retain only the relevant part. First of all, we assume that it is regular enough to be rewritten as

$$\mathscr{P}_0[\varphi] = \frac{1}{\mathscr{Z}_0}\mathrm{e}^{-S_0} = \frac{1}{\mathscr{Z}_0}\mathrm{e}^{-\int \mathrm{d}^d x\,\mathscr{H}_0[\varphi]}, \tag{3.45}$$

where $\mathscr{Z}_0 = \int D\varphi_{t=0}\,\mathrm{e}^{-S_0}$ is a normalisation factor which ensures that $\mathscr{P}_0$ describes indeed a probability, i.e., $\int D\varphi_{t=0}\,\mathscr{P}_0 = 1$ and $\mathscr{H}_0$ is a functional which admits a power-series expansion in terms of φ; secondly, we also restrict to initial states which do not explicitly break the $O(n)$ symmetry. As a consequence, one finds

$$\mathscr{H}_I[\varphi] = \sum_{n=1}^{\infty}\frac{\tau_{n-1}}{(2n)!}\varphi^{2n} = \frac{\tau_0}{2}\varphi^2 + \frac{\tau_1}{4!}\varphi^4 + \dots, \tag{3.46}$$

from which, using Eqs. (3.44), one can determine that $[\tau_n] = 2 - n(d-2)$. For $d = 4$ this implies

$$[\tau_0] = 2, \qquad [\tau_1] = 0, \qquad [\tau_n] < 0 \quad \forall n > 1, \tag{3.47}$$

i.e., the quadratic term is the only relevant one. In principle, one should also take into account the marginal, quartic one, but, as we wish to keep the discussion as simple as possible, here we shall follow the example of Ref. [23] and neglect it. From a physical perspective, this amounts to requiring that at $t = 0$ the system be far from criticality, which implies that the introduction of the quartic term is irrelevant for the description, as the quadratic one dictates the behaviour. Therefore, if the initial state is sufficiently similar to the one described by

$$\mathscr{H}_0 = \frac{1}{2}\tau_0\varphi^2 \tag{3.48}$$

we can expect the universal features extracted by the RG to correctly capture the main properties of the dynamics already in its early stages. Equation (3.48) corresponds to a Gaussian state with vanishing mean and extremely short-range correlations

$$\langle\varphi(\vec{x},0)\varphi(\vec{y},0)\rangle = \int D\varphi_{t=0}\,\varphi(\vec{x},0)\varphi(\vec{y},0)\,\mathrm{e}^{-S_0} = \frac{1}{\tau_0}\delta\left(\vec{x}-\vec{y}\right). \tag{3.49}$$

effectively represented by a δ distribution at the mesoscopic level. Such features denote a highly-disordered state; in particular, for large τ_0 Eq. (3.49) effectively captures the features of an infinite-temperature state. Thus, any quench performed as a sudden cooling from very high temperatures to the critical value T_c is well described within this framework.

Note that S_0 defined in Eq. (3.45) can be regarded as a boundary action at $t = 0$, which makes the partition function (3.38) substantially analogous to the one (Eq. (3.13)) encountered in the case of static, semi-infinite systems. The main difference consists in the causal structure of the dynamical theory: a perturbation in the future cannot affect the past, whereas a perturbation in the bulk is generally able to reach the surface. On the other hand, this dynamical feature is encoded in the properties of the response field $\widetilde{\varphi}$, thus the same formalism sketched in the previous Section can indeed be applied to the present case [20, 23]. In particular, in complete analogy with c_0 in the previous Section, one finds that the only possible fixed points for the renormalisation flow of τ_0 are 0 and $\pm\infty$; however, here τ_0 is involved in the definition of a probability density, hence we are forced to exclude those values which make it non-normalisable. Because of this, the only one left is $\tau_0 = +\infty$, which corresponds to the ordinary transition and to Dirichlet initial conditions for the order parameter

$$\varphi(\vec{x},t=0) = \frac{1}{\tau_0}\widetilde{\varphi}(\vec{x},t=0) \to 0. \tag{3.50}$$

This completely determines the bare propagators of the theory, written here in a momentum-time representation, which are the previously-introduced correlation

$$C(\vec{k};t,s) = \left\langle\varphi(\vec{k};t)\varphi(-\vec{k};s)\right\rangle = \frac{1}{k^2}\left(\mathrm{e}^{-k^2|t-s|} - \mathrm{e}^{-k^2(t+s)}\right) \tag{3.51}$$

and response

$$R(\vec{k};t,s) = \left\langle\varphi(\vec{k};t)\widetilde{\varphi}(-\vec{k};s)\right\rangle = \theta(t-s)\mathrm{e}^{-k^2(t-s)}, \tag{3.52}$$

in which the causal structure is made apparent by the presence of the unit step function $\theta(t-s)$ with $\theta(t<0) = 0$ and $\theta(t>0) = 1$. Furthermore, one has to introduce the boundary fields φ_0, $\widetilde{\varphi}_0$

which enter the SDEs of φ and $\widetilde{\varphi}$, respectively, and can be identified with

$$\varphi_0 = \partial_t \varphi \,|_{t=0} \quad \text{and} \quad \widetilde{\varphi}_0 = \widetilde{\varphi}(t=0) \tag{3.53}$$

within a mean-field description. The difference in scaling dimension between the temporal "bulk" and "surface" defines a new critical exponent θ, usually referred to as *initial-slip exponent*, which appears in

$$\varphi(\vec{x},t) \sim t^{1-\theta}\varphi_0(\vec{x}) \quad \text{and} \quad \widetilde{\varphi}(\vec{x},t) \sim t^{-\theta}\widetilde{\varphi}_0(\vec{x}) \tag{3.54}$$

and governs the early-time dynamics of the system. Its value has been calculated up to the second order in a dimensional expansion ($d = 4-\varepsilon$, $\varepsilon \to 0^+$), which gives [23]

$$\theta = \frac{n+2}{n+8}\frac{\varepsilon}{4} + \frac{3}{2}\frac{n+2}{(n+8)^2}\left(\frac{n+3}{n+8} + \log 2\right)\varepsilon^2 + O\left(\varepsilon^3\right). \tag{3.55}$$

An example of early-time scaling has already been encountered in Fig. 2.1 in the Introduction. The fact that the two SDEs above share the same exponent (apart from a shift by 1 due to the presence of a time derivative) is related to the fact that this model, in the long-time limit, reaches thermal equilibrium at $T = T_c$, which implies that the fluctuation-dissipation relation [20]

$$-\frac{\partial_t C(t,s)}{R(t,s)} = k_B T_c \tag{3.56}$$

is asymptotically satisfied. This can be directly verified — recalling that we have set $k_B T_c = 1$ — from Eqs. (3.51) and (3.52) taking the limits $t \to \infty$, $s \to \infty$ with $t - s$ fixed; as a consequence, the scaling dimension of $\widetilde{\varphi}$ and $\partial_t \varphi$ must be the same, i.e.,

$$[\widetilde{\varphi}(t)] = [\partial_t \varphi(t)] = [\varphi(t)] + z. \tag{3.57}$$

On the other hand, by applying the Dirichlet initial condition (3.50) to the equation of motion

$$\left(\partial_t - \nabla^2 + \frac{g}{6}\varphi^2\right)\varphi_i = 2\widetilde{\varphi}_i \tag{3.58}$$

one finds $\partial_t \varphi_i \,|_{t=0} = 2\widetilde{\varphi}_i(t=0)$, which implies $[\varphi_0] = [\widetilde{\varphi}_0]$. Note that, since the last equation does not depend on any scaling parameter and the Dirichlet condition $\tau_0 = \infty$ does not flow under RG transformations, the identification of the two dimensions goes beyond the mean-field description and is actually valid at any perturbative order [23].

3.2 A model with both spatial and temporal boundaries

In order to investigate the subtle interplay between the breaking of space- and time-translational invariance we have studied a semi-infinite $O(n)$ model quenched from a disordered state to its critical temperature at time $t = 0$. We have combined analytical and numerical methods for the purpose of verifying whether effects beyond those resulting from each separate breaking [79] emerge. We have uncovered, unexpectedly but similarly to the case of a spatial wedge [65], a so-far undetected

power-law behaviour described by a critical exponent θ_E which emerges upon approaching the effective edge formed by the intersection of the spatial and temporal boundaries.

Consider the Langevin equation (3.36) with a Gaussian white noise that we take to be uniform throughout the system, as the one in Eq. (3.37). In order to account for the presence of a spatial surface, we introduce a boundary term in the Ginzburg-Landau effective free-energy density

$$\mathscr{H}[\varphi] = \int\limits_{\{x_\perp \geq 0\}} \mathrm{d}^d x \left[\frac{(\vec{\nabla}\varphi)^2}{2} + \frac{r}{2}\varphi^2 + \frac{g}{4!}\varphi^4 + \delta(x_\perp)\frac{c_0}{2}\varphi^2 \right]. \tag{3.59}$$

where we have employed the same notation as in Sec. 3.1, i.e., $x_\perp$ represents the coordinate orthogonal to the surface, $r \propto T - T_c$ describes the distance from the critical temperature, $g > 0$ constitutes a measure of the strength of interactions in the bulk and c_0 the relative difference with their counterparts at the surface. As a starting point for the dynamics, we take for simplicity the same high-temperature state (3.48) introduced in Sec. 3.1.2, thereby choosing not to explicitly break space-translational invariance from the very beginning. In the following we shall concentrate on the special ($c_0 = 0$) and ordinary ($c_0 \to +\infty$) transitions, since they admit a unified treatment, as they are both cases in which the bulk becomes critical in the absence of an explicit breaking of the $O(n)$ symmetry. The average order parameter $\langle\varphi(t)\rangle$ has been studied in Ref. [79], where it has been argued that no new field-theoretical divergences should arise at the spatio-temporal edge ($t = 0, x_\perp = 0$). In order to support such a statement, the following argument has been proposed: on the one hand, the new divergences which appear in an out-of-equilibrium context at the initial instant are logarithmic in nature (i.e., $O\left(\Lambda^0\right)$); on the other, as we have seen at the end of Sec. 3.1.1, moving a point from the bulk to the surface reduces the degree of divergence by 1. Thus, the corresponding novel singularity expected to emerge at the edge $(t = 0, x_\perp = 0)$ should be of order $O\left(\Lambda^{-1}\right)$, which represents an effective way to denote its absence. Although seemingly reasonable, this argument fails to capture the singular behaviour emerging from the calculation of perturbative corrections, as we show in App. 3.C. We think such reasoning not to be entirely correct and we propose to revisit the issue in the same light as it has been presented for the case of a static system with boundaries [53]. Focusing our attention for simplicity on the "tadpole" contribution in $d = 4$, corresponding to Fig. 3.3, we first have to subtract from its usual degree of divergence (Λ^2) the number of relevant integrations lost at the edge, which include one over $x_\perp$ and one over time. Recalling that this theory has (naive) dynamic exponent $z = 2$ and therefore time effectively counts as a squared spatial coordinate, we get indeed Λ^{-1} for the general degree of divergence of this diagram. On the other hand, in order to gain insight on the boundary-specific singularities, we have to consider the effect of removing an external line fixed at the edge; the intrinsic ultraviolet behaviour of two-point correlation is, in the dynamical case, $\sim 1/k^4$ and provides an increase of order 4. In fact, the Fuorier transform of the equilibrium part of (3.51) with respect to time is

$$C(\vec{k};\omega) = \frac{2}{\omega^2 + (k^2)^2}. \tag{3.60}$$

The relevant integration, which is performed along the edge, involves three spatial dimensions and thus decreases it by 3. The global effect is an increase by 1 which returns a degree of divergence of $O\left(\Lambda^0\right)$, thereby identifying a logarithmic divergence, compatibly with the results reported below.

The response function is slightly more complicated; while it is characterised by an ultraviolet behaviour $\propto k^{-2}$, one has to consider that, because of its causal structure, the integration over time is irrelevant already in the "bulk"; therefore, one is losing only one spatial integration. The overall effect is again an increase by 1, analogously to the case of the correlation function.

3.2.1 Field-theoretical approach

In the response function formalism [76–78] (see App. 3.B), the global action is given by $S_{TOT} = S + S_0 + S_1$, where the first term corresponds to Eq. (3.41) with $t_0 = 0$, the second describes the initial state

$$S_0(\varphi) = \frac{1}{2} \int\limits_{\{x_\perp \geq 0\}} \mathrm{d}^d x \; \tau_0 \, \varphi^2(t=0) \tag{3.61}$$

and the third is the surface term

$$S_1(\varphi, \widetilde{\varphi}) = \int_0^\infty \mathrm{d}t \int \mathrm{d}^{d-1} x \, c_0 \, \widetilde{\varphi}(x_\perp = 0) \varphi(x_\perp = 0) \tag{3.62}$$

which comes from the boundary term $\propto \delta(x_\perp)$ in Eq. (3.59). S_1 gives rise to Dirichlet and Neumann boundary conditions for both fields at the ordinary and special points, respectively. We carried out a field-theoretical perturbative calculation aimed at obtaining both two-point functions

$$\begin{cases} C(\vec{k}; x, t; y, s) = \left\langle \varphi(\vec{k}; x, t) \varphi(-\vec{k}; y, s) \right\rangle, \\ R(\vec{k}; x, t; y, s) = \left\langle \varphi(\vec{k}; x, t) \widetilde{\varphi}(-\vec{k}; y, s) \right\rangle \end{cases} \tag{3.63}$$

in dimensional regularisation at the first order in $\varepsilon = 4 - d$; as in the previous Sections, we employ here a mixed momentum-coordinate representation, denoting with x and y the distances from the spatial surface and with t and s the time elapsed from the quench. In order to simplify the notation, below we will omit the dependence on the momentum whenever this might not cause confusion.

Beyond correctly reproducing the previously-known results concerning separately each of the two boundaries $x_\perp = 0$ and $t = 0$, this approach highlights indeed the emergence of an additional dimensional pole $\propto \varepsilon^{-1}$ [11] when the coordinates of the correlation and response functions (3.63) are fixed at the spatio-temporal edge $y = s = 0$, analogously to what happens for the static critical behaviour in a wedge [65]. Adopting the same point of view as the one introduced in Sec. 3.1, these poles can be associated to new edge operators φ_E and $\widetilde{\varphi}_E$ which appear as the most relevant fields in the short-distance expansions [53] of the order parameter φ and the response field $\widetilde{\varphi}$ close to the edge. In the present case, due to the nature of the boundary conditions imposed, at the mean-field level we can identify them with

$$\varphi_E = \partial_t \varphi(t, x_\perp) \,|_{t = x_\perp = 0} \quad \text{and} \quad \widetilde{\varphi}_E = \widetilde{\varphi}(t = 0, x_\perp = 0) \tag{3.64}$$

for the special transition and with

$$\varphi_E = \partial_t \partial_{x_\perp} \varphi(t, x_\perp) \,|_{t = x_\perp = 0} \quad \text{and} \quad \widetilde{\varphi}_E = \partial_{x_\perp} \widetilde{\varphi}(t = 0, x_\perp) \,|_{x_\perp = 0} \tag{3.65}$$

for the ordinary one. The corresponding naive scaling dimensions are given by

$$[\widetilde{\varphi}_E]_{sp} = [\varphi_E]_{sp} = \frac{d+2}{2} = 3 - \frac{\varepsilon}{2} \quad \text{and} \quad [\widetilde{\varphi}_E]_{ord} = [\varphi_E]_{ord} = \frac{d+4}{2} = 4 - \frac{\varepsilon}{2}. \tag{3.66}$$

Note that, in contrast with the previous instances, this implies that the corresponding operators $\int \mathrm{d}^{d-1}x\, h_E\, \varphi_E(\vec{x})$ are irrelevant in the RG sense, since $[h_E]_{sp} = -\varepsilon/2$ and $[h_E]_{ord} = -1-\varepsilon/2$. This is similar to the case of the spatial wedge [65], where the edge operator, which controls the leading behaviour of the correlation function near the intersection of the two (spatial) surfaces, becomes irrelevant when the angle is smaller than π. Since, in general, irrelevant operators are known to increase the degree of divergence when inserted in an expectation [80, 81], this might provide an explanation to the peculiar behaviour encountered above when fixing the external leg of a Feynman diagram to the edge. Note that, despite its irrelevance, it stills dictates the leading scaling behaviour in this regime. In order to write the corresponding SDEs, one has to introduce a generic "radial" coordinate $(Ay)^z + s$, where A is a non-universal constant which depends on the units chosen to measure time and space; this coordinate controls the distance from the edge, so that

$$\varphi(y,s) \sim \left((Ay)^z + s\right)^{-c_E} \varphi_E, \qquad \widetilde{\varphi}(y,s) \sim \left((Ay)^z + s\right)^{-\tilde{c}_E} \widetilde{\varphi}_E, \tag{3.67}$$

where we have defined

$$c_E = \frac{[\varphi] - [\varphi_E]}{z} \quad \text{and} \quad \tilde{c}_E = \frac{[\widetilde{\varphi}] - [\widetilde{\varphi}_E]}{z}. \tag{3.68}$$

The same argument which has led us to identify the exponents in Eq. (3.54) allows one to conclude that $c_E = \tilde{c}_E - 1$. Taking into account all the asymptotic behaviours defined by Eqs. (3.27), (3.54) and (3.67), the most general scaling forms one can write for the two-point functions (3.63) are

$$C(x,t;y,s) = A_C\,(\Delta t)^a \left(\frac{s}{t}\right)^{1-\theta} \left(\frac{A^2 xy}{(\Delta t)^{\frac{2}{z}}}\right)^{\frac{\beta_1-\beta}{\nu}} \left(\frac{(Ay)^z + s}{\Delta t}\right)^{-\theta_E} F_C\left(\frac{(Ax)^z}{\Delta t}, \frac{(Ay)^z}{\Delta t}, \frac{s}{t}\right), \tag{3.69a}$$

$$R(x,t;y,s) = A_R\,(\Delta t)^{a-1} \left(\frac{s}{t}\right)^{-\theta} \left(\frac{A^2 xy}{(\Delta t)^{\frac{2}{z}}}\right)^{\frac{\beta_1-\beta}{\nu}} \left(\frac{(Ay)^z + s}{\Delta t}\right)^{-\theta_E} F_R\left(\frac{(Ax)^z}{\Delta t}, \frac{(Ay)^z}{\Delta t}, \frac{s}{t}\right), \tag{3.69b}$$

where we have assumed, without loss of generality, $t > s$ and introduced $\Delta t = t - s$. In the expressions above, $F_{C/R}$ are scaling functions (depending, inter alia, on the specific surface transition) with finite $F_{C/R}(0,0,0) \neq 0$ and such that the usual equilibrium scaling is recovered when $t \to s$ and $x \to y$; the non-universal constants $A_{R/C}$ are chosen such that

$$F_{C/R}(0,0,0) = 1. \tag{3.70}$$

The exponents a and $a-1$ denote the scaling dimensions of the correlation and response functions, respectively, once again related by the fluctuation-dissipation theorem (3.56), and can be expressed in terms of bulk critical exponents as

$$a = d - 1 - \frac{2\beta}{\nu} = 1 - \eta. \tag{3.71}$$

The exponent θ_E describes the only effect which is specifically due to the edge; to relate it with c_E defined in Eq. (3.67) we rewrite $(Ay)^z = u\cos\alpha$ and $s = u\sin\alpha$ and consider the limit $u \to 0$, which denotes an approach to the edge for any fixed "angle" α. The asymptotic behaviour of Eqs. (3.69a) and (3.69b) is then given by

$$C \sim u^{-c_E} \langle \varphi(x,t), \varphi_E \rangle \sim u^{1-\theta+\frac{\beta_1-\beta}{z\nu}-\theta_E}, \tag{3.72a}$$

$$R \sim u^{-c_E+1} \langle \varphi(x,t), \widetilde{\varphi}_E \rangle \sim u^{-\theta+\frac{\beta_1-\beta}{z\nu}-\theta_E}, \tag{3.72b}$$

which leads to the identification

$$c_E = -1 + \theta - \frac{\beta_1 - \beta}{z\nu} + \theta_E, \tag{3.73}$$

where, according to Eqs. (3.54) and (3.27), $z(-1+\theta) = [\varphi] - [\varphi_0]$ and $-(\beta_1-\beta)/(\nu) = [\varphi] - [\varphi_1]$ represent the initial-slip and surface contributions that would appear even in the absence of novel singularities localised at the edge. This clearly shows that θ_E entirely encodes the edge features. Up to $O(\varepsilon)$, the latter turns out to be [82]

$$\theta_{E,sp} = \left(\sqrt{3}-1\right)\frac{n+2}{n+8}\frac{\varepsilon}{4} \quad \text{and} \quad \theta_{E,ord} = -\left(1-\frac{1}{\sqrt{3}}\right)\frac{n+2}{n+8}\frac{\varepsilon}{4} \tag{3.74}$$

for the special and ordinary transitions, respectively. The factor $\sqrt{3}$ in these expressions is specific to the edge: up to the first order in the perturbative ε-expansion, in fact, it does not appear in any other static or dynamic, bulk [11] or surface [59, 60] exponent (see, e.g., Eqs. (3.173a), (3.173b), (3.33a), (3.33b) and (3.55)). Thus, it seems unlikely that θ_E could be expressed by means of a scaling relation in terms of these quantities. Furthermore, in the present picture θ_E is the only critical exponent associated with an edge operator; since this model lacks conservation laws which could relate the scaling dimension of φ_E with that of the order parameter φ in any other region (bulk, surface or initial time), the exponent θ_E appears to be an independent one.

Working with the effective radial coordinate $((Ay)^z + s)$, as we have done above, involves from a practical point of view varying simultaneously the time and the distance from the surface and may seem factitious; in order to highlight what novel effects the edge brings forth in a more easily controllable context, we now introduce what we refer to as the "edge regime", which is depicted in Fig. 3.5(a): x, y and t are fixed such that $y \ll x$ and $y^z \ll t - s$, while s varies within the range $y^z \ll s \ll t$; correspondingly, Eqs. (3.69a) and (3.69b) yield

$$C(\ldots,s) \propto s^{1-\theta-\theta_E} \quad \text{and} \quad R(\ldots,s) \propto s^{-\theta-\theta_E}, \tag{3.75}$$

where the proportionality constants depend, inter alia, on $t \gg s$, x^z/t and $y^z/t \ll 1$. Conversely, we name "short-time" (ST) the regime illustrated in Fig. 3.5(b), in which s is much smaller than any other (mesoscopic) scale, which can be obtained from the edge regime by moving s to the domain $s \ll y^z$ and in which we find

$$C(\ldots,s) \propto s^{1-\theta} \quad \text{and} \quad R(\ldots,s) \propto s^{-\theta}. \tag{3.76}$$

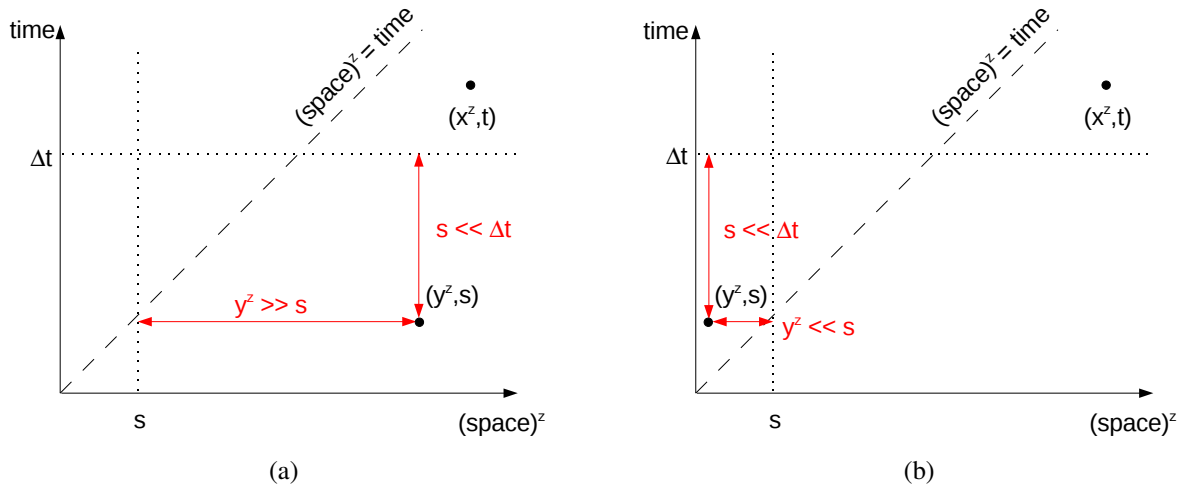

Figure 3.5: Schematic representation of (a) the edge and (b) the short-time regimes in a space^z-time plot. The two dots indicate the coordinates of the two-point functions (3.63). The dotted and dashed lines are reported in order to make the comparison between the various scales easier. The red arrows and text summarise the conditions which identify either of the two regimes.

Note that in the absence of edge effects (i.e., for $\theta_E = 0$) no alteration in the power-law behaviour could be observed by passing from one of these two regimes to the other [20, 83]; moreover, since the initial-slip exponent θ is oblivious of the surface transition, one would not find any differences between the ordinary and special cases. As we explicitly demonstrate in the next Section, these considerations can be used to set up an experimental or numerical verification of the presence of edge corrections to the scaling behaviour of observables; this approach has the significant advantage of not relying on a quantitative comparison with our predictions (3.74) which, coming from a first-order truncation of the perturbative series, could very well prove not to be accurate enough.

3.2.2 Monte Carlo study of the three-dimensional Ising universality class

While the ordinary transition is always present for $d > 2$, the special transition can be found in $d < 4$ only within the Ising universality class, i.e., for $n = 1$ [53]. For $d \geq 4$ (corresponding to $\varepsilon = 0$), the mean-field description becomes exact; therefore, since for both transitions the new exponent θ_E is of order $O(\varepsilon)$, no effects due to the edge are expected to emerge. Hence, we conclude that the three-dimensional Ising model is the most convenient choice for studying them. All the other bulk, surface and initial-slip exponents appearing in Eqs. (3.69a) and (3.69b) have been extensively studied in the past for this universality class; their numerical estimates, taken from Refs. [12, 25, 84], are approximately

$$a = \frac{1}{z}\left(d - 1 - 2\frac{\beta}{\nu}\right) \simeq 0.4725(4), \qquad \nu \simeq 0.6297(5), \qquad \beta \simeq 0.3274(9), \qquad z \simeq 2.04,$$
$$\beta_{1,ord} \simeq 0.80(1), \qquad \beta_{1,sp} \simeq 0.237(5), \qquad \theta \simeq 0.15. \tag{3.77}$$

By using the standard setup for studying surface criticality [25], we have simulated the Ising model on a three-dimensional cubic lattice made up of $H = 40$ consecutive planes with 60×60 spins per plane. Within each of these planes, periodic conditions are imposed at the boundaries to mimic the infinite extension of the system along the directions orthogonal to $x_\perp$. In order to reproduce the two different surface transitions considered above, we have let the coupling constant between any pair of surface spins J_s be in general different from the one defined in the rest of the lattice J_b; by setting the latter to $J_b = 1$ the ordinary case is realised for $0 \leq J_s < 1.5$, whereas the special transition is known to occur in three dimensions for $J_s \simeq 1.5$ [85]. The system is prepared at $t = 0$ in a completely disordered state corresponding to infinite temperature T and it subsequently evolves at its bulk critical value $T_c = 4.5115 J_b/k_B$ with Glauber dynamics. One

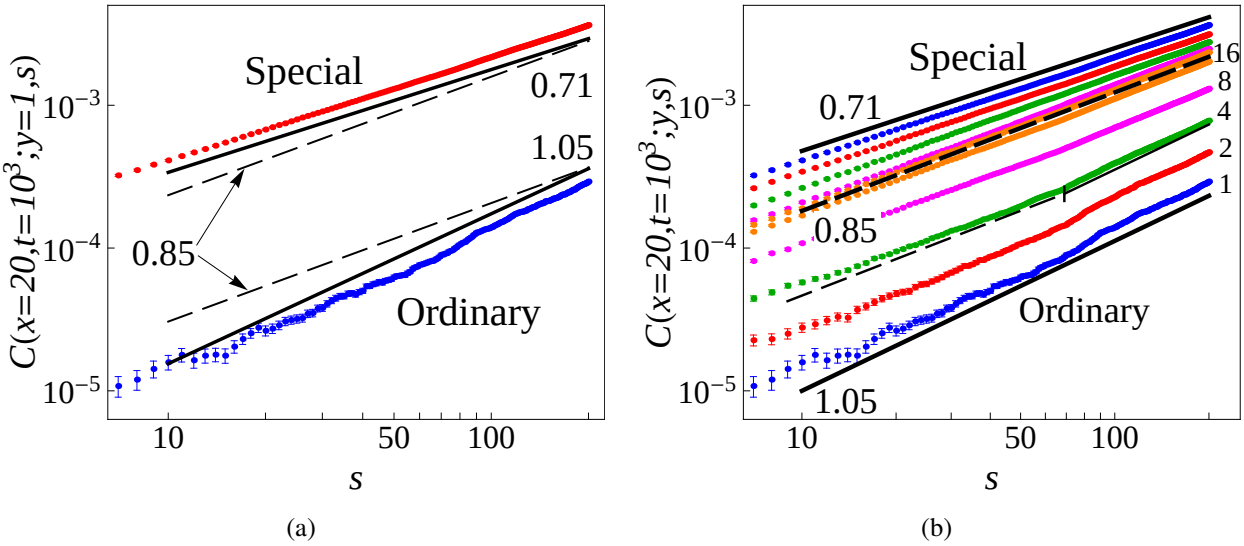

Figure 3.6: Time dependence of the correlation function $C(x,t;y,s)$ of the plane magnetisation of a three-dimensional Ising model evolving with Glauber dynamics after a quench from a completely disordered state to the bulk critical temperature. (a) The bulk-surface correlation function C with $x = H/2 = 20$ and $y = 1$ is plotted as a function of s for $t = 10^3$ sweeps (corresponding to the "edge regime" discussed in the main text). Data points result from averaging over 5×10^5 and 3×10^6 independent runs for the special (red upper dots) and ordinary (blue lower dots) case, respectively. The black solid lines correspond to power laws with the exponents reported to the right; the parallel dashed lines, instead, indicate, for comparison, the power law with exponent 0.85 observed within the short-time regime and predicted by Eq. (3.76). The data points with $s < 6$ have been disregarded as they might be affected by microscopic effects. (b) The same plot for various values of the position y. For the 5 lowermost (uppermost) curves, corresponding to the ordinary (special) transition, y increases from bottom to top (top to bottom) and takes the sequence of values reported for the ordinary case to the right. This plot highlights the crossover from the "edge" ($y^z \ll s$) to the "short-time" behaviour ($y^z \gg s$), which is common to the two instances. For the ordinary case and $y = 4$ this crossover can be observed as a function of s, as highlighted by the thin solid and dashed lines that meet at $s \simeq (Ay)^z$, which yields the indicative estimate $A \simeq 2$.

time step corresponds to one sweep in which on average every spin of the lattice has been updated once; this standard definition is conceptually akin to considering mesoscopic time scales. As we are interested in the behaviour close to the temporal surface, only rather short simulation times are needed and therefore we can restrict ourselves to rather small system sizes. In order to rule out the influence of finite-size effects we have also analysed some larger lattices, highlighting no significant discrepancies with the results we report below. For the purpose of investigating the edge regime we focused on the two-point correlation function $C(x,t;y,s)$ defined in Eq. (3.63), since the response is expected to behave in an analogous fashion (see Eqs. (3.75) and (3.76)). Here, $x = 1$ corresponds to the surface, whereas $x = H/2$ to the midplane of the lattice. The statistical average is taken over a large number of independent runs with different realisations of the thermal noise and of the initial state. In Fig. 3.6(a) we show the bulk-surface correlator $C(x = H/2,t;y = 1,s)$ for the ordinary case $J_s = 1$ and the special one $J_s = 1.5$, where we fix $t = 10^3$ and vary s within a range that, under the assumption $A \simeq 1$, corresponds to the edge regime (we verified that different instances of the value of t lead to the same slopes). From Fig. 3.6(b) one can indeed infer that the non-universal constant A is of order unity, thereby justifying our choice. We observe that $C(\ldots,s) \sim s^{\rho}$ increases algebraically, but with two different exponents $\rho_{sp} = 0.71(2)$ for the special case and $\rho_{ord} = 1.05(2)$ for the ordinary one. This result $\rho_{sp} \neq \rho_{ord}$ clearly shows that different surface universality classes display a different behaviour at the spatio-temporal edge, thus providing a confirmation to the presence of the novel effects discussed in Sec. 3.2.1. In particular, this picture is not in agreement with the power-counting argument of Ref. [79], which we have reported at the beginning of Sec. 3.2. The dashed lines, reported for comparison, denote the slope $\rho_{sp} = \rho_{ord} = 1 - \theta \simeq 0.85$ [84] which would be expected for the correlation function if no novel exponent were to appear at the edge.

Table 3.1 presents the comparison between the numerical estimates of ρ from Fig. 3.6(a) and the corresponding analytic expressions $\rho = 1 - \theta$ and $\rho = 1 - \theta - \theta_E$ which exclude and include the edge effects, respectively. The latter are calculated according to Eqs. (3.74) and (up to $O(\varepsilon)$) $\theta = \varepsilon/12$ [23], specialised to the three-dimensional Ising case (i.e., $n = 1$ and $\varepsilon = 1$). Note that, even

	Monte Carlo estimates	Analytical results ($\varepsilon = 1$)	
	Figs. 3.6(a) and 3.6(b)	$\rho = 1 - \theta$	$\rho = 1 - \theta - \theta_E$
Edge, sp	0.71(2)	0.917	0.856
Edge, ord	1.05(2)	0.917	0.952
Short-time, sp & ord	0.85(2)	0.917	0.917

Table 3.1: Comparison between the numerical and analytical estimates of the exponent ρ which controls $C(\ldots,s) \sim s^{\rho}$ in the edge and the short-time regimes, in the absence ($\rho = 1 - \theta$) and presence ($\rho = 1 - \theta - \theta_E$) of edge contributions, for the special (sp) and ordinary (ord) transitions.

if lacking quantitative accuracy, the factor relative to the edge introduced in Eq. (3.69a) correctly captures the qualitative behaviour as a function of s of the correlation function $C(x,t;y,s)$ within the edge regime: in fact, in the case of the ordinary and special transition $C(\ldots,s)$ grows respectively faster and slower than it does in the short-time regime; correspondingly, the first order correction

(3.74) is respectively negative and positive.

Figure 3.6(b) presents a study of the crossover between the edge regime of Fig. 3.6(a) and the short-time regime, which occurs upon increasing y above the scale set by $s^{1/z}/A$. This crossover is properly captured by the scaling function in Eq. (3.69a) because the additional multiplicative factor becomes approximately independent of s for $s \ll t$, so that $C(\ldots, s) \sim s^{1-\theta}$, as predicted for the short-time regime. Conversely, for a fixed $y \neq 1$ (i.e., not at the surface), the crossover between the short-time and the edge regimes occurs upon increasing s above $(Ay)^z$. With the present data, we could find reasonable evidence of its presence in the ordinary case with $y = 4$ (see Fig. 3.6(b)). We emphasize the fact that the edge regime is not the only one affected by the aforementioned factor; however, we focused on it in order to test a qualitative difference between our predictions and previous ones which had been based on the assumption that the edge plays no significant role, thus circumventing the need for a quantitatively accurate analytic determination of θ_E.

3.3 Conclusions

By studying the non-equilibrium relaxational (model A [68]) dynamics of the $O(n)$ model in the proximity of a surface within a field-theoretical formalism, we have identified novel singularities which affect the scaling behaviour of physical observables in the proximity of the spatio-temporal edge, defined as the intersection between the spatial and temporal boundaries. The asymptotic power-laws found in this regime can be understood in a boundary renormalisation group framework in terms of the difference between the scaling dimension of the order parameter φ (or the response field $\widetilde{\varphi}$) and the corresponding edge operator φ_E ($\widetilde{\varphi}_E$). Despite being irrelevant in the RG sense, the latter non-trivially affects the physics of the system as it represents the first non-vanishing contribution appearing in the short-distance expansion of the bulk field φ.

A power-counting argument had been proposed in the past to exclude the presence of novel universal effects at the edge [79]. All subsequent studies on systems presenting breaking of both space- and time-translational invariance assumed the validity of this statement in order to provide ansatzes for the scaling forms of observables. Since our calculations, which are not based on any a priori hypothesis, show a discrepancy in this respect, we have devised a suitable method to test their physical implications: we have identified a regime in which the presence or absence of effects due to the edge gives rise to qualitative differences in the behaviour of observables. In particular, in our framework the initial algebraic growth would be affected by the type of surface transition considered, whereas it would not if the aforementioned argument were correct. This avoids hinging upon a quantitative comparison which would in principle require an analytical approach to higher orders in the perturbative expansion. Our Monte Carlo simulations — which mainly focus on the edge regime and the crossover to the short-time one — provide numerical evidence of the correctness of our analytical predictions at a qualitative level. The consistency of these approaches, which concern two completely different systems at the microscopic level, i.e., a discrete spin model on a lattice and an interacting field theory in the continuum, provides additional support to the universality of the edge behaviour, which could be expected as a consequence of scale invariance at the critical point. This actually indicates that the scaling near the edge investigated here depends only on the gross features (symmetry, dimensionality and short-range interaction) which are shared

by both models.

It would be desirable to extend the present investigation to different static, dynamic and surface universality classes of experimental relevance. While the first experiments probing the static surface and equilibrium dynamical bulk properties of materials date back to the 1970s [68, 86], techniques with the sufficient accuracy to study bulk non-equilibrium behaviours have been available only since the 1990s [87]. Surface dynamics in condensed matter systems, instead, have not been observed until recently, though with a different purpose and not in the critical regime [88]. Extending recent investigations of ageing phenomena in liquid crystals [15] to the proximity of surfaces might provide a viable alternative for the experimental test of the present predictions in systems undergoing an Ising transition. Moreover, it would be interesting to understand whether the general framework of boundary renormalisation group could be applied in the early dynamical stages of *quantum* critical systems, as recent works highlighted the emergence of universal features in the non-equilibrium dynamics of one-dimensional [89] and higher-dimensional [90] bosonic systems after a quench. The introduction of initial-slip operators and the corresponding short-distance expansions in a quantum context would provide a substantial improvement in our ability to classify the aforementioned universal features, possibly shedding some light on the topical subject of dynamical phase transitions.

Appendix 3.A Divergences localised at the surface

In Sec. 3.1.1 we have sketched a procedure which allows one to determine the degree of divergence of Feynman graphs when one of their external legs is fixed at the boundary. Note that, while the more commonly used definition would refer to it as *superficial degree of divergence*, we will drop the attribute "superficial" in order not to cause confusion with the spatial surface. By focusing on the tadpole diagram of a φ^4 theory (although the argument is more generally valid [53]), we have found that the divergence at the surface is less pronounced than the bulk one. More precisely, introducing an ultraviolet (UV) momentum cutoff Λ, the latter is $\propto \Lambda^2$, whereas the former is $\propto \Lambda$. In this Appendix we explicitly show that this is indeed the case. Note that the cutoff provides a regularisation to the integration over momenta, making all the expressions appearing below finite. In the following, we shall always use the term "divergences" having in mind the removal of the cutoff $\Lambda \to \infty$. The tadpole contribution depicted in Fig. 3.3 is proportional to the convolution

$$\widetilde{G}^{(1)}(\vec{k};x,y) \propto \int_0^\infty \mathrm{d}z \int^\Lambda \frac{\mathrm{d}^3 q}{(2\pi)^3} \widetilde{G}^{(0)}(\vec{k};x,z)\, \widetilde{G}^{(0)}(\vec{q};z,z)\, \widetilde{G}^{(0)}(\vec{k};z,y). \tag{3.78}$$

For simplicity, we consider here the special point $c_0 = 0$, for which (see Eq. (3.29))

$$\widetilde{G}^{(0)}(\vec{k};x,y) = \frac{1}{2\omega_k}\left(\mathrm{e}^{-\omega_k|x-y|} + \mathrm{e}^{-\omega_k(x+y)}\right). \tag{3.79}$$

As we have argued in Sec. 3.1.1, as long as one's interest is focused on the UV behaviour, this does not represent a restriction, since for any choice of $c_0 > 0$ the large-momentum behaviour of the propagator is the same. The ordinary case $c_0 = \infty$ actually represents an exception to this rule; since the two-point function in this case vanishes at the boundary, a more subtle analysis would be required. However, by studying its normal derivative along the direction $x_\perp$ one could in principle follow the same steps illustrated below and retrieve analogous results. Note now that, according to our choice (3.79), the central term in Eq. (3.78) (corresponding to the tadpole "bubble") is given by

$$B(z,z) = \int^\Lambda \frac{\mathrm{d}^3 q}{(2\pi)^3}\, \widetilde{G}^{(0)}(\vec{q};z,z) = \int^\Lambda \frac{\mathrm{d}^3 q}{(2\pi)^3} \frac{1}{2\omega_q}\left[1 + \mathrm{e}^{-2\omega_q z}\right]. \tag{3.80}$$

Since $\omega_q \sim q$ for $q \to \infty$, the first term of this expression diverges as Λ^2 and, being independent of z, constitutes a renormalisation of the parameter r. In the following we shall focus on the second part, for which the integration over the z coordinate is not inconsequential, as we shall see. Without loss of generality, we assume $x < y$. Correspondingly, we divide the integral over z in Eq. (3.78) in three distinct parts and postpone the integration over $\vec{q}$:

$$I_1(\vec{q};x,y) = \int_0^x \mathrm{d}z\, \widetilde{G}^{(0)}(\vec{k};x,z) \frac{1}{2\omega_q} \mathrm{e}^{-2\omega_q z} \widetilde{G}^{(0)}(\vec{k};z,y), \tag{3.81a}$$

$$I_2(\vec{q};x,y) = \int_x^y \mathrm{d}z\, \widetilde{G}^{(0)}(\vec{k};x,z) \frac{1}{2\omega_q} \mathrm{e}^{-2\omega_q z} \widetilde{G}^{(0)}(\vec{k};z,y), \tag{3.81b}$$

$$I_3(\vec{q};x,y) = \int_y^\infty \mathrm{d}z\, \widetilde{G}^{(0)}(\vec{k};x,z) \frac{1}{2\omega_q} \mathrm{e}^{-2\omega_q z} \widetilde{G}^{(0)}(\vec{k};z,y). \tag{3.81c}$$

A direct calculation yields

$$I_1 = \frac{\mathrm{e}^{-\omega_k(x+y)}}{4\omega_q}\left[\frac{1}{\omega_q-\omega_k}\left(1-\mathrm{e}^{-2(\omega_q-\omega_k)x}\right)+\frac{2}{\omega_q}\left(1-\mathrm{e}^{-2\omega_q x}\right)+\frac{1}{\omega_q+\omega_k}\left(1-\mathrm{e}^{-2(\omega_q+\omega_k)x}\right)\right], \tag{3.82a}$$

$$I_2 = \cosh(\omega_k x)\,\frac{\mathrm{e}^{-\omega_k y-2\omega_q x}}{\omega_q}\left[\frac{1}{2\omega_q}\left(\mathrm{e}^{-2\omega_q x}-\mathrm{e}^{-2\omega_q y}\right)+\frac{1}{2(\omega_q+\omega_k)}\left(\mathrm{e}^{-2(\omega_q+\omega_k)x}-\mathrm{e}^{-2(\omega_q+\omega_k)y}\right)\right], \tag{3.82b}$$

$$I_3 = \frac{\cosh(\omega_k x)\cosh(\omega_k y)}{\omega_q(\omega_k+\omega_q)}\mathrm{e}^{-2(\omega_k+\omega_q)y}. \tag{3.82c}$$

For $x>0$ the leading ultraviolet behaviour of the expressions above is given by

$$I_1 = \frac{\mathrm{e}^{-\omega_k(x+y)}}{2\omega_q^2}\frac{2\omega_q^2-\omega_k^2}{\omega_q^2-\omega_k^2}+O\left(\mathrm{e}^{-q}\right), \qquad I_2 = O\left(\mathrm{e}^{-q}\right), \qquad I_3 = O\left(\mathrm{e}^{-q}\right), \tag{3.83}$$

where we denote with $O(\mathrm{e}^{-q})$ all the terms which are exponentially decreasing and thus cannot contribute to the divergence of the integral. Recalling that $\omega_q \sim q\left(1+O\left(q^{-2}\right)\right)$ one can see that I_1 behaves asymptotically as

$$I_1 \sim \frac{\mathrm{e}^{-\omega_k(x+y)}}{q^2}\left(1+O\left(q^{-2}\right)\right) \tag{3.84}$$

which, when integrated over the momenta, produces a divergence $\propto \Lambda$ for $\Lambda\to\infty$. Clearly, adding a counterterm

$$\mathscr{C}_1(\vec{q};x,y) = -\frac{\mathrm{e}^{-\omega_k(x+y)}}{q^2} \tag{3.85}$$

completely removes the divergence, i.e., it makes the integral convergent in the limit $\Lambda\to\infty$. If, instead, we fix one coordinate at the surface, i.e., $x=0$, then we have

$$I_1 \equiv 0, \qquad I_2 = \frac{\mathrm{e}^{-\omega_k y}}{2\omega_q^2(\omega_q+\omega_k)}\left(2\omega_q+\omega_k\right) \quad \text{and} \quad I_3 = O\left(\mathrm{e}^{-q}\right). \tag{3.86}$$

Therefore, the only term which can give rise to a divergence when integrated over $\vec{q}$ is now I_2, which asymptotically behaves as

$$I_2 \sim \mathrm{e}^{-\omega_k y}\left[\frac{1}{q^2}\left(1+O\left(q^{-2}\right)\right)-\frac{\omega_k}{2q^3}\left(1+O\left(q^{-2}\right)\right)\right]. \tag{3.87}$$

The first term, which produces a divergence $\propto\Lambda$, is exactly canceled by the counterterm $\mathscr{C}_1(\vec{q};0,y)$ introduced in Eq. (3.85). A second term, however, emerges which causes a logarithmic divergence "Λ^0" and requires a new counterterm

$$\mathscr{C}_2(\vec{q};y) = +\omega_k\frac{\mathrm{e}^{-\omega_k y}}{2q^3} \tag{3.88}$$

which must act only at the surface $x = 0$. In the remaining case $x = y = 0$, one has

$$I_1 = I_2 \equiv 0 \quad \text{and} \quad I_3 = \frac{1}{\omega_q(\omega_k + \omega_q)} \sim \frac{1}{q^2}\left(1 - \frac{\omega_k}{q} + O\left(q^{-2}\right)\right); \tag{3.89}$$

the divergence emerging from integrating the last expression can be removed by adding $\mathscr{C}_1 + 2\mathscr{C}_2$; the prefactor 2 accounts for the fact that in this case two points have been fixed at the surface and, consequently, the surface divergence is doubled. Generically, one would need a surface counterterm for every external leg fixed at the surface. Note that, as expected, no additional divergence appears which cannot be removed by the previously-introduced counterterms (3.85) and (3.88).

Appendix 3.B The response function formalism

In this Appendix we briefly discuss how one can recast a dynamical problem described by a stochastic equation into a path-integral formalism such as the one we have introduced in Sec. (3.2). The mapping we report below is usually referred to as *response function formalism* or *MSRDJ* or more briefly *MSR transformation*, owing its name to the people who first employed it in a physical context back in the 70s, i.e., Martin, Siggia, Rose [76], Janssen [77] and de Dominicis [78]. Consider a n-component real, classical field φ whose dynamics is described by the Langevin equation

$$\frac{\partial \varphi_i}{\partial t} = \mathscr{F}_i[\varphi] + \eta_i, \tag{3.90}$$

with a white Gaussian noise

$$\left\langle \eta_i(\vec{x},t)\eta_j(\vec{y},s)\right\rangle = 2\Omega_{ij}\,\delta(\vec{x}-\vec{y})\,\delta(t-s), \tag{3.91}$$

where we require Ω to be a positive-definite, symmetric matrix, as we want to avoid negative self-correlations. As the initial state distribution $\mathscr{P}_{t_0}[\varphi]$ does not play any significant role in the construction, we shall review here for simplicity the stationary case $t_0 = -\infty$. Moreover, we shall omit the space dependence and sum over repeated indices will always be understood. As it is the case for most path-integral constructions, also this provides an effective formalism which proves particularly useful for calculating relevant quantities, but has not to be interpreted as a formal definition from the mathematical point of view. For this reason, in the following we will not concern ourselves with problems of definition of the measures and distributions we are going to introduce.

In general, to every possible realisation of the noise η corresponds a well-defined solution φ_η of Eq. (3.90). Thereby, we can write the mean value of a generic observable $\mathscr{O}[\varphi]$ as

$$\langle \mathscr{O}[\varphi]\rangle = \int \mathscr{D}\eta\, \mathscr{P}[\eta]\, \mathscr{O}[\varphi_\eta], \tag{3.92}$$

where inside the integral the functional $\mathscr{O}$ is evaluated on the specific solution associated to the value of the "integration variable" η. By assumption, the probability distribution $\mathscr{P}[\eta]$ is Gaussian and therefore Eq. (3.91) implies

$$\mathscr{P}[\eta] = \mathscr{N}_\eta\, \mathrm{e}^{-\frac{1}{4}\int \mathrm{d}t\, \eta_i \left(\Omega^{-1}\right)_{ij} \eta_j} \quad \text{with} \quad \mathscr{N}_\eta^{-1} = \int \mathscr{D}\eta\, \mathrm{e}^{-\frac{1}{4}\int \mathrm{d}t\, \eta_i \left(\Omega^{-1}\right)_{ij} \eta_j}. \tag{3.93}$$

We now introduce an effective "delta" functional on the space of trajectories, such that

$$\int \mathscr{D}\varphi\, \mathscr{X}[\varphi]\, \delta(\varphi - \bar{\varphi}) = \mathscr{X}[\bar{\varphi}] \tag{3.94}$$

for every functional $\mathscr{X}$. This allows us to recast the average (3.92) in the form

$$\langle \mathscr{O}[\varphi] \rangle = \int \mathscr{D}\eta\, \mathscr{P}[\eta] \int \mathscr{D}\varphi\, \delta(\varphi - \varphi_\eta)\, \mathscr{O}[\varphi] = \int \mathscr{D}\varphi\, \mathscr{O}[\varphi] \int \mathscr{D}\eta\, \mathscr{P}[\eta]\, \delta(\varphi - \varphi_\eta), \tag{3.95}$$

where, in the last step, we have assumed that the integrals can be exchanged. The main advantage of this is that we can pull $\mathscr{O}$ out of the integral over the noise. We now focus on the "delta" term and define

$$\mathscr{S}_i[\varphi, \eta] = \partial_t \varphi_i - \mathscr{F}_i[\varphi] - \eta_i, \tag{3.96}$$

which casts the Langevin equation (3.90) in the more compact form $\mathscr{S}_i[\varphi, \eta] = 0$. Since for any choice of η only one solution φ_η exists, at least once the conditions at $t_0 = -\infty$ are fixed, upon performing a change of variable one obtains

$$\delta(\varphi - \varphi_\eta) = J[\varphi, \eta]\, \delta(\mathscr{S}_i[\varphi, \eta]) \quad \text{where} \quad J[\varphi, \eta] = \det \frac{\delta \mathscr{S}_i}{\delta \varphi_j}, \tag{3.97}$$

J being the corresponding Jacobian. Applying the well-known Fourier relation $\int \mathrm{d}x\, \mathrm{e}^{ikx} = 2\pi\delta(k)$, the new delta functional can now be exponentiated by means of an auxiliary, "imaginary" field $\widetilde{\varphi}$, yielding

$$\delta(\mathscr{S}_i[\varphi, \eta]) = \int \mathscr{D}(i\widetilde{\varphi})\, \mathrm{e}^{-\int \mathrm{d}t\, \widetilde{\varphi}\, \mathscr{S}[\varphi, \eta]}, \tag{3.98}$$

where we reabsorb any multiplicative constant in the measure. As a consequence, the average above can be written as

$$\langle \mathscr{O}[\varphi] \rangle = \int \mathscr{D}\varphi \mathscr{D}\widetilde{\varphi}\, \mathscr{O}[\varphi]\, \mathrm{e}^{-\int \mathrm{d}t \widetilde{\varphi}(\partial_t \varphi - \mathscr{F})} \int \mathscr{D}\eta\, \mathscr{P}[\eta]\, J[\varphi, \eta]\, \mathrm{e}^{\int \mathrm{d}t \widetilde{\varphi}\eta}. \tag{3.99}$$

By functional deriving Eq. (3.96) with respect to φ, one can express the Jacobian J as

$$J[\varphi, \eta] = \det \left\{ \partial_t \left[\delta(t-s)\delta_{ij} - \frac{\delta \mathscr{F}_i[\varphi(s)]}{\delta \varphi_j(s)} \theta(t-s) \right] \right\}, \tag{3.100}$$

where we have used for the second addend the distributional identity $\partial_t \theta(t-s) = \delta(t-s)$. Note that, for any choice of the path φ and the indices i and j, the argument of the determinant is a function $M_{ij}(t,s)$ of time which acts as an integral kernel over a generic space of test functions f, i.e.,

$$\left(M_{i,j} * f\right)(t) = \int \mathrm{d}\tau\, M_{i,j}(t,\tau) f(\tau). \tag{3.101}$$

The determinant can be thought as being comprised of two parts: one acting on this infinite-dimensional space for any choice of (i, j) and one on the remaining $n \times n$ matrix structure identified by the n different vector components. Thus, if one were able to solve the eigenvalue problem

$$M_{ij} * f_j^{(\alpha)} = \mu^\alpha f_i^{(\alpha)} \tag{3.102}$$

the determinant would be simply given by $\det(M) = \prod_\alpha \mu^\alpha$. The derivative in Eq. (3.100) is also an operator acting on test functions (the corresponding two-time kernel being $\partial_t \delta(t-s)$), hence Binet's theorem $\det(AB) = \det A \det B$ can be applied to separate the determinant in two parts

$$J[\varphi,\eta] = \det(\partial_t)\ \ \det\left\{\delta(t-s)\delta_{ij} - \frac{\delta \mathscr{F}_i[\varphi(s)]}{\delta\varphi_j(s)}\theta(t-s)\right\}, \tag{3.103}$$

the first of which does not depend on the fields and thus provides just a multiplicative factor; actually, the spectrum of the derivative is not bounded, which means we are reabsorbing into the measure a divergent quantity. However, as mentioned at the beginning of this Appendix, we shall not focus on the formal aspects, but just on the physically significant fact that it cannot contribute anything to the picture since it is independent of the fields. The remaining term can be written, in shorthand notation, as

$$\widetilde{J}[\varphi] = \det\left\{\mathbb{1} + u_{ij}(t,\tau)\right\}. \tag{3.104}$$

Now we use the relation $\det A = \mathrm{e}^{\mathrm{tr}\{\ln A\}}$ to exponentiate the argument in the expression above, aiming to make it part of what will look like the action of the fields φ and $\widetilde{\varphi}$. The logarithm of an operator is defined by its Taylor series, which in this case is

$$[\ln(\mathbb{1}+u)]_{ij}(t,s) = u_{ij}(t,s) - \frac{1}{2}\left(u_{ik} * u_{kj}\right)(t,s) + \frac{1}{3}\left(u_{ik} * u_{kl} * u_{lj}\right)(t,s) + \ldots. \tag{3.105}$$

Recalling that the step function $\theta(t-s)$ enters in the definition of u, the generic q-th convolution in this series is of the form

$$\int \left(\prod_{p=1}^{q} \mathrm{d}\tau_p\right)\left(\prod_{p=1}^{q}\theta(\tau_p - \tau_{p-1})\right)\Big[\ldots\Big], \tag{3.106}$$

where we denote $t = \tau_{q+1}$ and $s = \tau_0$. The product above implies that the integrand identically vanishes if the variables are not in increasing order, i.e., if there is at least one pair of variables which obeys $\tau_p < \tau_q$ with $p > q$. In particular, it does if $t < s$. Taking the trace means identifying the ending points and integrating over them. Because of this, the constraint on the q-th convolution becomes $t \geq \tau_q \geq \ldots \geq \tau_1 \geq t$, which means that the integrand has at best a support of null measure and thus its integral vanishes. The only term left, since the condition above becomes trivial ($t \geq t$), is the first one. This implies [11]

$$\mathrm{tr}\{\ln(\mathbb{1}+u)\} = \sum_i \int \mathrm{d}t\, u_{ii}(t,t) = -\theta(0)\sum_i \int \mathrm{d}t\, \mathscr{F}_i'[\varphi(t)], \tag{3.107}$$

with

$$\mathscr{F}_i'[\varphi(t)] = \frac{\delta \mathscr{F}_i[\varphi(t)]}{\delta\varphi(t)}. \tag{3.108}$$

Summarising, the Jacobian in Eq. (3.97) can be divided into two parts, a divergent factor independent of the fields which is incorporated into the integration measure, and a physically relevant one which can be written in exponential form. Furthermore, from Eq. (3.100) we see that it does not

depend on η, as φ represents now an independent integration variable. Thus, the integration over the noise in Eq. (3.99) can be performed according to the Gaussian rule

$$\int \mathscr{D}\eta\ \mathscr{P}[\eta]\,\mathrm{e}^{\int \mathrm{d}t\,\widetilde{\varphi}\eta} = \int \mathscr{D}\eta\ \mathscr{N}_\eta\,\mathrm{e}^{-\frac{1}{4}\int \mathrm{d}t\,\left[\eta_i\left(\Omega^{-1}\right)_{ij}\eta_j - 4\widetilde{\varphi}\eta\right]} = \mathrm{e}^{\int \mathrm{d}t\,\widetilde{\varphi}_i\Omega_{ij}\widetilde{\varphi}_j}. \tag{3.109}$$

Grouping together the various results above, one can re-express the average of the observable $\mathscr{O}$ as a path integral with two vector fields φ, $\widetilde{\varphi}$

$$\langle \mathscr{O}[\varphi]\rangle = \int \mathscr{D}\varphi\mathscr{D}\widetilde{\varphi}\ \mathscr{O}[\varphi]\,\mathrm{e}^{-S[\varphi,\widetilde{\varphi}]}, \tag{3.110}$$

where the action is given by

$$S[\varphi,\widetilde{\varphi}] = \int \mathrm{d}t\left\{\widetilde{\varphi}_i\left(\partial_t\varphi_i - \mathscr{F}_i[\varphi]\right) - \widetilde{\varphi}_i\Omega_{ij}\widetilde{\varphi}_j + \theta(0)\sum_i \mathscr{F}_i'[\varphi]\right\} \tag{3.111}$$

which would give back Eq. (3.41) when specialised to the φ^4 case were it not for the last term. Note that, in addition, the latter is ill-defined as it contains $\theta(0)$, which has no definite meaning: actually, the step function at the origin can take any real value, due to the fact that, despite its name, it is a distribution. Hence, on the one hand, the action seems to depend on such an arbitrary choice while, on the other, the physics requires that all observables be independent of it. In order to cope with this issue, we shall study how $\theta(0)$ enters in the calculation of observables; for this purpose, we shall assume that Wick's theorem holds. In general, one would have to require the state of the system to be Gaussian, such as the one defined by Eq. (3.48) [11]. We also take an effective force $\mathscr{F}$ which can be expanded as a power series of its argument, i.e.,

$$\mathscr{F}_i[\varphi] = D\nabla^2\varphi_i + C^{(1)}_{ij}\varphi_j + C^{(2)}_{ijk}\varphi_j\varphi_k + C^{(3)}_{ijkl}\varphi_j\varphi_k\varphi_l\ldots, \tag{3.112}$$

where we restrict for simplicity to cases in which the first, diffusive term is the only one containing a derivative. Note that the constant term $C^{(0)}$ needs not to be included as it constitutes a drift velocity which can be accounted for by redefining the field $\varphi \to \varphi + C^{(0)}t$. On the other hand, the introduction of an effective source $h(t)$ can be used to obtain information on the linear response of the system to external stimuli. In the action, this field would couple to $\widetilde{\varphi}$; this means that any expectation containing only response fields identically vanishes, since it corresponds to deriving the identity:

$$\langle \widetilde{\varphi}_{i_1}(t_1)\ldots\widetilde{\varphi}_{i_m}(t_m)\rangle = \frac{\delta}{\delta h_{i_1}(t_1)}\cdots\frac{\delta}{\delta h_{i_m}(t_m)}\langle \mathbb{1}\rangle = 0. \tag{3.113}$$

The higher-order coefficients in Eq. (3.112) are contracted with totally symmetric combinations of the fields and can be thus chosen to be totally symmetric under the exchange of the involved indices. Accordingly, the last term in the action (3.111) can be expanded as

$$\mathscr{F}_i'[\varphi] = D\nabla^2 + C^{(1)}_{ii} + 2C^{(2)}_{iij}\varphi_j + 3C^{(3)}_{iijk}\varphi_j\varphi_k + \ldots, \tag{3.114}$$

where the repeated indices i are not summed over yet. The first two terms can be neglected as they shift the action by just a constant; the remaining ones will be treated as an interaction, despite

the fact that they include linear and quadratic terms, which are usually employed to define the propagator, instead [11]. The reason is that, in the standard perturbative scheme we are going to employ, the action is expanded as a combined power-series of all the couplings of cubic and higher-order terms; according to Eq. (3.112), that would mean all coefficients starting from $C^{(2)}$, since the corresponding operator in the action is $\widetilde{\varphi}\varphi^2$. Thus, the expansion automatically involves all the relevant terms of Eq. (3.114).

Disregarding for the aforementioned reason the terms proportional to $\theta(0)$, the quadratic part is given by

$$\frac{1}{2}\begin{pmatrix} \varphi \\ \widetilde{\varphi} \end{pmatrix}^{\mathsf{T}} \begin{pmatrix} 0 & -\partial_t - D\nabla^2 - C^{(1)} \\ \partial_t - D\nabla^2 - C^{(1)} & -2\Omega \end{pmatrix} \begin{pmatrix} \varphi \\ \widetilde{\varphi} \end{pmatrix}. \tag{3.115}$$

The propagator is obtained by calculating the inverse of the matrix above; we are now particularly interested in the off-diagonal elements, which in Fourier transform $\vec{x} \to \vec{k}$ obey

$$\left(\partial_t + Dk^2 - C^{(1)}\right)_{ij} \left\langle \varphi_j(\vec{k},t)\, \widetilde{\varphi}_l(-\vec{k},s) \right\rangle = \delta_{il}\delta(t-s), \tag{3.116a}$$

$$\left(-\partial_t + Dk^2 - C^{(1)}\right)_{ij} \left\langle \widetilde{\varphi}_j(\vec{k},t)\, \varphi_l(-\vec{k},s) \right\rangle = \delta_{il}\delta(t-s). \tag{3.116b}$$

The equations above are solved by

$$R_{ij}(\vec{k};t,s) = \left\langle \varphi_i(\vec{k},t)\, \widetilde{\varphi}_j(-\vec{k},s) \right\rangle = \theta(t-s) \left(\mathrm{e}^{-\left(k^2\mathbb{1} - C^{(1)}\right)(t-s)}\right)_{ij}, \tag{3.117}$$

where the exponential in the r.h.s. has to be considered in a matrix sense. We wish to emphasize the fact that at equal times this function displays the same "troublesome" factor $\theta(0)$ as above.

We now group together all we want to treat as an interaction and define

$$V[\varphi,\widetilde{\varphi}] = \int \mathrm{d}\tau \sum_i \left[\widetilde{\varphi}_i \mathscr{F}_i^{(2)}[\varphi] - \theta(0)\mathscr{F}_i'[\varphi]\right], \tag{3.118}$$

where we introduced the notation $\mathscr{F}^{(2)} = \mathscr{F} - \left(D\nabla^2 + C^{(1)}\right)\varphi$; accordingly, the m-th perturbative correction to the expectation of a generic observable $\mathscr{O}[\varphi,\widetilde{\varphi}]$ (including response functions) will be

$$\frac{1}{m!}\left\langle (V[\varphi,\widetilde{\varphi}])^m \mathscr{O}[\varphi,\widetilde{\varphi}] \right\rangle_0, \tag{3.119}$$

where $\langle\cdot\rangle_0$ denotes the average calculated with just the quadratic part (3.115) of the action. For reasons that will become clear while proceeding with the discussion, we rewrite it as

$$\int \mathrm{d}\tau_1 \left\langle \left(\sum_i \left[\widetilde{\varphi}_i(\tau_1) \mathscr{F}_i^{(2)}[\varphi(\tau_1)] - \theta(0)\mathscr{F}_i'[\varphi(\tau_1)]\right] \right) \mathscr{O}'[\varphi,\widetilde{\varphi}] \right\rangle_0, \tag{3.120}$$

having reabsorbed $m-1$ powers of V into $\mathscr{O}'$. Now, we decompose every field into average and fluctuations

$$\varphi = \langle\varphi\rangle_0 + \delta\varphi \qquad \widetilde{\varphi} = \langle\widetilde{\varphi}\rangle_0 + \delta\widetilde{\varphi} = \delta\widetilde{\varphi}, \tag{3.121}$$

recalling that the average of the response field is always 0 (see Eq. (3.113)). Every average can be extracted from the expectation, while on the fluctuations one can use the standard Wick's contractions. Consider now the response field $\widetilde{\varphi}(\tau_1)$ appearing in Eq. (3.120). By the simple argument given above, this needs to be contracted with a field $\delta\varphi$ lying either within $\mathscr{F}^{(2)}[\varphi(\tau_1)]$ or $\mathscr{O}'[\varphi,\widetilde{\varphi}]$. We shall focus on the first case; this contraction will extract a field φ from every monomial starting with the second order in the expansion (3.114), thus acting like a derivative. This produces

$$\begin{aligned}
&\left\langle \widetilde{\varphi}_i(\tau_1)\,\mathscr{F}_i^{(2)}[\varphi(\tau_1)]\,\mathscr{O}'[\varphi,\widetilde{\varphi}]\right\rangle_0 = \\
&= \left\langle \widetilde{\varphi}_i(\tau_1)\varphi_j(\tau_1)\right\rangle_0 \left\langle \frac{\delta\mathscr{F}_i^{(2)}}{\delta\varphi_j}(\tau_1)\,\mathscr{O}'[\varphi,\widetilde{\varphi}]\right\rangle_0 + \left(\text{ contractions with }\mathscr{O}'\right) = \\
&= \left\langle \frac{\delta\mathscr{F}_i^{(2)}}{\delta\varphi_j}(\tau_1)\,\mathscr{O}'[\varphi,\widetilde{\varphi}]\right\rangle_0 R_{ji}(\tau_1,\tau_1) + \left(\text{ contractions with }\mathscr{O}'\right).
\end{aligned} \tag{3.122}$$

On the one hand, since τ_1 is an integration variable — see Eq. (3.120) — we can consider all the contractions with $\mathscr{O}'$ (which does not depend on it) as being performed at different times. On the other hand, according to Eq. (3.117), we find $R_{ij}(\tau_1,\tau_1) = \theta(0)\delta_{ij}$, which yields

$$\left\langle \widetilde{\varphi}_i(\tau_1)\,\mathscr{F}_i^{(2)}[\varphi(\tau_1)]\,\mathscr{O}'[\varphi,\widetilde{\varphi}]\right\rangle_0 = \theta(0)\left\langle \mathscr{F}_i'(\tau_1)\,\mathscr{O}'[\varphi,\widetilde{\varphi}]\right\rangle_0 + \left(\text{ contractions with }\mathscr{O}'\right). \tag{3.123}$$

The first term in Eq. (3.123) exactly cancels the second one in Eq. (3.120), thereby showing that indeed the observables are not affected by the value taken by $\theta(0)$ at any order in the perturbative expansion. The simplest choice would therefore be $\theta(0) = 0$, which renders the action

$$S[\varphi,\widetilde{\varphi}] = \int \mathrm{d}t\,\left\{\widetilde{\varphi}_i\left(\partial_t\varphi_i - \mathscr{F}_i[\varphi]\right) - \widetilde{\varphi}_i\,\Omega_{ij}\widetilde{\varphi}_j\right\} \tag{3.124}$$

which we have employed for our calculations.

Appendix 3.C One-loop calculations

In this Appendix we report the details of the calculations of the one-loop corrections to the two-point correlation and response functions

$$\begin{cases} C_{ij}(\vec{k};x,t;y,s) = \left\langle \varphi_i(\vec{k};x,t)\varphi_j(-\vec{k};y,s)\right\rangle, \\ R_{ij}(\vec{k};x,t;y,s) = \left\langle \varphi_i(\vec{k};x,t)\widetilde{\varphi}_j(-\vec{k};y,s)\right\rangle, \end{cases} \tag{3.125}$$

in our system, defined in Sec. 3.2. Since the problem is translationally invariant in all spatial directions parallel to the surface $x_\perp = 0$, we shall mostly adopt the same mixed $(\vec{k};x_\perp,t)$ representation that has been introduced previously in Sec. 3.1.1 (see, e.g., Eq. (3.29)). We start by determining

these functions for the non-interacting theory (i.e., for $g = 0$); with this purpose in mind, we note that Dirichlet and Neumann boundary conditions — corresponding to the ordinary and special transitions, respectively — can be obtained by applying the method of image charges to the respective functions in the bulk and at equilibrium [91]. In particular, we can obtain the response function by specialising Eq. (3.117) to the present case — meaning $\Omega = \mathbb{1}$, $D = 1$ and $C^{(1)} = -r = 0$ — which yields

$$R^{(0)}_{(bulk,eq),ij}(\vec{p};\Delta t) = \theta(\Delta t)\,\delta_{ij}\,\mathrm{e}^{-k^2\Delta t} \equiv \delta_{ij}\,R^{(0)}_{(bulk,eq)}(\vec{p};\Delta t)\,, \tag{3.126}$$

where $\Delta t = t - s$ and $\vec{p} = (\vec{k}, k_\perp)$ and we have made use of the fact that with our isotropic prescription among all $O(n)$ components, the latter are all equivalent and one can just study a specific one chosen as a representative. Since this is an equilibrium function, the correlation can be calculated via the fluctuation-dissipation relation (3.56), which yields

$$C^{(0)}_{(bulk,eq),ij}(\vec{p};\Delta t) = \int_{|\Delta t|}^{\infty} \mathrm{d}u\, R^{(0)}_{(bulk,eq),ij}(\vec{p},u) \equiv \delta_{ij} C^{(0)}_{(bulk,eq)}(\vec{p};\Delta t)\,. \tag{3.127}$$

Transforming $k_\perp \to x - y$ one gets

$$\begin{cases} R^{(0)}_{(bulk,eq)}\left(\vec{k}; x-y, t-s\right) = \theta(t-s)\left[4\pi(t-s)\right]^{-\frac{1}{2}}\mathrm{e}^{-k^2(t-s)-\frac{(x-y)^2}{4(t-s)}}, \\ C^{(0)}_{(bulk,eq)}\left(\vec{k}; x-y, t-s\right) = \int_{|t-s|}^{+\infty} du\, R^{(0)}_{(bulk,eq)}\left(x-y, u; \vec{k}\right). \end{cases} \tag{3.128}$$

Since the response function is only affected by the spatial surface, because no initial condition is actually cast on $\widetilde{\varphi}$, one finds

$$\begin{aligned} R^{(0)}\left(\vec{k}; x, t; y, s\right) &= R^{(0)}_{(bulk,eq)}\left(\vec{k}; x-y, t-s\right) \pm R^{(0)}_{(bulk,eq)}\left(\vec{k}; x+y, t-s\right) = \\ &= \frac{\theta(t-s)}{\sqrt{\pi(t-s)}}\mathrm{e}^{-k^2(t-s)-\frac{x^2+y^2}{4(t-s)}} f_\pm\left(\frac{xy}{2(t-s)}\right), \end{aligned} \tag{3.129}$$

where the upper and lower signs refer to the special and ordinary phase transitions, respectively, and $2f_\pm(\alpha) = \mathrm{e}^{\alpha} \pm \mathrm{e}^{-\alpha}$. For the correlation, instead, one has to take into account also the Dirichlet condition (3.50) at $t = 0$, which implies

$$\begin{aligned} &C^{(0)}(\vec{k}; x, t; y, s) = C^{(0)}_{(bulk,eq)}(\vec{k}; x-y, t-s) - C^{(0)}_{(bulk,eq)}(\vec{k}; x-y, t+s) + \\ &\pm C^{(0)}_{(bulk,eq)}(\vec{k}; x+y, t-s) \mp C^{(0)}_{(bulk,eq)}(\vec{k}; x+y, t+s) = \int_{|t-s|}^{t+s} \mathrm{d}u\ (\pi u)^{-\frac{1}{2}}\,\mathrm{e}^{-k^2 u - \frac{x^2+y^2}{4u}} f_\pm\left(\frac{xy}{2u}\right). \end{aligned} \tag{3.130}$$

The structure reported above for the two-point functions had been previously found in a few works focusing on the same setting and used to calculate the corrections due to the quartic term $\propto g\widetilde{\varphi}\varphi^3$ to the long-time behaviour of the correlation function [83], the scaling behaviour of the magnetisation [79] and the fluctuation-dissipation ratio within the Gaussian approximation $g = 0$ [20]. However, the previous attempts to perturbatively include the interaction relied on the expected absence of

novel effects due to the edge in order to introduce scaling ansatzes; therefore, to our knowledge, no direct calculation of the corrections has been attempted before the one reported below.

The first-order corrections to the functions in Eq. (3.125) are

$$\begin{aligned} C_{ij}^{(1)}(\vec{k};x,t;y,s) &= -\frac{g}{6}\int_0^\infty \mathrm{d}z\,\mathrm{d}\tau \left\langle \varphi_i(\vec{k};x,t)\,\varphi_j(-\vec{k};y,s)\,\left[\varphi^2\widetilde{\varphi}\cdot\varphi\right](z,\tau)\right\rangle_{g=0}, \\ R_{ij}^{(1)}(\vec{k};x,t;y,s) &= -\frac{g}{6}\int_0^\infty \mathrm{d}z\,\mathrm{d}\tau \left\langle \varphi_i(\vec{k};x,t)\,\widetilde{\varphi}_j(-\vec{k};y,s)\,\left[\varphi^2\widetilde{\varphi}\cdot\varphi\right](z,\tau)\right\rangle_{g=0}, \end{aligned} \tag{3.131}$$

where

$$\begin{aligned} \left[\varphi^2\widetilde{\varphi}\cdot\varphi\right](z,\tau) = \int \frac{\mathrm{d}^{d-1}q_1}{(2\pi)^{d-1}}\frac{\mathrm{d}^{d-1}q_2}{(2\pi)^{d-1}}\frac{\mathrm{d}^{d-1}q_3}{(2\pi)^{d-1}}\,\varphi_l(\vec{q}_1;z,\tau)\,\varphi_l(\vec{q}_2;z,\tau)\times \\ \times\,\widetilde{\varphi}_m(\vec{q}_3;z,\tau)\,\varphi_m(-\vec{q}_1-\vec{q}_2-\vec{q}_3;z,\tau) \end{aligned} \tag{3.132}$$

represents a short-hand for the usual momentum convolution of the fields. The only connected contributions coming from Eqs. (3.131) are those arising by contracting each of the external fields with one of those inside the square brackets. Note also that our convention $\theta(0)=0$, which implies $R^{(0)}(\ldots;\tau,\tau)=0$, forces us to contract either of the external legs with the response field coming from the interaction. The corresponding Feynman graphs are reported in Fig. 3.7, where undirected

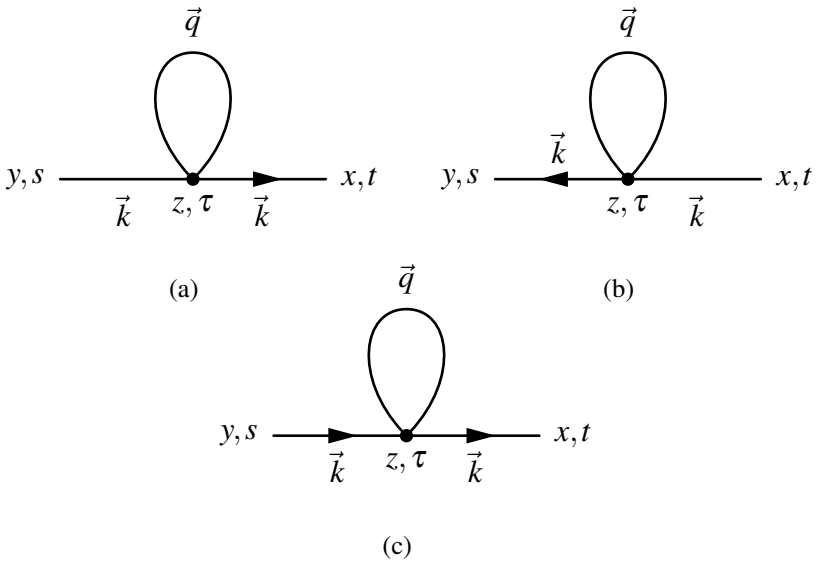

Figure 3.7: One-loop corrections to the two-point functions. (a) and (b) contribute to the correlation function $C^{(1)}(\vec{k};x,t;y,s)$, whereas (c) to the response function $R^{(1)}(\vec{k};x,t;y,s)$. Undirected lines correspond to $C^{(0)}$, whereas those accompanied by arrows stand for $R^{(0)}$; the arrows always point towards later times according to the causal structure of the response function.

lines represent $C^{(0)}$ propagators, while directed ones denote $R^{(0)}$ functions with the arrow pointing from earlier to later times. Diagrams 3.7(a) and 3.7(b) contribute to the correlation, whereas 3.7(c) to the response function. In order to determine the combinatorial factor, we shall for the moment

omit the coordinates and analyse the Wick contractions in the light of the rules determined above, which produce

$$\left\langle \varphi_i \varphi_j \left[\varphi^2 \widetilde{\varphi} \cdot \varphi \right] \right\rangle_{g=0} = \langle \varphi_i \widetilde{\varphi}_l \rangle_{g=0} \left\langle \varphi_j \varphi_m \right\rangle_{g=0} \left\langle \frac{\delta}{\delta \widetilde{\varphi}_l} \frac{\delta}{\delta \varphi_m} \varphi^2 \widetilde{\varphi} \cdot \varphi \right\rangle_{g=0} + \\ + \langle \varphi_i \varphi_l \rangle_{g=0} \left\langle \varphi_j \widetilde{\varphi}_m \right\rangle_{g=0} \left\langle \frac{\delta}{\delta \varphi_l} \frac{\delta}{\delta \widetilde{\varphi}_m} \varphi^2 \widetilde{\varphi} \cdot \varphi \right\rangle_{g=0} \tag{3.133}$$

for the correlation function and

$$\left\langle \varphi_i \widetilde{\varphi}_j \left[\varphi^2 \widetilde{\varphi} \cdot \varphi \right] \right\rangle_{g=0} = \langle \varphi_i \widetilde{\varphi}_l \rangle_{g=0} \left\langle \widetilde{\varphi}_j \varphi_m \right\rangle_{g=0} \left\langle \frac{\delta}{\delta \widetilde{\varphi}_l} \frac{\delta}{\delta \varphi_m} \varphi^2 \widetilde{\varphi} \cdot \varphi \right\rangle_{g=0} \tag{3.134}$$

for the response function. The functional derivatives in the expressions above all yield the same expression

$$\left\langle \frac{\delta}{\delta \widetilde{\varphi}_l} \frac{\delta}{\delta \varphi_m} \varphi^2 \widetilde{\varphi} \cdot \varphi \right\rangle_{g=0} = \left\langle \delta_{lm} \varphi^2 + 2 \varphi_m \varphi_l \right\rangle_{g=0} = \sum_i \delta_{lm} C^{(0)}_{ii} + 2 C^{(0)}_{lm} = (n+2)\, \delta_{lm} C^{(0)} \tag{3.135}$$

which ensures, as expected, that the matrix structure remains diagonal and proportional to the identity also at the first perturbative order. Note that the same conclusion can in principle be reached by accounting for the symmetries of the Feynman graphs. We can thus write

$$C^{(1)}(\vec{k}; x,t; y,s) = -\frac{n+2}{6} g \int_0^\infty \mathrm{d}z\, \mathrm{d}\tau \left[R^{(0)}(\vec{k}; x,t; z,\tau)\, C^{(0)}(\vec{k}; z,\tau; y,s) + \right. \\ \left. + C^{(0)}(\vec{k}; x,t; z,\tau)\, R^{(0)}(\vec{k}; y,s; z,\tau) \right] B(z,\tau) \tag{3.136a}$$

$$R^{(1)}(\vec{k}; x,t; y,s) = -\frac{n+2}{6} g \int_0^\infty \mathrm{d}z\, \mathrm{d}\tau\, R^{(0)}(\vec{k}; x,t; z,\tau)\, R^{(0)}(\vec{k}; z,\tau; y,s)\, B(z,\tau), \tag{3.136b}$$

where $B(z,\tau)$ represents the "bubble" in the diagrams of Fig. 3.7 and corresponds to

$$B(z,\tau) = \int \frac{\mathrm{d}^{d-1} q}{(2\pi)^{d-1}} C^{(0)}(\vec{q}; z,\tau; z,\tau). \tag{3.137}$$

The different contributions coming from the four terms in Eq. (3.130) shall be separately calculated in order to distinguish the effects of the various boundaries; in the following they will be denoted by indices 0, 1, 2, 3 respectively; accordingly, we define $B(z,\tau) = \sum_{i=0}^{3} \varepsilon_i \mathscr{B}(Z_i, T_i)$, where

$$\mathscr{B}(Z_i, T_i) = \int \frac{\mathrm{d}^{d-1} q}{(2\pi)^{d-1}} C^{(0)}_{(bulk,eq)}(\vec{q}; Z_i, T_i) = \int \frac{\mathrm{d}^{d-1} q}{(2\pi)^{d-1}} \int_{T_i}^\infty \frac{\mathrm{d}u}{\sqrt{4\pi u}} \mathrm{e}^{-q^2 u - \frac{Z_i^2}{4u}} \tag{3.138}$$

and

$$\begin{aligned} &Z_0 = 0, \quad Z_1 = 0, \quad Z_2 = 2z, \quad Z_3 = 2z, \\ &T_0 = 0, \quad T_1 = 2\tau, \quad T_2 = 0, \quad T_3 = 2\tau, \\ &\varepsilon_0 = 1, \quad \varepsilon_1 = -1, \quad \varepsilon_2 = \pm 1, \quad \varepsilon_3 = \mp 1. \end{aligned} \tag{3.139}$$

Again, the upper and lower signs distinguish the special from the ordinary transition. Using dimensional regularisation we explicitly find

$$\mathscr{B}_0 \equiv \mathscr{B}(Z_0, T_0) = 0, \tag{3.140a}$$

$$\mathscr{B}_1 \equiv \mathscr{B}(Z_1, T_1) = (4\pi)^{-\frac{d}{2}} \frac{(2\tau)^{1-\frac{d}{2}}}{\frac{d}{2}-1}, \tag{3.140b}$$

$$\mathscr{B}_2 \equiv \mathscr{B}(Z_2, T_2) = (4\pi)^{-\frac{d}{2}} z^{2-d} \Gamma\left(\frac{d}{2}-1\right), \tag{3.140c}$$

$$\mathscr{B}_3 \equiv \mathscr{B}(Z_3, T_3) = (4\pi)^{-\frac{d}{2}} z^{2-d} \gamma\left(\frac{d}{2}-1, \frac{z^2}{2\tau}\right), \tag{3.140d}$$

where $\gamma(\alpha, w) = \int_0^w \mathrm{d}z\, z^{\alpha-1} \mathrm{e}^{-z}$ is the incomplete gamma function. Correspondingly, we divide the first-order corrections into three parts each resulting from the various $\mathscr{B}$'s:

$$C^{(1)} = -\frac{n+2}{6} g \sum_{i=1}^{3} \varepsilon_i \mathscr{C}_i \quad \text{and} \quad R^{(1)} = -\frac{n+2}{6} g \sum_{i=1}^{3} \varepsilon_i \mathscr{R}_i, \tag{3.141}$$

the 0-th contribution associated with $\mathscr{B}_0$ being neglected due to the fact that, in general, in dimensional regularisation all the divergences which are not logarithmic in $d = 4$, and in particular the mass renormalisation term, vanish. In the following, we will analyse the asymptotic behaviour of the remaining terms in the proximity of the boundaries $y = 0$ and $s = 0$, in an attempt to recover the new universal exponents from the corresponding algebraic laws, as we discussed in Sec. 3.1.1. Note that the latter will appear here as logarithmic divergences, as can be seen by expanding in powers of g the exponent in

$$x^{\alpha} = x^{\alpha_0 + g\alpha_1 + \dots} = x^{\alpha_0}(1 + g\alpha_1 \ln x + \dots) \tag{3.142}$$

We shall restrict in the following to the response function, the correlation being similar, but more involved due to the presence of an additional integral (see its definition (3.130)). Furthermore, we will set for simplicity $\vec{k} = 0$ and $t > s$, so that we can omit the step function. The first term is particularly simple: exploiting the relation

$$\int_0^{\infty} \mathrm{d}z\, R^{(0)}(x,t;z,\tau) R^{(0)}(z,\tau;y,s) = R^{(0)}(x,t;y,s) \quad \text{valid} \quad \forall\, s < \tau < t \tag{3.143}$$

we find

$$\begin{aligned} &\frac{(4\pi)^{-\frac{d}{2}}}{\frac{d}{2}-1} \int_0^{\infty} \mathrm{d}z \int_s^t \mathrm{d}\tau\, (2\tau)^{1-\frac{d}{2}} R^{(0)}(x,t;z,\tau) R^{(0)}(z,\tau;y,s) = \\ &= \frac{(4\pi)^{-\frac{d}{2}}}{\frac{d}{2}-1} R^{(0)}(x,t;y,s) \int_s^t \mathrm{d}\tau\, (2\tau)^{1-\frac{d}{2}} = \frac{2(8\pi)^{-\frac{d}{2}}}{\frac{d}{2}-1} \left[\frac{t^{2-\frac{d}{2}} - s^{2-\frac{d}{2}}}{2-\frac{d}{2}}\right] R^{(0)}(x,t;y,s) \end{aligned} \tag{3.144}$$

which, for $d = 4$, gives

$$\mathscr{R}_1^{(1)}(x,t;y,s) = \frac{1}{2(4\pi)^2} \ln\left(\frac{t}{s}\right) R^{(0)}(x,t;y,s). \tag{3.145}$$

This function is singular only when $s \to 0$; thus, it identifies at least part of the temporal divergence, whilst it does not include any of the others. In particular, as generally stated in Eq. (3.142), this comes from a power law of the form

$$R^{(1)}(\ldots s) \sim s^{-a} R^{(0)}(\ldots s) = s^{-a_0}(1 - g a_1 \ln s) R^{(0)}(\ldots s) \qquad (s \to 0). \tag{3.146}$$

Substituting Eq. (3.145) in the definition (3.141) yields $a_0 = 0$ and

$$a_1 g = \frac{n+2}{12} \frac{1}{(4\pi)^2} g. \tag{3.147}$$

At the Wilson-Fisher fixed point $g = g^* = \frac{3}{n+8}(4\pi)^2 \varepsilon + O\left(\varepsilon^2\right)$ [11, 59, 60] the latter becomes

$$\widehat{a}_1 \varepsilon = \frac{n+2}{n+8} \frac{\varepsilon}{4} + O\left(\varepsilon^2\right), \tag{3.148}$$

which corresponds with the first-order of the expansion of the initial-slip exponent θ reported in Eq. (3.55). Thereby, this term completely encodes the divergence proper of the temporal boundary. Note that, alternatively, one could expand Eq. (3.144) in powers of $\varepsilon = 4 - d$; all terms would then be regular in the limit $\varepsilon \to 0$ except the one inside the square brackets, i.e.,

$$\frac{t^{\frac{\varepsilon}{2}} - s^{\frac{\varepsilon}{2}}}{\frac{\varepsilon}{2}}, \tag{3.149}$$

which would provide a pole $\propto \varepsilon^{-1}$ in the case $s = 0$, being regular otherwise. One could then extract the same result as in Eq. (3.148) by studying the coefficient of such a dimensional divergence. In particular, the latter can be reabsorbed by standard means, introducing a renormalisation factor Z_0 which multiplies the boundary fields φ_0 and $\widetilde{\varphi}_0$.

The second term $\mathscr{R}_2^{(1)}$ is slightly more complicated; its expression is

$$\begin{aligned}(4\pi)^{\frac{d}{2}} \mathscr{R}_2^{(1)} = \int_0^\infty \mathrm{d}z \int_s^t \mathrm{d}\tau \, \frac{z^{2-d}\,\Gamma\left(\frac{d}{2}-1\right)}{\sqrt{\pi^2 (t-\tau)(\tau-s)}} \times \\ \times \mathrm{e}^{-\frac{x^2}{4(t-\tau)} - \frac{y^2}{4(\tau-s)} - \frac{z^2}{4}\left(\frac{t-s}{(t-\tau)(\tau-s)}\right)} f_\pm\left(\frac{xz}{2(t-\tau)}\right) f_\pm\left(\frac{yz}{2(\tau-s)}\right).\end{aligned} \tag{3.150}$$

Now we employ the changes of variables

$$z = 2l\sqrt{\frac{(t-\tau)(\tau-s)}{t-s}} \quad \text{and} \quad \tau = (t-s)\vartheta + s \tag{3.151}$$

to rewrite it as

$$(4\pi)^{\frac{d}{2}}\mathscr{R}_2^{(1)} = A_d(\Delta t)\int_0^\infty \mathrm{d}l \int_0^1 \mathrm{d}\vartheta \mathrm{e}^{-\frac{1}{4}\left(\frac{\tilde{x}^2}{1-\vartheta}+\frac{\tilde{y}^2}{\vartheta}\right)}\left[\vartheta(1-\vartheta)\right]^{1-\frac{d}{2}} l^{2-d}\mathrm{e}^{-l^2}\times \\ \times f_\pm\left(\tilde{x}l\sqrt{\frac{\vartheta}{1-\vartheta}}\right) f_\pm\left(\tilde{y}l\sqrt{\frac{1-\vartheta}{\vartheta}}\right), \tag{3.152}$$

with

$$A_d(\Delta t) = \frac{2}{\pi}\Gamma\left(\frac{d}{2}-1\right)4^{1-\frac{d}{2}}(\Delta t)^{\frac{3-d}{2}}, \qquad \tilde{x} = \frac{x}{\sqrt{\Delta t}}, \qquad \tilde{y} = \frac{y}{\sqrt{\Delta t}}, \qquad \Delta t = t-s. \tag{3.153}$$

Recalling that $d = 4-\varepsilon$ and that dimensional regularisation implies [92]

$$\int_0^\infty \mathrm{d}l\, l^{-2+\varepsilon}F(l) = \int_0^1 \mathrm{d}l\, l^{-2+\varepsilon}\left(F(l)-F(0)-lF'(0)\right) + \int_1^\infty \mathrm{d}l\, l^{-2+\varepsilon}\left(F(l)-F(0)\right) + \frac{F'(0)}{\varepsilon} \tag{3.154}$$

on any function F which decreases sufficiently fast for $l\to\infty$, we find that the integral over l in Eq. (3.152) has actually to be interpreted as

$$\mathscr{I} \equiv \int_0^\infty \mathrm{d}l\, l^{-2+\varepsilon}\left(\mathrm{e}^{-l^2}f_\pm(Al)f_\pm(Bl) - f_\pm(0)^2\right), \tag{3.155}$$

with $A = \tilde{x}\sqrt{\frac{\vartheta}{1-\vartheta}}$ and $B = \tilde{y}\sqrt{\frac{1-\vartheta}{\vartheta}}$. Due to the fact that there are no explicitly divergent terms in ε, we can conveniently fix $d=4$ in the following. We use the identity

$$f_\pm(Al)f_\pm(Bl) = \frac{1}{2}\left[\cosh\left((A+B)l\right) \pm \cosh\left((A-B)l\right)\right], \tag{3.156}$$

noting that $f_\pm(0)^2$ can be rewritten as $(1\pm1)/2$, to recast Eq. (3.155) in the form $\mathscr{I} = H(A+B)\pm H(A-B)$, where

$$H(w) = \frac{1}{2}\int_0^\infty \frac{\mathrm{d}l}{l^2}\left[\left(\mathrm{e}^{-l^2}-1\right)+\mathrm{e}^{-l^2}\left(\cosh(wl)-1\right)\right]. \tag{3.157}$$

We now expand the hyperbolic cosine $f_+ \equiv \cosh$ in the r.h.s. as a power series to get

$$H(w) = \frac{1}{2}\left\{\int_0^\infty \frac{\mathrm{d}l}{l^2}\left(\mathrm{e}^{-l^2}-1\right) + \sum_{m=1}^\infty \frac{w^{2m}}{(2m)!}\int_0^\infty \mathrm{d}l\, l^{2m-2}\mathrm{e}^{-l^2}\right\} = \\ = \frac{1}{4}\left\{\Gamma\left(-\frac{1}{2}\right) + \sum_{m=1}^\infty \frac{w^{2m}}{(2m)!}\Gamma\left(m-\frac{1}{2}\right)\right\} = \frac{1}{4}\sum_{m=0}^\infty \frac{w^{2m}}{(2m)!}\Gamma\left(m-\frac{1}{2}\right), \tag{3.158}$$

where we assume (for now) that we can safely exchange the series with the integral. Thanks to this, we can re-express Eq. (3.152) as

$$(4\pi)^2\,\mathscr{R}_2^{(1)} = \frac{A_4(\Delta t)}{4}\mathrm{e}^{-\frac{1}{4}\left(\tilde{x}^2+\tilde{y}^2\right)}\sum_{m=0}^{\infty}\frac{\Gamma\left(m-\frac{1}{2}\right)}{(2m)!}\int_0^1\frac{\mathrm{d}\vartheta}{\vartheta(1-\vartheta)}\mathrm{e}^{-\frac{\tilde{x}}{4}\frac{\vartheta}{1-\vartheta}-\frac{\tilde{y}}{4}\frac{1-\vartheta}{\vartheta}}\times \\ \times\left[\left(\tilde{x}\sqrt{\frac{\vartheta}{1-\vartheta}}+\tilde{y}\sqrt{\frac{1-\vartheta}{\vartheta}}\right)^{2m}\pm\left(\tilde{x}\sqrt{\frac{\vartheta}{1-\vartheta}}-\tilde{y}\sqrt{\frac{1-\vartheta}{\vartheta}}\right)^{2m}\right]. \tag{3.159}$$

By performing the additional change of variables

$$\sqrt{\frac{1-\vartheta}{\vartheta}}=\sqrt{\tilde{x}\tilde{y}}\,\beta \quad \text{with} \quad \frac{\mathrm{d}\vartheta}{\vartheta(1-\vartheta)}=-2\frac{\mathrm{d}\beta}{\beta}, \tag{3.160}$$

we arrive at

$$(4\pi)^2\,\mathscr{R}_2^{(1)} = \frac{A_4(\Delta t)}{2}\mathrm{e}^{-\frac{1}{4}\left(\tilde{x}^2+\tilde{y}^2\right)}\sum_{m=0}^{\infty}\frac{\Gamma\left(m-\frac{1}{2}\right)}{(2m)!}(\tilde{x}\tilde{y})^m\int_0^{\infty}\frac{\mathrm{d}\beta}{\beta}\mathrm{e}^{-\frac{\tilde{x}\tilde{y}}{4}\left(\beta^2+\frac{1}{\beta^2}\right)}\times \\ \times\left[\left(\beta+\frac{1}{\beta}\right)^{2m}\pm\left(\beta-\frac{1}{\beta}\right)^{2m}\right]. \tag{3.161}$$

In order to verify that the series in the expression above is convergent for $\tilde{x}>0$, $\tilde{y}>0$, we introduce the shorthand notation $\omega=\tilde{x}\tilde{y}$ and define

$$S_{\pm}(\omega)=\sum_{m=1}^{\infty}\frac{\Gamma\left(m-\frac{1}{2}\right)}{(2m)!}\omega^m\int_0^{\infty}\frac{\mathrm{d}\beta}{\beta}\,\mathrm{e}^{-\frac{\omega}{4}\left(\beta^2+\frac{1}{\beta^2}\right)}\left(\beta\pm\frac{1}{\beta}\right)^{2m}, \tag{3.162}$$

postponing the discussion of the $m=0$ terms. Note now that all addends in these series are positive; therefore, since for every $\beta>0$ we have $(\beta-1/\beta)\leq(\beta+1/\beta)$, it is sufficient to study S_+ for, if the latter converges, S_- must converge too. Exploiting the symmetry of the integrand under the transformation $\beta\to 1/\beta$ we can rewrite it as

$$S_+(\omega)=2\sum_{m=1}^{\infty}\frac{\Gamma\left(m-\frac{1}{2}\right)}{\Gamma(2m+1)}\omega^m\mathrm{e}^{\frac{\omega}{2}}\int_1^{\infty}\frac{\mathrm{d}\beta}{\beta}\mathrm{e}^{-\frac{\omega}{4}\left(\beta+\frac{1}{\beta}\right)^2}\left(\beta+\frac{1}{\beta}\right)^{2m}, \tag{3.163}$$

where we have also slightly manipulated the integrand to extract a factor $\mathrm{e}^{\omega/2}$. Now we perform the change of variable $(\beta+1/\beta)=\alpha$ to get

$$S_+(\omega)=2\sum_{m=1}^{\infty}\frac{\Gamma\left(m-\frac{1}{2}\right)}{\Gamma(2m+1)}\omega^m\mathrm{e}^{\frac{\omega}{2}}\int_2^{\infty}\frac{\mathrm{d}\alpha}{\sqrt{\alpha^2-4}}\mathrm{e}^{-\frac{\omega}{4}\alpha^2}\alpha^{2m}. \tag{3.164}$$

We separate the integration domain into two parts, separated by $\alpha=\sqrt{5}$. When $\alpha\leq\sqrt{5}$ we use the fact that $\mathrm{e}^{-\alpha^2\omega/4}\leq 1$, $\alpha^{2m}\leq 5^m$ and when $\alpha>\sqrt{5}$ we use the property $\sqrt{\alpha^2-4}>\alpha/3$ to

provide an upper bound to Eq. (3.164)

$$\int_2^\infty \frac{\mathrm{d}\alpha}{\sqrt{\alpha^2-4}}\mathrm{e}^{-\frac{\omega}{4}\alpha^2}\alpha^{2m} \leq 5^m \int_2^{\sqrt{5}} \frac{\mathrm{d}\alpha}{\sqrt{\alpha^2-4}} + 3\int_{\sqrt{5}}^\infty \mathrm{d}\alpha\, \mathrm{e}^{-\frac{\omega}{4}\alpha^2}\alpha^{2m-1} \leq$$
$$5^m \int_2^{\sqrt{5}} \frac{\mathrm{d}\alpha}{\sqrt{\alpha^2-4}} + 3\int_0^\infty \mathrm{d}\alpha \mathrm{e}^{-\frac{\omega}{4}\alpha^2}\alpha^{2m-1} = 5^m \ln\left(\frac{\sqrt{5}+1}{2}\right) + \frac{3}{2}\left(\frac{4}{\omega}\right)^m \Gamma(m)\,. \tag{3.165}$$

Now, using the duplication formula

$$\frac{\Gamma\left(m+\frac{1}{2}\right)}{\Gamma(2m+1)} = \sqrt{\pi}\frac{4^{-m}}{\Gamma(m+1)} = \sqrt{\pi}\frac{4^{-m}}{m!} \tag{3.166}$$

and recalling, for the first term, that $\Gamma(m-1/2) \leq 2\Gamma(m+1/2)\ \forall m \geq 1$, we get

$$S_+(\omega) \leq 2\sqrt{\pi}\mathrm{e}^{\frac{\omega}{2}} \sum_{m=1}^\infty \left[\frac{2}{m!}\left(\frac{5\omega}{4}\right)^m \ln\left(\frac{\sqrt{5}+1}{2}\right) + \frac{3}{2}\frac{1}{m\left(m-\frac{1}{2}\right)}\right] =$$
$$4\sqrt{\pi}\mathrm{e}^{\frac{\omega}{2}}\left[\ln\left(\frac{\sqrt{5}+1}{2}\right)\left(\mathrm{e}^{\frac{5\omega}{4}}-1\right) + 3\ln 2\right]. \tag{3.167}$$

Consequently, S_+ converges for every $\omega \geq 0$ and so does S_-. This also ensures that exchanging the series with the integral above is a formally correct operation. The first term of the series is instead given by

$$\Gamma\left(-\frac{1}{2}\right)\int_0^\infty \frac{\mathrm{d}\beta}{\beta}\mathrm{e}^{-\frac{\omega}{4}\left(\beta^2+\frac{1}{\beta^2}\right)} = -2\sqrt{\pi}\int_0^\infty \mathrm{d}\lambda\, \mathrm{e}^{-\frac{\omega}{2}\cosh\lambda} = -2\sqrt{\pi}K_0\left(\frac{\omega}{2}\right), \tag{3.168}$$

where we have used the transformation $\beta = \mathrm{e}^{\lambda/2}$ and K_0 is one of the modified (or hyperbolic) Bessel functions of the second kind, whose asymptotic behaviour for small argument is $K_0(\omega/2) \sim -\ln\omega$. For the special transition — i.e., for Neumann boundary conditions — this implies that, in the limit $\omega \to 0$, Eq. (3.161) is dominated by the first term, which diverges logarithmically as

$$(4\pi)^2 \mathscr{R}_2^{(1)}\,|_{DIV} \sim 2\sqrt{\pi}A_4(\Delta t)\,\mathrm{e}^{-\frac{1}{4}\left(\tilde{x}^2+\tilde{y}^2\right)}\ln(\tilde{x}\tilde{y}) = \frac{2}{\sqrt{4\pi\Delta t}}\mathrm{e}^{-\frac{1}{4}\left(\tilde{x}^2+\tilde{y}^2\right)}\ln(\tilde{x}\tilde{y})\,. \tag{3.169}$$

Note that, as we are considering the limit $\omega \to 0$, i.e., either $x \to 0$ or $y \to 0$, we can safely multiply the expression above by any function which goes asymptotically to 1, such as $\cosh(\tilde{x}\tilde{y}/2)$; the advantage of doing so is that we recover, according to the definition (3.129) and to the notation introduced in (3.153),

$$\mathscr{R}_2^{(1)}\,|_{DIV} \sim \frac{1}{(4\pi)^2}\ln\left(\frac{xy}{\Delta t}\right)R^{(0)}(x,t;y,s)\,. \tag{3.170}$$

As we have done above, we trace back this behaviour to the emergence of a non-trivial power law

$$R^{(1)}(\ldots s) \sim \left(\frac{xy}{\Delta t}\right)^b R^{(0)}(\ldots) = \left(\frac{xy}{\Delta t}\right)^{b_0}\left[1+gb_1\ln\left(\frac{xy}{\Delta t}\right)\right]R^{(0)}(\ldots) \qquad (xy \to 0), \tag{3.171}$$

which implies $b_0 = 0$ and

$$b_1 g = -\frac{n+2}{6}\frac{g}{(4\pi)^2} \quad \text{while} \quad \hat{b}_1 \varepsilon = -\frac{n+2}{n+8}\frac{\varepsilon}{2} + O\left(\varepsilon^2\right). \tag{3.172}$$

By considering Eq. (3.33b) along with the bulk critical exponents [60]

$$\beta = \frac{1}{2} - \frac{3}{n+8}\frac{\varepsilon}{2} + \frac{1}{2}\frac{n+2}{(n+8)^3}(2n+1)\,\varepsilon^2 + O\left(\varepsilon^3\right), \tag{3.173a}$$

$$\nu = \frac{1}{2} + \frac{n+2}{4(n+8)}\varepsilon + \frac{(n+2)(n^2+23n+60)}{8(n+8)^3}\varepsilon^2 + O\left(\varepsilon^3\right), \tag{3.173b}$$

one can prove that $(\beta_{1,sp} - \beta)/\nu = \hat{b}_1 \varepsilon + O\left(\varepsilon^2\right)$; therefore, this term correctly and completely captures the surface divergence in the special case. For the ordinary transition, the two-point function obeys Dirichlet boundary conditions, which yields $b_0 = 1$; furthermore, the first (i.e., $m = 0$) term of the series in Eq. (3.161) identically vanishes. Therefore, one has to study the behaviour of the remaining ones for $\omega \to 0$. For this purpose, we define

$$I_m^{(\pm)}(\omega) = \int_0^\infty \frac{\mathrm{d}\beta}{\beta} \mathrm{e}^{-\frac{\omega}{4}\left(\beta^2 + \frac{1}{\beta^2}\right)} \left(\beta \pm \frac{1}{\beta}\right)^{2m}. \tag{3.174}$$

In terms of these quantities Eq. (3.161) becomes

$$(4\pi)^2 \mathscr{R}_2^{(1)} = \frac{A_4(\Delta t)}{2} \mathrm{e}^{-\frac{1}{4}\left(\tilde{x}^2 + \tilde{y}^2\right)} \sum_{m=1}^{\infty} \frac{\Gamma\left(m - \frac{1}{2}\right)}{(2m)!} \omega^m \left[I_m^{(+)}(\omega) - I_m^{(-)}(\omega)\right]. \tag{3.175}$$

Now, equation (3.174) can be rewritten as

$$\begin{aligned} I_m^{(\pm)}(\omega) &= \mathrm{e}^{\pm\frac{\omega}{2}} \int_0^\infty \frac{\mathrm{d}\beta}{\beta} \mathrm{e}^{-\frac{\omega}{4}\left(\beta \pm \frac{1}{\beta}\right)^2} \left(\beta \pm \frac{1}{\beta}\right)^{2m} = \\ &= \mathrm{e}^{\pm\frac{\omega}{2}} 4^m (-\partial_\omega)^m \int_0^\infty \frac{\mathrm{d}\beta}{\beta} \mathrm{e}^{-\frac{\omega}{4}\left(\beta \pm \frac{1}{\beta}\right)^2} = \mathrm{e}^{\pm\frac{\omega}{2}} 4^m (-\partial_\omega)^m \left[\mathrm{e}^{\mp\frac{\omega}{2}} I_0^{(\pm)}(\omega)\right], \end{aligned} \tag{3.176}$$

and from Eq. (3.168) we can extract $I_0^{(\pm)}(\omega) = K_0(\omega/2)$. Using the additional identity

$$-\partial_\omega \left(\mathrm{e}^{\mp\frac{\omega}{2}} f\right) = \mathrm{e}^{\mp\frac{\omega}{2}} \left(\pm\frac{1}{2} - \partial_\omega\right) f \tag{3.177}$$

valid for any test function f we find that

$$I_m^{(+)}(\omega) - I_m^{(-)}(\omega) = 4^m \left[\left(\frac{1}{2} - \partial_\omega\right)^m - \left(-\frac{1}{2} - \partial_\omega\right)^m\right] K_0\left(\frac{\omega}{2}\right). \tag{3.178}$$

Note that the highest-order derivative ∂_ω^m always cancels out. We now recall a few useful properties of these Bessel functions:

$$K_0\left(\frac{\omega}{2}\right) = -\ln\omega - \ln 4 - \gamma_E + O\left(\omega^2 \ln\omega\right) \qquad \text{for } (\omega \to 0), \tag{3.179a}$$

$$K_m\left(\frac{\omega}{2}\right) = \frac{1}{2}\left(\frac{4}{\omega}\right)^m \Gamma(m) + o\left(\omega^{-m}\right) \qquad \text{for } (\omega \to 0),\ (m > 0), \tag{3.179b}$$

$$-\partial_\omega K_0\left(\frac{\omega}{2}\right) = \frac{1}{2} K_1\left(\frac{\omega}{2}\right), \tag{3.179c}$$

$$-\partial_\omega K_m\left(\frac{\omega}{2}\right) = \frac{1}{4}\left[K_{m-1}\left(\frac{\omega}{2}\right) + K_{m+1}\left(\frac{\omega}{2}\right)\right] \qquad \text{for } (m > 0), \tag{3.179d}$$

$$\tag{3.179e}$$

Equations (3.179c) and (3.179d) imply that the j-th derivative of K_0 can be written as a sum of other Bessel functions with degree running from j back to 0 or 1, depending on the parity of j, i.e.,

$$(-\partial_\omega)^j K_0\left(\frac{\omega}{2}\right) = c_j K_j\left(\frac{\omega}{2}\right) + c_{j-2} K_{j-2}\left(\frac{\omega}{2}\right) + c_{j-4} K_{j-4}\left(\frac{\omega}{2}\right) + \dots \tag{3.180}$$

with suitable coefficients c_i. Among these terms, according to Eq. (3.179b), the leading behaviour for $\omega \to 0$ is given by $K_j \sim \omega^{-j}$. As we have mentioned above, the highest non-vanishing order in the derivatives of Eq. (3.178) is (at most) $m-1$, which means that

$$I_1^{(+)}(\omega) - I_1^{(-)}(\omega) = 4K_0\left(\frac{\omega}{2}\right) \sim -4\ln\omega \quad \text{while} \quad I_m^{(+)}(\omega) - I_m^{(-)}(\omega) \sim \omega^{1-m} \quad (m > 1). \tag{3.181}$$

As a consequence, all the terms of the series in Eq. (3.175) vanish as ω for $\omega \to 0$ except the first one which instead behaves as $\omega \ln\omega$. Hence, we can safely disregard all terms but the first, which yields

$$\mathscr{R}_2^{(1)}\,|_{DIV} \sim -\frac{1}{(4\pi)^2}\frac{1}{\sqrt{4\pi\Delta t}} \mathrm{e}^{-\frac{1}{4}\left(\tilde{x}^2+\tilde{y}^2\right)} \omega \ln\omega \tag{3.182}$$

Again, by noting that $\sinh(\omega/2) \sim \omega/2$ in proximity of the spatial surface, we can rewrite the expression above as

$$\mathscr{R}_2^{(1)}\,|_{DIV} \sim -\frac{1}{(4\pi)^2} \ln\omega\, R^{(0)}(x,t;y\to 0,s), \tag{3.183}$$

which coincides with Eq. (3.170) apart from the sign; on the other hand, this difference is re-absorbed in the change of sign of the prefactor ε_2 between the two transitions, as expressed in Eq. (3.139). Thus, also in this case we conclude that

$$b_1 g = -\frac{n+2}{6}\frac{g}{(4\pi)^2} \quad \text{and} \quad \hat{b}_1 \varepsilon = -\frac{n+2}{n+8}\frac{\varepsilon}{2} + O\left(\varepsilon^2\right), \tag{3.184}$$

which correctly reproduces the previously-known results for the ordinary transition at a spatial surface [60].

Finally, we consider the third term $\mathscr{R}_3^{(1)}$; its expression is

$$(4\pi)^{\frac{d}{2}}\mathscr{R}_3^{(1)} = \theta(t-s)\int_0^\infty \mathrm{d}z \int_s^t \mathrm{d}\tau \frac{z^{2-d}}{\sqrt{\pi^2(t-\tau)(\tau-s)}}\gamma\left(\frac{d}{2}-1,\frac{z^2}{2\tau}\right)\times \\ \times \mathrm{e}^{-\frac{x^2}{4(t-\tau)}-\frac{y^2}{4(\tau-s)}-\frac{z^2}{4}\left(\frac{t-s}{(t-\tau)(\tau-s)}\right)} f_\pm\left(\frac{xz}{2(t-\tau)}\right) f_\pm\left(\frac{yz}{2(\tau-s)}\right). \tag{3.185}$$

Using the change of variables (3.151) we arrive at

$$(4\pi)^{\frac{d}{2}}\mathscr{R}_3^{(1)} = \frac{A_d(\Delta t)}{\Gamma\left(\frac{d}{2}-1\right)}\int_0^\infty \mathrm{d}l \int_0^1 \mathrm{d}\vartheta\, \mathrm{e}^{-\frac{1}{4}\left(\frac{\tilde{x}^2}{1-\vartheta}+\frac{\tilde{y}^2}{\vartheta}\right)}\left[\vartheta(1-\vartheta)\right]^{1-\frac{d}{2}} l^{2-d}\mathrm{e}^{-l^2}\times \\ \times f_\pm\left(\tilde{x}l\sqrt{\frac{\vartheta}{1-\vartheta}}\right) f_\pm\left(\tilde{y}l\sqrt{\frac{1-\vartheta}{\vartheta}}\right)\gamma\left(\frac{d}{2}-1,\frac{2l^2\vartheta(1-\vartheta)}{\vartheta+\frac{s}{\Delta t}}\right), \tag{3.186}$$

Since the incomplete Gamma function vanishes as $\gamma(\alpha,w)\sim w^\alpha$ for vanishing argument $w\to 0$, it constitutes a sufficient regularisation to make the integral above convergent. We can thus immediately set $d=4$, noticing that $\gamma(1,w)=1-\mathrm{e}^{-w}$. Thus, the integral over l becomes

$$\widetilde{\mathscr{I}} = \int_0^\infty \mathrm{d}l\, \mathrm{e}^{-l^2} f_\pm(Al)\, f_\pm(Bl)\,\frac{1-\mathrm{e}^{-Cl^2}}{l^2}, \tag{3.187}$$

with A and B such as in Eq. (3.155) and

$$C = \frac{2\vartheta(1-\vartheta)}{\vartheta+\frac{s}{\Delta t}}. \tag{3.188}$$

We now divide $\widetilde{\mathscr{I}}$ as

$$\widetilde{\mathscr{I}} = \widetilde{\mathscr{I}}_1+\widetilde{\mathscr{I}}_2 = \int_0^\infty \mathrm{d}l\, \mathrm{e}^{-l^2}\left(f_\pm(Al)\, f_\pm(Bl)-f_\pm(0)^2\right)\frac{1-\mathrm{e}^{-Cl^2}}{l^2}+ \\ +\int_0^\infty \mathrm{d}l\, \mathrm{e}^{-l^2} f_\pm(0)^2\frac{1-\mathrm{e}^{-Cl^2}}{l^2} \tag{3.189}$$

and note that $\widetilde{\mathscr{I}}_1$ represents a more regular version of $\mathscr{I}$ (see Eq. (3.155)); thereby, all the arguments of convergence presented above can be applied also in this case and one needs only to consider $\widetilde{\mathscr{I}}_2$ for the special case and the first term of the series generated by the expansion of the hyperbolic functions of $\widetilde{\mathscr{I}}_1$ in the ordinary one. We consider first the special case and study the behaviour at the boundaries of

$$(4\pi)^2\mathscr{R}_3^{(1)}\,|_{DIV} = A_4(\Delta t)\int_0^1 \frac{\mathrm{d}\vartheta}{\vartheta(1-\vartheta)}\mathrm{e}^{-\frac{1}{4}\left(\frac{\tilde{x}^2}{1-\vartheta}+\frac{\tilde{y}^2}{\vartheta}\right)}\widetilde{\mathscr{I}}_2. \tag{3.190}$$

Exploiting the identity

$$\int_0^\infty \mathrm{d}l\, \mathrm{e}^{-l^2} \frac{1-\mathrm{e}^{-Cl^2}}{l^2} = -\sqrt{\pi}\left(1-\sqrt{1+C}\right) \tag{3.191}$$

and implementing the transformation

$$\sqrt{\frac{1-\vartheta}{\vartheta}} = \beta' \quad \text{with} \quad \frac{\mathrm{d}\vartheta}{\vartheta(1-\vartheta)} = -2\frac{\mathrm{d}\beta'}{\beta'}, \tag{3.192}$$

one finds

$$\begin{aligned}(4\pi)^2 \mathscr{R}_3^{(1)}\,|_{DIV} = -2\sqrt{\pi}\, A_4(\Delta t)\, \mathrm{e}^{-\frac{1}{4}\left(\tilde{x}^2+\tilde{y}^2\right)} \int \frac{\mathrm{d}\beta'}{\beta'} \mathrm{e}^{-\frac{1}{4}\left(\frac{\tilde{x}^2}{\beta'^2}+\tilde{y}^2\beta'^2\right)} \times \\ \times \left[1-\sqrt{1+\frac{2\beta'^2}{(\beta'^2+1)\,(1+\tilde{s}(\beta'^2+1))}}\right],\end{aligned} \tag{3.193}$$

where, analogously to the shorthands in Eq. (3.153), we have defined $\tilde{s} = s/\Delta t$. Denoting with $\mathscr{B}(\beta')$ the argument of the square brackets in the expression above, we have that

$$\mathscr{B}(\beta') = -\beta'^2 + O\left(\beta'^4\right) \qquad \text{for } (\beta' \to 0), \tag{3.194a}$$

$$\mathscr{B}(\beta') = -\frac{1}{\tilde{s}\beta'^2} + O\left(\beta'^{-4}\right) \qquad \text{for } (\beta' \to \infty), (s > 0), \tag{3.194b}$$

$$\mathscr{B}(\beta') = 1-\sqrt{3} + O\left(\beta'^{-2}\right) \qquad \text{for } (\beta' \to \infty), (s = 0). \tag{3.194c}$$

Thus, we see that even in the absence of the exponential (i.e., for $x = y = 0$) the integral is convergent for every $s > 0$. We also notice that the integral is still finite for $s = x = 0$, $y > 0$, as the exponential regularises the behaviour at $\beta' \to \infty$. Thus, the only divergence is obtained when $y = s = 0$, independently of the value taken by x. In the following, we shall employ the "radial" representation

$$y^2 = u\cos\alpha, \qquad s = u\sin\alpha \tag{3.195}$$

already introduced in Sec. (3.2.1). We now define

$$Q(u,\alpha) = \int_0^\infty \frac{\mathrm{d}\beta'}{\beta'} \mathrm{e}^{-\frac{1}{4}\left(\frac{\tilde{x}^2}{\beta'^2}+u\cos\alpha\beta'^2\right)} \left[1-\sqrt{1+\frac{2\beta'^2}{(\beta'^2+1)\,(1+u\sin\alpha(\beta'^2+1))}}\right]. \tag{3.196}$$

We expect a logarithmic behaviour to emerge as in the previous cases, i.e.,

$$Q(u,\alpha) = f(\alpha)\ln u + O(1) \qquad (u \to 0). \tag{3.197}$$

In order to verify this assumption and calculate the coefficient $f(\alpha)$, we derive this function with respect to u, which yields

$$Q'(u,\alpha) = J_1(u,\alpha) + J_2(u,\alpha) \tag{3.198}$$

with

$$J_1 = -\frac{\cos\alpha}{4}\int_0^\infty \mathrm{d}\beta'\,\beta' \mathrm{e}^{-\frac{1}{4}\left(\frac{\tilde{x}^2}{\beta'^2}+u\cos\alpha\beta'^2\right)}\left[1-\sqrt{1+\frac{2\beta'^2}{(\beta'^2+1)\,(1+u\sin\alpha(\beta'^2+1))}}\right] \tag{3.199}$$

and

$$\begin{aligned} J_2 = &\sin\alpha\int_0^\infty \mathrm{d}\beta'\,\beta' \mathrm{e}^{-\frac{1}{4}\left(\frac{\tilde{x}^2}{\beta'^2}+u\cos\alpha\beta'^2\right)}\left[1+\frac{2\beta'^2}{(\beta'^2+1)\,(1+u\sin\alpha(\beta'^2+1))}\right]^{-\frac{1}{2}}\times \\ &\times\left(1+u\sin\alpha(\beta'^2+1)\right)^{-2}. \end{aligned} \tag{3.200}$$

We now perform another change $\beta' = \gamma/\sqrt{u}$ which allows us to rewrite the expressions above as $J_i = (1/u)\widehat{J}_i$ with

$$\widehat{J}_1(u,\alpha) = -\frac{\cos\alpha}{4}\int_0^\infty \mathrm{d}\gamma\,\gamma \mathrm{e}^{-\frac{1}{4}\left(u\frac{\tilde{x}^2}{\gamma^2}+\gamma^2\cos\alpha\right)}\left[1-\sqrt{1+\frac{2\gamma^2}{(\gamma^2+u)\,[1+\sin\alpha(\gamma^2+u)]}}\right] \tag{3.201}$$

and

$$\begin{aligned} \widehat{J}_2(u,\alpha) = &\sin\alpha\int_0^\infty \mathrm{d}\gamma\,\gamma \mathrm{e}^{-\frac{1}{4}\left(u\frac{\tilde{x}^2}{\gamma^2}+\gamma^2\cos\alpha\right)}\left[1+\frac{2\gamma^2}{(\gamma^2+u)\,[1+\sin\alpha(\gamma^2+u)]}\right]^{-\frac{1}{2}}\times \\ &\times\left(1+\sin\alpha(\gamma^2+u)\right)^{-2}. \end{aligned} \tag{3.202}$$

Clearly, $f(\alpha)$ in Eq. (3.197) is given by the sum $\widehat{J}_1(0,\alpha)+\widehat{J}_2(0,\alpha)$ (provided it is finite), which we calculate in the following. We start from

$$\widehat{J}_1(0,\alpha) = -\frac{\cos\alpha}{4}\int_0^\infty \mathrm{d}\gamma\,\gamma \mathrm{e}^{-\frac{1}{4}\gamma^2\cos\alpha}\left[1-\sqrt{1+\frac{2}{1+\gamma^2\sin\alpha}}\right] = -\frac{1}{2}+\mathscr{J}(\alpha), \tag{3.203}$$

where we have defined

$$\mathscr{J}(\alpha) = \frac{\cos\alpha}{4}\int_0^\infty \mathrm{d}\gamma\,\gamma\sqrt{1+\frac{2}{1+\gamma^2\sin\alpha}}\,\mathrm{e}^{-\frac{1}{4}\gamma^2\cos\alpha}. \tag{3.204}$$

We now consider

$$\begin{aligned} &\widehat{J}_2(0,\alpha) = \sin\alpha\int_0^\infty \mathrm{d}\gamma\,\gamma \mathrm{e}^{-\frac{1}{4}\gamma^2\cos\alpha}\left[1+\frac{2}{1+\gamma^2\sin\alpha}\right]^{-\frac{1}{2}}\left(1+\gamma^2\sin\alpha\right)^{-2} = \\ &-\int_0^\infty \mathrm{d}\gamma\,\gamma \mathrm{e}^{-\frac{1}{4}\gamma^2\cos\alpha}\frac{1}{2\gamma}\partial_\gamma\left[1+\frac{2}{1+\gamma^2\sin\alpha}\right]^{\frac{1}{2}} = \left[-\frac{1}{2}\mathrm{e}^{-\frac{1}{4}\gamma^2\cos\alpha}\sqrt{1+\frac{2}{1+\gamma^2\sin\alpha}}\right]_0^\infty + \\ &+\frac{1}{2}\int_0^\infty \mathrm{d}\gamma\sqrt{1+\frac{2}{1+\gamma^2\sin\alpha}}\,\partial_\gamma \mathrm{e}^{-\frac{1}{4}\gamma^2\cos\alpha} = \frac{\sqrt{3}}{2}-\mathscr{J}(\alpha). \end{aligned} \tag{3.205}$$

This confirms that the divergence of $Q(u,\alpha)$ for $u \to 0$ is indeed logarithmic in nature. Moreover, it proves that the coefficient

$$f(\alpha) = \frac{\sqrt{3}-1}{2} \tag{3.206}$$

is actually independent of the choice of α, which means that the divergence is the same when approaching the edge from any "direction" in the $y^z - s$ plane. Thus, the divergent part (3.193) can be rewritten as

$$(4\pi)^2 \mathscr{R}_3^{(1)} \,|_{DIV} \sim -\frac{1}{\sqrt{4\pi\Delta t}} \mathrm{e}^{-\frac{1}{4}\tilde{x}^2} \left(\frac{\sqrt{3}-1}{2}\right) \ln u = -\left(\frac{\sqrt{3}-1}{2}\right) \ln u \, R^{(0)}(x,t;0,0). \tag{3.207}$$

The corresponding divergence of $R^{(1)}$ is obtained by multiplying it by $-(n+2)\varepsilon_3 g/6 = (n+2)g/6$. This contribution is entirely due to the edge behaviour, thereby it is related with the term

$$\left(\frac{(Ay)^z + s}{\Delta t}\right)^{-\theta_E} \sim u^{-\theta_E} \tag{3.208}$$

appearing in the scaling form (3.69b) (the specific value of the constant A is inconsequential for the leading asymptotic behaviour). Therefore, at the Wilson-Fisher fixed point $g = g^* = 3/(n+8)(4\pi)^{-2}\varepsilon + O\left(\varepsilon^2\right)$ we have

$$-\theta_E = -\theta_{E,0} - \theta_{E,1}\varepsilon + O\left(\varepsilon^2\right) = -\frac{n+2}{n+8}\left(\frac{\sqrt{3}-1}{4}\right)\varepsilon + O\left(\varepsilon^2\right), \tag{3.209}$$

which gives back the value for the special transition displayed in Eq. (3.74). For the ordinary case, $\widetilde{\mathscr{I}}_2 \equiv 0$ and we have to take the first non-trivial order of the expansion of the hyperbolic functions in $\widetilde{\mathscr{I}}_1$ in Eq. (3.189), i.e.,

$$\widetilde{\mathscr{I}}_1 \,|_{DIV} \sim \tilde{x}\tilde{y} \int_0^\infty \mathrm{d}l \, \mathrm{e}^{-l^2} \left(1 - \mathrm{e}^{-Cl^2}\right) = \tilde{x}\tilde{y} \frac{\sqrt{\pi}}{2} \left(1 - \frac{1}{\sqrt{1+C}}\right). \tag{3.210}$$

Analogously to the case above (see Eq. (3.193)), we have

$$(4\pi)^2 \mathscr{R}_3^{(1)} \,|_{DIV} = \sqrt{\pi} A_4(\Delta t) \, \mathrm{e}^{-\frac{1}{4}\left(\tilde{x}^2+\tilde{y}^2\right)} \tilde{x}\tilde{y} \, \widetilde{Q}(u,\alpha), \tag{3.211}$$

with

$$\widetilde{Q}(u,\alpha) = \int_0^\infty \frac{\mathrm{d}\beta'}{\beta'} \mathrm{e}^{-\frac{1}{4}\left(\frac{\tilde{x}^2}{\beta'^2} + u\cos\alpha\beta'^2\right)} \left[1 - \left(1 + \frac{2\beta'^2}{(\beta'^2+1)\left(1+u\sin\alpha(\beta'^2+1)\right)}\right)^{-\frac{1}{2}}\right]. \tag{3.212}$$

We apply again the same procedure employed for the special case, i.e., we derive with respect to u and define

$$\partial_u \widetilde{Q}(u,\alpha) = \frac{1}{u}\left(\widehat{K}_1(u,\alpha) + \widehat{K}_2(u,\alpha)\right), \tag{3.213}$$

where

$$\widehat{K}_1(u,\alpha) = -\frac{\cos\alpha}{4}\int_0^\infty \mathrm{d}\gamma\,\gamma\,\mathrm{e}^{-\frac{1}{4}\left(u\frac{\tilde{x}^2}{\gamma^2}+\gamma^2\cos\alpha\right)}\left[1-\left(1+\frac{2\gamma^2}{(\gamma^2+u)\,[1+\sin\alpha(\gamma^2+u)]}\right)^{-\frac{1}{2}}\right] \tag{3.214}$$

and

$$\widehat{K}_2(u,\alpha) = -\sin\alpha\int_0^\infty \mathrm{d}\gamma\,\gamma\,\mathrm{e}^{-\frac{1}{4}\left(u\frac{\tilde{x}^2}{\gamma^2}+\gamma^2\cos\alpha\right)}\left[1+\frac{2\gamma^2}{(\gamma^2+u)\,[1+\sin\alpha(\gamma^2+u)]}\right]^{-\frac{3}{2}}\times \\ \times\left(1+\sin\alpha(\gamma^2+u)\right)^{-2}. \tag{3.215}$$

We now have to calculate the sum of these two expressions for $u=0$, which gives

$$\widehat{K}_1(0,\alpha) = -\frac{\cos\alpha}{4}\int_0^\infty \mathrm{d}\gamma\gamma\,\mathrm{e}^{-\frac{1}{4}\gamma^2\cos\alpha}\left[1-\left(1+\frac{2}{1+\gamma^2\sin\alpha}\right)^{-\frac{1}{2}}\right] = -\frac{1}{2}+\mathscr{K}(\alpha), \tag{3.216}$$

with

$$\mathscr{K}(\alpha) = \frac{\cos\alpha}{4}\int_0^\infty \mathrm{d}\gamma\gamma\,\mathrm{e}^{-\frac{1}{4}\gamma^2\cos\alpha}\left(1+\frac{2}{1+\gamma^2\sin\alpha}\right)^{-\frac{1}{2}}, \tag{3.217}$$

and

$$\widehat{K}_2(0,\alpha) = -\sin\alpha\int_0^\infty \mathrm{d}\gamma\gamma\,\mathrm{e}^{-\frac{1}{4}\gamma^2\cos\alpha}\left(1+\frac{2}{1+\gamma^2\sin\alpha}\right)^{-\frac{3}{2}}\left(1+\gamma^2\sin\alpha\right)^{-2} = \\ = \int_0^\infty \mathrm{d}\gamma\gamma\,\mathrm{e}^{-\frac{1}{4}\gamma^2\cos\alpha}\frac{1}{2\gamma}\partial_\gamma\left(1+\frac{2}{1+\gamma^2\sin\alpha}\right)^{-\frac{1}{2}} = \frac{1}{2}\left[\mathrm{e}^{-\frac{1}{4}\gamma^2\cos\alpha}\left(1+\frac{2}{1+\gamma^2\sin\alpha}\right)^{-\frac{1}{2}}\right]_0^\infty + \\ -\frac{1}{2}\int_0^\infty \mathrm{d}\gamma\left(1+\frac{2}{1+\gamma^2\sin\alpha}\right)^{-\frac{1}{2}}\partial_\gamma\mathrm{e}^{-\frac{1}{4}\gamma^2\cos\alpha} = \frac{1}{2\sqrt{3}}-\mathscr{K}(\alpha). \tag{3.218}$$

As a consequence, in this case

$$\widetilde{Q}(u\alpha) \sim \frac{1}{2}\left(\frac{1}{\sqrt{3}}-1\right)\ln u + O(1) \quad \text{for} \quad (u\to 0), \tag{3.219}$$

which in turn implies

$$(4\pi)^2\mathscr{R}_3^{(1)}\,|_{DIV} \sim \frac{\sqrt{\pi}}{2}A_4(\Delta t)\,\mathrm{e}^{-\frac{1}{4}(\tilde{x}^2)}\,\tilde{x}\tilde{y}\left(\frac{1}{\sqrt{3}}-1\right)\ln u = \frac{1}{2}\left(\frac{1}{\sqrt{3}}-1\right)R^{(0)}(x,t;y\to 0,0). \tag{3.220}$$

This expression differs from Eq. (3.207) by the sign and the fact that $\sqrt{3} \to 1/\sqrt{3}$; on the other hand, the sign is reabsorbed by ε_3 in Eq. (3.139). Therefore, the value of θ_E in the ordinary case is given by

$$-\theta_E = -\theta_{E,0} - \theta_{E,1}\varepsilon + O\left(\varepsilon^2\right) = -\frac{n+2}{n+8}\left(\frac{1}{\sqrt{3}} - 1\right)\frac{\varepsilon}{4} + O\left(\varepsilon^2\right), \tag{3.221}$$

which again reproduces the result previously reported in Eq. (3.74).

3.C.1 Renormalisation factors

As we have mentioned while discussing the divergence at the initial time, i.e., the case of $\mathscr{R}_1^{(1)}$, one can analogously look for dimensional poles $\propto 1/\varepsilon$ by fixing the functions at the boundaries. These divergent part can be absorbed by standard multiplicative renormalisation techniques, as we briefly show here focusing for simplicity on the special case. We therefore introduce [11, 20, 23, 53]

$$\widetilde{\varphi} = \tilde{Z}^{\frac{1}{2}}\, \widetilde{\varphi}^{(R)}, \qquad [\widetilde{\varphi}] = \frac{d+z+\tilde{\eta}}{2}, \tag{3.222a}$$

$$\widetilde{\varphi}_0 = \tilde{Z}^{\frac{1}{2}}\, \tilde{Z}_0^{\frac{1}{2}}\, \widetilde{\varphi}_0^{(R)}, \qquad [\widetilde{\varphi}_0] = \frac{d+z+\tilde{\eta}+\tilde{\eta}_0}{2}, \tag{3.222b}$$

$$\widetilde{\varphi}_S = \tilde{Z}^{\frac{1}{2}}\, \tilde{Z}_1^{\frac{1}{2}}\, \widetilde{\varphi}_S^{(R)}, \qquad [\widetilde{\varphi}_1] = \frac{d+z+\tilde{\eta}+\tilde{\eta}_1}{2}, \tag{3.222c}$$

$$\widetilde{\varphi}_E = \tilde{Z}^{\frac{1}{2}}\, \tilde{Z}_1^{\frac{1}{2}}\, \tilde{Z}_0^{\frac{1}{2}}\, \tilde{Z}_E^{\frac{1}{2}}\, \widetilde{\varphi}_E^{(R)}, \qquad [\widetilde{\varphi}_E] = \frac{d+z+\tilde{\eta}+\tilde{\eta}_1+\tilde{\eta}_0+\tilde{\eta}_E}{2}, \tag{3.222d}$$

where $\widetilde{\varphi}^{(R)}$ generically denotes the renormalised response field. Here, $\tilde{Z}$ is the bulk renormalisation factor, $\tilde{Z}_0$ refers specifically to the temporal boundary, whereas $\tilde{Z}_1$ to the spatial one; finally, $\tilde{Z}_E$ takes care of the additional renormalisation of the edge fields $\widetilde{\varphi}_E$, according to the appearance of novel divergences in this regime. In order to account for the differences in the scaling dimensions, we have introduced three novel anomalous dimensions $\tilde{\eta}_0$, $\tilde{\eta}_1$ and $\tilde{\eta}_E$ [23, 53] in addition to the usual one $\tilde{\eta}$ [11] introduced in Eq. (3.8). According to standard RG techniques, these corrections can be obtained by taking the logarithmic derivatives

$$\tilde{\eta}_i = -\varepsilon\, g\, \partial_g \log \tilde{Z}_i. \tag{3.223}$$

From the three algebraic factors coming from the SDEs of Eq. (3.69b) one finds that the exponents we have discussed in the previous Sections can be completely rewritten in terms of the bulk ones and the boundary anomalous dimensions as

$$\tilde{\eta}_1 = 2\frac{\beta_1 - \beta}{\nu}, \qquad \tilde{\eta}_0 = -2\theta z, \qquad \tilde{\eta}_E = -2\theta_E z. \tag{3.224}$$

In the following, the coordinates shall be always thought to be different from 0, unless otherwise stated. In dimensional regularisation, one can extract from Eqs. (3.144), (3.150) and (3.185) the

one-loop corrections:

$$R(x,t;y,s) = R^{(0)}(x,t;y,s) + O\left(g^2\right), \tag{3.225a}$$

$$R(x,t;y,s=0) = R^{(0)}(x,t;y,0)\left(1+\frac{n+2}{3!}\frac{g}{(4\pi)^2\varepsilon}\right) + O\left(g^2\right), \tag{3.225b}$$

$$R(x,t;y=0,s) = R^{(0)}(x,t;0,s)\left(1+\frac{n+2}{3!}\frac{g}{(4\pi)^2\varepsilon}\right) + O\left(g^2\right), \tag{3.225c}$$

$$R(x,t;y=0,s=0) = R^{(0)}(x,t;0,0)\left(1+\frac{n+2}{3!}\frac{\left(\sqrt{3}+1\right)g}{(4\pi)^2\varepsilon}\right) + O\left(g^2\right). \tag{3.225d}$$

Equation (3.225a) implies $\tilde{Z} = 1 + O\left(g^2\right)$, which, at the Wilson-Fisher fixed point $g^* = \frac{3}{n+8}(4\pi)^2\varepsilon + O(\varepsilon^2)$, becomes $\tilde{Z} = 1 + O\left(\varepsilon^2\right)$ [11]. From Eq. (3.225b) we find instead the less trivial result

$$\tilde{Z}_0 = 1 - \frac{n+2}{3}\frac{g}{\varepsilon}\frac{1}{(4\pi)^2} + O\left(g^2\right). \tag{3.226}$$

Applying the logarithmic derivative (3.223) yields [23]

$$\tilde{\eta}_0 = -\frac{g}{(4\pi)^2}\frac{n+2}{3}. \tag{3.227}$$

The renormalisation factor associated to the spatial surface for the special transition can be extracted from Eq. (3.225c) and corresponds to [59]

$$\tilde{Z}_1 = 1 - \frac{n+2}{3}\frac{g}{\varepsilon}\frac{1}{(4\pi)^2} + O\left(g^2\right). \tag{3.228}$$

Again, by deriving according to Eq. (3.223), one obtains

$$\tilde{\eta}_1 = -\frac{g}{(4\pi)^2}\frac{n+2}{3}. \tag{3.229}$$

Finally, from Eq. (3.225d) one can calculate

$$\tilde{Z}_E = 1 - \frac{n+2}{3}\frac{g}{\varepsilon}\frac{\sqrt{3}-1}{(4\pi)^2} + O\left(g^2\right) \tag{3.230}$$

and, consequently,

$$\tilde{\eta}_E = -\left(\sqrt{3}-1\right)\frac{g}{(4\pi)^2}\frac{n+2}{3}. \tag{3.231}$$

At the fixed point Eqs. (3.227), (3.229) and (3.231) become

$$\tilde{\eta}_0 = -\frac{n+2}{n+8}\varepsilon, \qquad \tilde{\eta}_1 = -\frac{n+2}{n+8}\varepsilon, \qquad \tilde{\eta}_E = -\left(\sqrt{3}-1\right)\frac{n+2}{n+8}\varepsilon, \tag{3.232}$$

which, when inserted in Eqs. (3.224) and using the fact that $z = 2 + O\left(\varepsilon^2\right)$, render the first-order corrections to the exponents we have found above (see Eqs. (3.33b), (3.55) and (3.74)).

4 Quantum quenches: two alternative approaches

The development of quantum theories in the first half of the 20-th century completely revolutionised our view of the world at the microscopic scale. Actually, there are several macroscopic features which are affected by quantum effects, such as the photoelectric response of metals to high-frequency radiation, or the semiconducting behaviour of many metalloids. However, they are mostly the reflection of a large number of microscopic degrees of freedom independently behaving according to quantum mechanics. It is much more difficult to highlight quantum many-body effects, mainly due to the fact that the interaction of these degrees of freedom with the environment typically destroys the coherence between their constituents on extremely small time-scales. Only recently, thanks to the advances in cold-atomic techniques [29], it has become possible to engineer macroscopic systems which display non-microscopic coherence times, ranging from some milliseconds [35] up to a few seconds [27]. This allowed for the first time to undertake the study of quantum dynamics in an experimental setting, highlighting many intriguing effects, such as the ones, mentioned in the Introduction, which are illustrated in Figs. 2.2 and 2.3.

Among the various analytical methods which have been devised in order to approach the physics of quantum many-body systems, field-theoretical ones prove to be particularly useful, especially in the thermodynamic limit. In fact, they provide a rather general and versatile framework to investigate a variety of different systems and naturally allow one to address the possible emergence of collective phenomena, which typically defy other approaches. Field theories have been widely and successfully used in the past for describing the static and dynamic behaviour of many-body systems in *equilibrium* [11], greatly contributing in the progress of our understanding of condensed matter. Within this approach, one typically identifies asymptotic states of the theory for $t \to \pm\infty$ — corresponding to the absence of interaction, which is assumed to be switched on and off *adiabatically* in these limits — in such a way that the quantum state with no elementary excitations (vacuum) in the far past $t \to -\infty$ and in the far future $t \to +\infty$ differ at most by an overall phase factor (Gell-Mann and Low theorem [93–95]). Non-equilibrium processes, on the other hand, often involve sudden changes of the control parameters of the system which generically violate the condition of adiabaticity required above, rendering the identification of the asymptotic states in the past with those in the future problematic.

However, a strategy to deal with this problem has been known since the 60s [96, 97]: it is based on an effective time evolution running on the contour sketched in Fig. 4.1, which just requires the knowledge of the initial state, whilst not needing any kind of inference on the structure of the asymptotic state in the far future. This approach is usually referred to as *Keldysh* (or *Keldysh-*

Schwinger) *formalism* [98–103] and, for convenience, we summarize its main features in Sec. 4.1. Among the different protocols which may be employed to drive an isolated quantum system out

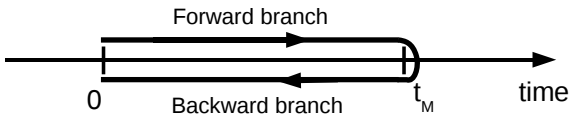

Figure 4.1: Sketch of the "time evolution" within the Keldysh formalism. Without loss of generality, we fix at $t = 0$ the time at which the initial condition ρ_0 is imposed. The rightmost time t_M has no specific physical significance: as long as it is larger than all the values of the time at which the various quantities are considered, its position along the real axis is inconsequential and can be chosen arbitrarily, as clarified in Section 4.1. Differently from the dynamics in equilibrium, the difficulty in identifying the asymptotic states in the future with the ones in the past does not allow the transformation of the backward branch of the contour into a forward one from t_M to $+\infty$ and therefore one has to deal with a closed-time path integral instead of with an "ordinary" one.

of equilibrium, in the following we focus on the one which is conceptually the simplest, i.e., the quench: as stated before, in spite of its simplicity, it actually encompasses a rich variety of cases and is currently under intensive theoretical and experimental study (see, e.g., Ref. [41]). From a formal point of view, two equivalent formulations may be given: the system is prepared in the ground state of a Hamiltonian H_0; at time $t = 0$ the Hamiltonian is switched with a new, time-independent one H, which governs the subsequent ($t > 0$) evolution. Alternatively, one can think of having only one Hamiltonian H while the system is prepared at $t = 0$ in a (pure) state which is not an energy eigenstate.

An alternative approach for studying the dynamics of an isolated quantum system after a quench has been recently proposed and successfully applied in Refs. [2, 3]. Instead of relying on the Keldysh contour, this method represents a generalisation of the usual Wick rotation [94] to non-equilibrium problems, as it maps the original dynamical system in d spatial dimensions to a static $(d+1)$-dimensional one, where the additional "spatial" direction is provided by the imaginary axis in the complex plane of times. A fundamental difference which arises with respect to equilibrium is that the Euclidean framework obtained in this way is actually confined within a film geometry, i.e., the system is defined in an effectively bounded interval of imaginary times $[-\varepsilon, \varepsilon]$, which can be conveniently thought to be centered on the real axis. This mapping makes it possible to take advantage of the available knowledge about the thermodynamic and structural properties (e.g., correlation functions) of statistical systems confined within films of finite thickness [25, 53, 61].

This Chapter provides a critical comparison of the two different approaches mentioned above, in order to highlight analogies and differences and elucidate them in the simplest possible cases. In Sec. 4.1 we provide a summary on the main concepts concerning the two-time Keldysh approach. The following Sec. 4.2 is instead devoted to briefly introducing the mapping to imaginary times for non-equilibrium quantum dynamical problems. In Sec. 4.3 we discuss how these two formalisms are related, paying particular attention to the relationship existing between the initial conditions

of the dynamical problem and the boundary conditions at the edges of the film in the euclidean one. We show that an interpretation in terms of a static system in a film is not always possible, but requires the initial state to be pure; on the other hand, we are still able to provide a formal definition of a theory in the film in the case of statistical mixtures. We also provide a detailed discussion of the issues one encounters in performing the analytic continuation from imaginary to real times, providing a prescription to retrieve the various Keldysh functions from the ones defined on imaginary times, working out explicitly a few simple examples. In Sec. 4.4 we make use of such an analysis to show that one can employ the euclidean formalism not only for calculating correlations, but also response functions. Finally, in Sec. 4.5 we summarise our main results.

4.1 The Keldysh formalism

Consider a generic quantum many-body system which can be described in terms of a given set of fields Ψ, $\Psi^\dagger$, either bosonic or fermionic (e.g., containing information on the density of charge carriers in a semiconductor), which evolve according to a Hamiltonian H in a d-dimensional space, starting from an initial condition encoded in a density matrix ρ_0. Since we consider below homogeneous, and thus space-translationally invariant, systems, the dependence of these fields on the spatial coordinates will play no significant role for our discussion and shall be implied by the notation $\Psi(t) \equiv \Psi(\vec{x},t)$ whenever confusion may not arise as a consequence. The typical observables one is interested in are correlation functions such as

$$\langle \Psi(t_1)\Psi(t_2)\dots\Psi(t_n)\rangle \equiv \mathrm{tr}\left\{\Psi(t_1)\Psi(t_2)\dots\Psi(t_n)\rho_0\right\}, \tag{4.1}$$

where the fields are expressed in the Heisenberg representation $\Psi(t) = \mathrm{e}^{iHt}\,\Psi\,\mathrm{e}^{-iHt}$. The Keldysh structure of the evolution reported in Fig. 4.1 emerges already at the level of the one-time function $\langle\Psi(t_1)\rangle = \left\langle \mathrm{e}^{iHt_1}\Psi\mathrm{e}^{-iHt_1}\right\rangle$: the operator e^{-iHt_1} represents the forward branch, as it evolves the initial state at $t=0$ to its counterpart at the measurement time $t=t_1$, whereas the backward branch is generated by e^{iHt_1}, which brings the state of the system back at $t=0$, where it is projected onto the initial state ρ_0 (by the cyclicity of the trace). Clearly, by introducing the identity in the form $\mathbb{1} = \mathrm{e}^{iH(t_M-t_1)}\mathrm{e}^{-iH(t_M-t_1)}$ to the immediate right (or left) of the field Ψ, one can indefinitely extend the contour to any point t_M on the right of the original "turning time" t_1, the value of the latter being completely inconsequential. On the other hand, the path has to definitely reach t_1, where Ψ is measured; trying to deform it to the left of t_1 enforces a more complicated structure, which we portray in Fig. 4.2. This explains, in the simplest case, the irrelevance of the precise position of the rightmost point and the requirement that it be greater than any measurement time. While the same argument can be repeated for two-time quantities, starting with three-time ones, the Keldysh structure enforces a constraint on the order in which fields may appear inside the expectation (4.1); for example, taking $\langle\Psi(t_1)\Psi(t_2)\Psi(t_1)\rangle$ with $t_2 < t_1$ and trying to apply the same interpretation as before, one ends up with a contour similar to the one displayed in Fig. 4.2, where however the central part does not represent the identity anymore, as the second field lies upon it. Thus, in order to identify those correlations which can be actually described in a Keldysh framework, it is convenient to define the corresponding time-ordering operator T_K, the action of which is to move all the operators lying on the backward branch to the left of those lying on the forward one, while

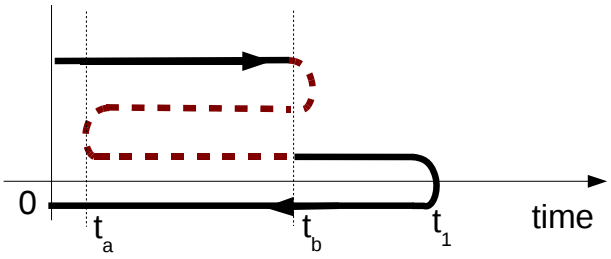

Figure 4.2: Example of the effect of inserting at time t_b on the Keldysh contour (black, solid line) the identity in the form $e^{iH(t_a-t_b)}e^{-iH(t_a-t_b)}$ (red, dashed line). This choice is completely equivalent to the original one as long as no field is positioned along the red, dashed part of the path. The vertical separation of the lines represents just a visual aid to distinguish them, while they should be collapsed onto the real axis, which implies that the time variable can be thought to be fourthly degenerate within the range $[t_a, t_b]$.

imposing the canonical time-ordering on the latter and the opposite ordering (*anti-ordering*) on the former. For the sake of clarity, consider a generic product of operators $\mathscr{O}$ at times $t_1, t_2, \dots t_m$ and $s_1, s_2, \dots s_n$, which are positioned along the Keldysh contour as shown in Fig. 4.3: T_K renders

$$T_K\left[\mathscr{O}(t_1)\dots\mathscr{O}(t_m)\mathscr{O}(s_1)\dots\mathscr{O}(s_n)\right] = (-1)^{\mathscr{P}}\mathscr{O}(s_1)\dots\mathscr{O}(s_n)\mathscr{O}(t_m)\dots\mathscr{O}(t_1), \tag{4.2}$$

where $\mathscr{P}$ corresponds to the parity of the permutation applied to the fermionic operators (e.g., it would be mn if they were all fermionic and identically vanish it they were all bosonic). Accordingly, reading from the left to the right the arguments of the operator, one always obtains an increasing sequence of times followed by a decreasing one.

Quite naturally, all the correlation functions of the fields which are T_K-ordered can be derived from the generating functional

$$Z[J,\bar{J}] = \mathrm{tr}\left\{T_K\left[\exp\left(i\int \mathrm{d}^d x \int_K \mathrm{d}t\left(J(t)\Psi(t) + \bar{J}(t)\Psi^\dagger(t)\right)\right)\right]\rho_0\right\}, \tag{4.3}$$

where J and $\bar{J}$ are suitable source terms defined on the Keldysh contour (we refer to App. 4.A for the explicit construction of the path integral). Indeed, time-ordered correlations are obtained by functional differentiation of Z with respect to the sources, e.g.,

$$\langle T_K\left[\Psi(t_1)\Psi(t_2)\dots\Psi(t_n)\right]\rangle = (-i)^n \frac{\delta^n Z[J,\bar{J}]}{\delta J(t_1)\dots\delta J(t_n)}\bigg|_{J=\bar{J}\equiv 0}, \tag{4.4}$$

where we have used the simplified notation $\langle\cdot\rangle = \mathrm{tr}\{(\cdot)\rho_0\}$. Naturally, the expectation of an observable at any given moment must be a well-defined quantity: in this context, this property may be rephrased as "being single-valued" in time, which means that its expectation at corresponding points on the forward and backward branches of K must coincide. However, at intermediate stages of the analysis it is actually convenient to distinguish them as if they were completely unrelated

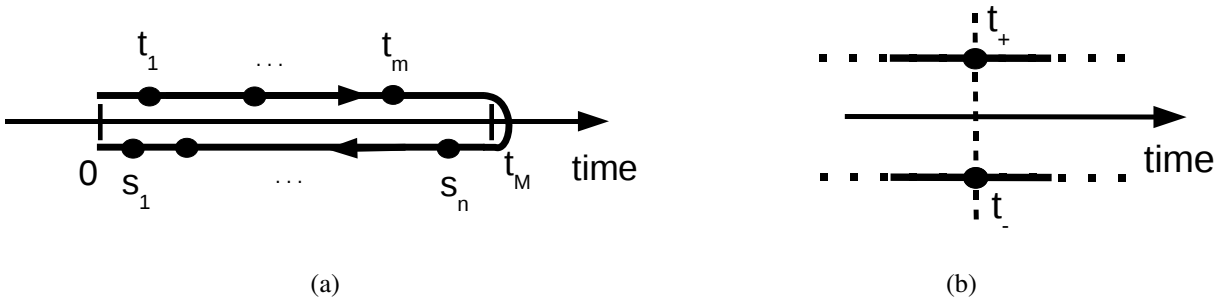

(a) (b)

Figure 4.3: Sketches of a collection of times defined on the two branches of the Keldysh contour. (a) As specified in the main text, the T_K-ordering of a product of operators taken at times $\{t_i, s_i\}$ moves to the left quantities lying near the end of the contour (i.e., on the backward branch) and to the right those lying next to its starting point (i.e., on the forward branch). Within the forward and backward branches operators are ordered according to the canonical time ordering and anti-ordering, respectively. Whenever ambiguities might arise, we shall distinguish points belonging to the forward and backward branches by adding the subscripts "+" and "−", respectively, to the corresponding time, as sketched in panel (b).

(see App. 4.A); for this purpose, we introduce the subscripts $+$ and $-$ for the forward and backward branch, respectively. Equivalently, one might think of the time t as taking two different values t_+ and t_- on the two branches, as depicted in Fig. 4.3(b). In particular, the source terms in Eq. (4.3) will be generally considered as double-valued, by distinguishing, e.g., the value $J_+(t) \equiv J(t_+)$ that J takes at time t on the forward branch from the value $J_-(t) \equiv J(t_-)$ it takes at the same time t on the backward branch. At the end of the analysis these two values have to be identified, i.e., $J_+(t) = J_-(t) \equiv J(t)$. Once this has been done and the ordering has been made explicit (as in Eq. (4.2)), the subscripts $\pm$ may be safely disregarded, and the time coordinates considered single-valued along the real axis, with no further distinction between the two branches.

Within this formalism, one introduces the two-time correlation functions of the fields as follows [98, 100]:

$$iG_{\pm\pm}(t,s) = -\left.\frac{\delta^2 Z[J,\bar{J}]}{\delta J(t_\pm)\delta\bar{J}(s_\pm)}\right|_{J=\bar{J}=0} = \left\langle T_K\left[\Psi(t_\pm)\Psi^\dagger(s_\pm)\right]\right\rangle, \tag{4.5}$$

where $t_\pm$ and $s_\pm$ are defined on the Keldysh contour K and t and s indicate their corresponding values along the time axis. The four different combinations of subscripts $+$ and $-$ give rise to

$$\begin{cases} iG^<(t,s) = iG_{+-}(t,s) = \pm\left\langle\Psi^\dagger(s)\Psi(t)\right\rangle, \\ iG^>(t,s) = iG_{-+}(t,s) = \left\langle\Psi(t)\Psi^\dagger(s)\right\rangle, \\ iG^T(t,s) = iG_{++}(t,s) = \left\langle T[\Psi(t)\Psi^\dagger(s)]\right\rangle, \\ iG^{T^*}(t,s) = iG_{--}(t,s) = \left\langle T^*[\Psi(t)\Psi^\dagger(s)]\right\rangle, \end{cases} \tag{4.6}$$

where, having already indicated explicitly on which branch each field lies, we have dropped the subscripts $\pm$ from the times. Here T and T^* denote the standard operations of time-ordering and

anti-ordering. In the case of $G^<$, the sign on the r.h.s. distinguishes the case of bosonic fields (+) from the case (−) of fermionic ones. These functions are known to satisfy the identity [98, 100]

$$G^T + G^{T^*} = G^> + G^< \tag{4.7}$$

and therefore at most three of them are actually independent. An often convenient reformulation is given by the so-called *physical representation*, which is defined in terms of the "classical" and "quantum" components of the fields

$$\Psi_c(t) = \Psi(t_+) + \Psi(t_-) \quad \text{and} \quad \Psi_q(t) = \Psi(t_+) - \Psi(t_-), \tag{4.8}$$

respectively. The corresponding two-point correlations are usually referred to as classical (or Keldysh), retarded, advanced and quantum functions:

$$\begin{cases} G^K(t,s) &= -\frac{i}{2}\left\langle T_K[\Psi_c(t)\Psi_c^\dagger(s)]\right\rangle &= G^>(t,s) + G^<(t,s), \\ G^r(t,s) &= -\frac{i}{2}\left\langle T_K[\Psi_c(t)\Psi_q^\dagger(s)]\right\rangle &= \theta(t-s)\left[G^>(t,s) - G^<(t,s)\right], \\ G^a(t,s) &= -\frac{i}{2}\left\langle T_K[\Psi_q(t)\Psi_c^\dagger(s)]\right\rangle &= -\theta(s-t)\left[G^>(t,s) - G^<(t,s)\right], \\ G^q(t,s) &= -\frac{i}{2}\left\langle T_K[\Psi_q(t)\Psi_q^\dagger(s)]\right\rangle &= 0, \end{cases} \tag{4.9}$$

where the rightmost equalities follow from Eq. (4.7). The physical representation is particularly useful as it makes the inherent causal structure of a dynamical theory apparent, due to the presence of the step function θ, with $\theta(t<0)=0$ and $\theta(t>0)=1$. For example, the retarded function G^r can be interpreted as the (linear) response of the classical field Ψ_c at time t to a small perturbation applied at time s [100], as it will be discussed in more detail in Section 4.4. Accordingly, causality implies that G^r vanishes for $t<s$ because physical effects cannot propagate in the past. This feature is analogous to the one encountered in Sec. 3.1.2 when discussing the properties of response functions in classical system. Actually, one can conceptually think of the classical component Ψ_c as being the analogous of the order parameter φ of Chap. 3, while the quantum component Ψ_q ideally corresponds to the response field $\widetilde{\varphi}$. Moreover, if the quantum system we are presently interested in is no longer isolated but linearly coupled to an equilibrium thermal bath of quantum harmonic oscillators, one can show that in the classical limit $\hbar \to 0$ (with $\Psi_q = (\Psi_+ - \Psi_-)/\hbar$) the action effectively describes a dynamics governed by a Langevin equation [8, 98]. In such a case, the noise constitutes an effective description of the degrees of freedom of the bath, which, thanks to the fact that they are Gaussian by assumption, can be conveniently integrated out.

4.1.1 Path-integral and initial conditions

In the present Section we focus on the case of a single real, scalar field $\Psi = \Psi^\dagger = \Phi$, although the following considerations extend straightforwardly to more general cases. The generating functional (4.3) can be cast in the path-integral formalism (see App. 4.A) as

$$Z[J] = \int \mathscr{D}\phi\, \mathrm{e}^{i(S_K[\phi] + J\cdot\phi)} \left\langle \phi(0_+)\right| \rho_0 \left|\phi(0_-)\right\rangle, \tag{4.10}$$

where J is the source coupled to the only field present. In this effective representation, the integration variable $\phi(\cdot)$ is a classical field whose evolution defines a "path", $S_K[\phi] = \int_K \mathrm{d}t L[\phi]$ is the action of the system, $L[\phi] = \int \mathrm{d}^d x \mathscr{L}[\phi]$ its Lagrangian, which can be obtained from the Hamiltonian H via the Legendre transformation $L[\Phi] = \int \mathrm{d}^d x \Pi(\vec{x},t)\,\Phi(\vec{x},t) - H$, where Π denotes the quantum field conjugate to Φ:

$$[\Phi(\vec{x},t), \Pi(\vec{y},t)] = i\hbar\delta(\vec{x}-\vec{y}). \tag{4.11}$$

In Eq. (4.10) $J\cdot\phi \equiv \int_K \mathrm{d}t\, \mathrm{d}^d x\, J(\vec{x},t)\,\phi(\vec{x},t)$ is a shorthand for the source term, and the "functional measure" is thought to be normalised such that $Z[0] = 1$. The density matrix ρ_0 which characterises the initial condition of the system plays the role of a "boundary" term for the path integral. In order to better highlight this fact, it is convenient to adopt a slightly different approach: we introduce two fields $\phi_\pm$, which are single-valued in time and correspond to the original field ϕ defined on either branch of the Keldysh contour, according to the notation introduced before: $\phi_+(t) \equiv \phi(t_+)$ and $\phi_-(t) \equiv \phi(t_-)$. The Keldysh action can be rewritten as $S_K[\phi] = S[\phi_+] - S[\phi_-]$, where $S[\phi_\pm] = \int_0^{t_M} \mathrm{d}t\, \mathrm{d}^d x \mathscr{L}[\phi_\pm]$ has the same Lagrangian density as S_K, but, while the former is integrated along the whole contour, the latter runs only on the real axis from 0 to t_M; the overall minus sign appearing in front of S_- is due to the fact that the backward branch is actually covered in the reversed direction (i.e., from t_M towards 0, see Fig. 4.1). By performing an analogous redefinition of the source J, we can rewrite Eq. (4.10) as [100]

$$Z[J_+,J_-] = \int_{\mathscr{K}} \mathscr{D}\phi_+ \mathscr{D}\phi_-\, \mathrm{e}^{i(S[\phi_+]-S[\phi_-]+J_+\cdot\phi_+ - J_-\cdot\phi_-)}\, \langle\phi_+(0)|\,\rho_0\,|\phi_-(0)\rangle\,, \tag{4.12}$$

where the functional integral is performed over the configurations (paths) of the fields that coincide at $t = t_M$, i.e.,

$$\mathscr{K} = \{\text{paths defined on the interval } [0,t_M] \text{ such that } \phi_+(t_M) = \phi_-(t_M)\}\,. \tag{4.13}$$

As we pointed out above, t_M can be chosen arbitrarily, as long as it is larger or equal than any other time involved in the correlation functions one is interested in. In particular, t_M can be identified with the largest time involved in a certain correlation function and therefore the condition $\phi_+(t_M) = \phi_-(t_M)$ allows one to move the corresponding field from one branch of the contour to the other.

The expectation $\langle\phi_+(0)|\,\rho_0\,|\phi_-(0)\rangle$ is in general a functional $F[\phi_+(0),\phi_-(0)]$ of the initial fields which, rewritten as $F = \mathrm{e}^{iS_0}$, can be incorporated into the action:

$$Z[J_+,J_-] = \int_{\mathscr{K}} \mathscr{D}\phi_+ \mathscr{D}\phi_-\, \mathrm{e}^{i(S[\phi_+,J_+]-S[\phi_-,J_-]+S_0[\phi_+(0),\phi_-(0)])}, \tag{4.14}$$

with

$$\begin{cases} S[\phi,J] \equiv S[\phi] + J\cdot\phi = \int_0^{t_M} \mathrm{d}t \int \mathrm{d}^d x\, [\mathscr{L}[\phi(\vec{x},t)] + J(\vec{x},t)\phi(\vec{x},t)]\,, \\ S_0[\phi_+(0),\phi_-(0)] = \int \mathrm{d}^d x \mathscr{L}_0[\phi_+(\vec{x},0),\phi_-(\vec{x},0)], \end{cases} \tag{4.15}$$

where $\mathscr{L}$ is the Lagrangian density which enters in the action S_K of Eq. (4.10). The functional $\mathscr{L}_0$ encodes the properties of the initial state and is generally a rather complicated function of its arguments. In terms of the fields ϕ_+ and ϕ_-, the generating functional in Eq. (4.14) has the

same structure as the partition function that we have encountered in the Chapter 3 when studying classical systems in the presence of boundaries [53] (see, e.g., Eq. (3.13)). Within this setting, the term S in Eq. (4.14) plays the role of a "bulk" action of the field, whereas S_0 is identified with a boundary term, which is indeed localized at the surface $t = 0$ of the semi-infinite system. In addition, as long as one is interested in emerging collective behaviours of the classical system close to the surface, one can suitably construct a combined renormalisation-group flow for both S and S_0, a fact which leads to the notion of *surface universality* and fixed-point surface actions that we have discussed in Sec. 3.1. In these cases, one can typically assume that not only the most relevant terms of the bulk action are captured by a series expansion of S in the field and its derivatives, but that the same idea applies also to the surface term S_0 [53]. Analogously to what we have done in Chapter 3, below we focus on initial states of the quantum evolution for which S_0 can be expanded in a power series of its arguments.

As in the case of classical systems in the presence of a boundary, the effect of the action S_0 in Eq. (4.14) is to generate effective boundary conditions for the fields $\phi_\pm$, as one can readily verify by determining the configuration of the fields which renders the total action extremal (i.e., solving the "classical" variational problem, see, e.g., Eq. (3.15)). In fact, assuming for the bulk Lagrangian $\mathscr{L}$ the canonical structure

$$\mathscr{L}[\phi] = \frac{1}{2}((\partial_t\phi)^2 - (\vec{\nabla}\phi)^2) - V[\phi], \tag{4.16}$$

where V is a regular function (e.g., a polynomial) of its argument, the functional derivative with respect to the fields generates a boundary condition of the form

$$\partial_t\phi_\pm(x,t)\,|_{t=0} = \pm\frac{\delta S_0[\phi_+(0),\phi_-(0)]}{\delta\phi_\pm(x,0)}, \tag{4.17}$$

which holds at the "classical" level, i.e., for the extremal field. The l.h.s. of this expression is generated by the term $(\partial_t\phi)^2$ which appears in $\mathscr{L}$ (see also the discussion following Eq. (3.15)): a small variation $\phi \to \phi + \delta\phi$ of the field, in fact, yields

$$\int_0^{t_M} \mathrm{d}t\,[\partial_t(\phi(t)+\delta\phi(t))]^2 = \int_0^{t_M} \mathrm{d}t\,\left\{(\partial_t\phi(t))^2 + 2\,(\partial_t\delta\phi(t))\,\partial_t\phi(t) + \ldots\right\}, \tag{4.18}$$

to linear order in $\delta\phi$; integrating by parts the linear contribution, one finds

$$\delta S[\phi,J] = \int \mathrm{d}^d x\left\{\delta\phi(t_M)\partial_t\phi(t)\,|_{t=t_M} - \delta\phi(0)\partial_t\phi(t)\,|_{t=0} + \text{bulk terms}\right\}. \tag{4.19}$$

Accordingly, the variation of the total action with respect to the boundary field $\phi_-(0)$ is given by

$$0 = \frac{\delta(S[\phi_+,J_+] - S[\phi_-,J_-] + S_0[\phi_+(0),\phi_-(0)])}{\delta\phi_-(0)} = \partial_t\phi_-(t)\,|_{t=0} + \frac{\delta S_0[\phi_+(0),\phi_-(0)]}{\delta\phi_-(0)}, \tag{4.20}$$

which, together with the corresponding expression for ϕ_+, yields Eq. (4.17).

If the system under investigation evolves in the proximity of a critical point, collective behaviours are expected to emerge and to affect the resulting non-equilibrium evolution. In this case, the effects of fluctuations become predominant and simple mean-field-like (or Gaussian) approximations fail. As long as one is interested in the leading scaling behaviour which characterises

these emerging phenomena, renormalisation-group arguments allow one to simplify significantly the structure of the total action because terms which are irrelevant by power counting can be discarded, as we have already discussed in Chap. 3. For example, in a theory near four spatial dimensions with a potential containing a term $\propto \phi^4$, the only relevant terms in the initial action S_0 which are symmetric under $\mathbb{Z}_2$ transformations (i.e., $\phi \to -\phi$) are those quadratic in the fields. Consequently, the initial conditions generated by Eq. (4.17) are linear

$$\begin{cases} \partial_t \phi_+(t)\,|_{t=0} = c_{++}\phi_+(0) + c_{+-}\phi_-(0), \\ \partial_t \phi_-(t)\,|_{t=0} = c_{--}\phi_-(0) + c_{-+}\phi_+(0), \end{cases} \tag{4.21}$$

with suitable (generically complex) coefficients $c_{\pm,\pm}$. Constraints of this form are also known as *Robin boundary conditions*. In Sec. 4.3.1 we discuss in detail the constraints which the values of $c_{\pm,\pm}$ are subject to due to the general properties of ρ_0. Linear boundary conditions (or, equivalently, a quadratic $\mathscr{L}_0$) offer the advantage of producing closed equations for the correlation functions, i.e., once inserted into a n-point correlation function, Eq. (4.21) gives rise to an equation which involves only other n-point correlation functions and their time derivatives. Instead, if higher-order terms were included in S_0 (e.g., ϕ^k with $k > 2$) this would generate a hierarchy of equations (connecting, e.g., n-point correlations to $(n+k-2)$-point ones). A quadratic S_0 actually encompasses a wide and physically relevant class of initial states, which include — as we show further below in a simple case — all possible generalised thermal ensembles of an infinite set of harmonic oscillators [103], i.e.,

$$\rho_0 = \mathscr{N}\, \mathrm{e}^{-\int \frac{\mathrm{d}^d k}{(2\pi)^d} \beta_k\, \omega_k\, a_k^\dagger a_k}, \tag{4.22}$$

where $a_k^\dagger$ and a_k are bosonic creation and annihilation operators corresponding to the momentum k, ω_k is the dispersion law, $\beta_k > 0$ a mode-dependent temperature-like variable and $\mathscr{N}$ a normalisation constant which ensures that $\mathrm{tr}\{\rho_0\} = 1$.

4.2 The Euclidean formalism

Here, we briefly discuss the formalism introduced in Refs. [2, 3] in order to describe the dynamics after a quantum quench, presenting it according to the notations introduced above. In particular, consider the expectation value on a pure state $\rho_0 = |\psi_0\rangle\langle\psi_0|$ of an observable $\mathscr{O}$ at time t:

$$\langle \mathscr{O}(t) \rangle = \langle \psi_0 |\, \mathrm{e}^{iHt}\, \mathscr{O}\, \mathrm{e}^{-iHt}\, |\psi_0\rangle\,. \tag{4.23}$$

As mentioned in the previous Sections, this expectation value can be calculated in a path-integral formalism which runs on the evolution contour sketched in Fig. 4.4(a). On the other hand, we can rewrite the expectation above as [3]

$$\langle \mathscr{O}(t) \rangle = \lim_{\varepsilon \to 0^+} \langle \mathscr{O}(t) \rangle_\varepsilon \equiv \lim_{\varepsilon \to 0^+} Z^{-1}\, \langle \psi_0 |\, \mathrm{e}^{iHt - \varepsilon H}\, \mathscr{O}\, \mathrm{e}^{-iHt - \varepsilon H}\, |\psi_0\rangle\,, \tag{4.24}$$

where the two factors $\mathrm{e}^{-\varepsilon H}$ with $\varepsilon > 0$ have been introduced in order to make the corresponding path-integral representation absolutely convergent, while $Z = \langle \psi_0 |\, \mathrm{e}^{-2\varepsilon H}\, |\psi_0\rangle$ normalises the expectation of the identity to 1. The regulator $\mathrm{e}^{-\varepsilon H}$ can be effectively regarded as the evolution

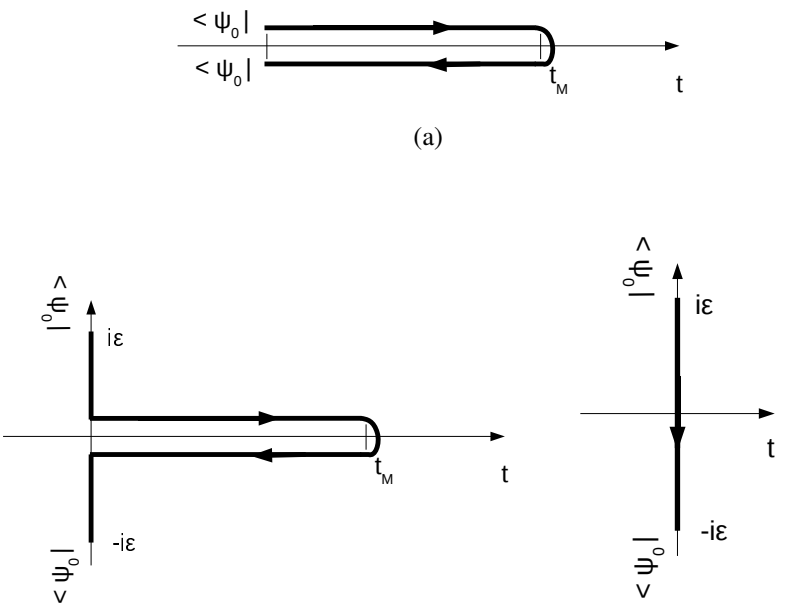

Figure 4.4: Analytic deformation of the Keldysh contour in the plane of complex times: starting from (a), the initial and final points (which correspond, e.g., to the ground state $|\psi_0\rangle$ of some Hamiltonian, i.e., to a pure initial state $\rho_0 = |\psi_0\rangle\langle\psi_0|$) of the oriented contour are moved along the imaginary axis as shown in (b). At the price of relinquishing the direct evaluation of expectation values of operators taken at times on the real axis, the original Keldysh path can be seen as a representation of the identity $\mathrm{e}^{-iHt_M}\mathrm{e}^{iHt_M}$ and can be therefore shrunk to 0, bringing the whole contour onto the imaginary axis, as presented in (c).

operator from complex time T to $T - i\varepsilon$, leading to a path-integral of the form

$$\langle \mathscr{O}(t)\rangle_\varepsilon = \int \mathscr{D}\phi\ \langle\psi_0|\,\phi(-i\varepsilon)\rangle\,\langle\phi(i\varepsilon)|\,\psi_0\rangle\ \langle\phi(t)|\,\mathscr{O}\,|\phi(t)\rangle\ \mathrm{e}^{i\int_\gamma \mathrm{d}t\, L[\phi]}, \tag{4.25}$$

where the contour γ is shown in Fig. 4.4(b). Note that our convention is slightly different from the one adopted in Refs. [2, 3], because we take $T = i\varepsilon$ as the starting point of our contour, instead of $T = 0$. The path displayed in Fig. 4.4(b) constitutes clearly a specific choice which involves a separation of the evolution with imaginary and real time (e.g., in the upper half-plane of complex times we take first $\mathrm{e}^{-\varepsilon H}$ and then e^{-itH}). Actually, a different discretisation of the time interval would result in any path which proceeds from $i\varepsilon$ on the imaginary axis downwards and rightwards towards t on the real axis and from there downwards and leftwards towards $-i\varepsilon$ on the imaginary axis; by introducing the identity operator in the form $\mathrm{e}^{-iHt'}\mathrm{e}^{iHt'}$ with generic real t' one can relax the constraint about the rightwards and leftwards motion in the upper and lower complex half-plane, respectively (see Fig. 4.2); by analogy, one could think of doing the same for the downwards motion by adding a product $\mathrm{e}^{-H\tau'}\mathrm{e}^{H\tau'}$ (with non-vanishing, real τ'), which is again an acceptable

rewriting of the identity; however, this expression poses serious problems to the construction of the path integral whenever the spectrum of H is not bounded from above. For example, for an infinitesimal interval $\tau' = \delta\tau > 0$ one would find a propagator of the form $\langle\phi(\tau_0+\delta\tau)|\,\mathrm{e}^{\delta\tau H}\,|\phi(\tau_0)\rangle$, where τ_0 is the point of insertion, which is generally ill-defined, as it can be easily checked in the example reported in the next Section (see Eq. (4.63)). As a consequence, the path in Fig. 4.4(b) can be actually deformed in an arbitrary way which keeps the end points $\pm i\varepsilon$ fixed and still passes through t (i.e., the time at which the observable $\mathscr{O}$ is measured), but never proceeds upwards. This freedom in the choice of the path appears to clash with the fact that Eq. (4.24) is uniquely defined; thus, Eq. (4.25) must not depend on the choice of the contour γ and, since the latter appears only in the argument of the exponential, this in turn implies that the Lagrangian $L[\phi(t)]$ must be treated as an analytic function of the time variable. This conclusion allows one to calculate $\langle\mathscr{O}(t)\rangle$ with a different approach: in fact, assuming that this quantity is analytic in t, the analysis can be restricted entirely to the imaginary axis by determining

$$\langle\mathscr{O}(i\tau)\rangle_\varepsilon \equiv Z^{-1}\,\langle\psi_0|\,\mathrm{e}^{-(\varepsilon+\tau)H}\,\mathscr{O}\,\mathrm{e}^{-(\varepsilon-\tau)H}\,|\psi_0\rangle\,, \tag{4.26}$$

on the interval $-\varepsilon < \tau < \varepsilon$ — which ensures that all expressions are well-defined — and by performing an eventual analytic continuation to real times. The path-integral representation of Eq. (4.26) becomes equivalent to one describing a static system confined in a film of width 2ε, i.e.,

$$\langle\mathscr{O}(i\tau)\rangle_\varepsilon = \int \mathscr{D}\phi\;\langle\psi_0|\,\phi(-i\varepsilon)\rangle\,\langle\phi(i\varepsilon)|\,\psi_0\rangle\,\langle\phi(i\tau)|\,\mathscr{O}\,|\phi(i\tau)\rangle\,\mathrm{e}^{-\int_{-\varepsilon}^{\varepsilon}\mathrm{d}\tau L_E[\phi]}, \tag{4.27}$$

where $L_E = \int \mathrm{d}^d x\,\mathscr{L}_E$ is the Euclidean Lagrangian which is obtained from $-L$ by substituting ∂_t with $i\partial_\tau$; for example, for a Lagrangian of the canonical form (4.16) one has

$$\mathscr{L}_E = \frac{1}{2}((\partial_\tau\phi)^2 + (\vec{\nabla}\phi)^2) + V[\phi]. \tag{4.28}$$

The integration contour associated with Eq. (4.27) is sketched in Fig. 4.4(c). Thereby, the initial dynamical problem has been reformulated in terms of an Euclidean field theory with surfaces, where the initial state $|\psi_0\rangle$ encodes the boundary conditions. The approach that we have just described proves to be particularly useful in the case of conformal theories in two dimensions, which — being exactly solvable — can be rather straightforwardly continued to real times; boundary states which preserve the conformal invariance, however, are in general not normalisable [73, 104]. In order to overcome this difficulty it is then preferable to consider an initial state $|\psi_0\rangle$ which is slightly different from one of them. In fact, following Refs. [2, 3] one can argue that, as long as the interest is in the leading scaling behaviour close to quantum critical points, the expectation value in Eq. (4.24) is not actually determined by $|\psi_0\rangle$ but by the boundary state $|\psi_0^*\rangle$ to which $|\psi_0\rangle$ flows under renormalisation group (RG) transformations. In this respect, the state $|\psi_0\rangle$ gives rise to boundary conditions which are approximately equivalent to the ones generated by $|\psi_0^*\rangle$, the main difference being that they are translated from the actual edges $\pm\varepsilon$ to effective boundaries positioned at $\pm(\tau_0+\varepsilon)$. In a sense, τ_0 can be regarded as being equivalent to the *extrapolation length* [24, 53] that we have introduced in Sec. 3.1.1 and illustrated in Figs. 3.2. In fact, as in the classical case it provides a measure of the "distance" from the corresponding surface critical point, in the Euclidean one it encodes the distance from the RG-invariant state. Consequently to

its introduction, the limit $\varepsilon \to 0$ can be safely taken; the width of the resulting film is then twice the extrapolation length τ_0. The considerations above, which hold for a one-time expectation, can be straightforwardly generalised to the case of n-time correlation functions

$$\langle T^* [\mathscr{O}(i\tau_1)\dots\mathscr{O}(i\tau_n)]\rangle_\varepsilon = \int \mathscr{D}\phi \, \langle\psi_0|\,\phi(-i\varepsilon)\rangle \langle\phi(i\varepsilon)|\,\psi_0\rangle \, O(i\tau_1)\dots O(i\tau_n)\, \mathrm{e}^{-\int_{-\varepsilon}^{\varepsilon} \mathrm{d}\tau L_E[\phi]}, \quad (4.29)$$

where $O(i\tau_k) = \langle\phi(i\tau_k)|\,\mathscr{O}\,|\phi(i\tau_k)\rangle$. The time anti-ordering T^* takes into account the orientation of the path along the imaginary axis (see Fig. 4.4(c)). The real-time correlation functions one is actually interested in can be obtained by analytically continuing Eq. (4.29) back to real values and then by taking the limit $\varepsilon \to 0$. Thus, whenever the Euclidean theory is analytically solvable in a confined geometry, the corresponding non-equilibrium dynamics is also exactly solvable.

4.2.1 Conformal field theories

In critical systems, the emergence of scale invariance, combined with the preexisting translational and rotational ones, gives rise to conformal symmetry [73]. As a matter of fact, this increases the constraints imposed on observables to the point that one can completely fix the scaling behaviour of two- and three-point functions to

$$\begin{aligned} \langle\Phi_{i_1}(\vec{x}_1)\Phi_{i_2}(\vec{x}_2)\rangle &= \frac{C_{i_1 i_2}\,\delta_{\Delta_{i_1}\Delta_{i_2}}}{|\vec{x}_1-\vec{x}_2|^{2\Delta_{i_1}}}, \\ \langle\Phi_{i_1}(\vec{x}_1)\Phi_{i_2}(\vec{x}_2)\Phi_{i_3}(\vec{x}_3)\rangle &= \frac{C_{i_1 i_2 i_3}}{x_{12}^{\Delta_{i_1}+\Delta_{i_2}-\Delta_{i_3}}\, x_{23}^{\Delta_{i_2}+\Delta_{i_3}-\Delta_{i_1}}\, x_{13}^{\Delta_{i_3}+\Delta_{i_1}-\Delta_{i_2}}}, \end{aligned} \quad (4.30)$$

where $\Delta_{i_j} \equiv \left[\Phi_{i_j}\right]$ denotes the scaling dimension of the j-th field and where we introduced the shorthand notation $x_{ab} = |\vec{x}_a - \vec{x}_b|$. On the other hand, should four or more points be involved, conformal invariants such as the *anharmonic ratio* $x_{12}x_{34}/(x_{23}x_{14})$ can be constructed, making it impossible to completely determine the corresponding scaling forms. Four-point functions, for instance, can be generically cast as

$$\langle\Phi_{i_1}(\vec{x}_1)\dots\Phi_{i_4}(\vec{x}_4)\rangle = F\left(\frac{x_{12}x_{34}}{x_{13}x_{24}}, \frac{x_{12}x_{34}}{x_{14}x_{23}}\right) \prod_{a<b}^{4} x_{ab}^{\frac{1}{3}\left(\sum_{j=1}^{4}\Delta_{i_j}\right)-\Delta_{i_a}-\Delta_{i_b}}, \quad (4.31)$$

with F a regular function of its arguments which depends on the specific model.

The case of two-dimensional systems is special in the fact that the conformal symmetry is characterised by an infinite set of generators and therefore provides an extremely stringent constraint on their physical properties [73, 74, 105]. In particular, a generic *conformal transformation*

$$x' = f_1(x,t), \qquad t' = f_2(x,t) \quad (4.32)$$

must obey the conditions [73]

$$\frac{\partial f_1}{\partial x} = \frac{\partial f_2}{\partial t} \qquad \frac{\partial f_2}{\partial x} = -\frac{\partial f_1}{\partial t} \quad (4.33)$$

which become completely equivalent to Cauchy-Riemann conditions when rewritten in a complex formalism $z = x + it$, $f = f_1 + if_2$. This implies that f must be holomorphic (to be more precise, also the corresponding antiholomorphic part must be generally included). Fields which transform according to this extended set of transformations are referred to as *primary* and completely encode the operator content of the theory, i.e., every other one can be derived from them. Under a conformal map $w \to z(w)$, their expectations are reshaped as

$$\langle \Phi_{i_1}(w_1) \dots \Phi_{i_n}(w_n) \rangle = \left| \frac{dw}{dz} \right|^{-\Delta_{i_1}}_{w=w_1} \dots \left| \frac{dw}{dz} \right|^{-\Delta_{i_n}}_{w=w_n} \langle \Phi_{i_1}(z(w_1)) \dots \Phi_{i_n}(z(w_n)) \rangle \,. \tag{4.34}$$

Moreover, the number of independent anharmonic ratios is reduced; for a single field Φ, the four-point function (4.31) takes the simpler form

$$\langle \Phi(z_1) \dots \Phi(z_4) \rangle = \left(\frac{z_{14}\, z_{23}}{z_{12}\, z_{13}\, z_{34}\, z_{24}} \right)^{2\Delta} F(\eta) \quad \text{with} \quad \eta = \frac{z_{13}\, z_{24}}{z_{14}\, z_{23}}. \tag{4.35}$$

As we have mentioned above, conformal symmetry can still be employed in systems with surfaces, provided that the boundary conditions do not break it completely [104, 106]. In particular, for semi-infinite systems one can think of the real axis as a mirror reflecting the holomorphic part into the upper complex half-plane (UHP) into the antiholomorphic one in the lower half-plane (LHP). As a consequence, such as in the case of image charges in the presence of a flat surface, the number of points is effectively doubled and one can write a generic n-point function in the bounded geometry as a $2n$-point function in the bulk depending on the original coordinates $z_1, \dots z_n$ and their conjugates $\bar{z}_1, \dots \bar{z}_n$. For example, the two-point function in the UHP can be rewritten as the four-point one in Eq. (4.35) with $z_3 \to \bar{z_1}$ and $z_4 \to \bar{z}_2$ [3, 106]

$$\langle \Phi(z_1) \Phi(z_2) \rangle_{UHP} = \left(\frac{z_{1\bar{2}}\, z_{2\bar{1}}}{z_{12}\, z_{\bar{1}\bar{2}}\, z_{1\bar{1}}\, z_{2\bar{2}}} \right)^{2\Delta} F_s(\eta) \quad \text{with} \quad \eta = \frac{z_{1\bar{1}}\, z_{2\bar{2}}}{z_{1\bar{2}}\, z_{2\bar{1}}}, \tag{4.36}$$

where now F_s does not depend just on the model, but also on the boundary conditions chosen. For example, for the free boson one has $F_s \equiv 1$, whereas for the critical Ising model $\Delta = 1/16$ and

$$F_s(\eta) = \frac{\sqrt{1+\eta^{\frac{1}{2}}} \pm \sqrt{1-\eta^{\frac{1}{2}}}}{\sqrt{2}}, \tag{4.37}$$

where the $\pm$ sign distinguishes fixed from free boundary conditions, respectively. The great advantage of considering conformal-invariant systems is that this particular geometry substantially encodes every other one which can be reached by a holomorphic transformation. In particular, a strip of width $2\tau_0$ such as the one defined in the previous Section can be obtained by applying the map

$$w(z) = \frac{2\tau_0}{\pi} \ln z - i\tau_0 \quad \text{,i.e.,} \quad z(w) = \mathrm{e}^{\frac{\pi(w+i\tau_0)}{2\tau_0}}, \tag{4.38}$$

the effects of which are sketched in Fig. 4.5. Correspondingly, observables in the strip can be

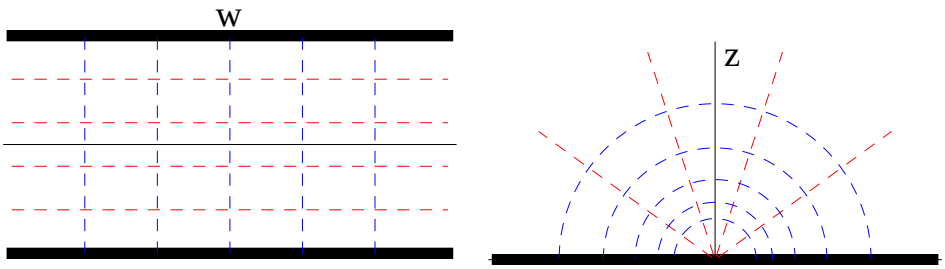

Figure 4.5: Effect of the conformal transformation (4.38); the strip (a) in the w plane is mapped into the upper half plane (b) in z coordinates; its boundaries correspond to the positive and negative real semi-axes and the real axis in the former description becomes the upper imaginary axis in the latter. The coloured lines are meant to depict how the remaining part of the space is mapped.

calculated from their counterparts in the upper half-plane by means of Eq. (4.34); accounting for simplicity for observables built with just a single primary operator one obtains

$$\begin{aligned}\langle\Phi(w_1)\dots\Phi(w_n)\rangle_{strip} &= \prod_{j=1}^{n}\left|\frac{2\tau_0}{\pi}\exp\left\{-\frac{\pi(w_j+i\tau_0)}{2\tau_0}\right\}\right|^{-\Delta}\times \\ \times\left\langle\Phi\left(\exp\left\{\frac{\pi(w_1+i\tau_0)}{2\tau_0}\right\}\right)\dots\Phi\left(\exp\left\{\frac{\pi(w_n+i\tau_0)}{2\tau_0}\right\}\right)\right\rangle_{UHP}&.\end{aligned} \tag{4.39}$$

In the previous Section, we have seen that a dynamical problem can be mapped into an Euclidean one confined in a film; thus, we now rewrite the complex coordinate as $w = r + i\tau$, where τ denotes the imaginary part of complex times, which is forced to satisfy $-\tau_0 < \tau < \tau_0$. We now wish to apply the transformation (4.39) to the two-point function (4.36); for scalar fields, the antiholomorphic part can be accounted for simply by doubling the dimension of the Jacobians, i.e.,

$$\left|\frac{dw}{dz}\right|^{-\Delta}\left|\frac{d\bar{w}}{d\bar{z}}\right|^{-\Delta}\to\left|\frac{dw}{dz}\right|^{-2\Delta}, \tag{4.40}$$

yielding

$$\begin{aligned}\langle\Phi(r,i\tau_1)\Phi(0,i\tau_2)\rangle_{strip} &= \left|\left(\frac{2\tau_0}{\pi}\right)^2 e^{-\rho}\right|^{-2\Delta}\times \\ \times\left(\frac{\cosh\rho+\cos(\theta_1+\theta_2)}{2e^{\rho}\left[\cos(\theta_1-\theta_2)+\cos(\theta_1+\theta_2)\right]\left[\cosh\rho-\cos(\theta_1-\theta_2)\right]}\right)^{2\Delta}&F_s(\eta),\end{aligned} \tag{4.41}$$

where we have introduced the shorthand notation

$$\rho=\frac{\pi r}{2\tau_0}\quad\text{and}\quad\theta_j=\frac{\pi\tau_j}{2\tau_0}\quad\text{with}\quad\theta_j\in\left[-\frac{\pi}{2},\frac{\pi}{2}\right], \tag{4.42}$$

which expresses distances and times in units of the strip width — i.e., of the extrapolation length — and

$$\eta = \frac{\cos(\theta_1 - \theta_2) + \cos(\theta_1 + \theta_2)}{\cosh\rho + \cos(\theta_1 + \theta_2)} = \frac{2\cos\theta_1 \cos\theta_2}{\cosh\rho + \cos(\theta_1 + \theta_2)}. \tag{4.43}$$

We recall that we are considering systems which are translationally-invariant in space, thus our choice of r and 0 as spatial coordinates of the fields involved in the expectation is completely general.

The properties of the dynamics in real time are recovered upon performing the analytic continuation $\tau_j \to -it_j$ of Eq. (4.41), which however requires the knowledge of the function F_s. Although the specific form of this function is system-dependent and not many instances are known, as was pointed out in Refs. [2, 3] its asymptotic features for $\eta \to 0$ and 1 are universal: in fact, from Eq. (4.43), one can see that at the boundaries $\theta_j = \pm\pi/2$ the anharmonic ratio η linearly vanishes, whilst the argument of the round brackets in Eq. (4.41) diverges as $(\theta_j \mp \pi/2)^{-1}$. Since in the proximity of a surface $\theta_j \to \pm\pi/2$, the short-distance expansion

$$\Phi(\rho, i\theta_j) \sim \left(\theta_j \mp \frac{\pi}{2}\right)^{2(\Delta_b - \Delta)} \Phi_b(\rho) \tag{4.44}$$

is expected to hold in terms of the boundary operator Φ_b corresponding to the field Φ and of its scaling dimension $2\Delta_b = [\Phi_b]$, one concludes that [3]

$$F_s(\eta) \sim \eta^{2\Delta_b} \quad \text{for} \quad \eta \to 0. \tag{4.45}$$

On the other hand, far from the boundaries the two-point function must reproduce the bulk behaviour and, in particular, the ultraviolet divergence at coincident points, which is already captured by the prefactors in Eq. (4.41). Setting $\rho = 0$ and $\theta_1 = \theta_2$ yields $\eta = 1$, which implies that $F_s(1) = 1$. Thus, the prescription $\tau_j \mapsto -it_j$ allows the determination of the general asymptotic behaviour of the two-time correlation function after a quench: for fixed times t_j it does not depend on r for $r \ll |t_1 - t_2|$ and takes a value $\propto \mathrm{e}^{-\Delta\pi|t_1 - t_2|/\tau_0}$. It decays exponentially $\propto \mathrm{e}^{-\pi\Delta r/\tau_0}$ for $|t_1 - t_2| \ll r \ll t_1 + t_2$, while $\propto \mathrm{e}^{-\Delta_b \pi r/\tau_0 - \Delta\pi(t_1+t_2)/\tau_0}$ for $r \gg t_1 + t_2$.

4.3 Two approaches, the same physics: a detailed comparison

Clearly, physics demands that different approaches to the same problem yield the same conclusions. Therefore, the Keldysh and the Euclidean frameworks for studying non-equilibrium quantum dynamics described in the previous two Sections ought to be equivalent. This Section is devoted to establishing a relationship between them; in particular, the imaginary-time formalism employs concepts which are proper of the theory of static systems with boundaries (introduced in Chapter 3), hence it is important to understand how the initial conditions (4.17) actually affect the boundary conditions at the edges of the film. Furthermore, note that in the Euclidean scheme the time coordinate is "single-valued", i.e., times along the imaginary axis are visited just once by the integration path in Fig. 4.4(c); as a consequence, choosing n points on the imaginary axis uniquely defines the expectation (4.29). Conversely, in the Keldysh formalism fixing n times on the real axis is not sufficient, as one generally needs to distinguish between those lying on the forward

and backward branches of the contour in Fig. 4.1. This brings forth in principle a 2^n degeneracy for n-point functions, i.e., one can define 2^n different ones depending on the ordering. Therefore, it remains to be determined how to extract 2^n functions defined on real times from the analytic continuation of just a single one defined on the imaginary axis.

In Sec. 4.3.1 we treat in detail these issues in the simplest possible instance, i.e., a $0+1$-dimensional system. In Sec. 4.3.2 we generalise the discussion to the case of quantum field theories and provide a few relevant examples on how to reconstruct Keldysh correlations from the Euclidean formalism.

4.3.1 Quantum mechanics

In order to better understand the properties of the imaginary-time formalism discussed in Sec. 4.2 we consider it in the simplest possible instance, i.e., the (non-relativistic) quantum mechanics of a single particle which is initially prepared in a state described by the density matrix $\boldsymbol{\rho_0}$ and then evolves according to the Hamiltonian

$$H = \frac{\mathbf{p}^2}{2} + V(\mathbf{x}). \tag{4.46}$$

Here $\mathbf{x}$ and $\mathbf{p}$ are the canonically conjugate "position" and "momentum" variables, respectively, with $[\mathbf{x},\mathbf{p}] = i$ (we set $\hbar = 1$), while the mass of the particle has been fixed for simplicity to 1, and the potential V is assumed to be physical, i.e., such that H has a spectrum bounded from below. In the Heisenberg picture any observable $\mathscr{O}$ evolves according to $\mathscr{O}(t) = \mathrm{e}^{iHt}\mathscr{O}\mathrm{e}^{-iHt}$; in what follows, if the time t is not explicitly indicated as an argument, the observable is meant to be evaluated at time $t = 0$. Note that the present case is a special zero-dimensional instance of the dynamics of the field discussed in Sec. 4.1.1: indeed if one identifies the field ϕ with the position $\mathbf{x}$ and consequently $\partial_0\phi$ with the momentum $\mathbf{p}$, the Hamiltonian in Eq. (4.46) has the same structure as $\mathscr{L}[\phi]$ in Eq. (4.16), up to the additional spatial degrees of freedom. Accordingly, all the path-integral formalism discussed in Sec. 4.1.1 applies to the present case and in particular Eq. (4.21) becomes

$$\begin{cases} \partial_t \mathbf{x}(t)|_{t=0_+} \equiv \dot{\mathbf{x}}(0_+) = c_{++}\,\mathbf{x}(0_+) + c_{+-}\,\mathbf{x}(0_-), \\ \partial_t \mathbf{x}(t)|_{t=0_-} \equiv \dot{\mathbf{x}}(0_-) = c_{--}\,\mathbf{x}(0_-) + c_{-+}\,\mathbf{x}(0_+). \end{cases} \tag{4.47}$$

A discussion of the implications deriving from choosing linear boundary conditions will be provided further below. We emphasize again that the distinction between times lying on the forward (0_+) and backward (0_-) branch of the Keldysh contour is relevant for ordering purposes only; once the order of the operators has been made explicit, the indices can be dropped. In order to relate Eq. (4.47) to the properties of the density matrix $\boldsymbol{\rho_0}$ which actually defines the initial state of the quench, consider a generic expectation of a product $\mathscr{O}'\mathscr{O}$ of quantities defined over the Keldysh contour, such that $\mathscr{O}' = \mathscr{O}'(t_1,\ldots,t_m)$ depends on generic but non-vanishing times $t_1,\ldots,t_n$, whereas $\mathscr{O}$ is taken at time $0_\pm$. Under the ordering T_K, $\mathscr{O}(0_-)$ is moved to the left of such a product, whereas $\mathscr{O}(0_+)$ to its right (see Eq. (4.2)):

$$T_K\left[\mathscr{O}'\mathscr{O}(0_+)\right] = T_K\left[\mathscr{O}'\right]\mathscr{O}(0), \tag{4.48}$$

$$T_K\left[\mathscr{O}'\mathscr{O}(0_-)\right] = \mathscr{O}(0)T_K\left[\mathscr{O}'\right]. \tag{4.49}$$

Hence, one can readily verify that the average $\langle T_K[\mathscr{O}'\mathbf{x}(t)]\rangle \equiv \mathrm{tr}\{T_K[\mathscr{O}'\mathbf{x}(t)]\,\boldsymbol{\rho_0}\}$ obeys, at $t=0^+$, the boundary condition

$$\begin{aligned}\partial_t \left\langle T_K\left[\mathscr{O}'\mathbf{x}(t)\right]\right\rangle|_{t=0^+} &= \mathrm{tr}\left\{T_K\left[\mathscr{O}'\dot{\mathbf{x}}(0_+)\right]\boldsymbol{\rho_0}\right\} = \\ &= c_{++}\,\mathrm{tr}\left\{T_K\left[\mathscr{O}'\right]\mathbf{x}(0)\boldsymbol{\rho_0}\right\} + c_{+-}\,\mathrm{tr}\left\{T_K\left[\mathscr{O}'\right]\boldsymbol{\rho_0}\mathbf{x}(0)\right\},\end{aligned} \tag{4.50}$$

which follows from Eq. (4.47) and in which the cyclic property of the trace has been used in order to rewrite the last term. On the other hand, $\dot{\mathbf{x}}$ is an observable in its own right and therefore obeys Eq. (4.48); consequently,

$$\mathrm{tr}\left\{T_K\left[\mathscr{O}'\right]\dot{\mathbf{x}}(0)\boldsymbol{\rho_0}\right\} = c_{++}\,\mathrm{tr}\left\{T_K\left[\mathscr{O}'\right]\mathbf{x}(0)\boldsymbol{\rho_0}\right\} + c_{+-}\,\mathrm{tr}\left\{T_K\left[\mathscr{O}'\right]\boldsymbol{\rho_0}\mathbf{x}(0)\right\}. \tag{4.51}$$

Since Eq. (4.50) must hold for every possible choice of $\mathscr{O}'$, one concludes that

$$\dot{\mathbf{x}}(0)\boldsymbol{\rho_0} = c_{++}\,\mathbf{x}(0)\boldsymbol{\rho_0} + c_{+-}\,\boldsymbol{\rho_0}\mathbf{x}(0). \tag{4.52}$$

Repeating the same procedure for the boundary condition at $t=0_-$, one finds

$$\boldsymbol{\rho_0}\dot{\mathbf{x}}(0) = c_{--}\,\boldsymbol{\rho_0}\mathbf{x}(0) + c_{-+}\,\mathbf{x}(0)\boldsymbol{\rho_0} \tag{4.53}$$

and, because of the form of the Hamiltonian (4.46), one can use the equation of motion $\dot{\mathbf{x}} = \mathbf{p}$ in order to rewrite Eqs. (4.52) and (4.53) as

$$\begin{cases} \mathbf{p}\,\boldsymbol{\rho_0} = c_{++}\,\mathbf{x}\,\boldsymbol{\rho_0} + c_{+-}\,\boldsymbol{\rho_0}\,\mathbf{x}, \\ \boldsymbol{\rho_0}\,\mathbf{p} = c_{--}\,\boldsymbol{\rho_0}\,\mathbf{x} + c_{-+}\,\mathbf{x}\,\boldsymbol{\rho_0}. \end{cases} \tag{4.54}$$

In terms of the "kernel" $\rho_0(x,y) = \langle x|\,\boldsymbol{\rho_0}\,|y\rangle$, with $\mathbf{x}|x\rangle = x|x\rangle$ (and $\mathbf{p}|x\rangle = -i\partial_x|x\rangle$), Eq. (4.54) turns into a system of differential equations

$$\begin{cases} (i\partial_x + c_{++}x + c_{+-}y)\rho_0(x,y) = 0, \\ (-i\partial_y + c_{--}y + c_{-+}x)\rho_0(x,y) = 0, \end{cases} \tag{4.55}$$

which admits solution only if $c_{+-} = -c_{-+}$; under this condition one then finds

$$\rho_0(x,y) = \mathscr{N}\exp\left\{\frac{i}{2}[c_{++}x^2 - c_{--}y^2 + 2c_{+-}xy]\right\}, \tag{4.56}$$

where $\mathscr{N}$ is a normalisation constant. In order for ρ_0 to be a bona-fide density matrix, it has to satisfy the conditions [107] (i) $\boldsymbol{\rho_0} = \boldsymbol{\rho_0}^\dagger$, (ii) $\mathrm{tr}\{\boldsymbol{\rho_0}\} = 1$, and (iii) $\mathrm{tr}\{\boldsymbol{\rho_0}^2\} \leq 1$ which, in turn, imply: (i) $c_{++} = c_{--}^*$ and $c_{+-} = -c_{+-}^*$, so that $c_{++} = a+ib$, $c_{--} = a-ib$ and $c_{+-} = id$, with real coefficients a, b, and d; (ii) $b+d>0$ and $\mathscr{N} = \sqrt{(b+d)/\pi}$; (iii) $b>0$ and $d\leq 0$. The expressions for $\rho_0(x,y)$ and the corresponding boundary conditions thus become

$$\rho_0(x,y) = \sqrt{\frac{b+d}{\pi}}\exp\left\{-\frac{1}{2}\left[b(x^2+y^2) + 2dxy - ia(x^2-y^2)\right]\right\}. \tag{4.57}$$

and

$$\begin{cases} \partial_t \mathbf{x}(t)|_{t=0_+} = (a+ib)\,\mathbf{x}(0_+) + id\,\mathbf{x}(0_-), \\ \partial_t \mathbf{x}(t)|_{t=0_-} = (a-ib)\,\mathbf{x}(0_-) - id\,\mathbf{x}(0_+), \end{cases} \tag{4.58}$$

respectively. By a direct calculation, the square of the density matrix turns out to be

$$\langle x|\,\boldsymbol{\rho}_{\mathbf{0}}^2\,|y\rangle = \rho_0(x,y)\sqrt{1+\frac{d}{b}}\exp\left\{d\,xy + \frac{d^2}{4b}(x+y)^2\right\}, \tag{4.59}$$

and therefore the initial state is pure, i.e., $\boldsymbol{\rho}_{\mathbf{0}}^2 = \boldsymbol{\rho}_{\mathbf{0}}$ [107], if and only if $d = 0$. Furthermore, for $a = 0$ the resulting density matrix in Eq. (4.57) can be attributed a precise physical meaning for every allowed choice of b and d: in fact, if we parametrise these coefficients as

$$b = m_0\omega_0\frac{\cosh(\beta_0\omega_0)}{\sinh(\beta_0\omega_0)} \quad \text{and} \quad d = -m_0\omega_0\frac{1}{\sinh(\beta_0\omega_0)} \tag{4.60}$$

in terms of the parameters $\beta_0\omega_0$ and $m_0\omega_0$, one may recognise in Eq. (4.56) the Gibbs distribution of a quantum harmonic oscillator of mass m_0, frequency ω_0 and inverse temperature $\beta_0 = 1/(k_B T_0)$. On the other hand, the pure states $|\psi_{a,b}\rangle$ obtained for $d = 0$, with $\langle x|\psi_{a,b}\rangle = \mathcal{N}^{-1/2}\exp\{-(b-ia)x^2/2\}$, do not seem to have a clear interpretation for $a \neq 0$, although they can be obtained as $\mathrm{e}^{ia\mathbf{x}^2/2}\,|\psi_{0,b}\rangle$, where $|\psi_{0,b}\rangle$ is the ground-state wave function of a harmonic oscillator of frequency b and unit mass (i.e., with $\beta_0 \to +\infty$, $\omega_0 = b$ and $m_0 = 1$ in Eq. (4.60)).

Summarising, at least in this simple case we have been able to determine the exact form of the initial state which eventually gives rise to the linear boundary conditions (4.47); moreover, it turns out that the assumption of their linearity, although representing a rather strong constraint, nonetheless captures all thermal ensembles of an harmonic oscillator. In addition, we determined the operatorial identities associated with these states (Eqs. (4.52) and (4.53)), which will prove useful in the following because they remain valid also when the formalism is extended to encompass complex times.

In order to compare the Keldysh approach briefly reviewed in Secs. 4.1 and 4.1.1 with the one presented in Sec. 4.2, we discuss below how to construct n-time correlation functions of the system with Hamiltonian H defined in imaginary time $i\tau$ in such a way that they correctly reproduce the results of the former approach after analytic continuation to the real axis. With this purpose in mind, we introduce the quantum evolution in imaginary time as a straightforward extension of the case in real time:

$$\mathscr{O}(i\tau) = \mathrm{e}^{-\tau H}\mathscr{O}\mathrm{e}^{\tau H}. \tag{4.61}$$

The corresponding kernel representation is

$$K(x,y,i\tau) = \langle x|\,\mathrm{e}^{\tau H}\,|y\rangle\,, \tag{4.62}$$

which is well-defined for every $\tau \leq 0$, while this might not be the case for $\tau > 0$ since the spectrum of the Hamiltonian H is often unbounded from above. In the simple but paradigmatic case of a free particle of mass m in one spatial dimension

$$K(x,y,i\tau) = \int_{-\infty}^{+\infty}\frac{\mathrm{d}p}{2\pi}\,\mathrm{e}^{ip(x-y)}\,\mathrm{e}^{\tau p^2/(2m)}, \tag{4.63}$$

which, as expected, describes a diffusion process with diffusion coefficient $D = m^{-1}$ for $\tau \leq 0$ while it is not defined for $\tau > 0$. In order to remain within the domain of definition of K, it is therefore necessary to guarantee that $\tau \leq 0$. The consequences of this request may be better understood with an example: consider the average

$$\langle \mathscr{O}(i\tau_1)\dots\mathscr{O}(i\tau_n)\rangle = \left\langle \mathrm{e}^{-\tau_1 H}\mathscr{O}\mathrm{e}^{-(\tau_2-\tau_1)H}\mathscr{O}\dots\mathrm{e}^{-(\tau_n-\tau_{n-1})H}\mathscr{O}\mathrm{e}^{\tau_n H}\right\rangle; \tag{4.64}$$

by inserting the resolution of the identity $\mathbb{1} = \int \mathrm{d}x\,|x\rangle\langle x|$ between consecutive operators, one can see that the resulting kernels depending on $\tau_{i+1}-\tau_i$ require a time ordering along the imaginary axis $\tau_i \leq \tau_{i+1}$ with $i = 1\dots n$, as indicated in Fig. 4.6(a), whereas the first and the last one, which depend on τ_1 and τ_n, impose the additional constraints $\tau_n \leq 0 \leq \tau_1$. These conditions can be simultaneously satisfied only if all τ_i vanish, i.e., $\tau_i = 0$, $\forall i$. In order to have a sound imaginary-time theory we therefore need to introduce some kind of regularisation at the boundaries which relaxes the last of these constraints. In particular, this can be done at the two extremes of the string of operators, by introducing terms $\mathrm{e}^{-\varepsilon H}$ with arbitrary $\varepsilon > 0$, such that the resulting conditions become $\tau_n \leq \varepsilon$ and $-\varepsilon \leq \tau_1$. Accordingly, we define

$$\langle \mathscr{O}(i\tau_1)\dots\mathscr{O}(i\tau_n)\rangle_\varepsilon = \frac{\left\langle \mathrm{e}^{-\varepsilon H}\,T^*\left[\mathscr{O}(i\tau_1)\dots\mathscr{O}(i\tau_n)\right]\mathrm{e}^{-\varepsilon H}\right\rangle}{\left\langle \mathrm{e}^{-2\varepsilon H}\right\rangle}, \tag{4.65}$$

where T^* is analogous to the time anti-ordering operator introduced in Eq. (4.2), the only difference being that it now orders the imaginary part of the (imaginary) times. The normalisation factor at the denominator is chosen in such a way that $\langle \mathbb{1}\rangle_\varepsilon = 1$. Equation (4.65) is the straightforward generalisation of Eq. (2) of Ref. [2] to n-point functions. Differently from Eq. (4.64), Eq. (4.65) admits a well-defined representation for $-\varepsilon \leq \tau_i \leq \tau_j \leq \varepsilon\ \forall\, i \leq j$, i.e., the resulting theory is defined on a film of width 2ε symmetric with respect to the real axis, as sketched in Fig. 4.6(b). (Note that, in principle, one could introduce two different values $\varepsilon_R > 0$ and $\varepsilon_L > 0$ at the right and left extremes of the string of operators and a suitable normalisation factor; however, for our purposes, this represents an unnecessary complication.) The translation of the boundary conditions (4.47) from $t = 0$ to $\tau = \pm i\varepsilon$ is more easily understood by considering their formulation (4.54) in terms of operators: in fact, from Eq. (4.61) one has

$$\partial_\tau \mathbf{x}(i\tau) = \mathrm{e}^{-\tau H}\,[\mathbf{x}, H]\,\mathrm{e}^{\tau H} = \mathrm{e}^{-\tau H}\,i\mathbf{p}\,\mathrm{e}^{\tau H}, \tag{4.66}$$

which implies, for the operator within $\langle \mathbf{x}(i\tau)\rangle_\varepsilon \propto \mathrm{tr}\left\{\mathrm{e}^{-\varepsilon H}\boldsymbol{\rho}_0\mathrm{e}^{-\varepsilon H}\mathbf{x}(i\tau)\right\}$, the identity

$$\begin{aligned}\partial_\tau\left(\mathrm{e}^{-\varepsilon H}\,\boldsymbol{\rho}_0\,\mathrm{e}^{-\varepsilon H}\mathbf{x}(i\tau)\right)|_{\tau=-\varepsilon} &= \mathrm{e}^{-\varepsilon H}\,i\,\boldsymbol{\rho}_0\,\mathbf{p}\,\mathrm{e}^{-\varepsilon H}\mathrm{e}^{-\varepsilon H}\left[(b+ia)\boldsymbol{\rho}_0\,\mathbf{x} + d\,\mathbf{x}\,\boldsymbol{\rho}_0\right]\mathrm{e}^{-\varepsilon H} = \\ &= (b+ia)\mathrm{e}^{-\varepsilon H}\,\boldsymbol{\rho}_0\,\mathrm{e}^{-\varepsilon H}\,\mathbf{x}(-i\varepsilon) + d\,\mathbf{x}(i\varepsilon)\,\mathrm{e}^{-\varepsilon H}\boldsymbol{\rho}_0\,\mathrm{e}^{-\varepsilon H},\end{aligned} \tag{4.67}$$

and therefore $\partial_\tau \langle \mathbf{x}(i\tau)\rangle_\varepsilon\,|_{\tau=-\varepsilon} = (b+ia)\,\langle \mathbf{x}(-i\varepsilon)\rangle_\varepsilon + d\,\langle \mathbf{x}(i\varepsilon)\rangle_\varepsilon$. Now, indicating by $\mathscr{O}'(i\tau_1,\dots,i\tau_n)$ a generic n-time function, it is not difficult to prove that, thanks to the ordering, the same kind of relation holds for any expectation $\langle \mathbf{x}(i\tau)\mathscr{O}'\rangle_\varepsilon$, i.e.,

$$\partial_\tau \left\langle \mathbf{x}(i\tau)\mathscr{O}'\right\rangle_\varepsilon|_{\tau=-\varepsilon} = (b+ia)\left\langle \mathbf{x}(-i\varepsilon)\mathscr{O}'\right\rangle_\varepsilon + d\left\langle \mathbf{x}(i\varepsilon)\mathscr{O}'\right\rangle_\varepsilon, \tag{4.68}$$

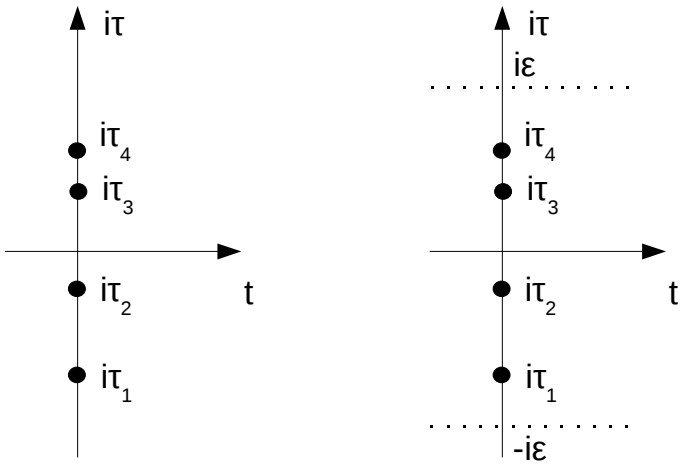

(a) (b)

Figure 4.6: (a) Sketch of the ordering enforced on the times along the imaginary axis by the requirement of having a well-defined expectation value in Eq. (4.64). (b) In order to allow for the ordering and regularise the behaviour at the boundaries, all the times must be within an effective film of width 2ε, delimited and enclosed by the two dotted lines.

as long as none of the times τ_i lies at the boundaries. This implies that the identity

$$\partial_\tau \mathbf{x}(i\tau)\,|_{\tau=-\varepsilon} = (b+ia)\,\mathbf{x}(-i\varepsilon) + d\,\mathbf{x}(i\varepsilon) \tag{4.69}$$

is valid when inserted in any time-ordered expectation. An analogous relation can be obtained at the other boundary:

$$\partial_\tau \mathbf{x}(i\tau)\,|_{\tau=\varepsilon} = (-b+ia)\,\mathbf{x}(i\varepsilon) - d\,\mathbf{x}(-i\varepsilon). \tag{4.70}$$

For the sake of clarity, we recall that while $\mathbf{x}(t)$ is a hermitian operator for any $t \in \mathbb{R}$, $\mathbf{x}(i\tau)$ in general is not, since $\mathbf{x}(i\tau)^\dagger = \mathrm{e}^{\tau H}\mathbf{x}\mathrm{e}^{-\tau H}$ is different from Eq. (4.61) if $\mathbf{x}$ is not a conserved quantity. By inspecting Eqs. (4.69) and (4.70) it is clear that the initial conditions (4.47) for the temporal evolution in real time — which are induced by an initial density matrix of the form (4.56) — are translated into proper boundary conditions which involve the values of $\mathbf{x}$ and $\dot{\mathbf{x}}$ at *the same* boundary of the film if and only if $d = 0$, i.e., if the initial density matrix describes a pure state ($\boldsymbol{\rho_0} = \boldsymbol{\rho_0^2}$). In addition, the conditions (4.69) and (4.70) at the two edges, reformulated in terms of (outgoing or ingoing) normal derivatives, are not independent, but complex conjugates. For $d \neq 0$, instead, Eqs. (4.69) and (4.70) mix the properties at the two edges. This implies that if we consider the path-integral formulation of this theory, we cannot interpret $\rho_0 = \mathrm{e}^{iS_0}$ as a boundary action since it will not be just a sum of two terms $S_{0,+i\varepsilon}$ and $S_{0,-i\varepsilon}$ separately concentrated at each boundary, but it will also include terms depending on both. While perfectly consistent from a mathematical point of view, these terms lack a definite reinterpretation in terms of an effective Euclidean theory

with boundaries. This difficulty — which emerged here in the simple case of ordinary quantum mechanics — is actually completely general, as shown in Section 4.3.2.

In order to characterise the non-equilibrium evolution, one is interested in determining (time-ordered) expectation values of operators, which physically correspond to measurable correlations and response functions (susceptibilities). Accordingly, a relevant issue is to understand whether and how such expectations in real time can be recovered from the imaginary-time formulation of the problem discussed above. Assuming that

$$K(x,y,t) = \langle x| \, \mathrm{e}^{-itH} \, |y\rangle \tag{4.71}$$

is defined, as a function of x and y, for every $t \geq 0$, also $K(x,y,t+i\tau)$ is defined for every non-positive value of τ, since the difference amounts to the introduction of a regularising term. By direct calculation, one can verify that K satisfies the Cauchy-Riemann conditions

$$\begin{cases} \partial_t \mathrm{Re}\, K = \partial_\tau \mathrm{Im}\, K, \\ \partial_t \mathrm{Im}\, K = -\partial_\tau \mathrm{Re}\, K. \end{cases} \tag{4.72}$$

Accordingly, $K(x,y,T)$ is an analytic function of T in the lower half of the complex plane and upon approaching the real axis it renders the real-time propagator. As an extension of the correlation function in Eq. (4.65), let us consider a generic multi-"time" correlation function

$$\langle \mathscr{O}(T_1) \ldots \mathscr{O}(T_n) \rangle_\varepsilon \,, \tag{4.73}$$

where $\tau_i = \mathrm{Im}\, T_i$ lies within the film, i.e., $|\tau_i| < \varepsilon$ and where we assume for simplicity that $\tau_1 \leq \tau_2 \leq \ldots \leq \tau_n$. The representation of this expectation value in terms of kernels can be obtained by introducing the resolution of the identity $\mathbb{1} = \int \mathrm{d}x \, |x\rangle \langle x|$ between subsequent operators:

$$\ldots \mathscr{O}(T_j) \ldots = \ldots \mathrm{e}^{iT_jH} \mathscr{O} \mathrm{e}^{-iT_jH} \ldots = \int \mathrm{d}x_j \mathrm{d}y_j \left[\ldots \mathrm{e}^{iT_jH} \left|y_j\right\rangle \left\langle y_j\right| \mathscr{O} \left|x_j\right\rangle \left\langle x_j\right| \mathrm{e}^{-iT_jH} \ldots \right] . \tag{4.74}$$

Once the evolution operators associated with adjacent operators are taken into account, this portion of the expectation becomes

$$\ldots \int \mathrm{d}x_j \mathrm{d}y_j \, K(x_{j-1}, y_j, T_{j-1} - T_j) \left\langle y_j\right| \mathscr{O} \left|x_j\right\rangle K(x_j, y_{j+1}, T_j - T_{j+1}) \ldots ; \tag{4.75}$$

this expression encompasses also the case of the boundaries if one identifies $T_{n+1} = i\varepsilon$ and $T_0 = -i\varepsilon$. We assume in the following that all $\left\langle y_j\right| \mathscr{O} \left|x_j\right\rangle$ and the kernels $\rho_0(y_{n+1}, x_0) \equiv \langle y_{n+1}| \, \boldsymbol{\rho_0} \, |x_0\rangle$ are regular functions of the respective coordinates and that the integrals exist and are finite. If the integrations in Eq. (4.75) commute with the derivatives with respect to the T_j's, Eq. (4.72) implies that the expectation (4.73) is an analytic function of the variables T_j as long as the ordering $\tau_j \leq \tau_{j+1}$ of the imaginary parts of T_j is preserved. Figure 4.7 presents a sketch of the required ordering of the complex times T_i in the case $n = 4$. This requirement of commutativity translates into conditions on the possible forms that the potential V can take in the Hamiltonian. While it is sufficient that both $K(x,y,t)$ and its time derivative $\partial_t K$ are continuous functions of x and y, the determination of the general class of potentials for which this holds true goes far beyond the scope of our discussion (the interested reader may find a detailed study of the kernel's continuity in

Ref. [108]). Note that the real parts $t_1,\dots,t_n$, of $T_1,\dots,T_n$ are not necessarily ordered, as sketched in Fig. 4.7 in the case $n=4$. As a consequence, from the analytic continuation to the real axis obtained by letting $\tau_j \to 0$, $\forall j$, i.e., $T_j \to t_j$ one recovers

$$\frac{\left\langle \mathrm{e}^{-\varepsilon H}\mathscr{O}(t_1)\dots\mathscr{O}(t_n)\mathrm{e}^{-\varepsilon H}\right\rangle}{\left\langle \mathrm{e}^{-2\varepsilon H}\right\rangle} \tag{4.76}$$

which, in the limit $\varepsilon \to 0^+$, renders the generic n-point function

$$\langle \mathscr{O}(t_1)\dots\mathscr{O}(t_n)\rangle\,, \tag{4.77}$$

with no time ordering. Time-ordered expectations can be quite easily reconstructed from these non-ordered quantities, as we demonstrate below. Consider for example a three-point function

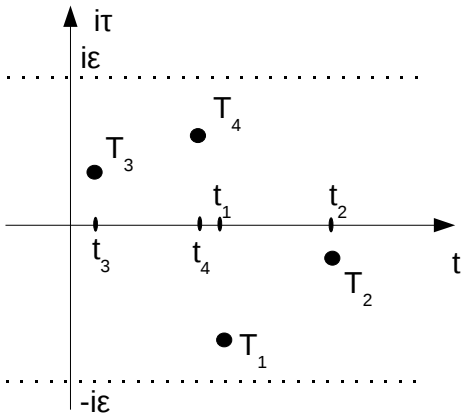

Figure 4.7: Sketch of the ordering of the complex times $T_1,\dots,T_4$ which allow a proper definition of correlation functions, where each of these times is indicated by a point $T_j = t_j + i\tau_j$ (with $t_j = \mathrm{Re}\,T_j$ and $\tau_j = \mathrm{Im}\,T_j$) in the complex-time plane. While performing the continuation from the complex plane to the real axis the ordering of the imaginary parts τ_j has to be preserved, whereas no ordering is required for the real parts t_j.

$\left\langle T_K\left[\mathscr{O}_1(t_{1,+})\mathscr{O}_2(t_{2,+})\mathscr{O}_3(s_-)\right]\right\rangle$, where for simplicity we restrict to bosonic operators $\mathscr{O}_i$, in order not to have to account for phases acquired under commutation. This quantity is associated to the imaginary-time expectation $\langle T^*\left[\mathscr{O}_1(\tau_1)\mathscr{O}_2(\tau_2)\mathscr{O}_3(\sigma)\right]\rangle$ and, according to the definition (4.2) of the T_K-ordering, it can be rewritten in terms of non-ordered functions as

$$\begin{aligned}\left\langle T_K\left[\mathscr{O}_1(t_{1,+})\mathscr{O}_2(t_{2,+})\mathscr{O}_3(s_-)\right]\right\rangle = \theta(t_1-t_2)\left\langle \mathscr{O}_3(s)\mathscr{O}_1(t_1)\mathscr{O}_2(t_2)\right\rangle + \\ + \theta(t_2-t_1)\left\langle \mathscr{O}_3(s)\mathscr{O}_2(t_2)\mathscr{O}_1(t_1)\right\rangle .\end{aligned} \tag{4.78}$$

In the r.h.s. of the expression above, the first expectation derives from an analytic continuation performed for $\sigma \le \tau_1 \le \tau_2$, whereas the second for $\sigma \le \tau_2 \le \tau_1$. For generic correlations, with n

points on the forward branch and m on the backward branch, such as the particular case depicted in Fig. 4.3(a), one has

$$\begin{aligned}\langle T_K\left[\mathscr{O}(t_1)\dots\mathscr{O}(t_n)\mathscr{O}(s_1)\dots\mathscr{O}(s_m)\right]\rangle = \sum_{P,P'}\theta\left(t_{P_1}\dots t_{P_n}\right)\bar{\theta}\left(s_{P'_1}\dots s_{P'_m}\right)\times \\ \times\left\langle\mathscr{O}\left(s_{P'_1}\right)\dots\mathscr{O}\left(s_{P'_m}\right)\mathscr{O}\left(t_{P_1}\right)\dots\mathscr{O}\left(t_{P_n}\right)\right\rangle,\end{aligned} \tag{4.79}$$

where for simplicity we have dropped the indices on the observables (but one can straightforwardly reintroduce them by considering that they match those of the respective times), P and P' represent all the possible permutations of n and m objects, respectively, and the generalised step functions

$$\begin{aligned}\theta(t_1\dots t_n) &= \prod_{j=1}^{n-1}\theta(t_j - t_{j+1}), \\ \bar{\theta}(s_1\dots s_m) &= \prod_{j=1}^{m-1}\theta(t_{j+1} - t_j)\end{aligned} \tag{4.80}$$

equal 1 if the sequences in their arguments are decreasing or increasing, respectively, whilst they vanish otherwise. This structure highlights the relevance of the non-analyticity of the imaginary-time function at coincident imaginary parts $\tau_i = \tau_j$: if the results obtained by analytically continuing it to the same points on the real axis but with different imaginary orderings were to be the same, then the Keldysh ordering would be inconsequential and the Keldysh-ordered functions would exactly coincide with their non-ordered counterparts. This would in turn imply the commutativity of the quantum fields at all times, which is known not to be the case in general. As a matter of fact, the domain of the Euclidean n-point functions is split into $n!$ analytic sectors, each identified by a specific choice of the ordering of the points along the imaginary axis. Within each subdomain, the continuation to real values is uniquely defined, as we have discussed above. We can now solve the apparent paradox of having to extract 2^n (in principle) different n-point dynamical functions from just a single, Euclidean one. The point is that different functions can be obtained by performing the analytic continuation within different sectors. Note that for $n > 1$ there are 2^n Keldysh functions and $n!$ sectors, which is compatible with the fact that the Euclidean approach allows to reproduce not only T_K-ordered correlations, but more generally non-ordered ones. Explicit examples involving two-point functions will be given in Sec. 4.3.2.

We focus now on the properties of the initial state. According to the discussion following Eq. (4.56), an initial density matrix $\boldsymbol{\rho_0}$ with $a = 0$ can be interpreted as a thermal state of a quantum harmonic oscillator, where the two remaining parameters b and d are related to those of the thermal distribution by Eq. (4.60). More generally, one would like to relate the parameters a, b, and d of the initial density matrix implied by the linear boundary conditions in Eq. (4.47) to expectation values of relevant observables, in order to understand their actual physical meaning. Taking into account the expression

$$\rho_0(x,y) = \sqrt{\frac{b+d}{\pi}}\mathrm{e}^{-\frac{b}{2}(x^2+y^2)+i\frac{a}{2}(x^2-y^2)-dxy}, \tag{4.81}$$

which follows from Eq. (4.56) and the requirements (i), (ii), and (iii) discussed after it, one easily finds

$$\langle \mathbf{x}^2 \rangle \equiv \int \mathrm{d}x\, x^2 \rho_0(x,x) = \frac{1}{2(b+d)}, \tag{4.82}$$

and, by taking advantage of Eq. (4.54),

$$\langle \{\mathbf{x},\mathbf{p}\} \rangle = \langle \mathbf{x}\mathbf{p} + \mathbf{p}\mathbf{x} \rangle = \frac{a}{b+d}, \tag{4.83}$$

$$\langle \mathbf{p}^2 \rangle = \frac{a^2+b^2-d^2}{2(b+d)}. \tag{4.84}$$

Accordingly, the parameters a, b, and d can be expressed as

$$\begin{cases} a = \dfrac{\langle \{\mathbf{x},\mathbf{p}\} \rangle}{2\langle \mathbf{x}^2 \rangle}, \\ b = \dfrac{1 - [\langle \{\mathbf{x},\mathbf{p}\} \rangle^2 - 4\langle \mathbf{p}^2 \rangle \langle \mathbf{x}^2 \rangle]}{4\langle \mathbf{x}^2 \rangle}, \\ d = \dfrac{1 + [\langle \{\mathbf{x},\mathbf{p}\} \rangle^2 - 4\langle \mathbf{p}^2 \rangle \langle \mathbf{x}^2 \rangle]}{4\langle \mathbf{x}^2 \rangle}. \end{cases} \tag{4.85}$$

Note that now the constraint $b+d>0$ emerges as a straightforward consequence of Eq. (4.82); the ones on the signs of b and d can be obtained instead from the Cauchy-Schwarz inequality $\langle \mathbf{p}^2 \rangle \langle \mathbf{x}^2 \rangle \geq |\langle \mathbf{p}\mathbf{x} \rangle|^2$; in fact, by decomposing the r.h.s. as $4|\langle \mathbf{p}\mathbf{x} \rangle|^2 = |\langle [\mathbf{p},\mathbf{x}] \rangle + \langle \{\mathbf{p},\mathbf{x}\} \rangle|^2 = |-i + \langle \{\mathbf{p},\mathbf{x}\} \rangle|^2 = 1 + \langle \{\mathbf{p},\mathbf{x}\} \rangle^2$, where the last equality comes from the fact that the anticommutator is hermitian and thus its expectation real, one finds

$$1 + \{\mathbf{p},\mathbf{x}\}^2 - 4\langle \mathbf{p}^2 \rangle \langle \mathbf{x}^2 \rangle \leq 0, \tag{4.86}$$

which is the same expression appearing in some of the numerators in the system (4.85) and implies $d \leq 0$ and, since $b+d>0$, also $b \geq 0$. Furthermore, since $\mathbf{p} = \dot{\mathbf{x}}$ we can rewrite a as

$$a = \partial_t \log \sqrt{\langle \mathbf{x}^2(t) \rangle}\,|_{t=0} \tag{4.87}$$

and therefore conclude that the condition $a=0$ is tantamount to requiring that the time derivative of the root-mean square position $\sqrt{\langle \mathbf{x}^2 \rangle}$ (we recall that our choice for the initial state implies $\langle \mathbf{x} \rangle = 0$) vanishes at the initial time. Actually, the analytic structure discussed above allows us to extend this result to any sufficiently smooth function of the position $F(\mathbf{x}(t))$: in fact, if $a=0$ the boundary conditions (4.69) and (4.70) at the two edges are symmetric, hence the system is symmetric under reflections of the complex time with respect to the real axis, which implies that $\langle F(\mathbf{x}(i\tau)) \rangle$ must be an even function of τ and therefore its derivative with respect to τ has to vanish in $\tau = 0$. Moreover, for a function to be analytic in a given point it is required that the derivative be independent of the direction along which it is calculated and therefore one concludes that $a=0$ generically implies $\partial_t \langle F(\mathbf{x}(t)) \rangle\,|_{t=0} = 0$. Note, however, that the converse statement is not true because even if $a \neq 0$ it is always possible to find functions of $\mathbf{x}(t)$ with vanishing initial derivative.

Summarizing, the previous discussion focused on the case of a single quantum particle with Hamiltonian $H = \mathbf{p}^2/2 + V(\mathbf{x})$ and assumed that its position $\mathbf{x}$ satisfies linear "boundary" conditions at time $t = 0$ (see Eq. (4.47)), which naturally emerge within the renormalisation-group framework as a consequence of keeping only the most relevant (symmetry-preserving) terms. A generalisation of this case is actually discussed further below. Under the additional but natural assumptions that $K(x,y,t) = \langle x| \, \mathrm{e}^{-itH} \, |y\rangle$ is well-defined $\forall x$, y, and $t \geq 0$ and that in the coordinate representation the integrals over the spatial coordinates and the derivatives with respect to time commute (see, e.g., Eq. (4.75)) we argued that: (A) The kernel representation of the initial density matrix is Gaussian, see Eq. (4.81), with $d \leq 0$ and $b \geq -d$. (B) An equivalent theory can be constructed in which time assumes complex values ($T = t + i\tau$) within a film of width 2ε, i.e., $\mathrm{Re}\, T \geq 0$ and $|\mathrm{Im}\, T| \leq \varepsilon$. In order to be well-defined, the expectation values of observables of this theory at complex times $T_1, \ldots, T_n$ are required to be time-anti-ordered along the imaginary direction, such that $\mathrm{Im}\, T_1 \leq \mathrm{Im}\, T_2 \leq \ldots \leq \mathrm{Im}\, T_n$; by explicitly introducing the ordering operator T^* in the definition (4.65) of these quantities, one is actually partitioning their domains into $n!$ analytic sectors, each corresponding to a specific order of the imaginary parts $\mathrm{Im}\, T_j$, separated by non-analytic boundaries. Therefore, analytic continuations of a given Euclidean n-point function performed from different subdomains provide different results: as a matter of fact, once the width of the film is made to vanish ($\varepsilon \to 0^+$), one can recover every generic (non-time-ordered) real-time expectation of the same observables at times $\mathrm{Re}\, T_1, \ldots, \mathrm{Re}\, T_n$. (C) If the density matrix $\boldsymbol{\rho_0}$ describing the initial state corresponds to a pure state $\boldsymbol{\rho_0} = |\psi\rangle \langle\psi|$, the equivalent theory on the film obeys Robin boundary conditions at $T = \pm i\varepsilon$ which are similar to the ones realised in real time at $t = 0$, the only difference being a multiplication of the coefficients by $\pm i$ (compare Eqs. (4.69) and (4.70) with Eq. (4.58)). If $\boldsymbol{\rho_0}$ is not a pure state, instead, the equivalent theory on the film does not obey proper boundary conditions at the edges, in the sense that the equation that $\mathbf{x}$ has to satisfy at one of these boundaries also involves the values $\mathbf{x}$ takes at the other.

Inspired by the previous discussion, we consider below a more general class of initial conditions for the real-time evolution. However, as we have done in Sec. 4.1.1, we shall account only for those which can be expanded as power series, i.e., which are of the form

$$\partial_t \mathbf{x}(t) \, |_{t=0_\pm} = \sum_{n,m=0}^{\infty} c^{(\pm)}_{n,m} \, \mathbf{x}^n(0_+) \mathbf{x}^m(0_-). \tag{4.88}$$

Linear conditions such as those in Eq. (4.47) are recovered with a suitable choice of $c^{(\pm)}_{n,m}$ (i.e., $c^{(+)}_{1,0} = a + ib$, $c^{(+)}_{0,1} = id$, $c^{(-)}_{1,0} = -id$ and $c^{(-)}_{0,1} = a - ib$, while all the remaining ones vanish). Analogously to the latter case, by inserting Eq. (4.88) in a generic T_K-ordered expectations one recovers the identities

$$\begin{cases} \mathbf{p}\, \boldsymbol{\rho_0} = \sum\limits_{n,m=0}^{\infty} c^{(+)}_{n,m} \, \mathbf{x}^n \, \boldsymbol{\rho_0} \, \mathbf{x}^m, \\ \boldsymbol{\rho_0}\, \mathbf{p} = \sum\limits_{n,m=0}^{\infty} c^{(-)}_{n,m} \, \mathbf{x}^n \, \boldsymbol{\rho_0} \, \mathbf{x}^m, \end{cases} \tag{4.89}$$

from which the kernel of the density matrix $\rho_0(x,y) = \langle x| \, \boldsymbol{\rho_0} \, |y\rangle$ may be reconstructed:

$$\rho_0(x,y) = \mathscr{N} \exp\left\{ i \left[\sum_{n=0}^{\infty} \left(\frac{c^{(+)}_{n0}}{n+1} x^{n+1} - \frac{c^{(-)}_{0n}}{n+1} y^{n+1} \right) - \sum_{n,m=0}^{\infty} \frac{c^{(-)}_{n+1,m}}{m+1} x^{n+1} y^{m+1} \right] \right\}. \tag{4.90}$$

Note that, in order for the solution (4.90) to exist, it is necessary that $c^{(+)}_{nm} = -\frac{n+1}{m} c^{(-)}_{n+1,m-1}$ for all $n \geq 0$ and $m > 0$. Moreover, the requirement $\boldsymbol{\rho_0} = \boldsymbol{\rho_0}^\dagger$ implies that $c^{(-)}_{n,m} = (c^{(+)}_{m,n})^*$. We have in general no closed formula to express the normalisation constant $\mathscr{N}$ in terms of the coefficients $c^{(\pm)}_{n,m}$, however, in the case of polynomials, which is again a very natural restriction from a renormalisation group point of view, it is at least quite clear, by putting $x = y$ in the expression above, that the condition of existence of the trace is that the highest-order term (i.e., the x^{n+m+2} with largest power) shall be even (which implies $n+m = 2N$, with N an integer) and the corresponding total coefficient, which is in general given by the sum

$$C_M = \frac{c^{(+)}_{2N+1,0}}{2N+2} - \frac{c^{(-)}_{0,2N+1}}{2N+2} - \sum_{n=0}^{2N} \frac{c^{(-)}_{n+1,2N-n}}{2N-n+1} \tag{4.91}$$

must have positive imaginary part ($\mathrm{Im}\,(C_M) > 0$, which indeed reduces to $b+d > 0$ in the simpler case discussed above). The remaining positivity condition $\langle\psi|\,\boldsymbol{\rho_0}\,|\psi\rangle \geq 0$ for all choices of $|\psi\rangle$, instead, is not so easy to implement. One can however notice that the kernel of a pure state would be separable in x and y; therefore, $\boldsymbol{\rho_0}$ describes a pure state only if the last term in Eq. (4.90) vanishes, i.e., $c^{(-)}_{n,m} \neq 0 \Leftrightarrow nm = 0$.

Equation (4.89) allows one to infer the conditions satisfied by $\mathbf{x}$ at the boundaries of the complex film: in fact, following a procedure analogous to the one employed in order to derive Eq. (4.67), one can write

$$\begin{aligned}\partial_\tau \left(\mathrm{e}^{-\varepsilon H}\boldsymbol{\rho_0}\mathrm{e}^{-\varepsilon H}\mathbf{x}(i\tau)\right)|_{\tau=-\varepsilon} &= \mathrm{e}^{-\varepsilon H}\boldsymbol{\rho_0}\, i\mathbf{p}\, \mathrm{e}^{-\varepsilon H} = i\mathrm{e}^{-\varepsilon H}\left(\sum_{n,m=0}^{\infty} c^{(-)}_{n,m}\mathbf{x}^n\,\boldsymbol{\rho_0}\,\mathbf{x}^m\right)\mathrm{e}^{-\varepsilon H} \\ &= i\sum_{n,m=0}^{\infty} c^{(-)}_{n,m}\,\mathbf{x}^n(i\varepsilon)\,\mathrm{e}^{-\varepsilon H}\,\boldsymbol{\rho_0}\,\mathrm{e}^{-\varepsilon H}\,\mathbf{x}^m(-i\varepsilon)\end{aligned} \tag{4.92}$$

which, in turn, finally gives

$$\begin{cases} \partial_\tau \mathbf{x}(i\tau)\,|_{\tau=-\varepsilon} = i\sum\limits_{n,m=0}^{\infty} c^{(-)}_{n,m}\,\mathbf{x}^m(-i\varepsilon)\,\mathbf{x}^n(i\varepsilon), \\ \partial_\tau \mathbf{x}(i\tau)\,|_{\tau=\varepsilon} = i\sum\limits_{n,m=0}^{\infty} c^{(+)}_{n,m}\,\mathbf{x}^m(-i\varepsilon)\,\mathbf{x}^n(i\varepsilon). \end{cases} \tag{4.93}$$

As it was the case for Eqs. (4.69) and (4.70), these identities are valid for all time-anti-ordered (on the imaginary axis) correlation functions. Accordingly, a property analogous to the one mentioned above at point (C) holds: equation (4.93) renders proper boundary conditions only if $c^{(+)}_{nm} = \delta_{m0}\, c^{(+)}_{n0}$, which is tantamount to requiring that $\boldsymbol{\rho_0}$ is a pure state. Hence, we can conclude that the relation between the initial state being pure and the boundary conditions being proper is a general feature of dynamical systems when mapped in a complex-time formalism.

4.3.2 Field Theories

Most of the implications of the discussion reported in Section 4.3.1 apply also to the non-equilibrium quantum field theories introduced in Sections 4.1 and 4.1.1, as we illustrate below. For the sake

of simplicity, we focus on the case of a real, scalar field $\Psi = \Psi^\dagger = \Phi$ because the extension to other cases is rather straightforward, although it generally involves more complicated boundary conditions. In the present case, linear boundary conditions such as those discussed in the previous Sections emerge for the fields if the two following conditions are satisfied: (i) All terms containing time derivatives in the Lagrangian density $\mathscr{L}$ of Eq. (4.15) — which generate boundary terms by integration by parts — are (at most) quadratic in the fields, as happens in the standard case of Eq. (4.16) with, say, a polynomial V; (ii) S_0 (see, e.g., Eq. (4.14)) is quadratic in the initial fields with coefficients which may depend on the coordinates. For an isotropic system, for example, a quite general choice can be written down in momentum space as follows:

$$S_0[\phi_+,\phi_-] = \int \frac{\mathrm{d}^d k}{(2\pi)^d} \left\{ \frac{c_{++}(k)}{2}\phi_+^2 - \frac{c_{--}(k)}{2}\phi_-^2 + c_{+-}(k)\phi_+\phi_- \right\}, \tag{4.94}$$

where $k = |\vec{k}|$. Conditions (i) and (ii) correspond to Eqs. (4.46) and (4.56). The conditions $\boldsymbol{\rho_0} = \boldsymbol{\rho_0}^\dagger$ and $\mathrm{tr}\{\boldsymbol{\rho_0}\} = 1$ translate into $c_{++}(k) = c_{--}^*(k)$, $c_{+-}(k) = -c_{+-}^*(k)$ and $\mathrm{Im}\,[c_{++}(k) + c_{+-}(k)] \geq 0$, while $\mathrm{Im}\ c_{+-}(k) \leq 0$ is a sufficient condition for $\mathrm{tr}\{\boldsymbol{\rho_0}^2\} \leq 1$ to hold. Moreover, if all coefficients are purely imaginary, in analogy with the discussion which led to Eq. (4.60), one can rewrite them as

$$c_{++}(k) = -c_{--}(k) = im_0\omega_0 \frac{\cosh(\beta_k\omega_0)}{\sinh(\beta_k\omega_0)} \quad \text{and} \quad c_{+-}(k) = -im_0\omega_0 \frac{1}{\sinh(\beta_k\omega_0)}, \tag{4.95}$$

where β_k is a mode-dependent (inverse) temperature; accordingly, the initial state corresponds to a set of independent harmonic oscillators each fixed at its own temperature [103].

By following the line of argument illustrated in the previous Section one reaches the same conclusions, i.e., that it is possible to construct an effective theory with imaginary times, such as the one introduced at the end of Sec. 4.2,

$$Z = \int_{\mathscr{I}} \mathscr{D}\phi\, \mathrm{e}^{-S_\varepsilon[\phi] + iS_0[\phi(i\varepsilon),\phi(-i\varepsilon)]}, \tag{4.96}$$

where

$$S_\varepsilon[\phi] = \int_{-\varepsilon}^{\varepsilon} \mathrm{d}\tau \int \mathrm{d}^d x \left\{ (\partial_j\phi)(\partial_j\phi) + V[\phi] \right\} \tag{4.97}$$

is the Euclidean action associated with (4.16) and the domain $\mathscr{I}$ of integration includes field configurations which are defined in imaginary time within the film $-i\varepsilon \leq i\tau \leq i\varepsilon$. The time runs on the contour depicted in Fig. 4.4(c) and the time derivative has the same sign as the spatial ones, i.e., $(\partial_j\phi)(\partial_j\phi) = (\partial_\tau\phi)^2 + |\vec{\nabla}\phi|^2$. Again, $S_0[\phi(i\varepsilon),\phi(-i\varepsilon)]$ — which may be easily inferred from Eq. (4.94) — constitutes a "proper" boundary term (i.e., generates proper boundary conditions) only if $c_{+-} = 0$, which in turn implies that $\boldsymbol{\rho_0}$ describes a pure state. Of course, we still have to demand that the potential term be regular enough for the correlation functions to be analytic in the upper complex half-plane, as long as the ordering along the imaginary direction is preserved. As usual, the generating functional of correlation functions is obtained from Z in Eq. (4.96) by adding a source term $J\cdot\phi \equiv \int_{-\varepsilon}^{\varepsilon} \mathrm{d}\tau \int \mathrm{d}^d x\, J(\tau,\vec{x})\,\phi(\tau,\vec{x})$ (see also Eq. (4.15)) in the exponent of the integrand. At the conceptual level, via functional derivation with respect to J one can then obtain any

time anti-ordered (along the imaginary-time axis) expectation and, as explained in Section 4.3.1, determine the non-time-ordered correlation functions in real time by performing the analytic continuation of the former to the real axis, followed by the limit $\varepsilon \to 0^+$, from any analytic sector.

In Section 4.3.1 we have shown that indeed one can retrieve an Euclidean theory starting from one defined on the Keldysh contour. However, since this construction straightforwardly carries over to the case of quantum field theories discussed here, one concludes on the basis of the discussion in Sec. 4.2 that also in this case the mapping of a dynamical problem into a static one with boundaries is possible only if the initial state of the dynamics is pure. If, instead, it is a statistical mixture, the boundaries at $\pm i\varepsilon$ are inextricably intertwined and the corresponding equations (see, e.g., Eqs. (4.69), (4.70), and (4.93)) — although formally correct, valid, and in principle solvable — cannot be interpreted as physical boundary conditions because each of them involves fields evaluated at the two distinct boundaries of the resulting film.

In order to illustrate the inherent analytic structure of the theory, we discuss below two simple examples.

The Gaussian theory

First, consider the Gaussian scalar field theory described by the action (4.97) (in imaginary time) with $V[\Phi] = m^2\Phi^2/2$ and a pure initial condition (i.e., Eq. (4.94) with $c_{+-} = 0$). Indicating by Φ_k the Fourier transform in space of Φ, the two-time correlation function

$$G_k^\varepsilon(i\tau, i\sigma) = \langle \Phi_k(i\tau)\Phi_{-k}(i\sigma)\rangle_\varepsilon, \tag{4.98}$$

in which we factored out $(2\pi)^d\delta^{(d)}(\vec{k}+\vec{q})$ due to the conservation of momenta, solves the equations

$$\begin{cases} (\partial_\tau^2 - \omega_k^2)G_k^\varepsilon(i\tau, i\sigma) = -\delta(\tau-\sigma), \\ (\partial_\sigma^2 - \omega_k^2)G_k^\varepsilon(i\tau, i\sigma) = -\delta(\tau-\sigma), \end{cases} \tag{4.99}$$

where $\omega_k = \sqrt{k^2+m^2}$ is the free-particle dispersion relation and ε indicates explicitly the width of the film in imaginary time. Recalling that $c_{--} = c_{++}^*$, the boundary conditions which G_k^ε satisfies as a consequence of the assumption on the initial condition are:

$$\begin{cases} \partial_\tau G_k^\varepsilon(i\tau, i\sigma)\,|_{\tau=-\varepsilon} = ic_{++}^* G_k^\varepsilon(-i\varepsilon, i\sigma), \\ \partial_\sigma G_k^\varepsilon(i\tau, i\sigma)\,|_{\sigma=-\varepsilon} = ic_{++}^* G_k^\varepsilon(i\tau, -i\varepsilon), \\ \partial_\tau G_k^\varepsilon(i\tau, i\sigma)\,|_{\tau=\varepsilon} = ic_{++} G_k^\varepsilon(i\varepsilon, i\sigma), \\ \partial_\sigma G_k^\varepsilon(i\tau, i\sigma)\,|_{\sigma=\varepsilon} = ic_{++} G_k^\varepsilon(i\tau, i\varepsilon). \end{cases} \tag{4.100}$$

The solution of Eqs. (4.99) and (4.100) is given by [53]

$$G_k^\varepsilon(i\tau, i\sigma) = \frac{\mathrm{e}^{-\omega_k|\sigma-\tau|}}{2\omega_k} + A_k\mathrm{e}^{-\omega_k(\tau+\sigma)} + 2B_k\cosh\left(\omega_k(\sigma-\tau)\right) + C_k\mathrm{e}^{\omega_k(\tau+\sigma)}, \tag{4.101}$$

where

$$\begin{gathered} A_k = \frac{1}{2\omega_k}\frac{\alpha_k}{\alpha_k^*}\frac{1}{\alpha_k\mathrm{e}^{2\omega_k\varepsilon} - (\alpha_k^*)^{-1}\mathrm{e}^{-2\omega_k\varepsilon}}, \quad B_k = \frac{\mathrm{e}^{-2\omega_k\varepsilon}}{\alpha_k}A_k, \\ C_k = \frac{\alpha_k^*}{\alpha_k}A_k \quad \text{and} \quad \alpha_k = \frac{\omega_k - ic_{++}}{\omega_k + ic_{++}}. \end{gathered} \tag{4.102}$$

The only term in Eq. (4.101) which explicitly depends on the choice of the sector is the first one, due to the presence of the absolute value which makes it non-analytic in the neighbourhood of $\tau = \sigma$. The continuation to the real axis, which corresponds to the substitutions $\sigma \to -is$ and $\tau \to -it$, must be performed without leaving either of the two sectors $\tau < \sigma$ and $\sigma < \tau$ within which Eq. (4.101) is separately analytic, which is tantamount to preserving the chosen ordering. Correspondingly, two different results are rendered, namely

$$\frac{\mathrm{e}^{-i\omega_k(t-s)}}{2\omega_k} \quad \text{for} \quad \tau < \sigma \qquad \text{and} \qquad \frac{\mathrm{e}^{i\omega_k(t-s)}}{2\omega_k} \quad \text{for} \quad \tau > \sigma \tag{4.103}$$

We emphasize that the time anti-ordering which is understood in Eq. (4.98) (see the definition of $\langle\cdot\rangle_\varepsilon$ in Eq. (4.65)) plays a fundamental role: if it were not present, in fact, the first term of Eq. (4.101) could be exponentially divergent for $k \to \infty$ and therefore would have no Fourier transform, invalidating the previous treatment. The remaining terms, instead, are regularised by the factors A_k, B_k, C_k, which, in the limit $k \to +\infty$, asymptotically behave as

$$A_k \sim C_k \sim \mathrm{e}^{-2k\varepsilon} \quad \text{and} \quad B_k \sim \mathrm{e}^{-4k\varepsilon}. \tag{4.104}$$

Consider also that the ordering of the fields depends on the choice of the analytic sector: for $\tau < \sigma$ the analytic continuation of Eq. (4.101) renders $\langle\Phi(t)\Phi(s)\rangle$, whereas $\langle\Phi(s)\Phi(t)\rangle$ is recovered from its continuation within the sector $\tau > \sigma$. In fact, in this last case, by definition one gets $\langle T^*[\Phi(\tau)\Phi(\sigma)]\rangle = \langle\Phi(\sigma)\Phi(\tau)\rangle$. Of course, this general statement holds beyond the simple case we are analyzing here, once the proper phases generated by commuting non-bosonic fields have been taken into account. These phases are included in the definition of the time-ordering, as is the case with fermions, i.e., $T^*[\Psi(\tau > 0)\Psi(0)] = -\Psi(0)\Psi(\tau)$.

According to Eqs. (4.101) and (4.103), the real-time two-point function for $\tau < \sigma$ is given by

$$G_k^\varepsilon(t,s) = \frac{\mathrm{e}^{-i\omega_k(t-s)}}{2\omega_k} + A_k \mathrm{e}^{i\omega_k(t+s)} + 2B_k \cos\left(\omega_k(t-s)\right) + C_k \mathrm{e}^{-i\omega_k(t+s)}. \tag{4.105}$$

In order to recover the actual correlation function of the fields, one has eventually to take the limit $\varepsilon \to 0^+$ of the expression above, which becomes

$$G_k(t,s) = \frac{\mathrm{e}^{-i\omega_k(t-s)}}{2\omega_k} + \mathscr{A}_k \mathrm{e}^{i\omega_k(t+s)} + 2\mathscr{B}_k \cos\left(\omega_k(t-s)\right) + \mathscr{C}_k \mathrm{e}^{-i\omega_k(t+s)} \tag{4.106}$$

where

$$\begin{cases} \alpha_k = (\omega_k - ic_{++})/(\omega_k + ic_{++}), \\ \mathscr{A}_k = \frac{1}{2\omega_k}\frac{\alpha_k}{|\alpha_k|^2-1}, \\ \mathscr{B}_k = \frac{1}{2\omega_k}\frac{1}{|\alpha_k|^2-1}, \\ \mathscr{C}_k = \frac{1}{2\omega_k}\frac{\alpha_k^*}{|\alpha_k|^2-1}. \end{cases} \tag{4.107}$$

As we argued above, this expression of $G_k(t,s)$ corresponds to the expectation $\langle\Phi(t)\Phi(s)\rangle$ and hence, by comparing it with the definitions in Eq. (4.6), this correlation function coincides, up to a

trivial factor, with $G^{>}$, i.e., $G_k(t,s) = iG_k^{>}(t,s)$: in fact, it can be additionally verified that $G_k(t,s)$ satisfies the same equations

$$\begin{cases} (\partial_t^2 + \omega_k^2) G_k^{>}(t,s) = 0, \\ (\partial_s^2 + \omega_k^2) G_k^{>}(t,s) = 0, \end{cases} \tag{4.108}$$

and the same boundary conditions

$$\begin{cases} \partial_t G_k^{>}(t,s)\,|_{t=0} = c_{++}^* G_k^{>}(0,s), \\ \partial_s G_k^{>}(t,s)\,|_{s=0} = c_{++} G_k^{>}(t,0), \end{cases} \tag{4.109}$$

as $G_k^{>}(t,s)$, which follow from the equations of motion of a Gaussian theory in real time, when applied to two-point functions. Moreover, specialising it to the case of a quench in the mass $m_0 \to m$, which corresponds to an initial condition of the form $c_{++} = i\omega_{0k} \equiv i\sqrt{k^2 + m_0^2}$, one finds

$$\alpha_k = \frac{\omega_k + \omega_{0k}}{\omega_k - \omega_{0k}}, \qquad \mathscr{A}_k = \mathscr{C}_k = \frac{\omega_k^2 - \omega_{0k}^2}{8\omega_k^2 \omega_{0k}} \quad \text{and} \quad \mathscr{B}_k = \frac{(\omega_k - \omega_{0k})^2}{8\omega_k^2 \omega_{0k}}, \tag{4.110}$$

which yields

$$iG_k^{>}(t,s) = \frac{\mathrm{e}^{-i\omega_k(t-s)}}{2\omega_k} + \frac{\omega_k^2 - \omega_{0k}^2}{4\omega_k^2\omega_{0k}} \cos\left(\omega_k(t+s)\right) + \frac{(\omega_k - \omega_{0k})^2}{4\omega_k^2\omega_{0k}} \cos\left(\omega_k(t-s)\right). \tag{4.111}$$

This expression coincides with ones previously found for this dynamical problem in Refs. [3, 109].

Analogously, one can verify that the analytic continuation of Eq. (4.101) within the complementary sector corresponds to the correlation function $\langle \Phi(s)\Phi(t)\rangle$ which, according to Eq. (4.6), can be identified with $G^{<}$. In the very simple case of the real scalar field considered here one can actually recover one from the other by exploiting the additional symmetry

$$G_k^{>}(t,s) = G_k^{<}(s,t), \tag{4.112}$$

which can be straightforwardly obtained from Eq. (4.6) after imposing $\Psi = \Psi^\dagger = \Phi$ and which is indeed correctly reproduced by Eq. (4.103).

The conformal Ising model

Second, we specialise to the $1+1$-dimensional case and consider the two-point correlation of the order parameter of the Ising model at criticality, which is again a scalar field. As we are going to work in coordinate space, we shall adopt here the same notation of Sec. 4.2.1, i.e., we will measure distances and times in units of the extrapolation length, as defined by Eqs. (4.42). For later convenience, we also introduce the corresponding notation in real time $\hat{t}_j = \pi t_j/(2\tau_0)$. Due to the conformal symmetry of the model, the correlation function is given by Eqs. (4.41) and (4.37), from which one finds [2, 3]

$$\langle \Phi(r, i\tau_1)\Phi(0, i\tau_2)\rangle = \xi^{1/8} \left[\sqrt{\frac{1+\sqrt{\eta}}{2}} \pm \sqrt{\frac{1-\sqrt{\eta}}{2}} \right] \tag{4.113}$$

with

$$\xi = \left(\frac{\pi}{2\tau_0}\right)^2 \frac{\cosh\rho + \cos(\theta_1+\theta_2)}{4\cos\theta_1\cos\theta_2[\cosh\rho - \cos(\theta_1-\theta_2)]}, \tag{4.114}$$

and η given in Eq. (4.43). This case appears to be more subtle than the previous one because these expressions do not display a clear point of non-analyticity at $\tau_1 = \tau_2$. The naive analytic continuation $\tau_j \to -it_j$ (i.e., $\theta_j \to -i\hat{t}_j$) renders

$$\langle\Phi(r,t_1)\Phi(0,t_2)\rangle = u^{1/8}\left[\sqrt{\frac{1+\sqrt{\mathrm{n}}}{2}} \pm \sqrt{\frac{1-\sqrt{\mathrm{n}}}{2}}\right], \tag{4.115}$$

where

$$u = \left(\frac{\pi}{2\tau_0}\right)^2 \frac{\cosh\rho + \cosh(\hat{t}_1+\hat{t}_2)}{4\cosh\hat{t}_1\cosh\hat{t}_2\,[\cosh\rho - \cosh(\hat{t}_1-\hat{t}_2)]} \tag{4.116}$$

and

$$\mathrm{n} = \frac{\cosh(\hat{t}_1-\hat{t}_2)+\cosh(\hat{t}_1+\hat{t}_2)}{\cosh\rho+\cosh(\hat{t}_1+\hat{t}_2)}. \tag{4.117}$$

Equation (4.115) is symmetric under the exchange of times $\hat{t}_1 \leftrightarrow \hat{t}_2$ (i.e., $t_1 \leftrightarrow t_2$); according to Eq. (4.112), this would make it impossible to distinguish $G^<$ from $G^>$. However, the analytic continuation has to be performed with care: in fact, different continuations arise as a consequence of the structure of these functions: indeed, Eq. (4.115) features two branching points of algebraic order $1/8$ for $t_1 - t_2 = \pm r$, as schematically represented in Fig. 4.8. Moreover, from expression

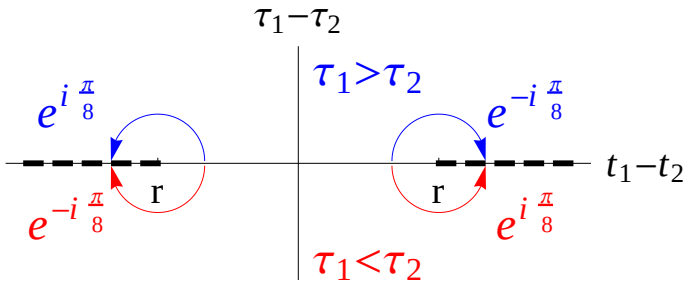

Figure 4.8: Schematic representation of the analytic structure of the function $\xi^{1/8}$ (Eq. (4.114)) in the complex plane $\tau_1 - \tau_2$. The branch points are positioned at $|t_1 - t_2| = r$; our choice for the branch cuts is indicated by the thick, dashed lines superimposed to the real axis. The lower-half plane (red) represents the sector associated to $G^>$, whereas the upper half-plane (blue) to $G^<$. One can see that for $|t_1 - t_2| > r$ the phase of $u^{1/8}$ depends on the choice of the sector, as also highlighted by Eqs. (4.118) and (4.119).

(4.117) one can infer that $n = 1$ at the same points, which implies that $1 - n^{1/2}$ changes sign. As a consequence, an additional branching point has to be considered, which is associated to the second square root in Eq. (4.115) and is of algebraic order $1/2$. Thus, a picture completely similar to the one sketched in Fig. 4.8 holds for this term, the only difference being that the acquired phases are in this case $\mathrm{e}^{\mp i(\pi/2)} = \mp i$. Thus, although the distinction is not as neat as in the previous example,

it is still fundamental to determine whether the real axis is being reached from one sector or the other; overall, introducing the shorthand notation $\sigma = \mathrm{sign}\,(t_1 - t_2)$, one finds indeed

$$iG^{<}(t_1,t_2) = |u|^{\frac{1}{8}} \times \begin{cases} \left[\sqrt{\frac{1+\sqrt{n}}{2}} \pm \sqrt{\frac{1-\sqrt{n}}{2}}\right] & \text{for} \quad |t-s| < r \\ e^{i\sigma\frac{\pi}{8}}\left[\sqrt{\frac{1+\sqrt{n}}{2}} \mp i\sigma\sqrt{\frac{\sqrt{n}-1}{2}}\right] & \text{for} \quad |t-s| > r \end{cases} \tag{4.118}$$

for $\tau_1 > \tau_2$ and

$$iG^{>}(t_1,t_2) = |u|^{\frac{1}{8}} \times \begin{cases} \left[\sqrt{\frac{1+\sqrt{n}}{2}} \pm \sqrt{\frac{1-\sqrt{n}}{2}}\right] & \text{for} \quad |t-s| < r \\ e^{-i\sigma\frac{\pi}{8}}\left[\sqrt{\frac{1+\sqrt{n}}{2}} \pm i\sigma\sqrt{\frac{\sqrt{n}-1}{2}}\right] & \text{for} \quad |t-s| > r \end{cases} \tag{4.119}$$

for $\tau_1 < \tau_2$. In the expressions above, the only term which is affected by the exchange $t_1 \leftrightarrow t_2$ is σ, which changes sign; thus, it is straightforward to verify that Eqs. (4.118) and (4.119) satisfy the identity (4.112).

It may be interesting to note that a similar structure arises in the Gaussian case when treated in coordinate space $(\vec{r},t)$. Focusing for simplicity just on the first term of Eq. (4.101), since it bears full responsibility for the non-analytic behaviour, and setting $m = 0$, we find that its Fourier transform is given by

$$G_0(\vec{r},i\tau,i\sigma) = K_d\left(r^2 + (\tau-\sigma)^2\right)^{-\frac{d-1}{2}} \quad \text{with} \quad K_d = \frac{\pi^{-\frac{d+1}{2}}}{4}\Gamma\left(\frac{d-1}{2}\right). \tag{4.120}$$

Clearly, this is a symmetric function under the exchange $\tau \leftrightarrow \sigma$; on the other hand, as in the conformal case, it generically displays two branching points at $(\tau - \sigma) = \mp ir$. Thus, on the real axis one finds two different functions

$$iG_0^{<}(\vec{r},t,s) = K_d\left|r^2 - (t-s)^2\right|^{-\frac{d-1}{2}} \exp\left\{i\pi\left(\frac{d-1}{2}\right)\chi(\vec{r},t,s)\right\} = iG_0^{>}(\vec{r},s,t), \tag{4.121}$$

where

$$\chi(\vec{r},t,s) = \begin{cases} \mathrm{sign}\,(t-s) & \text{for } |t-s| > r \\ 0 & \text{for } |t-s| < r. \end{cases} \tag{4.122}$$

The case of odd spatial dimensions $d > 1$, which seemingly entails $G^{<} \equiv G^{>}$, will be discussed in Sec. 4.4. Although we lack the actual expressions, it is possible to demonstrate that the same analytic structure carries over to the gapped case $m \neq 0$.

4.4 Response functions

In the previous Sections, we have shown how an Euclidean formalism can be set up in order to calculate correlation functions of observables at imaginary times and then perform an analytic continuation back to the real axis, i.e., to real times. This allows one to exploit the methods

developed for treating static systems confined in a film geometry in order to calculate dynamical features following a quench. In this Section we focus on a second but equally relevant class of quantities of interest which characterise the dynamics of a system, i.e., *response functions*. Their definition is analogous to the one we have given in a classical setting (see Eq. (3.42)), i.e., they describe the linear variation of some quantity at time t (e.g., the average $\langle\Phi(t)\rangle$ of some field Φ) due to the action of a small external perturbation h at an earlier time (see also the analogous discussion in Sec. 3.1.2):

$$R(t,s) = \left.\frac{\delta\langle\Phi(t)\rangle}{\delta h(s)}\right|_{h\equiv 0}. \tag{4.123}$$

The perturbation h couples linearly to one of the fields of the Hamiltonian and therefore acts like a source term; for example, consider a theory defined in terms of a set of fields $\{\Phi_i\}_i$. The perturbation of the Hamiltonian would then be $\sum_i h_i\Phi_i$ with a set of external fields $\{h_i\}_i$ in terms of which one can define generalised responses

$$R_{i_1,\ldots,i_n;j_1,\ldots j_m}(t_1,\ldots,t_n;s_1,\ldots,s_m) = \left.\frac{\delta^m\langle\Phi_{i_1}(t_1)\ldots\Phi_{i_n}(t_n)\rangle}{\delta h_{j_1}(s_1)\ldots\delta h_{j_m}(s_m)}\right|_{\{h_i\}_i\equiv 0}. \tag{4.124}$$

Clearly, the causality of the response of any physical system is reflected in the fact that the response function (4.124) vanishes identically whenever $\max_i\{t_i\} < \max_j\{s_j\}$. Within the Keldysh formalism discussed in Sec. 4.1, response functions can be obtained as follows: in the physical representation introduced by Eqs. (4.8) and (4.9), the effective action (4.15) is rewritten as $\mathscr{S}[\phi_c,\phi_q,J_c,J_q]+\mathscr{S}_0[\phi_c(0),\phi_q(0)]$, with

$$\begin{cases} \mathscr{S}[\phi_c,\phi_q,J_c,J_q] = S[\frac{\phi_c+\phi_q}{2}] - S[\frac{\phi_c-\phi_q}{2}] + \frac{1}{2}\left(J_c\cdot\phi_q + J_q\cdot\phi_c\right), \\ \mathscr{S}_0[\phi_c(0),\phi_q(0)] = S_0[\frac{\phi_c(0)+\phi_q(0)}{2}, \frac{\phi_c(0)-\phi_q(0)}{2}], \end{cases} \tag{4.125}$$

where the classical and quantum components $J_{c/q}$ of the sources $J_\pm$ are defined analogously to the fields $J_{c/q} = J_+ \pm J_-$. As we have mentioned above, the distinction between the two time branches is a convenient artifice, but all physical observables must be single-valued in time; hence, actual perturbations (i.e., sources such as h mentioned above) must satisfy $J_+ = J_-$, i.e., $J_q = 0$. According to the definition in Eqs. (4.123) and (4.124), one has to calculate the variation of a given correlation function with respect to the turning on of an external perturbation applied at time s, which is formally obtained by taking its functional derivative with respect to J_c; in turn, this translates into the appearance of a quantum component $\phi_q(s)$ in the average such that, e.g.,

$$-2i\frac{\delta\langle\phi_c(t)\rangle}{\delta J_c(s)} = \left\langle\phi_c(t)\phi_q(s)\right\rangle = 2iG^r(t,s). \tag{4.126}$$

Hence, the retarded component coincides with the response function except for the sign, i.e., $G^r \equiv -R$. Consequently, this expression of the retarded function on the l.h.s. as a correlation function on the r.h.s. with a suitable field is completely analogous to the one we have encountered in Chapter 3 when studying classical systems with dissipative dynamics (see, e.g., Eq. (3.42)) [18, 20, 76]. In the latter case, the response of the fluctuating order parameter φ — which corresponds to the classical

component of the field within the Keldysh formalism — is encoded in the auxiliary response field $\tilde{\varphi}$ whose role is here played by the quantum component. We recall now that the contour onto which the time runs can be deformed arbitrarily in the complex plane but in such a way that it does not include any part going upwards (see the discussion following Eq. (4.25)). In particular, this implies that the forward and backward branches of the Keldysh contour can actually be deformed only within the upper and lower half-plane, respectively. As a consequence, we lack a clear prescription for the analytical continuation of ϕ_c and ϕ_q, outside the real axis because this is the only domain along which ϕ_+ and ϕ_- are simultaneously defined. On the one hand, this limitation does not imply that the two-time functions in Eq. (4.9) do not admit a local analytic continuation; on the other, it is related to the fact that G^r and G^a clearly have a point of non-analyticity for $t = s$ due to their causal structure which makes them vanish identically for $t < s$ and $t > s$, respectively. Nonetheless, one may reconstruct them by combining the imaginary time formalism described in Sec. 4.3.2 with the relations (4.9): starting from any response function (say, involving n times), one can expand the "classical" and "quantum" fields involved into "forward" $(+)$ and "backward" $(-)$ components (see Eq. (4.8)); correspondingly, this quantity can be re-expressed in terms of a sum of 2^n Keldysh-ordered correlations which, as we have mentioned in Sec. 3.2, constitute a subset of all possible non-time-ordered correlations and can therefore be recovered by the imaginary-time formalism. Reverting to the physical representation, one can reconstruct the desired response. Below, we illustrate this point with few simple, but relevant examples.

The Gaussian theory

First of all, consider the Gaussian scalar field theory we have discussed near the end of the previous Section. Substituting Eq. (4.106) into

$$G^r_k(t,s) = \theta(t-s)\left[G^>_k(t,s) - G^>_k(s,t)\right], \tag{4.127}$$

one obtains

$$G^r_k(t,s) = -\frac{1}{\omega_k}\theta(t-s)\sin\left(\omega_k(t-s)\right). \tag{4.128}$$

This expression for the retarded two-point function is exactly the same as the one that could be found by solving directly the problem in real time. In coordinate representation, according to Eq. (4.121), the expression above becomes

$$G^r(\vec{r},t,s) = 2\theta(t-s-r)\,K_d\,\sin\left(\pi\frac{1-d}{2}\right)\left[(t-s)^2 - r^2\right]^{-\frac{d-1}{2}}, \tag{4.129}$$

where K_d is the same constant as in Eq. (4.120). From this expression it would appear that for odd $d \neq 1$ the response function identically vanishes, which reflects the fact that the exponent of the algebraic law in Eqs. (4.120) is an integer, implying that no branching cut emerges in the complex plane. On the other hand, a system which displays no response to external perturbations is clearly unphysical, and moreover the null function could not have Eq. (4.128) as a Fourier counterpart. The point here is that the limit implied by the analytic continuation has to be interpreted in the sense of distributions. For example, for $d = 3$ one finds

$$G_0(\vec{r},i\tau,i\sigma) = \frac{(2\pi)^{-2}}{r^2+(\tau-\sigma)^2} = \frac{(2\pi)^{-2}}{2r}\left(\frac{1}{r+i(\tau-\sigma)} + \frac{1}{r-i(\tau-\sigma)}\right); \tag{4.130}$$

its analytic continuation to real values for $\tau < \sigma$ corresponds to the limit

$$\begin{aligned} iG_0^{>}(\vec{r},t,s) &= \lim_{\vartheta\to 0^+} G_0(\vec{r},t,s+i\vartheta) = \lim_{\vartheta\to 0^+} \frac{(2\pi)^{-2}}{2r}\left(\frac{1}{r+(t-s)-i\vartheta}+\frac{1}{r-(t-s)+i\vartheta}\right) = \\ &= \frac{(2\pi)^{-2}}{2r}\left[\mathbf{P}\frac{1}{r+(t-s)}+i\pi\delta(r+t-s)+\mathbf{P}\frac{1}{r-(t-s)}-i\pi\delta\left(r+s-t\right)\right] = \\ &= \frac{1}{4\pi^2}\mathbf{P}\frac{1}{r^2-(t-s)^2}+i\frac{1}{8\pi r}\left[\delta(r+t-s)-\delta\left(r+s-t\right)\right], \end{aligned} \tag{4.131}$$

where $\mathbf{P}$ denotes the principal value. On the other hand, for $\tau > \sigma$ one finds that the imaginary part changes sign, i.e.,

$$iG_0^{<}(\vec{r},t,s) = \frac{1}{4\pi^2}\mathbf{P}\frac{1}{r^2-(t-s)^2}-i\frac{1}{8\pi r}\left[\delta(r+t-s)-\delta\left(r+s-t\right)\right]. \tag{4.132}$$

This implies that the response function actually exists as a distribution and is equal to

$$-G^r(\vec{r},t,s) = \frac{1}{4\pi r}\delta\left(r-(t-s)\right). \tag{4.133}$$

Thereby, in three spatial dimensions the response of a system is not absent, but pointwise. This holds true also in higher, odd dimensions $d = 2n+1$ (with integer n), since one can rewrite G_0 as

$$G_0(\vec{r},i\tau,i\sigma) = \frac{K_d}{\left(r+i\left(\tau-\sigma\right)\right)^n+\left(r-i\left(\tau-\sigma\right)\right)^n}\left[\frac{1}{\left(r+i(\tau-\sigma)\right)^n}+\frac{1}{\left(r-i(\tau-\sigma)\right)^n}\right]. \tag{4.134}$$

The argument of the square brackets can be recast in the form

$$\frac{1}{(n-1)!}\left(-\partial_r\right)^{n-1}\left[\frac{1}{r+i(\tau-\sigma)}+\frac{1}{r-i(\tau-\sigma)}\right]. \tag{4.135}$$

Consequently, one can apply these same derivatives in the real-time formulation in a distributional sense and get

$$\begin{aligned} iG_0^{>}(\vec{r},t,s) = iG_0^{<}(\vec{r},s,t) &= K_d\mathbf{P}^{(n-1)}\frac{1}{\left(r^2-(t-s)^2\right)^n}+ \\ &+i\frac{(-1)^{n-1}\pi K_d}{\left(r+(t-s)\right)^n+\left(r-(t-s)\right)^n}\left[\delta^{(n-1)}(r+t-s)-\delta^{(n-1)}\left(r+s-t\right)\right], \end{aligned} \tag{4.136}$$

where we recall that the $(n-1)$-th derivative of the principal value $\mathbf{P}^{(n-1)}\frac{1}{(x-y)^n}$ acts on test functions f as

$$\mathbf{P}^{(n-1)}\int \mathrm{d}x\frac{f(x)}{(x-y)^n} = \mathbf{P}\int \mathrm{d}x\frac{1}{(x-y)^n}\left[f(x)-\sum_{j=0}^{n-2}f^{(j)}(y)\frac{(x-y)^j}{j!}\right]. \tag{4.137}$$

Hence, one finds

$$-G^r(\vec{r},t,s) = \frac{2\pi(-1)^{n-1}K_d}{\left(r+(t-s)\right)^n+\left(r-(t-s)\right)^n}\,\delta^{(n-1)}\left(r-(t-s)\right) \tag{4.138}$$

The conformal Ising model

We now consider the $1+1$-dimensional conformal case. Although in general the expression of the response function G^r depends on the specific form of F_s in Eq. (4.36), we can still highlight a general feature, i.e., the fact that G^r always vanishes for $|t-s|<r$. In fact, on the one hand the function $u^{2\Delta}$ (with u as in Eq. (4.116)) is single-valued in this range, as can be inferred from Fig. 4.8. On the other hand, within this domain n in Eq. (4.117) is smaller than 1 and thus lies within the domain of analyticity of F_s. As a general consequence, $G^> = G^<$ for all values $|t-s|<r$, which yields, correspondingly, $G^r = 0$. As an example, for the critical Ising model one finds from the subtraction of Eqs. (4.119) and (4.118)

$$G^r(r,t,s) = -2\theta(t-s-r)\,|u|^{\frac{1}{8}}\left[\sin\left(\frac{\pi}{8}\right)\sqrt{\frac{n^{\frac{1}{2}}+1}{2}} \mp \cos\left(\frac{\pi}{8}\right)\sqrt{\frac{n^{\frac{1}{2}}-1}{2}}\right] \tag{4.139}$$

We tested this prediction against numerical data previously obtained in Ref. [4] and found a reasonable agreement, as illustrated in Fig. 4.9, mainly spoiled by the oscillations which unavoidably appear when considering systems of finite size. The function in Eq. (4.139) is also depicted in

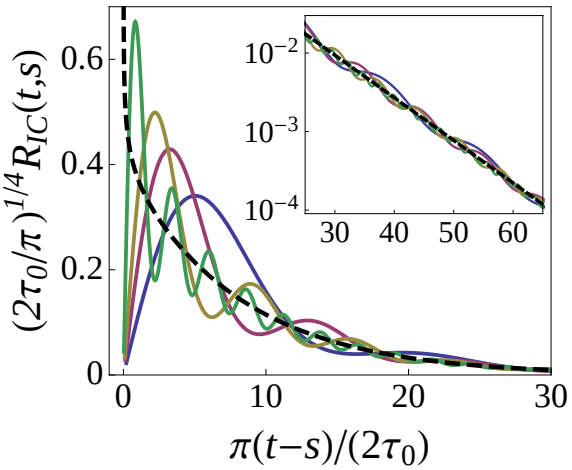

Figure 4.9: Response function $-G^r(r=0,t,s) = R_{IC}(t,s)$ of the order parameter of the quantum Ising chain in a transverse field g, prepared in an initial state corresponding to the ground state of its Hamiltonian with $g=g_0$ and quenched at time $t=0$ to the critical value $g=g_c=1$. The response is measured at the same point in which the perturbation is applied, i.e., $r=0$, within the regime in which t, s are large enough for R_{IC} to become stationary. The solid lines represent the numerical data (courtesy of L. Foini, L. Cugliandolo and A. Gambassi [4]), with $g_0 = 0.8$, 0.5, 0.3, and 0 in order of decreasing slope at the origin. The data have been rescaled with the values of $\tau_0(g_0)$ determined from the exponential slope $\propto e^{\pi(t-s)/16\tau_0}$ observed for $t-s \gg r$. The dashed line, instead, corresponds to the rescaled theoretical prediction in Eq. (4.139). The inset shows the same curves as in the main plot but in a logarithmic scale and on a wider range of values of the abscissa.

Fig. 4.10 for different values of the distance r and the "waiting time" s, for both fixed (upper sign in Eq. (4.139)) and free (lower sign) boundary conditions. This highlights the emergence of a light-

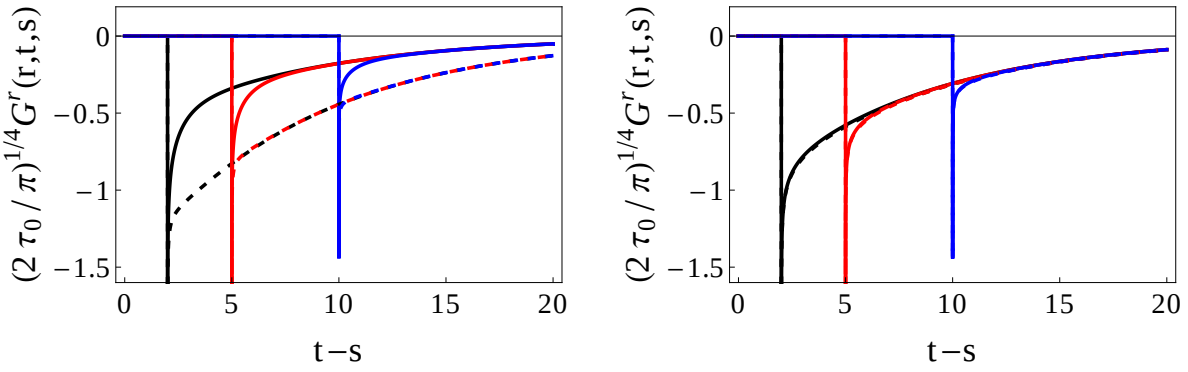

Figure 4.10: Retarded component $G^r(r,t,s)$ (i.e., minus the response function $-R(r,t,s)$) for the Ising model as a function of the difference of times $t-s$ for $r=2$ (black), $r=5$ (red) and $r=10$ (blue). Solid lines correspond to fixed, whereas dashed ones to free boundary conditions. For a given r, G^r vanishes identically for $t-s<r$, while it displays an algebraic divergence as $t-s\to r^+$. Panel (a) corresponds to $s=1$, while panel (b) to $s=5$. As s increases, G^r becomes effectively independent of the boundary conditions.

cone effect which is very similar to the one discussed in Refs. [2, 3] for correlations. In this case, however, instead of being related to the value of $t+s$, it depends on the difference $t-s$. This can be explained in terms of the same picture that has been proposed in Ref. [2]: upon performing the quench, entangled quasiparticles are created which propagate across the system at a finite velocity $v=1$, building up correlations in their wake. Thus, a time $t+s=r$ is required in order to observe a change in the correlations at distance r due to non-equilibrium effects. Analogously, applying a local perturbation $h(x,s)$ generates at time s excitations confined in a neighbourhood of the point x, which move at the same finite speed $v=1$. Therefore, in order for the system to respond to the external perturbation at a distance r, at least a time r has to elapse.

The light-cone structure emerges quite clearly also in the Gaussian case discussed above, as one can infer from Eqs. (4.129), (4.133) and (4.138). Moreover, in odd spatial dimension $d\neq 1$ the response function is non-vanishing only for $r=t-s$, i.e., exactly on the boundary of the light-cone.

On a side note, the imaginary-time formalism also provides a natural framework within which one can easily retrieve the expression of the response functions for the limiting cases $-ic_{++}=b\to 0$ and $b\to+\infty$ (with $a=d=0$), which give rise to Dirichlet and Neumann boundary conditions for the field, respectively (see Eq. (4.106)). For example, considering the quantum harmonic oscillator (with mass $m=1$) and adding to its Hamiltonian H_{QHO} a "source term" $h(t)\mathbf{x}$ one can explicitly calculate

$$G^r(t,s)=\left\langle \frac{\delta \mathbf{x}(t)}{\delta h(s)}\,|_{h\equiv 0}\right\rangle=-\frac{1}{\omega}\theta(t-s)\sin\left(\omega(t-s)\right), \tag{4.140}$$

which can be straightforwardly obtained from the antisymmetric part (see Eq. (4.112)) of

$$G^{>}(t,s) = -i\cos(\omega(t-s))\left[\frac{1}{4b}+\frac{b}{4\omega^2}\right] - i\cos(\omega(t+s))\left[\frac{1}{4b}-\frac{b}{4\omega^2}\right] - \frac{1}{2\omega}\sin(\omega(t-s)). \tag{4.141}$$

In the limits $b \to 0, +\infty$, however, the initial state becomes non-normalisable, being either an eigenstate of the momentum or of the position (as can be inferred from Eqs. (4.82) and (4.84)); this is reflected in the divergence of the expression above, which therefore must be normalised in a different way, the simplest one being taking the aforementioned limits after multiplying Eq. (4.141) by a suitable regularisation factor (i.e., $2b/\omega$ for $b \to 0$ and $2\omega b^{-1}$ for $b \to +\infty$), which yields

$$G^{>}(t,s) = -\frac{i}{2\omega}\left[\cos(\omega(t-s)) \pm \cos(\omega(t+s))\right], \tag{4.142}$$

where the sign $\pm$ refers to $b \to 0$, $b \to +\infty$, respectively. Clearly, $G^{>}$ is symmetric under the exchange $t \leftrightarrow s$, which implies that the response function (4.140) cannot be obtained from it. On the other hand, from the analytic continuation, before collapsing the film to the real axis one finds

$$G^{>}_{\varepsilon}(t,s) = -\frac{i}{2\omega}\left[\mathrm{e}^{-i\omega(t-s)} + \frac{\mathrm{e}^{-2\omega\varepsilon}\cos(\omega(t-s)) \pm \cos(\omega(t+s))}{\sinh(2\omega\varepsilon)}\right] \tag{4.143}$$

and therefore it is possible to derive

$$G^{r}(t,s) = \theta(t-s)\lim_{\varepsilon\to 0}\left[G^{>}_{\varepsilon}(t,s) - G^{>}_{\varepsilon}(s,t)\right], \tag{4.144}$$

which coincides exactly with Eq. (4.140). We emphasize again that this would have been impossible starting directly from expression (4.142).

4.5 Conclusions

Inspired by previous works which make use of the effective imaginary-time formalism in order to describe the dynamics of quantum systems after a quench [2, 3], we have investigated the conditions under which such a method can actually be employed. By using quantum mechanics as a very simple, but paradigmatic framework, we have formulated a constructive proof to show that, in general, an imaginary-time formalism can indeed be constructed. We have shown that the kernel representation of the evolution (4.62), which constitutes a necessary step in the introduction of the path-integral formalism, requires a specific time-ordering, i.e., in any expectation on the imaginary axis the time coordinates must appear in an increasing sequence. This condition would not be sufficient, however, if not supported by the introduction of a regularisation which may be expressed as $\rho_0 \to \frac{\mathrm{e}^{-\varepsilon H}\rho_0\mathrm{e}^{-\varepsilon H}}{\langle \mathrm{e}^{-2\varepsilon H}\rangle}$, where $\varepsilon > 0$ is an auxiliary parameter. Consequently, all times must lie within a film of width 2ε in the complex plane (which is sketched in Fig. 4.6(b)).

In this way, the problem can be reformulated in terms of an Euclidean description (which, from a practical point of view, is obtained through the substitution $t \to i\tau$ in the equations of motion),

while the boundary conditions are moved from $t = 0$ to the edges $\pm i\varepsilon$ of the film. We provide a general prescription of such a mapping in Eqs. (4.88) and (4.93). This procedure, however, does not always return properly-defined boundary conditions on the imaginary axis. In fact, this occurs only if the initial state is pure; in the case of a statistical mixture ($\rho_0 \neq \rho_0^2$), instead, one identifies equations which depend on the properties of both edges (e.g., see Eq. (4.69)). While consistent from the mathematical point of view, this means that an interpretation of the new system as a static film in $d+1$ dimensions (since Euclidean time is akin to a spatial coordinate) is no longer possible.

In the Euclidean picture, which features complex times, the various quantities are analytical as long as one does not change the ordering of the imaginary parts of the involved time variables; no constraint is imposed instead on the real parts. As a consequence, every sufficiently regular expectation defined on the imaginary axis and time-anti-ordered according to the prescription above can be analytically continued to the corresponding non-ordered function on the real-axis. Clearly, the knowledge of these quantities is sufficient to reconstruct any time-ordered quantity. We emphasize here, as done in Section 4.4, that the original ordering of times along the imaginary axis is not inconsequential: in fact, for each possible choice a different domain of analyticity is defined and, while performing the analytical continuation towards the real axis, one ideally cannot cross between them. The effect of this is that the original order of the operators is kept; for example, for a generic field Ψ define

$$G^{\varepsilon}(t,s) = \left\langle \Psi(i\tau)\Psi^{\dagger}(i\sigma) \right\rangle_{\varepsilon}.$$

Starting from the domain $\tau < \sigma$ one finds, according to the definitions (4.6), $iG^{>}(t,s)$ in real-time, whereas $\pm iG^{<}(t,s)$ is retrieved if the other domain ($\sigma < \tau$) is chosen, while the sign distinguishes between bosonic ($+$) and fermionic ($-$) fields.

We have also shown that, although response functions do not admit a global extension to the complex plane, due to their causal structure, their expressions can be derived from the imaginary time formalism by defining them in terms of non-ordered functions such as $G^{<}$ and $G^{>}$, which instead can be directly reproduced. Rather generically, the response function of one-dimensional systems quenched to criticality as well as the one of the Gaussian model in generic dimension $d > 1$ displays sharp light-cone effects which are analogous to those theoretically predicted [2–4, 110] and experimentally observed [39] for correlation functions: this describes the fact that information travels across the system at a finite speed ($v = 1$ in our units), and therefore one must wait for a local perturbation to propagate up to the considered point before being able to observe any response there. Finally, we have tested our predictions for the Ising conformal class against numerical data extracted from a finite one-dimensional Ising chain [4], finding a reasonable agreement.

Appendix 4.A Keldysh path-integral construction

In this Appendix we describe how the path-integral discussed in Sec. 4.1.1 can be constructed starting from Eq. (4.3). In doing this, many features mentioned in the previous Sections, such as the doubling of fields $\Phi \to \Phi_\pm$, will be made clearer. We wish to remark that the path-integral is not really a well-defined integral, but rather a quite convenient effective notation to use for the calculation of relevant quantities. For this reason, as was done in the original work by Feynman [111] which introduced the concept, we shall not concern ourselves with formal problems regarding the proper definition of the functionals and measures we will introduce below. As we have done before, we focus here on the case of a single, real scalar field $\Psi = \Psi^\dagger = \Phi$ and we assume that its evolution is governed by a Hamiltonian

$$H = \int \mathrm{d}^d x \left[\frac{\Pi(\vec{x})^2}{2} + U(\Phi(\vec{x})) \right] = \int \mathrm{d}^d x \left[\frac{\Pi(\vec{x})^2}{2} + \frac{(\vec{\nabla}\Phi(\vec{x}))^2}{2} + V\left(\Phi(\vec{x})\right) \right], \tag{4.145}$$

where Π is the field conjugate to Φ (see Eq. (4.11)) and V is a generic, regular function of its argument (typically, a polynomial). The first step of the procedure consists in discretising the contour in Fig. 4.1, i.e., dividing it into $2N$ equal parts of "small" width $\varepsilon = t_M/N$; the corresponding points are defined by

$$t_n = \theta(N-n)n\varepsilon + \theta(n-N)(2N-n)\varepsilon \quad \text{with} \quad n = 0, \dots 2N, \tag{4.146}$$

where θ indicates the Heaviside step function, with the convention $\theta(0) = 1/2$. Note that, with this choice, $t_n = t_{2N-n}\ \forall n$. We also introduce the instantaneous "eigenbasis" of the field $\{|\phi, t\rangle\}$, where $\phi(\vec{x})$ is supposed to be a real function of the spatial coordinates:

$$\Phi(\vec{x}, t)\,|\phi, t\rangle = \phi(\vec{x})\,|\phi, t\rangle\,. \tag{4.147}$$

By definition, the identity $F(\phi_1)\,\langle\phi_1|\,\phi_2\rangle = \langle\phi_1|\,F(\Phi)\,|\phi_2\rangle = F(\phi_2)\,\langle\phi_1|\,\phi_2\rangle$ holds for any function F, which implies $\langle\phi_1|\,\phi_2\rangle = c\,\delta(\phi_1 - \phi_2)$, where c depends on the normalisation of the eigenstates, which we fix at $c = 1$, while $\delta(\phi_1 - \phi_2)$ effectively represents a "delta functional" in the space of functions. Also note that the vector $|\phi, t\rangle$ does not evolve according to the Schrödinger representation, but its adjoint $|\phi, t\rangle = \mathrm{e}^{iHt}\,|\phi, 0\rangle$: in fact, by taking the equation above at $t = 0$ and multiplying it on the left by e^{iHt}, one obtains

$$\phi(\vec{x})\,\mathrm{e}^{iHt}\,|\phi, 0\rangle = \mathrm{e}^{iHt}\Phi(\vec{x}, 0)\,|\phi, 0\rangle = \mathrm{e}^{iHt}\,\Phi(\vec{x}, 0)\mathrm{e}^{-iHt}\,\mathrm{e}^{iHt}\,|\phi, 0\rangle = \Phi(\vec{x}, t)\,\mathrm{e}^{iHt}\,|\phi, 0\rangle\,. \tag{4.148}$$

At every instant t_n we introduce in expression (4.3) a representation of the identity

$$\mathbb{1} = \int \mathrm{D}\phi_n\,|\phi_n, t_n\rangle\,\langle\phi_n, t_n|\,, \tag{4.149}$$

where $\mathrm{D}\phi$ is assumed to be an appropriately normalised measure on the space of functions. By doing this, the generating functional takes the form

$$\int D\phi_0 \dots D\phi_{2N} \left(\prod_{n=0}^{2N-1} \chi_n \right) \langle\phi_0, t_0|\,\rho_0\,|\phi_{2N}, t_{2N}\rangle \tag{4.150}$$

in which, by recalling that $t_0 = t_{2N} = 0$, we are already able to recognise the initial term $\langle\phi(0_+)|\,\rho_0\,|\phi(0_-)\rangle$ appearing in Eq. (4.10), whereas

$$\chi_n = \langle\phi_{n+1},t_{n+1}|\,T_n\left[exp\left(i\int \mathrm{d}^d x\int_{t_n}^{t_{n+1}} dt\,J(\vec{x},t)\Phi(\vec{x},t)\right)\right]|\phi_n,t_n\rangle\,. \tag{4.151}$$

Here T_n stands for the standard time-ordering operator T for $n < N/2$, and for the anti-ordering one T^* for $n \geq N/2$. Note that for each pair t_n, t_{2N-n} of corresponding points, two different functions ϕ_n and ϕ_{2N-n} have been introduced, which are being integrated upon independently. The only exception lies at the rightmost point, i.e., $t_n = t_M$, where there is only ϕ_N. This reflects the necessity, already encountered in Sec. 4.1.1, of introducing two distinct fields ϕ_+ and ϕ_- which have to coincide at t_M.

Since for $N \gg 1$ the time interval ε becomes very short, one can think of the integrand in formula (4.151) as being almost constant over $[t_n,t_{n+1}]$, and hence approximate it with the value it takes at the lower bound t_n. This yields

$$\mathrm{e}^{i\,\alpha_n\,\varepsilon\int \mathrm{d}^d x\,J(\vec{x},t_n)\,\phi_n(\vec{x})}\;\langle\phi_{n+1},t_{n+1}|\,\phi_n,t_n\rangle \equiv \mathrm{e}^{i\,\alpha_n\,\varepsilon\,J(t_n)\circ\phi_n}\;\langle\phi_{n+1},t_{n+1}|\,\phi_n,t_n\rangle\,, \tag{4.152}$$

with $\alpha_n = 1$ for $n < N$ and $\alpha_n = -1$ for $n \geq N$. Now, in order to re-express the bracket on the right in a similar way, we recall that

$$\langle\phi_{n+1},t_{n+1}| = \langle\phi_{n+1},t_n|\,\mathrm{e}^{-iH(t_{n+1}-t_n)} = \langle\phi_{n+1},t_n|\,\mathrm{e}^{-iH\varepsilon\alpha_n}. \tag{4.153}$$

We now expand the exponent in powers of ε up to the first order:

$$\langle\phi_{n+1},t_n|\,\mathrm{e}^{-iH\varepsilon\alpha_n}\,|\phi_n,t_n\rangle \approx \langle\phi_{n+1},t_n|\,\mathbb{1} - iH\varepsilon\alpha_n\,|\phi_n,t_n\rangle\,; \tag{4.154}$$

in order to proceed, we focus on the calculation of $\langle\phi_2,t|\,H\,|\phi_1,t\rangle$, which, according to Eq. (4.145), can be readily rewritten as

$$\int \mathrm{d}^d x\left[\frac{1}{2}\,\langle\phi_2,t|\,\Pi(\vec{x},t)^2\,|\phi_1,t\rangle + U(\phi_1(\vec{x}))\,\langle\phi_2,t|\,\phi_1,t\rangle\right] \tag{4.155}$$

In the first addend, the conjugate field Π appears; from the canonical commutation relations (4.11) one can very easily prove that, for any function F which can be expanded as a power series, the identity

$$[F(\Phi(\vec{x},t)),\Pi(\vec{y},t)] = iF'(\Phi(\vec{x},t))\,\delta(\vec{x}-\vec{y}) \tag{4.156}$$

holds, and thus conclude that Π acts as a (functional) derivative on the field Φ; more precisely,

$$\Pi(\vec{x},t)\,|\phi,t\rangle = \left(-i\frac{\delta}{\delta\phi(\vec{x})}\right)|\phi,t\rangle\,, \tag{4.157}$$

which, introducing the instantaneous eigenbasis $\Pi(\vec{x},t)\,|\pi,t\rangle = \pi(\vec{x},t)\,|\pi,t\rangle$, that is completely analogous to the one introduced before for Φ, leads to

$$-i\frac{\delta}{\delta\phi(\vec{x})}\,\langle\pi,t|\,\phi,t\rangle = \langle\pi,t|\,\Pi(\vec{x},t)\,|\phi,t\rangle = \pi(\vec{x})\,\langle\pi,t|\,\phi,t\rangle\,, \tag{4.158}$$

implying $\langle\pi,t|\,\phi,t\rangle = \mathrm{e}^{i\int \mathrm{d}^d x\,\pi(\vec{x})\,\phi(\vec{x})} \equiv \mathrm{e}^{i\pi\circ\phi}$, where the multiplying factor that in principle would appear in front can be chosen to be 1 by appropriately fixing the normalisation of the new eigenbasis. Introducing the identity $\mathbb{1} = \int \mathrm{D}\pi\,|\pi,t\rangle\,\langle\pi,t|$ in the first addend of Eq. (4.155) one finds

$$\begin{aligned}&\langle\phi_2,t|\Pi(\vec{x},t)^2\,|\phi_1,t\rangle = \\ &\quad = \int D\pi\,\langle\phi_2,t|\,\pi,t\rangle\,\pi(\vec{x})^2\,\langle\pi,t|\,\phi_1,t\rangle = \int D\pi\,\pi(\vec{x})^2 \mathrm{e}^{i\pi\circ(\phi_1-\phi_2)},\end{aligned} \tag{4.159}$$

which can be finally used to rewrite Eq. (4.154) as

$$\int D\pi_n\,\mathrm{e}^{i\pi_n\circ(\phi_n-\phi_{n+1})}\left[1 - i\varepsilon\alpha_n\int \mathrm{d}^d x\left(\frac{1}{2}\pi_n(\vec{x})^2 + U(\phi_n(\vec{x}))\right)\right], \tag{4.160}$$

which, since we are disregarding higher-order (i.e., $O\left(\varepsilon^2\right)$) terms, can be conveniently rewritten as

$$\int D\pi_n\,\mathrm{e}^{i\pi_n\circ(\phi_n-\phi_{n+1}) - i\varepsilon\alpha_n\int \mathrm{d}^d x\left(\frac{\pi_n^2}{2}+U(\phi_n)\right)} = \mathscr{N}_n\,\mathrm{e}^{i\varepsilon\alpha_n\int \mathrm{d}^d x\left[\frac{(\phi_{n+1}-\phi_n)^2}{2\varepsilon^2} - U(\phi_n)\right]}, \tag{4.161}$$

where the spatial dependence has been made implicit, the Gaussian integral over π_n has been performed with the regularisation $\varepsilon \to \varepsilon - i0^+$ and $\mathscr{N}_n = \sqrt{\frac{2\pi}{i\varepsilon\alpha_n}}$ is a multiplying factor which we shall reabsorb into the measure $D\phi_n$. Now, if we introduce a curve $\phi(\vec{x},t)$ which obeys $\phi(\vec{x},t_n) = \phi_n(\vec{x})$ for all n, i.e., which reproduces the corresponding functions at every point of the discretisation, we can make the approximation

$$\frac{(\phi_{n+1}-\phi_n)^2}{2\varepsilon^2} = \frac{1}{2}\left(\frac{\phi(t_n+\alpha_n\varepsilon)-\phi(t_n)}{\varepsilon}\right)^2 \approx \frac{1}{2}\left(\partial_t\phi(t)\right)^2\,|_{t=t_n}. \tag{4.162}$$

By substituting this expression in Eq. (4.161) we obtain

$$\chi_n \propto \mathrm{e}^{i\varepsilon\alpha_n[L[\phi(t_n)]+J(t_n)\circ\phi(t_n)]} \equiv \mathrm{e}^{i\varepsilon\alpha_n L_J[\phi(t_n)]}, \tag{4.163}$$

where $L_J[\phi] = \int \mathrm{d}^d x\left[\frac{1}{2}\left(\partial_t\phi(\vec{x},t)\right)^2 - U(\phi(\vec{x},t)) + J(\vec{x},t)\phi(\vec{x},t)\right]$ is the Lagrangian corresponding to $H - J(t)\circ\phi$. In the limit $N\to\infty$ the discretisation t_n fills the contour and the corresponding integrations over ϕ_n can be thought to ideally become an integration over all paths $\phi(t)$. As we have specified above, however, with the exception of t_M, there are two independent integration variables for every point $t < t_M$; therefore, we actually need to introduce two different paths ϕ_+ (for $n < N$) and ϕ_- (for $n \geq N$). By recalling that $\alpha_n = 1$ for $n < N$ and $\alpha_n = -1$ for $n \geq N$ one finds

$$\left(\prod_{n=0}^{2N-1}\chi_n\right) \propto \mathrm{e}^{i\sum_{n=0}^{N-1}\varepsilon L_J[\phi_+(t_n)] - i\sum_{n=N}^{2N-1}\varepsilon L_J[\phi_-(t_n)]} \approx \mathrm{e}^{i\int_0^{t_M}\mathrm{d}t\,(L_J[\phi_+(t)]-L_J[\phi_-(t)])}, \tag{4.164}$$

eventually recovering Eq. (4.12). Note that the same reasoning applies also in the case of a time-dependent Hamiltonian (e.g., one with a polynomial V with evolving coefficients), the only difference being that one has to perform the substitution

$$\mathrm{e}^{-i\varepsilon\alpha_n H} \to T_n\left[exp\left(-i\alpha_n\int_{t_n}^{t_{n+1}} dt\,H(t)\right)\right], \tag{4.165}$$

starting from Eq. (4.153) onwards. Moreover, the choice (4.146) we have made of taking intervals $[t_n,t_{n+1}]$ of equal length can be relaxed as well.

5 Relaxation in closed quantum systems

In the past decade, the impressive progress in manipulating cold atomic gases has made it possible, for the first time, to gain experimental insight on the non-equilibrium dynamics of isolated, interacting quantum many-body systems, renewing the theoretical interest in the subject. Observations such as the lack of thermalisation in (almost) integrable one-dimensional Bose gases [35] (see Fig. 2.2(b)) and the appearance of an intermediate, metastable prethermal regime in a non-integrable system on time-scales much shorter than those required for its equilibration [51], call for a better understanding of the mechanisms underlying quantum relaxation. In this Chapter, we focus on the problem of *prethermalisation*, the basic features of which we recall below: in integrable systems, the existence of a maximal set of conserved quantities prevents the occurrence of thermalisation; instead, observables show an effective relaxation towards a non-thermal generalised Gibbs ensemble (GGE) [43, 49, 50], which encodes information on the whole set of constants of motion. When integrability is weakly broken, a many-body system initially prepared in the ground state of an integrable Hamiltonian may be trapped in an intermediate, quasi-stationary state, called *prethermal*, whose properties are mainly dictated by the GGE of the integrable counterpart, while being perturbatively corrected by the newly-introduced integrability-breaking term. This regime has been analytically studied both for closed systems, such as Fermi [112, 113] and Luttinger [114] liquids, and for open ones [115]. Despite this progress, the description of the breaking of integrability is technically challenging and generally difficult to capture without strong approximations.

The goal of this Chapter is to provide a simple model apt for the study of prethermalisation in a numerical fashion up to a considerable accuracy; starting from an integrable quantum Ising chain, whose properties will be briefly summarized in Sec. 5.1.1, we introduce a long-range spin-spin interaction which breaks many, but not all, of the original conservation laws, as will be detailed in Sec. 5.1.2. We show in Sec. 5.1.3 that an exact mapping exists to a model of hard-core bosons on a fully-connected lattice. As long as said quasi-particles' densities remain sufficiently low, one can think of the hard-core constraint as being substantially ineffective, and thus treat them as if they were ordinary bosons. This approximation, which holds for small quenches up to very large times (see, e.g., Fig. 5.3), renders the theory non-interacting and allows us to reinterpret the prethermalisation of the original non-integrable system in terms of the relaxation to the GGE of an approximately equivalent integrable one. We then proceed to solve numerically the latter up to quite a large size, highlighting, in the dynamics of some physically relevant observables, plateaux which are typically approached algebraically in time; our main results are reported in Sec. 5.2. For very long times the hard-core nature of the quasi-particles cannot be ignored anymore and, in fact, it effectively gives rise to scattering processes which lead the dynamics away from this integrable scenario and are thus expected to cause the asymptotic thermalisation of the system.

5.1 The model

Among many integrable models which could constitute a valid starting point, we have chosen for our analysis the one-dimensional *quantum Ising model in transverse magnetic field*, as its inherent simplicity makes it possible to obtain analytical expressions for many different quantities. The reason behind taking a long-range integrability-breaking term lies instead in the fact that it considerably simplifies the analytical study of the dynamics both within perturbative and self-consistent schemes, allowing in principle to gain insight on both prethermalisation and thermalisation regimes. Although we are not including in the present discussion any of the preliminary analytical results we have obtained, we shall demonstrate further below that the interaction term we introduce proves to be quite a convenient choice also in a numerical setting.

5.1.1 Integrable part: the Ising chain

The one-dimensional Ising model constitutes of a chain with N sites, each accommodating a $S = 1/2$ quantum spin; these spins are simultaneously subject to a nearest-neighbour interaction with strength J, which favours configurations in which they are all aligned along a specific direction (say, x), and an external magnetic field directed orthogonally to it (e.g., towards z), which instead tends to destroy such an ordering and has an amplitude gJ; its Hamiltonian is

$$H_0(g) = -\frac{J}{2}\sum_{i=1}^{N}\left(\widehat{\sigma}_i^x\,\widehat{\sigma}_{i+1}^x + g\widehat{\sigma}_i^z\right). \tag{5.1}$$

For simplicity, for the remainder of our discussion we shall set $J = 1$. The notation $\widehat{\sigma}_i^\mu$ ($\mu = x, y, z$) denotes the standard spin operators acting on the i-th site, i.e., from a technical point of view, for every $i = 1\ldots N$ they constitute a two-dimensional representation of a $SU(2)$ algebra with commutation relations

$$\left[\widehat{\sigma}_i^\mu, \widehat{\sigma}_i^\nu\right] = 2i\,\varepsilon^{\mu\nu\rho}\,\widehat{\sigma}_i^\rho, \tag{5.2}$$

where $\varepsilon^{\mu\nu\rho}$ is the completely antisymmetric tensor $\varepsilon^{xyz} = 1$, $\varepsilon^{\mu\mu\nu} = 0$, which changes sign upon permuting any pair of indices $\varepsilon^{\mu\nu\rho} = -\varepsilon^{\mu\rho\nu}$. In the eigenbasis of the z component $\{|\uparrow\rangle_i, |\downarrow\rangle_i\}$ these operators correspond to the Pauli matrices $\widehat{\sigma}_i^\mu \to \sigma^\mu$, with

$$\sigma^x = \begin{pmatrix} 0 & 1 \\ 1 & 0 \end{pmatrix}, \quad \sigma^y = \begin{pmatrix} 0 & -i \\ i & 0 \end{pmatrix}, \quad \sigma^z = \begin{pmatrix} 1 & 0 \\ 0 & -1 \end{pmatrix}. \tag{5.3}$$

By definition, each $\widehat{\sigma}_i^\mu$ leaves unaffected spins at any position $j \neq i$ and therefore these operators commute at different sites:

$$\left[\widehat{\sigma}_i^\mu, \widehat{\sigma}_j^\nu\right] = 0 \qquad \forall\, i \neq j \quad \forall\, \mu, \nu. \tag{5.4}$$

The Hamiltonian (5.1) is invariant under the $\mathbb{Z}_2$ transformation $\widehat{\sigma}_i^x \to -\widehat{\sigma}_i^x$, $\widehat{\sigma}_i^z \to \widehat{\sigma}_i^z$, which corresponds to the unitary operator $U_{\mathbb{Z}_2} = \prod_i \widehat{\sigma}_i^z$. Although being utterly insufficient to integrate the theory, this symmetry still possesses some physical relevance; in fact, in the thermodynamic limit $N \to \infty$, due to the competing effects of the two terms in Eq. (5.1), this model undergoes a prototypical quantum phase transition [13]; for $g > g_c = 1$ the system is *paramagnetic* and the

longitudinal magnetisation $\langle\widehat{\sigma}_i^x\rangle$ identically vanishes, whereas for $g<1$ a *ferromagnetic* ordering ensues which entails a spontaneous breaking of the $\mathbb{Z}_2$ symmetry, i.e., $\langle\widehat{\sigma}_i^x\rangle\neq 0$.

Integrability is made apparent after a Jordan-Wigner transformation accompanied by a Bogoliubov rotation [13] (refer to App. 5.A for the details), which allow the Ising chain to be rewritten as a free model with N independent fermionic modes (or *quasi-particles*). For simplicity, in the following we shall always assume that N is an even number. The Hamiltonian (5.1) becomes

$$H_0(g)=\sum_{\substack{k=1\\ odd}}^{N-1}\varepsilon_k\psi_k^\dagger\sigma^z\psi_k\,, \tag{5.5}$$

where

$$\psi_k=\begin{pmatrix}\gamma_k\\ \gamma_{-k}^\dagger\end{pmatrix}\quad\text{and}\quad\psi_k^\dagger=\begin{pmatrix}\gamma_k^\dagger\\ \gamma_{-k}\end{pmatrix}^{\mathsf{T}} \tag{5.6}$$

are Nambu spinors (here T denotes transposition), $\gamma_k^\dagger$ and γ_k are fermionic creation and annihilation operators at momentum k, respectively, which depend on the value of g and obey the canonical anticommutation relations

$$\left\{\gamma_k,\gamma_q^\dagger\right\}=\delta_{kq},\quad\left\{\gamma_k,\gamma_q\right\}=\left\{\gamma_k^\dagger,\gamma_q^\dagger\right\}=0, \tag{5.7}$$

and

$$\varepsilon_k\equiv\sqrt{1+g^2+2g\cos\left(\frac{\pi}{N}k\right)} \tag{5.8}$$

is the dispersion relation of the quasi-particles. Note that here σ_z is not a quantum spin operator, but represents instead a Pauli matrix acting on spinor indices. One may note that our conventions are slightly different from the ones which are most commonly employed in the literature and which lead, e.g., to a dispersion relation of the form $\varepsilon_k^2=1+g^2-2g\cos k$; the latter are exact only in the paramagnetic phase of the odd $\mathbb{Z}_2$ sector, while they constitute a good approximation for the even one in the thermodynamic limit. Since the typical quenching protocol ends up in the second sector, in order not to be forced to account for $O(1/N)$ corrections, we have adopted an exact formalism for the even case. One can prove that the N fermionic populations

$$\hat{n}_k=\gamma_k^\dagger\gamma_k \tag{5.9}$$

are conserved, as they commute with the Hamiltonian (5.5). Thus, their dynamics is trivial, as their expectations do not evolve, while the GGE is defined by the values they take on the initial state. Moreover, it becomes evident that these N constraints include and are actually much stronger than the original $\mathbb{Z}_2$ symmetry identified above, once the latter is rewritten in this picture as

$$U_{\mathbb{Z}_2}=\prod_k(1-2\hat{n}_k)=\mathrm{e}^{\,i\pi\sum_k\hat{n}_k}, \tag{5.10}$$

which describes, in this new language, the parity of the total number of fermions N_p, i.e., it evaluates to 1 if N_p is even and to -1 if odd, and where the rightmost equality comes from the fact that $\hat{n}_k^m\equiv\hat{n}_k$ for every integer $m\geq 1$, due to the anticommutation relations (5.7).

The typical procedure employed to drive this system out of equilibrium is a quench in the transverse magnetic field $g_0 \to g$; the subsequent dynamics has been thoroughly investigated when the system is isolated, both in the thermodynamic limit [116–120] and at finite size [121], and when it is open, either being coupled to an external thermal bath [122], or subject to a classical source of noise [115]. Although the issue may become more subtle, integrability can be highlighted also in spin variables; for example, considering the non-equilibrium dynamics of the total transverse magnetisation $M^z = \sum_i \widehat{\sigma}_i^z$ after a quench, it turns out that its connected correlation function (i.e., schematically, $\langle M^z M^z \rangle_c = \langle M^z M^z \rangle - \langle M^z \rangle \langle M^z \rangle$) in the long-time limit

$$\lim_{\tau\to\infty} \lim_{t\to\infty} \langle M^z(t+\tau) M^z(t) \rangle_c > 0 \tag{5.11}$$

violates the cluster property [4, 110]. From a physical point of view, this means that there is a given amount of information about this observable which is never really lost, as measurements separated by an arbitrary time τ are still correlated.

5.1.2 Integrability breaking and quench

The peculiar structure of the dynamics following a quench in the magnetic field is generally spoiled by breaking the integrability of the model, which introduces scattering between the quasi-particle modes γ_k; as a consequence, the energy initially injected into the system gets redistributed among them, and thermalisation eventually ensues. Our attention, however, is focused here on the effects that the breaking produces on much shorter time-scales, where integrability still plays a role; for the purpose of providing new insight on prethermalisation it is particularly valuable to have at hand a simple enough model, amenable to being studied in a controlled and physically transparent way. As we shall demonstrate in the following, such an instance can be obtained by adding an interaction term

$$V = \frac{\lambda}{N} \left(M^z - \overline{M^z} \right)^2 , \tag{5.12}$$

to the Ising Hamiltonian (5.1), where M^z is the total transverse magnetisation already introduced before Eq. (5.11) and $\overline{M^z}$ represents its long-time average calculated for $\lambda = 0$, i.e.,

$$\overline{M^z} = \lim_{T\to\infty} \frac{1}{T} \int_0^T \mathrm{d}t \left(\mathrm{e}^{iH_0(g)t} M^z \mathrm{e}^{-iH_0(g)t} \right) . \tag{5.13}$$

This subtraction is meant to cancel the "integrable" part of the operator M^z, i.e., the constants of motion $\hat{n}_k$ which enter its definition (see Eqs. (5.69) and (5.72)) and, indeed, one can prove that the connected correlation function of the remainder satisfies, in the thermodynamic limit, the cluster property at long times

$$\lim_{\tau\to\infty} \lim_{t\to\infty} \left\langle \left(M^z(t+\tau) - \overline{M^z}(t+\tau) \right) \left(M^z(t) - \overline{M^z}(t) \right) \right\rangle_c = 0. \tag{5.14}$$

Since the total magnetisation is a global quantity, V represents a long-range interaction, as we have already anticipated above and as will be made clearer below; furthermore, being extensive, it requires that the new term be divided by the dimension N of the system, in order not to spoil the extensivity of the energy.

Although turning on the interaction would be in principle sufficient to drive the system out of equilibrium, it is still preferable to accompany it with a quench $g_0 \to g$ in the magnetic field, which has the effect of populating the various modes to an extent; more precisely,

$$ {}_{\gamma(g_0)}\langle 0|\,\hat{n}_k(g)\,|0\rangle_{\gamma(g_0)} = {}_{\gamma(g_0)}\langle 0|\,\gamma_k^\dagger(g)\gamma_k(g)\,|0\rangle_{\gamma(g_0)} = \sin^2\left(\theta_k(g)-\theta_k(g_0)\right), \tag{5.15} $$

where $|0\rangle_{\gamma(g_0)}$ denotes the vacuum of the Hamiltonian $H_0(g_0)$, $\gamma_k^\dagger(g)$ and $\gamma_k(g)$ represent the operatorial basis which diagonalises $H_0(g)$ (see App. 5.A), θ_k is the Bogoliubov angle

$$ \tan 2\theta_k(g) = \frac{\sin\left(\frac{\pi}{N}k\right)}{g+\cos\left(\frac{\pi}{N}k\right)} \tag{5.16} $$

and $\hat{n}_k(g)$ is the number operator introduced in Eq. (5.9). The reason that makes this a convenient choice is twofold; on the one hand, as we specified above, the GGE is determined by the initial values of the N fermionic populations $\hat{n}_k$; thus, the analysis is made more comprehensive by including different possibilities. From a slightly different point of view, this allows to increase the amount of energy injected into the system without necessarily increasing the strength of the interaction. On the other hand, in the quasi-particle picture we are adopting, V introduces scattering among different modes; thus, it is very reasonable to account for the possibility of actually having fermions that scatter from the very beginning.

Recalling that the $\mathbb{Z}_2$ transformation $U_{\mathbb{Z}_2}$ introduced in the previous Section commutes with H_0 and each and every $\widehat{\sigma}_i^z$ (and thereby with their sum M^z), it is not difficult to show, from Eq. (5.13) that $\overline{M^z}$ is left invariant too. Consequently, the total, perturbed Hamiltonian $H = H_0 + V$ is still $\mathbb{Z}_2$-symmetric, and thus preserves the parity of the number N_p of quasi-particles. We now show that, although the same does not hold for the single populations $\hat{n}_k$, one can still identify an extensive number of conserved quantities. For this purpose, we recast the interaction V in the fermionic formalism

$$ V = \frac{\lambda}{N}\Big[\sum_{\substack{k=1\\ odd}}^{N-1} \sin(2\theta_k)\ \psi_k^\dagger \sigma^y \psi_k\Big]^2, \tag{5.17} $$

where θ_k denotes the Bogoliubov angle defined in Eq. (5.16) (see also Eqs. (5.51)). In this expression the long-range nature of this term becomes apparent, as it connects every possible pair of momenta k, q. The total Hamiltonian H is thus

$$ H = \sum_{\substack{k=1\\ odd}}^{N-1} \varepsilon_k\ \psi_k^\dagger \sigma^z \psi_k + \frac{\lambda}{N}\left[\sum_{\substack{k=1\\ odd}}^{N-1} \sin(2\theta_k)\ \psi_k^\dagger \sigma^y \psi_k\right]^2. \tag{5.18} $$

Exploiting the identity $\left[A^2,B\right]=A\left[A,B\right]+\left[A,B\right]A$, one can show that

$$[H,\hat{n}_k]=[V,\hat{n}_k]=i\frac{\lambda}{N}\left\{\left(M^z-\overline{M^z}\right)\sum_{\substack{k=1\\odd}}^{N-1}\left[\sin\left(2\theta_k\right)\left(\gamma_k^\dagger\gamma_{-k}^\dagger+\gamma_{-k}\gamma_k\right)\right]+\right.$$
$$\left.+\sum_{\substack{k=1\\odd}}^{N-1}\left[\sin\left(2\theta_k\right)\left(\gamma_k^\dagger\gamma_{-k}^\dagger+\gamma_{-k}\gamma_k\right)\right]\left(M^z-\overline{M^z}\right)\right\}, \tag{5.19}$$

which proves that, for any finite N, not even a single population is conserved. In fact, according to definition (5.51), $\sin\left(2\theta_k\right)>0$ for every odd, positive integer k. Nonetheless, since both the Bogoliubov angle θ_k and the two-particle operators $\gamma_k^\dagger\gamma_{-k}^\dagger$ and $\gamma_{-k}\gamma_k$ appearing above are odd with respect to the momentum, i.e., $\gamma_k\gamma_{-k}=-\gamma_{-k}\gamma_k$, the global expression remains the same under the shift $k\rightarrow-k$, which implies $[H,\hat{n}_k]=[H,\hat{n}_{-k}]$, and thus every

$$I_k=\hat{n}_k-\hat{n}_{-k} \tag{5.20}$$

commutes with the Hamiltonian H (the properties of these operators in the Ising models are discussed in Ref. [121]).

5.1.3 Mapping to hard-core bosons and low-density approximation

Thanks to the presence of the I_k's, which represent a set of $N/2$ mutually commuting constants of motion, the spin chain described by H can be exactly mapped onto a quadratic (yet non-diagonal) Hamiltonian of hard-core bosons, as we show here. First of all, we analyse the structure of the Hilbert space in the light of these constraints: each I_k admits only three distinct eigenvalues, 0 and ±1, which correspond to states in which two quasi-particles with momenta $\pm k$ are either simultaneously present or absent ($|k,-k\rangle$ and $|\emptyset_k\rangle$), and to states in which only one of the two is present ($|k\rangle$ or $|-k\rangle$), respectively. We shall refer to the space spanned by these 4 vectors as the k-th "subsector". We remark that its vacuum $|\emptyset_k\rangle$ is in principle different from the global vacuum $|0\rangle=\bigotimes_k|\emptyset_k\rangle$. Every possible choice of the $N/2$ eigenvalues mentioned above identifies an eigenspace, which in the following we will call "eigensector", or "sector", for short; for example, for $N=4$ the string $\{I_1=1,I_3=1\}$ corresponds to the vector $|k=1\rangle\otimes|k=3\rangle$, whereas the string $\{I_1=0,I_3=-1\}$ is associated to the two-dimensional space generated by $|\emptyset_1\rangle\otimes|-3\rangle$ and $|1,-1\rangle\otimes|-3\rangle$. Since the aforementioned strings are $N/2$-characters long and the "alphabet" includes only three possibilities, the total number of sectors in which the global configuration space is split is $3^{\frac{N}{2}}$. The dimension of each is 2^{N_0}, with N_0 the total number of 0s appearing in the corresponding string, because there are two possible choices for each 0, the two quasi-particles at opposite momenta being either both absent or present, whereas every ±1 unambiguously fixes the related vector, as seen in the example above. The number of ±1s dictates instead the $\mathbb{Z}_2$-parity of the eigensector, as it counts the number of unpaired quasi-particles present. For example, for $N=8$, $\{0,0,1,-1\}$ identifies an even subspace of dimension 4, whereas $\{0,1,1,-1\}$ an odd one of dimension 2. By construction, each sector carries also a definite momentum $k\times I_k$ in each subsector. Thereby, the only possible operators which leave all eigensectors invariant are those which,

in every subsector, preserve both parity and momentum. Among all possible combinations of the fundamental operators $\gamma_{\pm k}$ and $\gamma^\dagger_{\pm k}$, the only (non-trivial) ones satisfying these constraints are the quadratic operators

$$\hat{n}_{\pm k} = \gamma^\dagger_{\pm k}\gamma_{\pm k}, \qquad b^\dagger_k = \gamma^\dagger_k\gamma^\dagger_{-k}, \qquad b_k = \gamma_{-k}\gamma_k\,, \tag{5.21}$$

which represent the populations and the creation and annihilation of pairs with zero net momentum, respectively, and the quartic one

$$\hat{n}_k\hat{n}_{-k} = b^\dagger_k b_k. \tag{5.22}$$

All other possibilities can be re-expressed in terms of these by making use of the canonical anti-commutation relations (5.7).

Like every operator which commutes with each I_k, the Hamiltonian H clearly constitutes a combination of the operators above. Less trivial is the fact that it can actually be rewritten entirely in terms of pair operators (for the derivation, see App. 5.B):

$$\begin{cases} H = \sum\limits_{\substack{k=1\\ odd}}^{N-1}\left[\varepsilon_k - \frac{\lambda}{N}\sin^2(2\theta_k)\right]\left(I_k^2 - 1\right) + H', \\ H' = \sum\limits_{\substack{k,q=1\\ odd}}^{N-1}\left[2\beta_{kq}b^\dagger_k b_q - \alpha_{kq}(b^\dagger_k b^\dagger_q + b_k b_q)\right], \end{cases} \tag{5.23}$$

with

$$\alpha_{kq} = \frac{\lambda}{N}(1-\delta_{kq})\sin(2\theta_k)\sin\left(2\theta_q\right) \quad \text{and} \quad \beta_{kq} = \varepsilon_k\delta_{kq} + \alpha_{kq}. \tag{5.24}$$

This implies that the relevant dynamics is described by the interaction of zero-momentum pairs, rather than single fermionic modes, and that we can therefore reformulate the problem in terms of these new quasi-particles. In order to do that, we shall first uncover their nature: as they obey

$$\begin{gathered} \left[b_k^{(\dagger)}, b_q^{(\dagger)}\right] = 0 \quad \forall k \neq q, \qquad \left\{b^\dagger_k, b^\dagger_k\right\} = \left\{b_k, b_k\right\} = 0, \\ \left\{b_k, b^\dagger_k\right\} = 1 - I_k^2, \end{gathered} \tag{5.25}$$

they behave almost, but not exactly, as hard-core bosons, which would require the last anticommutator to be 1. On the other hand, by noticing that, in a sector with $I_k = \pm 1$, both b_k and $b^\dagger_k$ act as the null operator, we can effectively expunge them from H'. This operation leaves behind only those corresponding to momenta q for which $I_q = 0$, which then satisfy the hard-core constraint. Thereby, within a sector characterised by having $N/2 - N_0$ unpaired quasi-particles, the projected Hamiltonian effectively describes a fully-connected model of hard-core bosons on a lattice with N_0 sites. The corresponding base can be obtained by setting, for every involved k, the correspondence $|\emptyset_k\rangle \to |\mathbf{0}_k\rangle$, $|k,-k\rangle \to |\mathbf{1}_k\rangle$, where $\mathbf{0}$ and $\mathbf{1}$ stand for the boson being absent or present, respectively.

This reinterpretation efficiently highlights the effect produced by V on the integrability of the model: as we have seen that there are still $N/2$ conserved quantities, in fact, we cannot expect the latter to be completely lost and, indeed, we identify sectors in which the theory is trivially solvable, which are the ones that are almost completely lacking pairs (i.e., those whose strings display just a few 0s). For example, the $2^{\frac{N}{2}}$ totally-unpaired sectors collectively represent the zero-energy

eigenspace of the Hamiltonian H and coincide with the corresponding one of H_0; furthermore, each of the $\frac{N}{2}2^{\frac{N}{2}-1}$ sectors having a single pair is two-dimensional and the corresponding reduced Hamiltonian is already cast in diagonal form

$$\begin{pmatrix} -\varepsilon_k + \frac{\lambda}{N}\sin^2(2\theta_k) & 0 \\ 0 & \varepsilon_k + \frac{\lambda}{N}\sin^2(2\theta_k) \end{pmatrix} \tag{5.26}$$

in the basis $\{|\mathbf{0}_k\rangle, |\mathbf{1}_k\rangle\}$ introduced above. This is due to the presence of an additional symmetry in this model which separates each sector in two halves of equal dimension and involves the parity of the number of pairs, i.e.,

$$\left[H, \mathrm{e}^{i\pi\Sigma_k b_k^\dagger b_k}\right] = 0. \tag{5.27}$$

From a physical point of view, this is associated to the fact that the action of H' in Eq. (5.23) either leaves their total number untouched, or it simultaneously creates or destroys two bosons. Therefore, for any choice of N, there are always $2^{N/2-2}(N+4)$ shared eigenvectors between H and H_0. Although the structure becomes progressively more complicated as N_0 grows, it is clear that it cannot really display non-integrable features as long as the dynamics remains confined in the low-N_0 sectors.

The situation is reversed for $N_0 \approx N/2 \gg 1$; even though the corresponding eigensectors are exponentially smaller than the global Hilbert space (whose dimension is 2^N), their dimensions are still exponentially large in the number of sites, as expected for a truly many-body problem. Note that, even though the Hamiltonian (5.23) is quadratic in the pair operators, it does not define a free theory, due to the hard-core nature of the bosons; indeed, if one tried to diagonalise it by applying a generic Bogoliubov rotation

$$b_k = A_{kq} b'_k + B_{kq} b'^\dagger_k \tag{5.28}$$

would immediately face the problem that there is no choice for the matrices A and B which can preserve the mixed commutation/anticommutation relations (5.25) other than the trivial one $A \equiv \mathbb{1}$, $B \equiv 0$. This relates to the fact that hard-core bosons are intrinsically interacting particles, for they can be thought as ordinary bosons subject to infinite interparticle repulsion.

Within our setting, the dynamics always starts from the totally-paired sector $N_0 = N/2$, independently of the values of the quench parameters g_0, g and λ. The initial state, in fact, can be represented as [110, 117]

$$|0\rangle_{\gamma(g_0)} \propto \mathrm{e}^{i\Sigma_k t_k b_k^\dagger} |0\rangle_{\gamma(g)}, \tag{5.29}$$

where $t_k = \tan(\theta_k(g) - \theta_k(g_0))$ (see also Eq. (5.61)) and the effect of the operator in the r.h.s. is to generate pairs on the vacuum. Thereby, this class of initial states constitutes a suitable choice for highlighting the effects of V on the dynamics. Still, for $N \gg 1$, the interacting problem is hard to solve; instead of employing the usual perturbative expansion in the interaction strength one can take in this case a different approach, which makes use of the quadratic structure of the Hamiltonian. The point is that the hard-core constraint is expected to become effective only when the filling of a given mode approaches 1; as long as the quasi-particles' densities remain much lower than that, they behave approximately as standard bosons. From a formal point of view, the pair operators b_k, $b_k^\dagger$ can be expressed in terms of truly bosonic ones a_k, $a_k^\dagger$ by means of a Holstein-Primakoff

transformation [123]

$$b_k = \sqrt{\mathbb{1} - a_k^\dagger a_k}\, a_k \quad \text{and} \quad b_k^\dagger = a_k^\dagger \sqrt{\mathbb{1} - a_k^\dagger a_k}; \tag{5.30}$$

one can then think of expanding the square roots as power series of their arguments

$$\begin{aligned} b_k &= \left(\mathbb{1} - \frac{1}{2}\widehat{N}_k - \frac{1}{8}\widehat{N}_k^2 + \dots\right) a_k, \\ b_k^\dagger &= a_k^\dagger \left(\mathbb{1} - \frac{1}{2}\widehat{N}_k - \frac{1}{8}\widehat{N}_k^2 + \dots\right), \end{aligned} \tag{5.31}$$

where $\widehat{N}_k = a_k^\dagger a_k$ is the bosonic number operator. Hence, as long as the average and the fluctua-

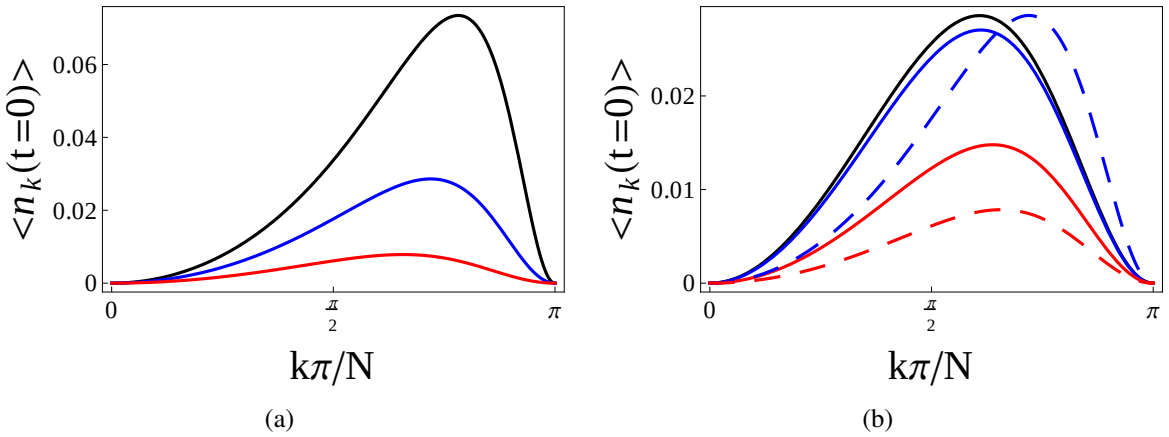

Figure 5.1: Initial populations $\langle \hat{n}_k(t=0)\rangle$ as functions of the rescaled momentum NK/π for various choices of the quench parameters. (a) Curves at fixed $g_0 - g = 3$; different colours correspond to $g = 1.5$ (black), $g = 2$ (blue) and $g = 3$ (red); the filling of the modes increases the closer g is to the critical value $g_c = 1$. (b) Curves at fixed $g = 3$; the different colors for the solid lines are associated to $g_0 = 10^4$ (black), $g_0 = 10^2$ (blue) and $g_0 = 10$ (red). Unsurprisingly, the populations increase with the quench amplitude $|g - g_0|$, however they seem to saturate far from their maximal value 1. The dashed lines correspond to the ones with the same colours in Fig. 5.1(a); by comparing them with the solid lines, one can conclude that the initial value of the populations is much more affected by the distance from the critical point $g - 1$ than by the relative distance of the quench parameters $|g_0 - g|$.

tions of $\widehat{N}_k$ remain small, one can conveniently truncate the expansions to just a few of the first terms. Further details on this approximation are provided in App. 5.C. What makes this approach particularly convenient is that, by expanding at the lowest order $b_k^\dagger \approx a_k^\dagger$ and $b_k \approx a_k$, we obtain in each sector a quadratic, bosonic Hamiltonian which can now be diagonalised by a Bogoliubov rotation. Calling K_S the set of paired momenta present in a given sector S, the expression of this Hamiltonian is

$$\begin{cases} H_S = -\sum\limits_{k \in K_S} \left[\varepsilon_k - \frac{\lambda}{N}\sin^2(2\theta_k)\right] + H_S', \\ H_S' = \sum\limits_{k,q \in K_S} \left[2\beta_{kq} a_k^\dagger a_q - \alpha_{kq}(a_k^\dagger a_q^\dagger + a_k a_q)\right], \end{cases} \tag{5.32}$$

where the absence of terms such as b_k^2 is still reflected in our definition of the matrix α_{kq}, which has vanishing diagonal part.

Quenches in the magnetic field such as the ones we consider here typically produce small initial populations, i.e., $\langle \hat{n}_k \rangle \ll 1 \ \forall k$ — and are thus suitable to be studied within the approximation introduced above — as long as g is not too close to the critical point $g_c = 1$. On the other hand, the actual amplitude of the quench $|g - g_0|$ is relatively inconsequential, as illustrated in Fig. 5.1. For $t > 0$, the time frame of validity of the low-density approximation is determined also by the strength of the interaction λ: intuitively, the term $a_k^\dagger a_q^\dagger$ in Eq. (5.32) is the one mainly responsible for the breakdown of the latter, since it is the only one which can actually populate the system to higher levels, and its coefficient α_{kq} is proportional to λ. At longer times, the integrable picture provided by the Hamiltonian (5.32) is spoiled because higher-order terms in the expansion of the Holstein-Primakoff representation (5.31) introduce novel interactions. The latter are expected to eventually drive the system away from its GGE towards a thermal distribution.

5.2 Numerical diagonalisation and results

As we have shown in the previous Section, the ground state of $H_0(g_0)$ lies in the totally-paired sector of H. This implies that, as long as we focus on invariant quantities (such as the populations $\hat{n}_k$) it is sufficient to restrict the analysis to this sector, since the dynamics will never leave it. The main advantage of working with the bosonic Hamiltonian (5.32) is that, being quadratic, it is not necessary to diagonalise it on the whole eigensector, which would imply an exponential complexity of order $2^{\frac{N}{2}}$, but it is sufficient to solve the one-particle problem by applying an appropriate Bogoliubov rotation

$$a_k = A_{k,q}\eta_q + B_{k,q}\eta_q^\dagger, \qquad a_k^\dagger = A_{k,q}^*\eta_q^\dagger + B_{k,q}^*\eta_q, \tag{5.33}$$

(the summation over repeated indices is understood) which casts H' in the form

$$H' = \sum_{\substack{q=1 \\ odd}}^{N-1} E_q \eta_q^\dagger \eta_q + C, \tag{5.34}$$

where $\left\{E_q\right\}_q$ is the single-particle spectrum and C an unimportant constant. This problem amounts to the diagonalisation of a $N \times N$ matrix, and is thus of polynomial complexity in N. As a consequence, one can conduct a numerical analysis up to quite large system sizes. Details about the diagonalisation procedure and the numerical computation of the relevant observables are provided in App. 5.D. For $\lambda = 0$, one readily obtains from Eq. (5.24) that $\beta_{kq} = \varepsilon_k \delta_{kq}$ and this implies that the unperturbed bosonic one-particle spectrum is $E_k = 2\varepsilon_k$, where the factor 2 accounts for the fact that each boson represents a pair of fermions with equal energies. The unperturbed eigenvalues are reported in Fig. 5.2(a), which clearly shows that the spectrum is non-degenerate. As a consequence, the first non-trivial corrections due to the interaction are of order $O\left(\lambda^2\right)$, as shown in Fig. 5.2(b) and 5.2(c). Moreover, they scale as $1/N$ with the system size, as we have also verified numerically.

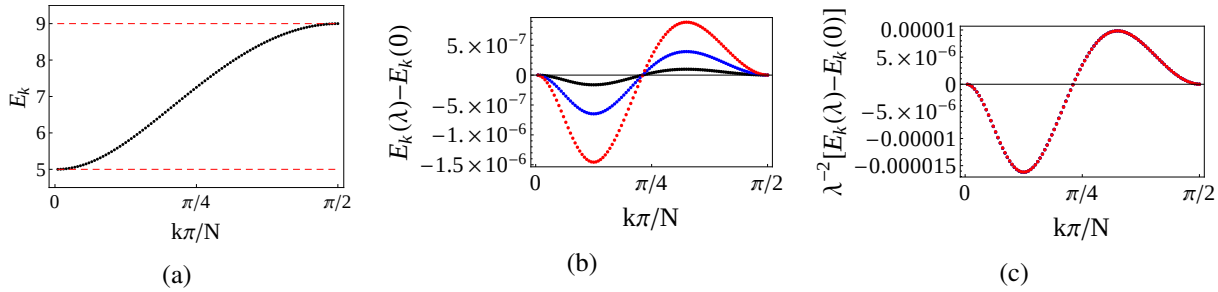

Figure 5.2: (a) Plot of the non-interacting one-particle bosonic spectrum $E_k(\lambda = 0) = 2\varepsilon_k$ (i.e., twice expression (5.8)) in increasing order for $N = 200$ and $g = 3.5$; the two dashed red lines denote the two extrema $g-1$ and $g+1$. (b) Difference $E_k(\lambda) - E_k(0)$ between the perturbed and unperturbed eigenvalues for $\lambda = 0.1$ (black), 0.2 (blue) and 0.3 (red). (c) As expected for a non-degenerate spectrum such as the one shown in panel (a), the first non-trivial correction is of order $O\left(\lambda^2\right)$; this plot shows the same curves of panel (b) after being rescaled by $1/\lambda^2$, which makes them collapse on a single master curve.

In order to gain some insight on the range of validity of the low-density expansion, we have diagonalised exactly the fermionic Hamiltonian (5.23) in the aforementioned, totally-paired sector up to $N = 20$ (this constitutes an exponentially-complex problem, so we had to consequently limit the system size) and compared the so-obtained dynamics with the one extracted from the bosonic

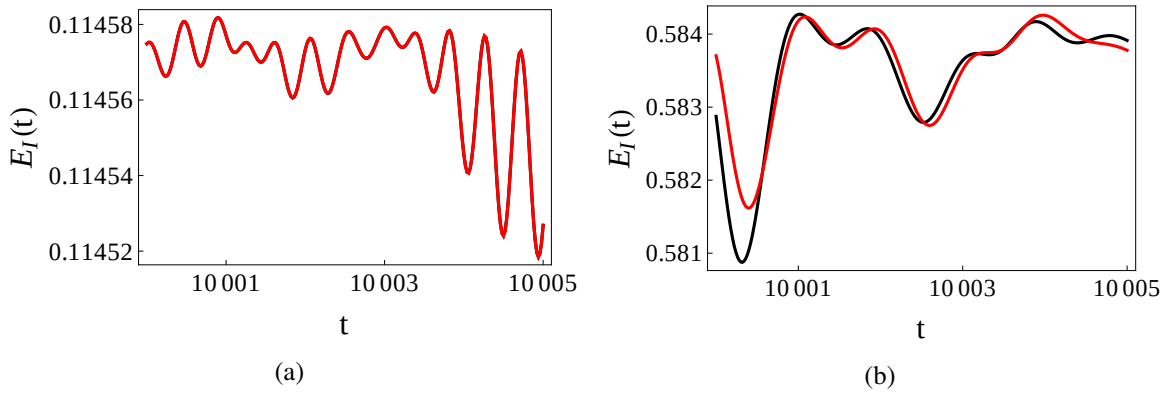

Figure 5.3: Temporal evolution of the Ising energy $E_I(t) = \langle H_0(t)\rangle$ for $g_0 = 8$, $\lambda = 0.1$ and $N = 20$ within the time interval $t \in [10000, 10005]$. Black lines represent data calculated in the fermionic formalism, whereas red ones refer to the bosonic one. (a) For $g = 3.5$ the two curves are indistinguishable in this time range. (b) For $g = 1.5$, which means closer to the critical point than (a), the red curve still resembles the black one. However, the low-density approximation breaks down much earlier than in the previous instance.

formalism. In Fig. 5.3 we report the evolution of the Ising energy

$$E_I^{(b/f)}(t) = \langle H_0(g,t)\rangle = \sum_{\substack{k=1\\ odd}}^{N-1} \varepsilon_k \langle \hat{n}_k(t)\rangle \tag{5.35}$$

calculated in the bosonic (b) and fermionic (f) formalism for $N = 20$, $g_0 = 8$, $\lambda = 0.1$ and two different values of g in the time frame $\left[10^4, 10^4+5\right]$ which, as we will show in the following, includes very large times with respect to the typical scales at which prethermalisation emerges. As panel (a) corresponds to $g = 3.5$ and panel (b) to $g = 1.5$, it becomes apparent that the low-density approximation fails on shorter and shorter time-scales the closer the quench ends to the critical point $g_c = 1$. This is related to the fact that, as we mentioned at the end of Sec. 5.1.3, the closer g is to its critical value, the larger are the initial populations $\langle \hat{n}_k(t=0)\rangle$. On the other hand, we have numerically verified that for $g = 1.01$ and all the other parameters fixed as above, the agreement of the two curves remains within 2% up to $t \simeq 10^3$, which implies that, as long as the interaction λ is small, the low-density approximation enjoys a very large range of validity. In order to understand the effect of the interaction, we have also performed the same comparison at different values of λ and N; the results are shown in Fig. 5.4, where we report the relative error

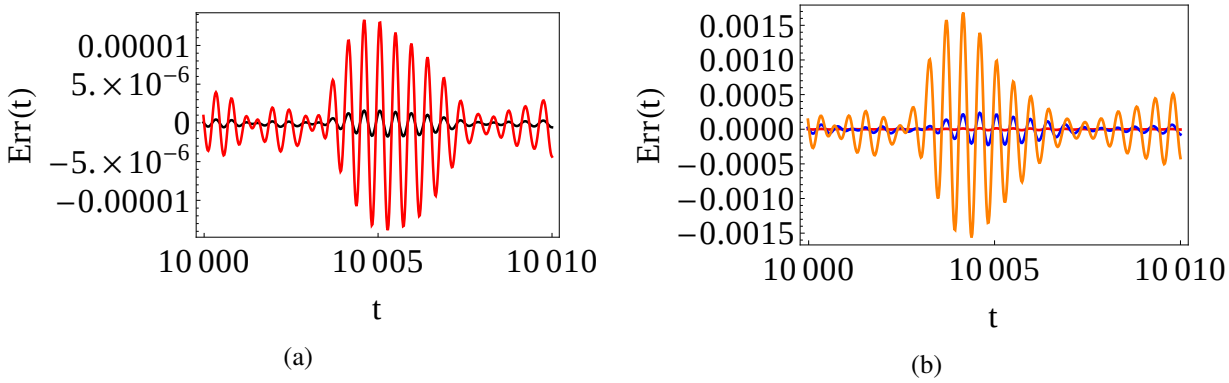

Figure 5.4: Plots of the relative error $Err(t)$ defined in Eq. (5.36) as a function of time for $N = 20$, $g_0 = 8$, $g = 3.5$ and various values of the interaction strength $\lambda = 0.1$ (black), 0.2 (red), 0.5 (blue) and 0.9 (orange). (a) Both choices $\lambda = 0.1$ and 0.2 display very small error up to very long time scales. (b) This plot highlights the fact that the error grows considerably when increasing λ; as stated above, the red line, which here looks almost constant, coincides with the one displayed in panel (a).

$$Err(t) = \frac{E_I^{(f)}(t) - E_I^{(b)}(t)}{E_I^{(b)}(t)} \tag{5.36}$$

on the Ising energy due to the low-density approximation. From them, we infer that indeed strong interactions tend to spoil the approximation much before, even though their effect seems to be less drastic than ending the quench near the critical point. Even if just in the limited range $N \leq 20$, we have also verified that the accuracy improves when increasing the size N.

By comparing panels (a) and (b) in Fig. 5.3 one can see that the typical frequency of oscillations depends on the value of g. As a matter of fact, the expectations of operators such as n_k, a_k and $a_k^\dagger$ can be expressed as sums of terms oscillating in time with frequencies $|E_n - E_m|$ and $E_n + E_m$, which we will be referring to as "slow" and "fast", respectively. Comparing the discrepancy of the actual spectrum with respect to the unperturbed one in Fig. 5.2(b) with the energy scales of Fig. 5.2(a), it emerges clearly that for small λ the spectrum of H_0 is very weakly perturbed, and thus $E_k \approx 2\varepsilon_q$; this implies that the slow frequencies range approximately from 0 to 4, whereas the fast ones from $4(g-1)$ to $4(g+1)$, which justifies our naming conventions for $g > 2$. This separation

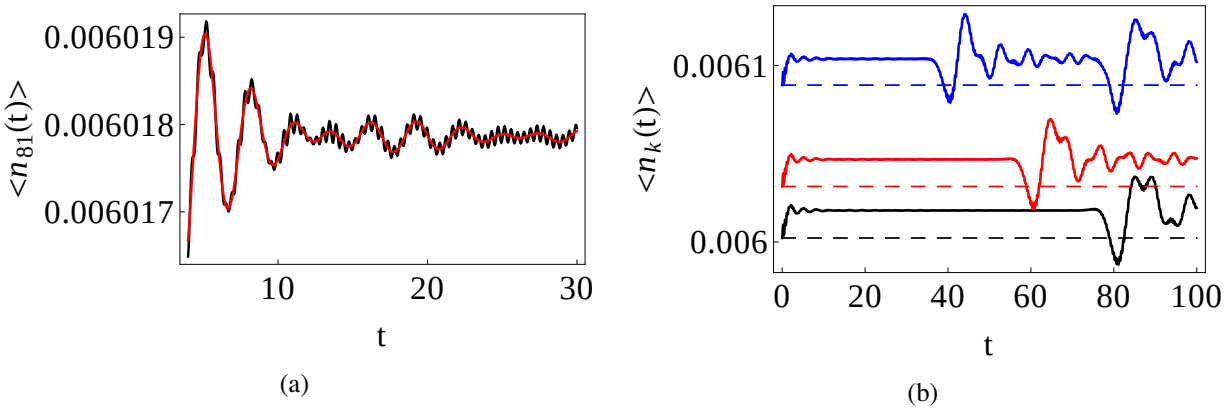

Figure 5.5: Population dynamics $\langle \hat{n}_k(t) \rangle$ for $g_0 = 8$, $g = 3$ and $\lambda = 1$. (a) The black curve represents the evolution of the central ($k = 81$) population $\langle \hat{n}_{81}(t) \rangle$ for $N = 160$. The red one is the corresponding evolution calculated taking into account only the slow modes. This plot clearly highlights the presence of fast modes which "dress" the curve described by the slow ones. (b) Dynamics for various values of the system size N: the black solid line denotes the population for $k = 81$ and $N = 160$; the red one $k = 61$ and $N = 120$; the blue one $k = 41$ and $N = 80$. The dashed lines of the respective colours keep track of the initial ($t = 0$) value of each curve. Thus, it emerges clearly that the populations relax towards a prethermal value which is different from the initial one. The plateaux last until a recurrence time t_R which marks the reappearance of oscillations and corresponds approximately to $N/2$.

of time scales is highlighted in Fig. 5.5(a) in the dynamics of a single population $\langle \hat{n}_{81}(t) \rangle$, which is representative of the typical behaviour.

As we have mentioned at the end of Sec. 5.1.3, thermalisation cannot occur without scattering (and thus energy and momentum redistribution) among the modes. This requires the breakdown of the low-density approximation, since within its scheme the Hamiltonian (5.32) is substantially free. Therefore, the typical time scales on which it ensues have to be larger than the regime of validity of the numerical picture we are providing. Actually, as can be read from Fig. 5.4, for a wide range of the quench parameters they are some orders of magnitude greater than the typical scales required for prethermalisation. The latter can be gleaned from Fig. 5.5(b), where marked plateaux arise in the evolution of the bosonic populations (which, at this level, are substantially equal to the fermionic ones): these quasi-stationary values are typically reached within $t \sim 10$, independently of the system size. As mentioned above, however, the dynamics of observables such as these is characterised by a finite collection of frequencies; therefore, the destructive interference

which gives rise to the aforementioned plateaux cannot last indefinitely at finite size and, in fact, oscillations reappear at a recurrence time $t_R \approx N/2$.

The same prethermal behaviour is reflected in the evolution of extensive observables such as the total number of quasi-particles $N_p(t) = \sum_k \langle \hat{n}_k(t) \rangle$ and the Ising energy (5.35), which represent two examples of a wider class of quantities which can be written as linear combinations of the populations

$$\mathcal{O}(t) = \sum_{\substack{k=1 \\ odd}}^{N-1} c_k \langle \hat{n}_k(t) \rangle , \tag{5.37}$$

corresponding to $c_k = 1$ and $c_k = \varepsilon_k$, respectively. Figure 5.6 displays the evolution of said observables and highlights, as expected, the presence of quasi-stationary values preceded by oscillations which decay algebraically as $t^{-\alpha}$, with $\alpha \approx 3$; to render apparent the latter, we also provide the same plots in double-logarithmic scale. The fact that the same exponent $\alpha \approx 3$ appears in both

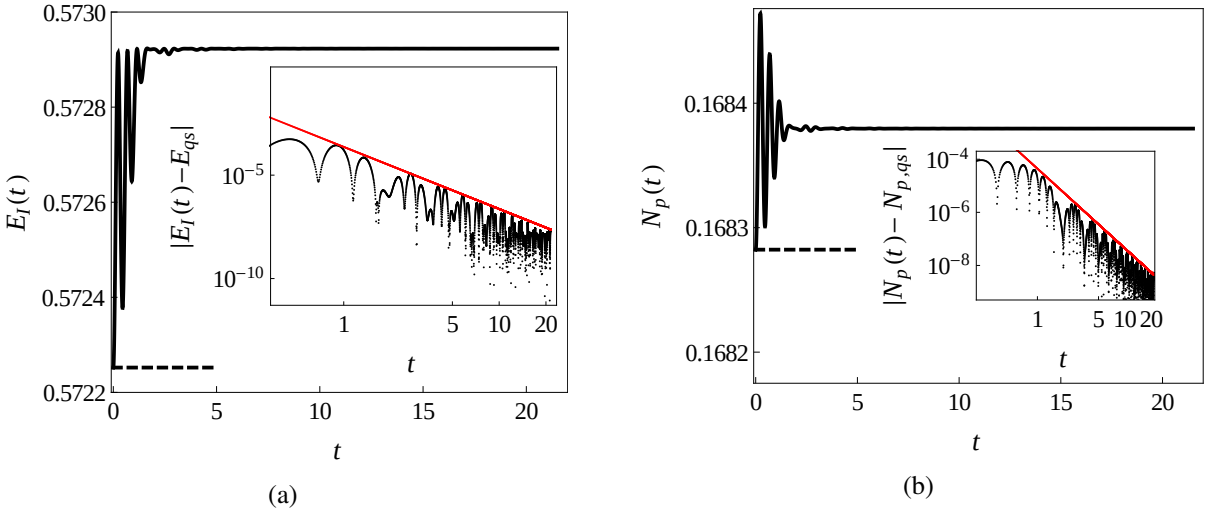

Figure 5.6: (a) Time evolution of the Ising energy $E_I(t)$ for $N = 100$, $g_0 = 8$, $g = 3.5$, and $\lambda = 0.1$. E_I attains a quasi-stationary value E_{qs} with an oscillating behaviour whose amplitude decays algebraically as $t^{-\alpha}$ with $\alpha \approx 3$. (b) Time evolution of the total number of quasi-particles $N_p(t)$ for the same parameters. The behaviour is substantially the same: $N_p(t)$ shows algebraically decreasing oscillations towards a quasi-stationary value $N_{p,qs}$. In both cases, the short dashed lines indicate the starting points of the evolution, i.e., the initial values $E_I(0)$ and $N_p(0)$. The insets show $\left|E_I(t) - E_{qs}\right|$ and $|N_p(t) - N_{p,qs}|$ in double logarithmic scale and highlight the algebraic decays $\propto t^{-\alpha}$; the straight red lines, corresponding to $\alpha = 3$, have been superimposed for comparison.

quantities is likely to be related to the fact that they belong to the same class defined by expression (5.37). Therefore, we can reasonably expect this exponent to characterise the whole set, apart from specific choices of the coefficients c_k. In Fig. 5.7 we study the same two quantities for different values of N and λ, showing that the typical amplitude of the oscillations around the respective quasi-stationary values scales as λN as long as λ is small enough (i.e., $\lambda \lesssim 0.5$) and N large enough ($N \gtrsim 40$). Note, however, that the recurrence time t'_R explicitly depends on N, thus curves

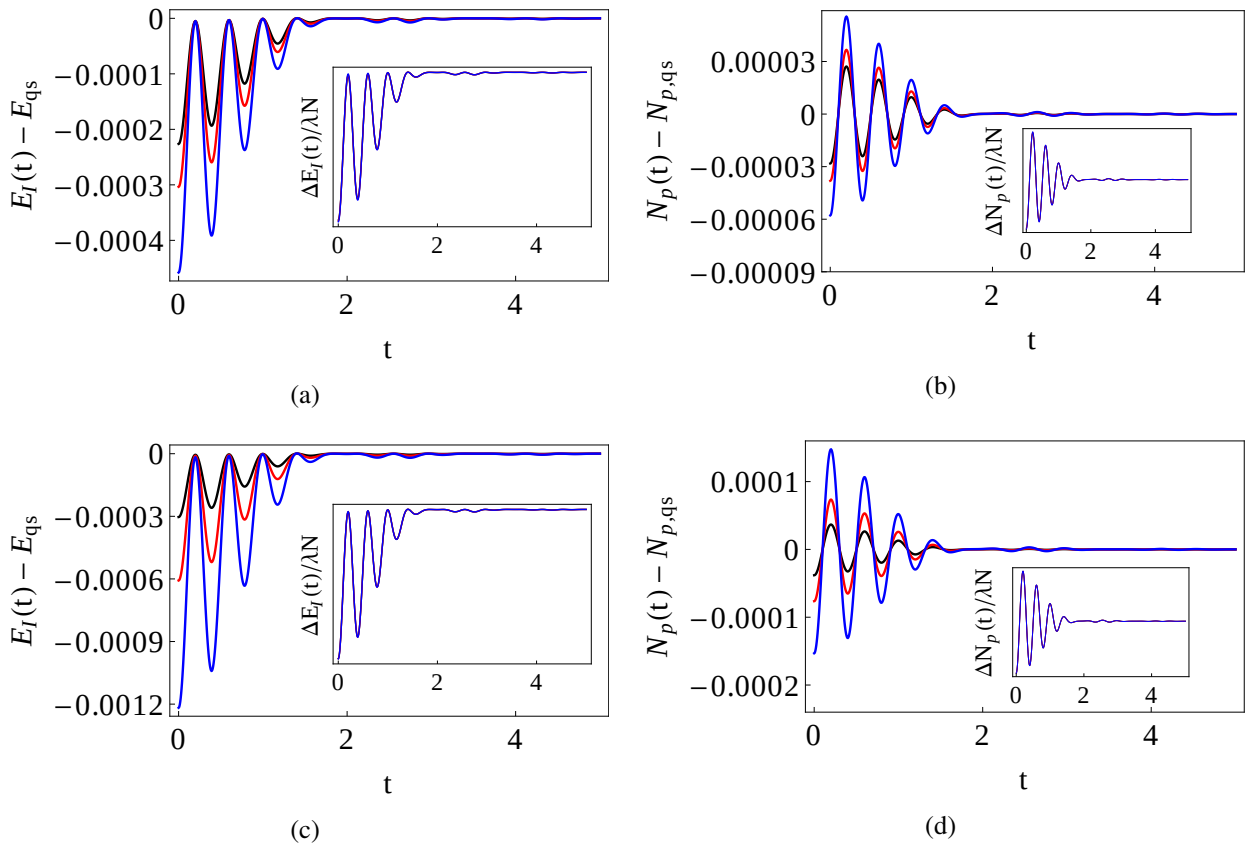

Figure 5.7: Displacement from the stationary value of the Ising energy $\Delta E_I(t) = E_I(t) - E_{qs}$ and total number of quasiparticles $\Delta N_p(t) = N_p(t) - N_{p,qs}$ for $g_0 = 9$ and $g = 4$. (a) and (b) At $\lambda = 0.1$, the different curves correspond to different system sizes $N = 60$ (black), 80 (red), and 120 (blue). (c) and (d) For $N = 80$, different colours stand for $\lambda = 0.1$ (black), 0.2 (red), 0.4 (blue). In each inset the curves of the corresponding main plot are rescaled by $1/(\lambda N)$, which leads them to collapse to a single master curve.

at different N can be collapsed one onto the other, as in Fig. 5.7 only until the first recurrence. On the other hand, this proves that the exponent α of the algebraic decay does not explicitly depend on N nor on λ. We have also studied the algebraic decay for a slightly different choice of the quench parameters $g_0 = 9$, $g = 4$ with respect to our analysis illustrated in Fig. 5.6 and verified that the exponent does not change.

Figure 5.8 highlights the peculiar fact that, for both the Ising energy $E_I(t)$ and the total number of excitations $N_p(t)$, the oscillating behaviour reappears sooner than in the case of the single populations (which constitute their building blocks, according to Eq. (5.37)). Moreover, this feature appears to be entirely due to the fast modes; this means that, while the slow ones are subject to mutual destructive interference up to $t_R \approx N/2$, the fast ones belonging to different modes k interfere constructively starting from a different time t_R' which, as we have verified numerically, corresponds approximately to $t_R/2 \approx N/4$.

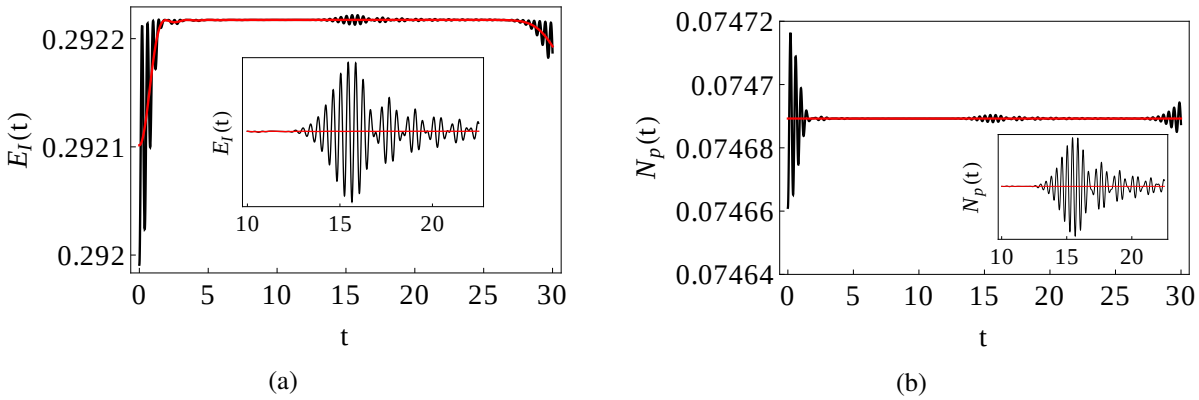

(a) (b)

Figure 5.8: Time evolution of (a) the Ising energy $E_I(t)$ and (b) the total number of quasi-particles $N_p(t)$ for $N = 60$, $g_0 = 9$, $g = 4$ and $\lambda = 0.1$. The red lines illustrate the contribution of the slow modes to the same quantities. Unexpectedly, oscillations reappear before the recurrence time $t_R \approx 30$ found in the case of single populations $\hat{n}_k$; moreover, since this effect does not arise in the slow modes, it must be entirely due to constructive interference between the fast modes belonging to different populations (i.e., different ks). In order to better highlight this fact, in the insets we magnify for each plot the central part.

5.3 Conclusions

In this Chapter we have studied a particular perturbation (Eq. (5.17)) of the quantum Ising chain which breaks a large number, although not all, of its conservation laws, thereby spoiling its integrability; in particular, we have focused our attention on the non-equilibrium dynamics after a composite quench of both the perturbation strength λ and the transverse field g. Opting for a numerical approach, we benefited from a suitable mapping of this model into the hard-core boson Hamiltonian (5.23), which at the lowest order in the low-density approximation, i.e., for small quenches and far from the critical point, is exactly solvable. This allows us to describe the approach towards a quasi-stationary prethermal state of our non-integrable model in terms of the effective relaxation towards the GGE of an approximately equivalent, integrable one.

The evolution of observables such as the populations $\hat{n}_k$ of the fermionic modes display, when the system size is adequately large, i.e., $N \gtrsim 40$, marked plateaux which last up to a recurrence time $t_R \approx N/2$. Global, extensive observables such as the total number of excitations N_p and the Ising energy E_I show a similar behaviour; their oscillations, however, reappear sooner, at a typical scale $t'_R \approx N/4$. The approach to their quasi-stationary values is, disregarding the superimposed oscillations, algebraic with exponent $\alpha \approx 3$. This value does not explicitly depend on the system size N nor on the interaction strength λ and seems to be also independent of the values g_0 and g of the transverse magnetic field, as long as they are kept far from the critical point. We argue that finding the same decay for both quantities reflects the fact that they belong to the same class (5.37) of observables which can be expressed as linear combinations of the populations $\langle \hat{n}_k \rangle$.

On the one hand, there is still room for improvement in our numerical approach: as a matter of fact, it would be interesting to expand our description by accounting for all the other quantities

which leave the sectors invariant; as we have argued above, this means taking into account every possible — not necessarily linear — combination of the operators introduced in Eqs. (5.21) and (5.22). This would allow us to compute some typical quantities related with the spin representation, such as average and correlations of the transverse magnetisation M^z, and verify whether the relaxational behaviour shows a different law or a different algebraic exponent. On the other hand, by construction our numerics is completely based on the pair formalism and cannot thus distinguish the features encoded in single fermionic operators. A different, analytical approach would be in principle required to capture the latter.

Appendix 5.A The quantum Ising model: from spins to fermions

This Appendix is devoted to providing a brief overview on the diagonalisation procedure of the Ising Hamiltonian (5.1) and to showing how the main features of the model emerge; for a comprehensive discussion of this and the more general case of the XY chain, we refer the reader to Refs. [124, 125]. In the following, we will consider for simplicity only even values of the number of sites N and assume periodic boundary conditions at the ends of the chain, i.e., $\widehat{\sigma}^{\mu}_{N+1} \equiv \widehat{\sigma}^{\mu}_{1}$; note that, as long as one is mainly interested in the bulk behaviour, especially in the thermodynamic limit, the latter does not constitute a restriction. First of all, we employ a Jordan-Wigner transformation [126, 127]

$$\begin{cases} \widehat{\sigma}^{x}_{i} = \prod_{j=1}^{i-1} \left(1-2c^{\dagger}_{i}c_{i}\right)\left(c^{\dagger}_{i}+c_{i}\right), \\ \widehat{\sigma}^{y}_{i} = i\prod_{j=1}^{i-1} \left(1-2c^{\dagger}_{i}c_{i}\right)\left(c^{\dagger}_{i}-c_{i}\right), \\ \widehat{\sigma}^{z}_{i} = 1-2c^{\dagger}_{i}c_{i}, \end{cases} \tag{5.38}$$

which is defined in terms of fermionic creation ($c^{\dagger}_{i}$) and annihilation (c_{i}) operators. Note that, thanks to the anticommuting nature of the latter, the relations (5.2) are recovered. The Hamiltonian thus becomes

$$\begin{aligned} H_{0}(g) = &-\frac{1}{2}\sum_{i=1}^{N-1}\left[c^{\dagger}_{i}c_{i+1}+c^{\dagger}_{i+1}c_{i}+c^{\dagger}_{i}c^{\dagger}_{i+1}+c_{i+1}c_{i}\right]+ \\ &+\frac{1}{2}U_{\mathbb{Z}_2}\left(c^{\dagger}_{N}c_{1}+c^{\dagger}_{1}c_{N}+c^{\dagger}_{N}c^{\dagger}_{1}+c_{1}c_{N}\right)-g\left(\frac{N}{2}-\widehat{N}\right), \end{aligned} \tag{5.39}$$

where $\widehat{N}=\sum_{i}c^{\dagger}_{i}c_{i}$ denotes the total number operator and $U_{\mathbb{Z}_2}=\mathrm{e}^{i\pi\widehat{N}}$ constitutes the parity operator and coincides with the $\mathbb{Z}_2$ transformation already introduced in Sec. 5.1.1 (see, e.g., Eq. (5.10)). Since $[H_0(g),U_{\mathbb{Z}_2}]=0$, we can conveniently separate the Hilbert space into the two eigensectors with $U_{\mathbb{Z}_2}=\pm 1$, corresponding to even and odd number of fermions, respectively. Note that the only part of Eq. (5.39) which is affected by this dichotomy is the boundary term, i.e., the one connecting the ends of the chain. As a consequence, the choice of the sector translates into different boundary conditions for the operators; in particular, periodic ones ($c_{N+1}=c_1$) are obtained in the odd sector, whereas anti-periodic ones ($c_{N+1}=-c_1$) appear in the even one [117]. Thus, one can employ a unified notation

$$H_{0}(g) = \frac{1+U_{\mathbb{Z}_2}}{2}H^{E}_{0}(g)+\frac{1-U_{\mathbb{Z}_2}}{2}H^{O}_{0}(g), \tag{5.40}$$

$$H^{E/O}_{0} = -\frac{1}{2}\sum_{i=1}^{N}\left[c^{\dagger}_{i}c_{i+1}+c^{\dagger}_{i+1}c_{i}+c^{\dagger}_{i}c^{\dagger}_{i+1}+c_{i+1}c_{i}\right]-g\left(\frac{N}{2}-\widehat{N}\right), \tag{5.41}$$

where the appropriate boundary conditions are understood. We focus now on the even sector and apply an antiperiodic, discrete Fourier transform

$$\begin{cases} c_j = \frac{1}{\sqrt{N}} \sum_{p=0}^{N-1} \mathrm{e}^{-\frac{2\pi i}{N} j\left(p+\frac{1}{2}\right)} c_p, \\ c_j^\dagger = \frac{1}{\sqrt{N}} \sum_{p=0}^{N-1} \mathrm{e}^{\frac{2\pi i}{N} j\left(p+\frac{1}{2}\right)} c_p^\dagger \end{cases} \tag{5.42}$$

to H_0^E, which yields

$$\begin{aligned} H_0^E = -\sum_{p=0}^{N-1} \Bigg[& \cos\left(\frac{2\pi}{N}\left(p+\frac{1}{2}\right)\right) c_p^\dagger c_p + \\ & -\frac{i}{2}\sin\left(\frac{2\pi}{N}\left(p+\frac{1}{2}\right)\right)\left(c_p^\dagger c_{-p-1}^\dagger - c_{-p-1} c_p\right)\Bigg] - g\left(\frac{N}{2} - \widehat{N}\right). \end{aligned} \tag{5.43}$$

As long as one is interested in the behaviour of the system in the thermodynamic limit, it is possible to define a continuum variable $\kappa_p = 2\pi p/N$ and neglect the addends $1/2$ in the expression above. Since we are interested instead in an exact, numerical approach, we introduce a new momentum $k = N-1-2p$, running only over odd integers, from $-N+1$ to $N-1$; clearly, the correspondence between k and p momenta is one to one (modulo N). Correspondingly, we define new operators

$$\begin{cases} d_k \equiv c_{\frac{N-1-k}{2}} = c_p, \\ d_{-k} \equiv c_{\frac{N-1+k}{2}} = c_{-p-1}. \end{cases} \tag{5.44}$$

which are obviously still fermionic in nature; the even-sector Hamiltonian is thereby recast in the form

$$H_0^E = \sum_{\substack{k=1-N \\ odd}}^{N-1} \left[\cos\left(\frac{\pi}{N}k\right) d_k^\dagger d_k + \frac{i}{2}\sin\left(\frac{\pi}{N}k\right)\left(d_k^\dagger d_{-k}^\dagger - d_{-k} d_k\right)\right] - g\left(\frac{N}{2} - \widehat{N}\right), \tag{5.45}$$

and it is quite easy to show that

$$\widehat{N} \equiv \sum_{p=1}^{N} c_p^\dagger c_p = \sum_{\substack{k=1-N \\ odd}}^{N-1} d_k^\dagger d_k. \tag{5.46}$$

We now introduce a Nambu spinor notation

$$\xi_k = \begin{pmatrix} d_k \\ d_{-k}^\dagger \end{pmatrix} \quad \text{and} \quad \xi_k^\dagger = \begin{pmatrix} d_k^\dagger \\ d_{-k} \end{pmatrix}^\intercal, \tag{5.47}$$

where $\intercal$ denotes transposition. This allows us to halve the momenta, by taking effectively into account only positive ones, and to give an even more compact expression for the even-sector Hamiltonian: in fact, by considering that $\xi_k^\dagger \sigma^z \xi_k = d_k^\dagger d_k - d_{-k} d_{-k}^\dagger = d_k^\dagger d_k + d_{-k}^\dagger d_{-k} - 1$, where we have made use of the anticommutation relations, and that $\xi_k^\dagger \sigma^y \xi_k = -i(d_k^\dagger d_{-k}^\dagger + d_{-k} d_k)$, one finds

$$H_0^E = \sum_{\substack{k=1 \\ odd}}^{N-1} \xi_k^\dagger \mathscr{M}_k \xi_k, \tag{5.48}$$

where

$$\mathscr{M}_k = \left(g + \cos\left(\frac{\pi}{N}k\right)\right)\sigma^z - \left(\sin\left(\frac{\pi}{N}k\right)\right)\sigma^y \tag{5.49}$$

is a collection of 2×2 matrices in spinorial space. The Hamiltonian (5.48) represents a quadratic theory of fermions; therefore, it can be diagonalised by a suitable Bogoliubov rotation which redefines the operators $d_k, d_k^\dagger$ in terms of new ones γ_k, $\gamma_k^\dagger$, while preserving the canonical anticommutation relations:

$$\psi_k = \begin{pmatrix} \gamma_k \\ \gamma_{-k}^\dagger \end{pmatrix} = \mathrm{e}^{i\theta_k\sigma^x}\xi_k, \qquad \psi_k^\dagger = \begin{pmatrix} \gamma_k \\ \gamma_{-k}^\dagger \end{pmatrix}^{\mathsf{T}} = \xi_k^\dagger \mathrm{e}^{-i\theta_k\sigma^x}, \tag{5.50}$$

where the Bogoliubov angles $\theta_k = -\theta_{-k} = \theta_k(g)$ are defined by the relations [13]

$$\cos(2\theta_k) = \frac{g+\cos\left(\frac{\pi}{N}k\right)}{\varepsilon_k} \qquad \text{and} \qquad \sin(2\theta_k) = \frac{\sin\left(\frac{\pi}{N}k\right)}{\varepsilon_k}, \tag{5.51}$$

with $\varepsilon_k^2 = \left(g+\cos\left(\frac{\pi}{N}k\right)\right)^2 + \left(\sin\left(\frac{\pi}{N}k\right)\right)^2$ the dispersion relation already encountered in Eq. (5.8). Note that the definition of the new spinors depends on the specific value of g. The result of this transformation is $H_0^E = \sum_{k>0} \psi_k^\dagger \mathscr{D}_k \psi_k$, with

$$\mathscr{D}_k = \mathrm{e}^{i\theta_k\sigma^x}\mathscr{M}_k\mathrm{e}^{-i\theta_k\sigma^x} = \mathrm{e}^{i\theta_k\sigma^x}\varepsilon_k\sigma_z\mathrm{e}^{i\theta_k\sigma^x} = \varepsilon_k\sigma^z, \tag{5.52}$$

where we used for the second equality the fact that, according to definitions (5.51), the matrix in Eq. (5.49) can be rewritten as

$$\mathscr{M}_k = \varepsilon_k\left(\cos(2\theta_k)\,\sigma^z - \sin(2\theta_k)\,\sigma^y\right) = \varepsilon_k\sigma^z\left(\cos(2\theta_k) + i\sin(2\theta_k)\,\sigma^x\right) = \varepsilon_k\sigma^z\mathrm{e}^{2i\theta_k\sigma^x}, \tag{5.53}$$

and for the third one the identity $\sigma^\mu\mathrm{e}^{\alpha\sigma^x} = \mathrm{e}^{-\alpha\sigma^x}\sigma^\mu$, which holds for $\mu = y,z$ for any value of the coefficient α. Thus, we obtain

$$H_0^E(g) = \sum_{\substack{k=1\\ odd}}^{N-1} \varepsilon_k \psi_k^\dagger \sigma^z \psi_k, \tag{5.54}$$

which is exactly the Hamiltonian in Eq. (5.5). The lowest energy state coincides with the vacuum $|0\rangle_\gamma$, i.e., the state with no particles, the corresponding eigenvalue being $E_0^E = -\sum_k \varepsilon_k$. Since the Bogoliubov rotation in this case is very simple, as it connects only modes at opposite momenta $\pm k$, it is fairly easy to relate it to the vacuum $|0\rangle_d$ in the basis of the d fermions: it is in fact sufficient to solve the problem separately in each subsector. Employing the same notation introduced at the beginning of Sec. 5.1.3 one finds

$$\begin{aligned}\gamma_k|\emptyset_k\rangle_\gamma &= \left(\cos\theta_k d_k + i\sin\theta_k d_{-k}^\dagger\right)\left(a_1|\emptyset_k\rangle_d + a_2|k\rangle_d + a_3|-k\rangle_d + a_4|k,-k\rangle_d\right) = \\ &= a_2\cos\theta_k|\emptyset_k\rangle_d + \left(a_4\cos\theta_k + ia_1\sin\theta_k\right)|-k\rangle_d + ia_2\sin\theta_k|-k,k\rangle_d = 0,\end{aligned} \tag{5.55}$$

which implies $a_2 = 0$ and $a_4 = -ia_1\tan\theta_k$; by applying instead γ_{-k} one obtains $a_3 = 0$, which completely determines the state. Overall, this yields

$$|0\rangle_\gamma = \left[\prod_{\substack{q=1\\ odd}}^{N-1}\left(\frac{1}{1+\tan^2\theta_q}\right)^{\frac{1}{2}}\right]\prod_{\substack{q=1\\ odd}}^{N-1}\left(\mathbb{1} - i\tan\theta_q\, d_q^\dagger d_{-q}^\dagger\right)|0\rangle_d, \tag{5.56}$$

where the normalisation inside the square brackets ensures that the vector has unit norm ${}_{\gamma}\langle 0|\,0\rangle_{\gamma} = 1$. When considering quenches $g_0 \to g$ starting from the ground state, it is often convenient to relate the vacuum of the theory with transverse field g_0 with the corresponding state for g; this can be done by noting that, since $\left(d_q^\dagger d_{-q}^\dagger\right)^2 = 0$,

$$\left(\mathbb{1} - i\,a\,d_q^\dagger d_{-q}^\dagger\right)\left(\mathbb{1} - i\,b\,d_q^\dagger d_{-q}^\dagger\right) = \left(\mathbb{1} - i\,(a+b)\,d_q^\dagger d_{-q}^\dagger\right) \tag{5.57}$$

for any choice of the coefficients a and b. Thus, by recalling that the d fermions do not depend on the specific value of the magnetic field, one can write

$$|0\rangle_{\gamma(g_0)} = \mathscr{N} \prod_{\substack{q=1\\ odd}}^{N-1} \left(\mathbb{1} - i\left(\tan\theta_{0,q} - \tan\theta_q\right) d_q^\dagger d_{-q}^\dagger\right) |0\rangle_{\gamma(g)}\,, \tag{5.58}$$

where we have introduced the shorthand notation $\theta_q = \theta_q(g)$, $\theta_{0,q} = \theta_q(g_0)$; the factor $\mathscr{N}$ is fixed in such a way to preserve the normalisation, i.e.,

$$\mathscr{N} = \left[\prod_{\substack{q=1\\ odd}}^{N-1} \left(\frac{1+\tan^2\theta_q}{1+\tan^2\theta_{0,q}}\right)^{\frac{1}{2}}\right]. \tag{5.59}$$

By re-expressing $d_q^\dagger d_{-q}^\dagger$ as

$$d_q^\dagger d_{-q}^\dagger = \left(i\sin\theta_q\gamma_{-q} + \cos\theta_q\gamma_q^\dagger\right)\left(-i\sin\theta_q\gamma_q + \cos\theta_q\gamma_{-q}^\dagger\right), \tag{5.60}$$

with the shorthand notation $\gamma_q \equiv \gamma_q(g)$, we obtain

$$|0\rangle_{\gamma(g_0)} = \mathscr{N}' \prod_{\substack{q=1\\ odd}}^{N-1} \left(\mathbb{1} - i\tan\left(\theta_{0,q} - \theta_q\right) \gamma_q^\dagger \gamma_{-q}^\dagger\right) |0\rangle_{\gamma(g)}\,, \tag{5.61}$$

where

$$\mathscr{N}' = \mathscr{N} \prod_{\substack{q=1\\ odd}}^{N-1} \frac{1+\tan\theta_{0,q}\tan\theta_q}{1+\tan^2\theta_q} = \prod_{\substack{q=1\\ odd}}^{N-1} \left(\frac{1}{1+\tan^2\left(\theta_q - \theta_{0,q}\right)}\right)^{\frac{1}{2}}. \tag{5.62}$$

Note that this peculiar, factorised structure of the quenched state produces an interesting consequence: any relevant observable $\mathscr{O}$, which is constructed as a combination of products of the elementary creation and annihilation operators $\gamma_k^{(\dagger)}$ can be associated to the set of momenta

$$\mathscr{K}(\mathscr{O}) = \left\{k \,|\, \gamma_k^{(\dagger)} \text{ or } \gamma_{-k}^{(\dagger)} \text{ appears in the definition of } \mathscr{O}\right\} \tag{5.63}$$

which actually appear in its definition. Then, for two generic observables $\mathscr{O}_1$ and $\mathscr{O}_2$, as long as $\mathscr{K}(\mathscr{O}_1) \cap \mathscr{K}(\mathscr{O}_2) = \emptyset$, their averages factorise

$${}_{\gamma(g_0)}\langle 0|\,\mathscr{O}_1\mathscr{O}_2\,|0\rangle_{\gamma(g_0)} = {}_{\gamma(g_0)}\langle 0|\,\mathscr{O}_1\,|0\rangle_{\gamma(g_0)}\ {}_{\gamma(g_0)}\langle 0|\,\mathscr{O}_2\,|0\rangle_{\gamma(g_0)}\,, \tag{5.64}$$

independently of the parameters g_0, g of the quench.

The Hamiltonian of the odd sector H_0^O can be diagonalised with a similar procedure, which yields

$$H_0^O(g) = (g-1)\left(\gamma_N^\dagger\gamma_N - \frac{1}{2}\right) + (g+1)\left(\gamma_0^\dagger\gamma_0 - \frac{1}{2}\right) + \sum_{\substack{q=2\\ even}}^{N-2} \varepsilon_q \psi_q^\dagger \sigma^z \psi_q; \tag{5.65}$$

the main differences with H_0^E are that here the sum runs over even values of the momenta and that the energy of the N-th elementary excitation is positive only for $g > 1$; for $g < 1$ the creation of a quasi-particle is actually an energetically favourable process. Taking into account that, in the odd sector, at least one particle must be present, the lowest energy state corresponds to the one in which only the N-th mode is populated, and the corresponding energy is

$$E_0^O = \frac{1}{2}(g-1) - \frac{1}{2}(g+1) - \sum_{\substack{q=2\\ even}}^{N-2} \varepsilon_q. \tag{5.66}$$

It is possible to prove that $E_0^E < E_0^O$ for any choice of g and thus conclude that the true ground state lies always in the even sector. Nonetheless, in the thermodynamic limit these two energies coincide for every $g \leq 1$, whereas they still differ by $g-1$ for $g > 1$. This feature gives rise to a quantum phase transition, allowing the longitudinal magnetisation $\langle \widehat{\sigma}_i^x \rangle$ to take non-vanishing values in the ferromagnetic phase $g < 1$. In fact, since $\widehat{\sigma}_i^x$ is an odd operator under the $\mathbb{Z}_2$ symmetry, it cannot connect states with the same parity. Only in the case of degeneracy between the even and odd sectors can it display a non-zero average.

5.A.1 The interaction term

In the following we relate the integrability-breaking term introduced in the spin formalism (5.12) to its corresponding expression in the fermionic one (5.17). The total transverse magnetisation explicitly appears in H_0, thus one can directly extract its fermionic representation from the last term of Eq. (5.43):

$$M^z = \widehat{N} - \frac{N}{2} = \sum_{\substack{k=1\\ odd}}^{N-1} \xi_k^\dagger \sigma^z \xi_k. \tag{5.67}$$

Applying the Bogoliubov rotation (5.50) we readily find $M^z = \sum_{\substack{k=1\\ odd}}^{N-1} \psi_k^\dagger \widetilde{\sigma}_k^z \psi_k$, with

$$\widetilde{\sigma}_k^z = \cos(2\theta_k)\sigma^z + \sin(2\theta_k)\sigma^y = \begin{pmatrix} \cos(2\theta_k) & -i\sin(2\theta_k) \\ i\sin(2\theta_k) & -\cos(2\theta_k) \end{pmatrix}, \tag{5.68}$$

which yields, once rewritten in "scalar" form,

$$M^z = -\frac{N}{2} + \sum_{\substack{k=1\\ odd}}^{N-1} \left[\cos(2\theta_k)(\hat{n}_k + \hat{n}_{-k}) - i\sin(2\theta_k)\left(\gamma_k^\dagger\gamma_{-k}^\dagger - \gamma_{-k}\gamma_k\right)\right], \tag{5.69}$$

with $\hat{n}_k = \gamma_k^\dagger \gamma_k$ the populations introduced via Eq. (5.9). Now, by applying the evolution in the Heisenberg picture $\partial_t \gamma_k(t) = i\left[H_0^E, \gamma_k(t)\right] = -i\varepsilon_k \gamma_k(t)$ and the identity $\varepsilon_k = \varepsilon_{-k}$, one finds for the magnetisation at time t after the quench

$$M^z(t) = -\frac{N}{2} + \sum_{\substack{k=1 \\ odd}}^{N-1} \left[\cos(2\theta_k)\,(\hat{n}_k + \hat{n}_{-k}) - i\sin(2\theta_k)\left(\mathrm{e}^{2i\varepsilon_k t}\,\gamma_k^\dagger \gamma_{-k}^\dagger - \mathrm{e}^{-2i\varepsilon_k t}\,\gamma_{-k}\gamma_k\right)\right]. \tag{5.70}$$

Since the one-particle spectrum ε_k does not include null values in the even sector (actually, with the exception of the critical point $g = 1$ in the thermodynamic limit), upon performing the long-time average (5.13) all oscillating terms vanish, leaving behind

$$\overline{M^z} = -\frac{N}{2} + \sum_{\substack{k=1 \\ odd}}^{N-1} \cos(2\theta_k)\,(\hat{n}_k + \hat{n}_{-k}) \equiv \sum_{\substack{k=1 \\ odd}}^{N-1} \cos(2\theta_k)\,\psi_k^\dagger \sigma^z \psi_k, \tag{5.71}$$

which in turn implies

$$M^z - \overline{M^z} = -i \sum_{\substack{k=1 \\ odd}}^{N-1} \left[\sin(2\theta_k)\left(\gamma_k^\dagger \gamma_{-k}^\dagger - \gamma_{-k}\gamma_k\right)\right] \equiv \sum_{\substack{k=1 \\ odd}}^{N-1} \sin(2\theta_k)\,\psi_k^\dagger \sigma^y \psi_k. \tag{5.72}$$

The expression above coincides with the one reported in Eq. (5.17) inside the brackets. Now, using the identity $[AB, C] = A\,[B, C] + [A, C]\,B$, along with the relations

$$\left[\gamma_k^\dagger, \hat{n}_k\right] = -\gamma_k^\dagger, \qquad \left[\gamma_k, \hat{n}_k\right] = \gamma_k, \tag{5.73}$$

it is not too difficult to prove that, for every fixed k,

$$\left[M^z - \overline{M^z}, \hat{n}_k\right] = -i\sin(2\theta_k)\left(\left[\gamma_k^\dagger, \hat{n}_k\right]\gamma_{-k}^\dagger - \gamma_{-k}\left[\gamma_k, \hat{n}_k\right]\right) = i\sin(2\theta_k)\left(\gamma_k^\dagger \gamma_{-k}^\dagger + \gamma_{-k}\gamma_k\right), \tag{5.74}$$

from which one can reconstruct the result in Eq. (5.19).

Appendix 5.B The mapping to hard-core bosons

Here we show in detail how the fermionic Hamiltonian (5.18) can be cast in the bosonic-like expression of Eq. (5.23). Expanding the spinorial products we find

$$H = \sum_{\substack{k=1 \\ odd}}^{N-1} \varepsilon_k\,(\hat{n}_k + \hat{n}_{-k} - 1) + \frac{\lambda}{N}\left(i\sum_{\substack{k=1 \\ odd}}^{N-1} \sin(2\theta_k)\left(\gamma_k^\dagger \gamma_{-k}^\dagger - \gamma_{-k}\gamma_k\right)\right)^2 = \sum_{\substack{k=1 \\ odd}}^{N-1} \varepsilon_k\,(\hat{n}_k + \hat{n}_{-k} - 1) +$$
$$- \frac{\lambda}{N} \sum_{\substack{k,q=1 \\ odd}}^{N-1} \left[\sin(2\theta_k)\sin(2\theta_q)\left(b_k^\dagger b_q^\dagger + b_k b_q - b_k^\dagger b_q - b_k b_q^\dagger\right)\right], \tag{5.75}$$

having introduced in the expression above the pair operators defined in Eq. (5.21). Note that it is possible to exchange $k \leftrightarrow q$ in the last term, as the coefficient in front

$$\widetilde{\alpha}_{kq} = \frac{\lambda}{N} \sin(2\theta_k) \sin(2\theta_q) \tag{5.76}$$

is symmetric. Using the commutation relations $\left[b_q, b_k^\dagger\right] = (1 - \hat{n}_k - \hat{n}_{-k})\,\delta_{kq}$, we find

$$H = \sum_{\substack{k=1 \\ odd}}^{N-1} \left(\varepsilon_k - \frac{\lambda}{N}\sin^2(2\theta_k)\right)(\hat{n}_k + \hat{n}_{-k} - 1) - \sum_{\substack{k,q=1 \\ odd}}^{N-1} \widetilde{\alpha}_{kq}\left(b_k^\dagger b_q^\dagger + b_k b_q - 2b_k^\dagger b_q\right). \tag{5.77}$$

Now we make use of the fermionic nature of the populations $\hat{n}_k = \hat{n}_k^2$ to rewrite

$$\hat{n}_k + \hat{n}_{-k} = \hat{n}_k^2 + \hat{n}_{-k}^2 = \hat{n}_k^2 + \hat{n}_{-k}^2 - 2\hat{n}_k\hat{n}_{-k} + 2\hat{n}_k\hat{n}_{-k} = (\hat{n}_k - \hat{n}_{-k})^2 + 2b_k^\dagger b_k, \tag{5.78}$$

where we have used the identity in Eq. (5.22) to rewrite the last term; inside the brackets we recognise the constant of motion $I_k = \hat{n}_k - \hat{n}_{-k}$. Applying the equality above to the first part of the Hamiltonian yields

$$\begin{aligned} H = &\sum_{\substack{k=1 \\ odd}}^{N-1} \left(\varepsilon_k - \frac{\lambda}{N}\sin^2(2\theta_k)\right)(I_k^2 - 1) - \sum_{\substack{k,q=1 \\ odd}}^{N-1} \widetilde{\alpha}_{kq}\left(b_k^\dagger b_q^\dagger + b_k b_q\right) + \\ &+ \sum_{\substack{k,q=1 \\ odd}}^{N-1} 2\left(\widetilde{\alpha}_{kq} + \left(\varepsilon_k - \frac{\lambda}{N}\sin^2(2\theta_k)\right)\delta_{kq}\right) b_k^\dagger b_q. \end{aligned} \tag{5.79}$$

Note that $\widetilde{\alpha}_{kk} = (\lambda/N)\sin^2(2\theta_k)$; we define now $\alpha_{kq} = \widetilde{\alpha}_{kq}\left(1 - \delta_{kq}\right)$, which coincides with the one appearing in Eq. (5.24) and notice that we can perform the substitution $\widetilde{\alpha}_{kq} \to \alpha_{kq}$ in the second sum of Eq. (5.79), since for $k = q$ the corresponding operators identically vanish. Thus, the Hamiltonian becomes

$$H = \sum_{\substack{k=1 \\ odd}}^{N-1} \left(\varepsilon_k - \frac{\lambda}{N}\sin^2(2\theta_k)\right)(I_k^2 - 1) - \sum_{\substack{k,q=1 \\ odd}}^{N-1} \alpha_{kq}\left(b_k^\dagger b_q^\dagger + b_k b_q\right) + \sum_{\substack{k,q=1 \\ odd}}^{N-1} 2\left(\alpha_{kq} + \varepsilon_k\delta_{kq}\right) b_k^\dagger b_q, \tag{5.80}$$

which, once we define $\beta_{kq} = \varepsilon_k\delta_{kq} + \alpha_{kq}$, yields the one reported in Eq. (5.23).

Appendix 5.C The Holstein-Primakoff transformation and its truncation

Hard-core bosons constitute a typical feature of $S = 1/2$ spin chains: as a matter of fact, by introducing the operators

$$\widehat{\sigma}_i^{\pm} = \frac{1}{2}\left(\sigma_i^x \pm \sigma_i^y\right), \tag{5.81}$$

where $\widehat{\sigma}_i^{\mu}$ represent the spin operators already encountered at the beginning of Sec. 5.1.1, the identification

$$\widehat{\sigma}_i^{+} \leftrightarrow b_i^{\dagger}, \qquad \widehat{\sigma}_i^{-} \leftrightarrow b_i, \qquad \widehat{\sigma}_i^{z} \leftrightarrow 2b_i^{\dagger}b_i - 1, \tag{5.82}$$

naturally ensues, where $b_i^{\dagger}$ and b_i are creation and annihilation operators for hard-core bosons. The Hilbert space can be reinterpreted accordingly by setting the correspondence $|\uparrow_i\rangle \leftrightarrow |\mathbf{1}\rangle$, $|\downarrow_i\rangle \leftrightarrow |\mathbf{0}\rangle$ between the spin and the particle states. The Holstein-Primakoff transformation [123] is meant to reproduce the hard-core constraint by means of a suitable combination of standard bosonic operators, therefore providing an alternative picture in which approximations can be based on considerations on the quasi-particles' densities and their fluctuations, rather than on the interaction strength. Here we shall focus, for simplicity, on a single mode b, $b^{\dagger}$, which is recast in the form

$$b = \sqrt{\mathbb{1} - \widehat{N}}\, a, \qquad b^{\dagger} = a^{\dagger}\sqrt{\mathbb{1} - \widehat{N}}, \tag{5.83}$$

with a, $a^{\dagger}$ bosonic operators and $\widehat{N} = a^{\dagger}a$. The Hilbert space is enlarged accordingly, from the two-dimensional space spanned by $|\mathbf{0}\rangle$ and $|\mathbf{1}\rangle$, to the infinite-dimensional one generated by the usual bosonic number basis $\{|n\rangle\}_{n\in\mathbb{N}}$. On the other hand, the latter is split into two sectors that cannot be connected by b and $b^{\dagger}$, which respectively include all the "physical" states $\{|n\rangle\}_{n=0,1}$ and all the "unphysical" ones $\{|n\rangle\}_{n>1}$. This represents a relevant aspect, as the anticommutation relations

$$\left\{b, b^{\dagger}\right\} = \mathbb{1} + 2\widehat{N} - 2\widehat{N}^2 = \mathbb{1} + 2\widehat{N}(\mathbb{1} - \widehat{N}) \tag{5.84}$$

are not correctly reproduced at the operatorial level; however, on both physical states (and, thus, in the whole physical subspace) one finds $\left\{b, b^{\dagger}\right\} \equiv \mathbb{1}$, thereby recovering the hard-core nature. When expanding the square roots in Eq. (5.83) as power series, and approximating the b operators by truncation at any finite order, the separation between the physical and unphysical subspaces becomes weaker. This feature emerges quite clearly when considering the simplest case, i.e., $b^{(\dagger)} \approx a^{(\dagger)}$; within this approximation, we find in fact that $b^{\dagger}|1\rangle = |2\rangle$, which connects the physical state $|1\rangle$ with the unphysical one $|2\rangle$. Consequently, the regime of validity of such an approximation is determined by the overlap of the state under study with the physical basis: the more it resembles its projection onto the physical space, the more accurate the result is. We shall now briefly discuss the implications that the truncation casts on the populations $\hat{n} = b^{\dagger}b$. First of all, we notice that

$$\hat{n} = a^{\dagger}(1 - \widehat{N})a = a^{\dagger}a - a^{\dagger}a(\widehat{N} - 1) = 2\widehat{N} - \widehat{N}^2 = 1 - \left(\widehat{N} - 1\right)^2, \tag{5.85}$$

which implies that, while the constraint $\langle\hat{n}\rangle \leq 1$ is preserved, the lower bound $\langle\hat{n}\rangle \geq 0$, which gives physical sense to the particle interpretation, holds only in the physical sector, whereas one finds $\langle\hat{n}\rangle < 0$ in the unphysical one.

In Sec. 5.2, we extensively used the approximation $\hat{n} \approx \widehat{N}$. Once again, this is valid in the physical sector: in fact, if we restrict the states to just $|0\rangle$ and $|1\rangle$, we can see that

$$\widehat{N}^m|0\rangle = 0 \quad \text{and} \quad \widehat{N}^m|1\rangle = |1\rangle \tag{5.86}$$

for every (integer) m. Thus, as long as the system is still lying approximately in the physical space, we can approximate $\widehat{N}^m \approx \widehat{N}$, which renders $\hat{n} \approx \widehat{N}$. Conversely, it is true that if, for any integer

$m \geq 2$, $\left\langle \widehat{N}^m \right\rangle \approx \left\langle \widehat{N} \right\rangle$, i.e.,

$$\frac{\left\langle \widehat{N}^m \right\rangle - \left\langle \widehat{N} \right\rangle}{\left\langle \widehat{N} \right\rangle} \ll 1, \tag{5.87}$$

then the truncation holds, as we prove below. Consider in fact a generic normalised state $|\psi\rangle = \sum_n a_n |n\rangle$; according to the discussion above, the latter can be considered "approximately physical" as long as $\sum_{n>1} |a_n|^2 \ll 1$. Calculating the averages in Eq. (5.87) on this state one finds

$$\sum_{n=0}^{\infty} |a_n|^2 (n^m - n) \ll \sum_{n=0}^{\infty} |a_n|^2 n. \tag{5.88}$$

The first two addends of the sum in the l.h.s. and the first one in the r.h.s. vanish, so that we can rewrite the expression above as

$$\sum_{n=2}^{\infty} |a_n|^2 (n^m - n) \ll |a_1|^2 + \sum_{n=2}^{\infty} |a_n|^2 n, \tag{5.89}$$

which is equivalent to

$$\sum_{n=2}^{\infty} |a_n|^2 (n^m - 2n) \ll |a_1|^2 . \tag{5.90}$$

Now, we note that if $m > 2$, then the expression $n^m - 2n$ is always greater than 1 for $n \geq 2$, which allows us to conclude that

$$\sum_{n=2}^{\infty} |a_n|^2 \leq \sum_{n=2}^{\infty} |a_n|^2 (n^m - 2n) \ll |a_1|^2 \leq \sum_{n=0}^{\infty} |a_n|^2 = 1, \tag{5.91}$$

proving that the state is indeed an "almost physical" one. For $m = 2$ we rewrite Eq. (5.89) as

$$2|a_2|^2 + \sum_{n=3}^{\infty} |a_n|^2 \left(n^2 - 2n\right) \ll |a_1|^2 + 2|a_2|^2 . \tag{5.92}$$

As the sum appearing in the l.h.s. is positive, this implies in particular $2|a_2|^2 \ll |a_1|^2 + 2|a_2|^2$, which can be true only if $|a_2|^2 \ll |a_1|^2$; consequently, we can effectively expunge a_2 from Eq. (5.92) and the rest of the proof follows as in the case $m > 2$ treated above.

From the discussion above, we understand that, although the truncation is sometimes referred to as "low-density approximation", it does not necessarily require, as that name would suggest, that $\left\langle \widehat{N} \right\rangle \ll 1$. Furthermore, the latter does not even represent a sufficient condition: take for instance $a_n = \mathcal{N}/(n^2+1)$, with $\mathcal{N} = 90/\pi^4 \approx 0.92$ a suitable normalisation factor. This produces $\left\langle \widehat{N} \right\rangle \approx 0.11$, which is quite small, but also $\left\langle \widehat{N}^2 \right\rangle \approx 0.3$, implying $\langle \hat{n} \rangle \approx -0.08$, which is clearly outside of the physical range On the other hand, $\left\langle \widehat{N} \right\rangle > 1$ constitutes a clear sign that unphysical states are populated; therefore, it is still safer to start from initial conditions — which must be defined entirely within the physical sector — that satisfy $\left\langle \widehat{N} \right\rangle \ll 1$. This condition thus represents a physically reasonable assumption, though not a mathematically precise one.

Appendix 5.D Diagonalisation procedure and calculation of the observables

The Bogoliubov rotation in Eq. (5.33), which is meant to diagonalise H', constitutes a change of basis and can therefore be expressed by a suitable unitary transformation. On the other hand, its implementation (5.33) is not realised via a unitary matrix. As a matter of fact, for the commutation relations to be preserved, the $\frac{N}{2} \times \frac{N}{2}$ matrices A and B must obey the identities

$$AA^\dagger - BB^\dagger = \mathbb{1}, \qquad AB^\intercal - BA^\intercal = 0, \tag{5.93}$$

which define a symplectic matrix (see App. 5.D.1)

$$M = \left(\begin{array}{c|c} A & B \\ \hline B^* & A^* \end{array}\right), \tag{5.94}$$

acting as $M\vec{\eta} = \vec{a}$ on the vectors

$$\begin{aligned} \vec{\eta} &= \left(\eta_1, \eta_2, \ldots, \eta_{\frac{N}{2}}, \eta_1^\dagger, \eta_2^\dagger, \ldots, \eta_{\frac{N}{2}}^\dagger\right), \\ \vec{a} &= \left(a_1, a_2, \ldots, a_{\frac{N}{2}}, a_1^\dagger, a_2^\dagger, \ldots, a_{\frac{N}{2}}^\dagger\right). \end{aligned} \tag{5.95}$$

The diagonalisation procedure reported in App. 5.D.1, which makes use of the constructive proof of Williamson's theorem [128], is exact in the sense that no approximation is involved other than the low-density one already employed to write down H' in Eq. (5.32). Single-particle eigenvalues and eigenvectors can therefore be obtained to any desired accuracy (e.g., for the data used to draw Fig. 5.2, to the 50-th digit). However, this is still not enough for studying the dynamics, which in general requires also to rewrite the initial state $|0\rangle_{\gamma(g_0)}$ in terms of the new Fock basis corresponding to the operators $\eta_k^\dagger$, η_k. Note that even though in the a-operators basis the state is a combination involving, for each mode k, only 0-particle and 1-particle states, this is not generically true in the new basis. This implies the necessity to approximate it with its projection on a finite subspace, thereby spoiling the exactness of the diagonalisation. On the other hand, since the system is free, this obstacle can be conveniently overcome by using the Heisenberg picture for the evolution, instead of the Schrödinger one: we consider for instance a population $\hat{n}_k$ and introduce the inverse transformation

$$M^{-1} = \left(\begin{array}{c|c} C & D \\ \hline D^* & C^* \end{array}\right), \tag{5.96}$$

which maps the η, $\eta^\dagger$ formalism back to the one built with a, $a^\dagger$: $M^{-1}\vec{a} = \vec{\eta}$. Note that, being in a sector with $I_k = 0$, we are authorised to treat the operators $\hat{n}_{\pm k}$ as if they were one and the same; thus, making use of the identity (5.22), we can rewrite

$$\hat{n}_k(t) = \hat{n}_k^2(t) = \hat{n}_k(t)\hat{n}_{-k}(t) = b_k^\dagger(t)b_k(t) \approx a_k^\dagger(t)a_k(t) \tag{5.97}$$

for any time t after the quench, as long as the last approximation holds (we recall that the last one is an equality at $t = 0$). Using the change of basis (5.33) we find

$$\left\langle a_k^\dagger(t)a_k(t)\right\rangle = \sum_{q_1,q_2} \left\{ 2Re\left[A_{kq_1}^* B_{kq_2} \left\langle \eta_{q_1}^\dagger(t)\eta_{q_2}^\dagger(t)\right\rangle\right] + \left[A_{kq_1}^* A_{kq_2} + B_{kq_1}B_{kq_2}^*\right] \left\langle \eta_{q_1}^\dagger(t)\eta_{q_2}(t)\right\rangle \right\}. \tag{5.98}$$

We now make use of the fact that the system is free for explicitly determining the temporal evolution of the operators involved: according to Eq. (5.34) we have

$$\eta_q^\dagger(t) = \mathrm{e}^{iE_q t}\eta_q^\dagger \quad \text{and} \quad \eta_q(t) = \mathrm{e}^{-iE_q t}\eta_q. \tag{5.99}$$

Consequently, the expectations in Eq. (5.98) oscillate as

$$\begin{aligned}\left\langle \eta_{q_1}^\dagger(t)\eta_{q_2}^\dagger(t)\right\rangle &= \left(Z_1^\dagger\right)_{q_1q_2}\mathrm{e}^{i\left(E_{q_1}+E_{q_2}\right)t},\\ \left\langle \eta_{q_1}^\dagger(t)\eta_{q_2}(t)\right\rangle &= \left(Z_0\right)_{q_1q_2}\mathrm{e}^{i\left(E_{q_1}-E_{q_2}\right)t},\end{aligned} \tag{5.100}$$

where we have introduced the matrices encoding all the initial values for operators quadratic in the bosons $Z_{0,q_1q_2} = \left\langle \eta_{q_1}^\dagger \eta_{q_2}\right\rangle$ and $Z_{1,q_1q_2} = \left\langle \eta_{q_1}\eta_{q_2}\right\rangle$. This makes apparent the separation between "fast" and "slow" modes already discussed in Sec. 5.2 and highlighted in Fig. 5.5(a). We also introduce the corresponding, analytically-known matrices

$$\begin{aligned}\left(W_0\right)_{k_1k_2} &= \left\langle a_{k_1}^\dagger a_{k_2}\right\rangle = \delta_{k_1k_2}\sin^2\left(\Delta\theta_{k_1}\right) + \left(\frac{1-\delta_{k_1k_2}}{4}\right)\sin\left(\Delta\theta_{k_1}\right)\sin\left(\Delta\theta_{k_2}\right),\\ \left(W_1\right)_{k_1k_2} &= \left\langle a_{k_1}a_{k_2}\right\rangle = -\left(\frac{1-\delta_{k_1k_2}}{4}\right)\sin\left(\Delta\theta_{k_1}\right)\sin\left(\Delta\theta_{k_2}\right),\end{aligned} \tag{5.101}$$

where $\Delta\theta_k = \theta_k(g) - \theta_k(g_0)$. In the $N\times N$ block representation introduced in Eq. (5.94) these matrices can be reorganised as

$$\mathscr{Z} = \langle \vec{\eta}\otimes\vec{\eta}\rangle = \left(\begin{array}{c|c} Z_1 & \mathbb{1}+Z_0^\intercal \\ \hline Z_0 & Z_1^\dagger \end{array}\right), \qquad \mathscr{W} = \langle \vec{a}\otimes\vec{a}\rangle = \left(\begin{array}{c|c} W_1 & \mathbb{1}+W_0 \\ \hline W_0 & W_1 \end{array}\right), \tag{5.102}$$

where we used the properties $W_0 = W_0^\intercal$ and $W_1 = W_1^\dagger$ which can be easily inferred from their explicit forms (5.101). Exploiting the inverse change of basis (5.96) we finally find

$$\mathscr{Z} = \left\langle M^{-1}\vec{a}\otimes M^{-1}\vec{a}\right\rangle = M^{-1}\mathscr{W}\left(M^{-1}\right)^\intercal, \tag{5.103}$$

which allows an exact numerical calculation of populations, in the sense described above. Unfortunately, this construction, which relies on the Heisenberg picture has the disadvantage of being specific to the operator chosen; for example, for a quartic one it would be necessary to calculate every possible entry of the average $\langle \vec{a}\otimes\vec{a}\otimes\vec{a}\otimes\vec{a}\rangle$, which denotes a 4-tensor of dimension $(N/2)^4$. On the other hand, once a specific tensor

$$\mathscr{W}^{(m)} \equiv \left\langle \underbrace{\vec{a}\otimes\vec{a}\otimes\ldots\otimes\vec{a}}_{m \text{ times}}\right\rangle \tag{5.104}$$

has been obtained, the corresponding dynamical expectation

$$C_{k_1\ldots k_m}(t_1,\ldots t_m) \equiv \left\langle \left(\vec{a}\right)_{k_1}(t_1)\otimes\left(\vec{a}\right)_{k_2}(t_2)\otimes\ldots\otimes\left(\vec{a}\right)_{k_m}(t_m)\right\rangle \tag{5.105}$$

can be in principle computed for any choice of the times by applying the formula

$$C_{k_1\dots k_m}(t_1,\dots t_m) = \left(M\mathscr{U}(t_1)M^{-1}\right)_{k_1k_1'}\dots\left(M\mathscr{U}(t_m)M^{-1}\right)_{k_mk_m'}\mathscr{W}^{(m)}_{k_1'\dots k_m'}. \tag{5.106}$$

Here $\mathscr{U}(t)$ represents the evolution matrix of the diagonal operator η, $\eta^\dagger$ and can be written as

$$\mathscr{U}(t) = \mathrm{e}^{-2i\mathscr{E}t}, \quad \text{with} \quad \mathscr{E} = \left(\begin{array}{c|c} \mathbf{E} & 0 \\ \hline 0 & -\mathbf{E} \end{array}\right) \tag{5.107}$$

and $\mathbf{E}$ the diagonal matrix $2\mathbf{E} = diag\left\{E_1, E_2, \dots E_{\frac{N}{2}}\right\}$, where $\{E_i\}_i$ is the one-particle spectrum. We emphasize that, for any fixed choice of the time coordinates, the only operation left is the contraction of the indices k_i' in Eq. (5.106), which just involves $(N/2)^m$ sums, and is thus of polynomial complexity.

5.D.1 Williamson's theorem

The Williamson's theorem [128] states that a symmetric, positive-definite, $2n\times 2n$ matrix J can be always brought into diagonal form by a symplectic transformation and that the corresponding spectrum is positive and doubly-degenerate. The proof is constructive and shows how to translate the problem into a standard diagonalisation one; since the algorithm we have employed follows its main steps, we will report it here. We start by recalling that a $2n\times 2n$ matrix S is said to be symplectic ($S\in Sp(2n,\mathbb{R})$) if

$$S\Omega S^{\intercal} = \Omega \quad \text{with} \quad \Omega = -\Omega^{\intercal} = \left(\begin{array}{c|c} 0 & \mathbb{1}_n \\ \hline -\mathbb{1}_n & 0 \end{array}\right), \tag{5.108}$$

where $\mathbb{1}_n$ is the $n\times n$ identity. As we have mentioned at the beginning of App. 5.D, the Bogoliubov rotation (5.94) defines in general a complex symplectic matrix, whereas the hypothesis here is that it is real. In order to avoid this issue, we employ the unitary transformation

$$\vec{r} = U\vec{a}, \qquad \vec{\rho} = U\vec{\eta}, \tag{5.109}$$

with

$$U = \frac{1}{\sqrt{2}}\left(\begin{array}{c|c} \mathbb{1}_n & \mathbb{1}_n \\ \hline -i\mathbb{1}_n & i\mathbb{1}_n \end{array}\right), \tag{5.110}$$

which represents (apart from a multiplicative factor) the usual transformation from ladder operators a_k, $a_k^\dagger$ to "position" an "momentum" ones

$$\begin{aligned} r_k &= \frac{a_k^\dagger + a_k}{\sqrt{2}}, \quad p_k = \frac{i(a_k^\dagger - a_k)}{\sqrt{2}}, \qquad \vec{r} = (r_1,\dots,r_{\frac{N}{2}},p_1,\dots,p_{\frac{N}{2}}), \\ \rho_k &= \frac{\eta_k^\dagger + \eta_k}{\sqrt{2}}, \quad \pi_k = \frac{i(\eta_k^\dagger - \eta_k)}{\sqrt{2}}, \qquad \vec{\rho} = (\rho_1,\dots,\rho_{\frac{N}{2}},\pi_1,\dots,\pi_{\frac{N}{2}}), \end{aligned} \tag{5.111}$$

obeying $\left[r_k, p_q\right] = \left[\rho_k, \pi_q\right] = i\delta_{kq}$. The change of basis

$$S = UMU^\dagger = \frac{1}{2}\left(\begin{array}{c|c} A+B+B^*+A^* & i\,(A-B+B^*-A^*) \\ \hline i\,(B^*+A^*-A-B) & (A-B-B^*+A^*) \end{array}\right) = \left(\begin{array}{c|c} Re\,(A+B) & Im\,(B-A) \\ \hline Im\,(A+B) & Re\,(A-B) \end{array}\right) \tag{5.112}$$

which maps $\vec{\rho}$ in $\vec{r}$ is now evidently real. To see that M is symplectic we simply apply the definition (5.108) to its form (5.94), which yields

$$\begin{aligned} M\Omega M^\intercal &= \left(\begin{array}{c|c} A & B \\ \hline B^* & A^* \end{array}\right)\left(\begin{array}{c|c} 0 & \mathbb{1}_n \\ \hline -\mathbb{1}_n & 0 \end{array}\right)\left(\begin{array}{c|c} A^\intercal & B^\dagger \\ \hline B^\intercal & A^\dagger \end{array}\right) = \\ &= \left(\begin{array}{c|c} AB^\intercal - BA^\intercal & AA^\dagger - BB^\dagger \\ \hline -\left(AA^\dagger - BB^\dagger\right)^\intercal & (AB^\intercal - BA^\intercal)^\dagger \end{array}\right) = \left(\begin{array}{c|c} 0 & \mathbb{1}_n \\ \hline -\mathbb{1}_n & 0 \end{array}\right) \equiv \Omega, \end{aligned} \tag{5.113}$$

where for the second to last equality we have used the identities (5.93). This implies that the matrix S preserves $\Omega' = U\Omega U^\intercal = i\Omega$, which is tantamount to say that it is symplectic too. We now proceed to show how this matrix can be determined. Using the canonical commutation relations, we rewrite the Hamiltonian H' in Eq. (5.32) as

$$H' = \vec{a}^\dagger J' \vec{a} - \sum_{k_1,k_2} \delta_{k_1 k_2}\beta_{k_1 k_2} \quad \text{with} \quad J' = \left(\begin{array}{c|c} \beta & -\alpha \\ \hline -\alpha & \beta \end{array}\right), \tag{5.114}$$

where α and β are the $n \times n$ matrices defined by (5.24) with $n = N/2$ (we recall that we have assumed N to be even). The corresponding form in coordinate space (r, p) is

$$J = UJ'U^\dagger = \left(\begin{array}{c|c} \beta - \alpha & 0 \\ \hline 0 & \beta + \alpha \end{array}\right). \tag{5.115}$$

Note that $(\beta - \alpha)_{k_1 k_2} = \delta_{k_1 k_2}\varepsilon_{k_1}$, so that half of this matrix is diagonal and displays the unperturbed eigenvalues $\varepsilon_k \geq |g-1|$, which makes it positive definite (if not at the critical point). The other half is given by

$$(\beta + \alpha)_{k_1 k_2} = \varepsilon_{k_1}\delta_{k_1 k_2} + 2\frac{\lambda}{N}\left(1 - \delta_{k_1 k_2}\right)\sin\left(2\theta_{k_1}\right)\sin\left(2\theta_{k_2}\right) \tag{5.116}$$

and we can safely assume that, as long as g is kept far from $g_c = 1$ and λ is not too large, also this part is positive definite and thus J satisfies all the requirements of the theorem. This implies that both the inverse J^{-1} and its "square root" $J^{-\frac{1}{2}}$ exist and are symmetric, positive-definite matrices. We now define $K = J^{-\frac{1}{2}}\Omega J^{-\frac{1}{2}}$, which is skew-symmetric and invertible due to the properties of Ω (see Eq. (5.108)). Therefore, by the spectral theorem, there exist an orthogonal matrix $R \in O\left(2n, \mathbb{R}\right)$ which performs the block diagonalisation

$$R^\intercal K R = \left(\begin{array}{c|c} 0 & \mathbf{E}^{-1} \\ \hline -\mathbf{E}^{-1} & 0 \end{array}\right), \tag{5.117}$$

where $\mathbf{E}^{-1}$ is a positive-definite, diagonal $n \times n$ matrix (which, as we are going to show, coincides with the one appearing in Eq. (5.107)). Its positivity is guaranteed by the fact that one can always exchange a negative diagonal entry with its opposite lying in the opposite block $-\mathbf{E}^{-1}$ by exchanging the two vectors identified by the corresponding row and column via an orthogonal transformation. Being positive-definite, its inverse square root $\mathbf{E}^{\frac{1}{2}}$ exists and we can use it to define the diagonal $2n \times 2n$ matrices

$$\mathbf{D} = \left(\begin{array}{c|c} \mathbf{E}^{\frac{1}{2}} & 0 \\ \hline 0 & \mathbf{E}^{\frac{1}{2}} \end{array}\right) \quad \text{and} \quad S = J^{-\frac{1}{2}} R \mathbf{D}. \tag{5.118}$$

The last one is exactly the symplectic transformation we were looking for; in fact,

$$S^{\intercal} \Omega S = \left(\mathbf{D} R^{\intercal} J^{-\frac{1}{2}}\right) \Omega \left(J^{-\frac{1}{2}} R \mathbf{D}\right) = \mathbf{D} R^{\intercal} K R \mathbf{D} = \Omega, \tag{5.119}$$

where we applied the definition in Eq. (5.117) and used the fact that the transposed of a symplectic matrix is still symplectic, and

$$S^{\intercal} J S = \left(\mathbf{D} R^{\intercal} J^{-\frac{1}{2}}\right) J \left(J^{-\frac{1}{2}} R \mathbf{D}\right) = \mathbf{D} R^{\intercal} R \mathbf{D} = \mathbf{D}^2, \tag{5.120}$$

where we used the fact that R is orthogonal, i.e., $R^{\intercal} = R^{-1}$. Thereby, we see that the Hamiltonian H' in Eq. (5.114) is recast into the form

$$H' = \vec{\rho}^{\intercal} \mathbf{D}^2 \vec{\rho} - \mathrm{tr}\{\beta\} = \vec{\rho}^{\intercal} \left(\begin{array}{c|c} \mathbf{E} & 0 \\ \hline 0 & \mathbf{E} \end{array}\right) \vec{\rho} - \sum_{\substack{q=1 \\ odd}}^{N-1} \varepsilon_q \tag{5.121}$$

which, applying the transformation $U^{\dagger} \mathbf{D}^2 U$ to retrieve the representation in terms of particle creation and annihilation operators and calling $\left\{E_q/2\right\}_q$ the spectrum of E, readily yields

$$H' = \vec{\eta}^{\,\dagger} \left(\begin{array}{c|c} \mathbf{E} & 0 \\ \hline 0 & \mathbf{E} \end{array}\right) \vec{\eta} - \sum_{\substack{q=1 \\ odd}}^{N-1} \varepsilon_q = \sum_{\substack{q=1 \\ odd}}^{N-1} \frac{E_q}{2} \left(\eta_q^{\dagger} \eta_q + \eta_q \eta_q^{\dagger}\right) - \sum_{\substack{q=1 \\ odd}}^{N-1} \varepsilon_q, \tag{5.122}$$

which corresponds to Eq. (5.34) with $C = \sum_q \left(E_q/2 - \varepsilon_q\right)$.

Bibliography

[1] M. Marcuzzi, A. Gambassi, and M. Pleimling, *Collective non-equilibrium dynamics at surfaces and the spatio-temporal edge*, EPL **100** (2012), 46004.

[2] P. Calabrese and J. L. Cardy, *Time dependence of correlation functions following a quantum quench*, Phys. Rev. Lett. **96** (2006), 136801.

[3] P. Calabrese and J. L. Cardy, *Quantum quenches in extended systems*, J. Stat. Mech. **P06008** (2007).

[4] L. Foini, L. F. Cugliandolo, and A. Gambassi, *Dynamic correlations, fluctuation-dissipation relations, and effective temperatures after a quantum quench of the transverse field Ising chain*, J. Stat. Mech. (2012), P09011.

[5] M. Marcuzzi and A. Gambassi, *Response functions after a quantum quench*, arXiv:cond-mat/1308.4665.

[6] M. Marcuzzi, J. Marino, A. Silva, and A. Gambassi, *Pre-thermalization in a non-integrable quantum spin chain after a quench*, arXiv:cond-mat/1307.3738 (2013).

[7] S. Ciliberto, *Experimental analysis of aging*, Slow Relaxations and Nonequilibrium Dynamics in Condensed Matter, vol. 77, Springer, 2003, p. 555.

[8] L. F. Cugliandolo, *Out of equilibrium dynamics of classical and quantum complex systems*, arXiv:cond-mat/1305.7126 (2012).

[9] J. P. Bouchaud, L. F. Cugliandolo, J. Kurchan, and M. Mézard, *Out of equilibrium dynamics in spin glasses and other glassy systems*, Spin Glasses and Random Fields, World Scientific (Singapore), 1998.

[10] S.-K. Ma, *Modern theory of critical phenomena*, Frontiers in Physics, Reading, MA: W. A. Benjamin,, 1976.

[11] J. Zinn-Justin, *Quantum field theory and critical phenomena*, 4th ed., International Series of Monographs on Physics, Clarendon Press, 2002.

[12] A. Pelissetto and E. Vicari, *Critical phenomena and renormalization group theory*, Phys. Rep. **368** (2002), 549.

[13] S. Sachdev, *Quantum phase transitions*, Cambridge University Press, 1999.

[14] W. H. Zurek, *Cosmological experiments in condensed matter systems*, Phys. Rep. **276** (1996), 177.

[15] S. Joubaud, B. Percier, A. Petrosyan, and S. Ciliberto, *Aging and effective temperatures near a critical point*, Phys. Rev. Lett. **102** (2009), 130601.

[16] L. Berthier, P. C. W. Holdsworth, and M. Sellitto, *Nonequilibrium critical dynamics of the two-dimensional XY model*, J. Phys. A **34** (2001), 1805.

[17] P. Mayer, L. Berthier, J. P. Garrahan, and P. Sollich, *Fluctuation-dissipation relations in the nonequilibrium critical dynamics of Ising models*, Phys. Rev. E **68** (2003), 016116.

[18] R. Bausch, H. K. Janssen, and H. Wagner, *Renormalized field theory of critical dynamics*, Z. Phys. B **24** (1976), 113.

[19] U. C. Täuber, *Field theory approaches to nonequilibrium dynamics*, Lecture Notes in Physics, Springer, 2007.

[20] P. Calabrese and A. Gambassi, *Ageing properties of critical systems*, J. Phys. A **38** (2005), R133.

[21] P. Calabrese, A. Gambassi, and F. Krzakala, *Critical ageing of Ising ferromagnets relaxing from an ordered state*, J. Stat. Mech. (2006), P06016.

[22] P. Calabrese and A. Gambassi, *Slow dynamics in critical ferromagnetic vector models relaxing from a magnetized initial state*, J. Stat. Mech. (2007), P01001.

[23] H. K. Janssen, B. Schaub, and B. Schmittmann, *New universal short-time scaling behaviour of critical relaxation processes*, Z. Phys. B **73** (1989), 539.

[24] K. Binder, *Critical behaviour at surfaces*, Phase Transitions and Critical Phenomena, vol. 8, London Academic Press, 1983.

[25] M. Pleimling, *Critical phenomena at perfect and non-perfect surfaces*, J. Phys. A **37** (2004), R79.

[26] L. Környei, *Nonequilibrium critical relaxation in the 2d random field Ising model*, J. Phys.: Conf. Ser. **40** (2006), 36.

[27] M. Greiner, O. Mandel, T. W. Hänsch, and I. Bloch, *Collapse and revival of the matter wave field of a Bose-Einstein condensate*, Nature **419** (2002), 51.

[28] W. H. Zurek, *Decoherence and the transition from quantum to classical - revisited*, Los Alamos Science **27** (2002).

[29] I. Bloch, J. Dalibard, and W. Zwerger, *Many-body physics with ultracold gases*, Rev. Mod. Phys. **80** (2008), 885.

[30] H. Feshbach, *Unified theory of nuclear reactions*, Ann. Phys. (N.Y.) **5** (1958), 337.

[31] T. Kinoshita, T. Wenger, and D. S. Weiss, *Observation of a one-dimensional Tonks-Girardeau gas*, Science **305** (2004), 1125.

[32] S. Hofferberth, I. Lesanovsky, T. Schumm, A. Imambekov, V. Gritsev, E. Demler, and J. Schmiedmayer, *Probing quantum and thermal noise in an interacting many-body system*, Nature Physics **4** (2008), 489.

[33] Z. Hadzibabic, P. Krüger, M. Cheneau, B. Battelier, and J. Dalibard, *Berezinskii-Kosterlitz-Thouless crossover in a trapped atomic gas*, Nature **441** (2006), 1118.

[34] M. Greiner, O. Mandel, T. Esslinger, T. W. Hänsch, and I. Bloch, *Quantum phase transition from a superfluid to a Mott insulator in a gas of ultracold atoms*, Nature **415** (2002), 39.

[35] T. Kinoshita, T. Wenger, and D. S. Weiss, *A quantum Newton's cradle*, Nature **440** (2006), 900.

[36] E. H. Lieb and D. Robinson, *The finite group velocity of quantum spin systems*, Commun. Math. Phys. **28** (1972), 251.

[37] P. Calabrese and J. L. Cardy, *Evolution of entanglement entropy in one-dimensional systems*, J. Stat. Mech. **P04010** (2005).

[38] M. A. Cazalilla, *The Luttinger model following a sudden interaction switch-on*, Phys. Rev. Lett. **97** (2006), 156403.

[39] M. Cheneau, P. Barmettler, D. Poletti, M. Endres, P. Schauß, T. Fukuhara, C. Gross, I. Bloch, C. Kollath, and S. Kuhr, *Light-cone-like spreading of correlations in a quantum many-body system*, Nature **481** (2012), 484.

[40] Oleg Lychkovskiy, *Dependence of decoherence-assisted classicality on the way a system is partitioned into subsystems*, Phys. Rev. A **87** (2013), 022112.

[41] A. Polkovnikov, K. Sengupta, A. Silva, and M. Vengalattore, *Nonequilibrium dynamics of closed interacting quantum systems*, Rev. Mod. Phys. **83** (2011), 863.

[42] J. von Neumann, *Beweis des ergodensatzes und des H-theorems in der neuen mechanik (proof of the ergodic theorem and the H-theorem in quantum mechanics)*, Z. Phys. **57** (1929), 30.

[43] E. T. Jaynes, *Information theory and statistical mechanics*, Phys. Rev. **106** (1957), 620.

[44] M. Stark and M. Kollar, *Kinetic description of thermalization dynamics in weakly interacting quantum systems*, arXiv:cond-mat/1308.1610 (2013).

[45] A. Mitra and T. Giamarchi, *Mode coupling induced dissipative and thermal effects at long times after a quantum quench*, Phys. Rev. Lett. **107** (2011), 150602.

[46] A. Mitra and T. Giamarchi, *Thermalization and dissipation in out of equilibrium quantum systems: A perturbative renormalization group approach*, Phys. Rev. B **85** (2012), 075117.

[47] M. Tavora and A. Mitra, *Quench dynamics of one-dimensional bosons in a commensurate periodic potential: A quantum kinetic equation approach*, arXiv:cond-mat/1306.6121 (2013).

[48] V. Gurarie, *Global large time dynamics and the generalized Gibbs ensemble*, J. Stat. Mech. (2013), P02014.

[49] M. Rigol, V. Dunjko, V. Yurovsky, and M. Olshanii, *Relaxation in a completely integrable many-body quantum system: An ab initio study of the dynamics of the highly excited states of 1D lattice hard-core bosons*, Phys. Rev. Lett. **98** (2007), 050405.

[50] T. Barthel and U. Schollwöck, *Dephasing and the steady state in quantum many-particle systems*, Phys. Rev. Lett. **100** (2008), 100601.

[51] J. Berges, Sz. Borsányi, and C. Wetterich, *Prethermalization*, Phys. Rev. Lett. **93** (2004), 142002.

[52] M. Gring, M. Kuhnert, T. Langen, T. Kitagawa, B. Rauer, M. Schreitl, L. Mazets, D. Adu Smith, E. Demler, and J. Schmiedmayer, *Relaxation and prethermalization in an isolated quantum system*, Science **337** (2012), 1318.

[53] H. W. Diehl, *Field-theoretic approach to critical behaviour at surfaces*, Phase Transitions and Critical Phenomena, vol. 10, London Academic Press, 1986.

[54] V. L. Berezinskii, *Destruction of long-range order in one-dimensional and two-dimensional systems having a continuous symmetry group I. Classical systems*, Sov. Phys. JETP **32** (1971), 493.

[55] J. M. Kosterlitz and D. J. Thouless, *Long range order and metastability in two dimensional solids and superfluids. (application of dislocation theory)*, J. Phys. C **5** (1972), L124.

[56] J. M. Kosterlitz and D. J. Thouless, *Ordering, metastability and phase transitions in two-dimensional systems*, J. Phys. C **6** (1973), 1181.

[57] K. G. Wilson, *Renormalization group and critical phenomena I*, Phys. Rev. B **4** (1971), 3174.

[58] M. N. Barber, *Finite-size scaling*, Phase Transitions and Critical Phenomena, vol. 8, London Academic Press, 1983.

[59] H. W. Diehl and S. Dietrich, *Multicritical behaviour at surfaces*, Z. Phys. B **50** (1983), 117.

[60] H. W. Diehl and S. Dietrich, *Field-theoretical approach to static critical phenomena in semi-infinite systems*, Z. Phys. B **42** (1981), 65.

[61] H. W. Diehl, *The theory of boundary critical phenomena*, Int. J. Mod. Phys. B **11** (1997), 3503.

[62] C. Ruge, S. Dunkelmann, and F. Wagner, *New method for determination of critical parameters*, Phys. Rev. Lett. **69** (1992), 2465.

[63] C. Ruge, S. Dunkelmann, F. Wagner, and J. Wulf, *Study of the three-dimensional Ising model on film geometry with the cluster Monte Carlo method*, J. Stat. Phys. **73** (1993), 293.

[64] H. Dosch, *Critical phenomena at surfaces and interfaces*, Springer Tracts in Modern Physics, vol. 126, Springer, 1992.

[65] J. L. Cardy, *Critical behaviour at an edge*, J. Phys. A **16** (1983), 3617.

[66] M. Pleimling and W. Selke, *Critical phenomena at edges and corners*, Eur. Phys. J. B **5** (1998), 805.

[67] U. Ritschel and H. W. Diehl, *Dynamical relaxation and universal short-time behavior in finite systems. the renormalization-group approach*, Nucl. Phys. B **464** (1996), 512.

[68] P. C. Hohenberg and B. I. Halperin, *Theory of dynamic critical phenomena*, Rev. Mod. Phys. **49** (1977), 435.

[69] S. Dietrich and H. W. Diehl, *The effects of surfaces on dynamic critical behavior*, Z. Phys. B **51** (1983), 343.

[70] N. D. Mermin and H. Wagner, *Absence of ferromagnetism or antiferromagnetism in one- or two-dimensional isotropic heisenberg models*, Phys. Rev. Lett. **17** (1966), 1133.

[71] T. W. Burkhardt and H. W. Diehl, *Ordinary, extraordinary, and normal surface transitions: Extraordinary-normal equivalence and simple explanation of* $|T - T_c|^{2-\alpha}$ *singularities*, Phys. Rev. B **50** (1994), 3894.

[72] K. G. Wilson, *Non-lagrangian models of current algebra*, Phys. Rev. **179** (1969), 1499.

[73] P. Di Francesco, P. Mathieu, and D. Senechal, *Conformal field theory*, Graduate Texts in Contemporary Physics, Springer (Berlin), 1997.

[74] G. Mussardo, *Statistical field theory*, Oxford Graduate Texts, Oxford University Press, 2009.

[75] C. Godrèche and J. M. Luck, *Nonequilibrium critical dynamics of ferromagnetic spin systems*, J. Phys.: Condens. Matter **14** (2002), no. 7, 1589.

[76] P. C. Martin, E. D. Siggia, and H. A. Rose, *Statistical dynamics of classical systems*, Phys. Rev. A **8** (1973), 423.

[77] H. K. Janssen, *On a lagrangean for classical field dynamics and renormalization group calculations of dynamical critical properties*, Z. Phys. B **23** (1976), 377.

[78] C. de Dominicis, *Techniques de renormalisation de la théorie des champs et dynamique des phénomènes critique*, J. Phys. (Paris) **37/C1** (1976), 247.

[79] U. Ritschel and P. Czerner, *Universal short-time behavior in critical dynamics near surfaces*, Phys. Rev. Lett. **75** (1995), 3882.

[80] D. J. Amit and L. Peliti, *On dangerous irrelevant operators*, Ann. Phys. **140** (1982), 207.

[81] H. W. Diehl, S. Dietrich, and E. Eisenriegler, *Universality, irrelevant surface operators, and corrections to scaling in systems with free surfaces and defect planes*, Phys. Rev. B **27** (1983), 2937.

[82] M. Marcuzzi and A. Gambassi, in preparation.

[83] S. N. Majumdar and A. M. Sengupta, *Nonequilibrium dynamics following a quench to the critical point in a semi-infinite system*, Phys. Rev. Lett. **76** (1996), 2394.

[84] M. Pleimling, *Aging phenomena in critical semi-infinite systems*, Phys. Rev. B **70** (2004), 104401.

[85] M. Hasenbusch, *Monte Carlo study of surface critical phenomena: The special point*, Phys. Rev. B **84** (2011), 134405.

[86] T. Wolfram, R. E. Dewames, W. F. Hall, and P. W. Palmberg, *Surface magnetization near the critical temperature and the temperature dependence of magnetic-electron scattering from nio*, Surf. Sci. **28** (1971), 45.

[87] N. Mason, A. N. Pargellis, and B. Yurke, *Scaling behavior of two-time correlations in a twisted nematic liquid crystal*, Phys. Rev. Lett. **70** (1993), 190.

[88] J. Serrano, A. Bosak, M. Krisch, F. J. Manjón, A. H. Romero, N. Garro, X. Wang, A. Yoshikawa, and M. Kuball, *InN thin film lattice dynamics by grazing incidence inelastic X-ray scattering*, Phys. Rev. Lett. **106** (2011), 205501.

[89] A. Mitra, *Time-evolution and dynamical phase transitions at a critical time in a system of one dimensional bosons after a quantum quench*, arXiv:cond-mat/1207.3777 (2012).

[90] E. G. della Torre, E. Demler, and A. Polkovnikov, *Universal rephasing dynamics after a quantum quench via sudden coupling of two initially independent condensates*, Phys. Rev. Lett. **110** (2013), 090404.

[91] J. D. Jackson, *Classical electrodynamics*, 3rd ed., New York: Wiley, 1999.

[92] I. M. Gelfand and G. E. Shilov, *Generalized functions, Vol. I*, New York: Acadmic Press, 1964.

[93] M. Gell-Mann and F. Low, *Bound states in quantum field theory*, Phys. Rev. **84** (1951), 350.

[94] S. Weinberg, *The quantum theory of fields, vol. I: Foundations*, International Series of Monographs on Physics, Cambridge University Press, 1995.

[95] G. D. Mahan, *Many-particle physics*, 2nd ed., Plenum Press, 1990.

[96] J. Schwinger, *Brownian motion of a quantum oscillator*, J. Math. Phys. **2** (1961), 407.

[97] L. V. Keldysh, *Diagram technique for nonequilibrium processes*, Sov. Phys. JETP **20** (1965), 1018.

[98] A. Kamenev and A. Levchenko, *Keldysh technique and non-linear σ-model: basic principles and applications*, Advances in Physics **58** (2009), 197.

[99] A. Kamenev, *Many-body theory of non-equilibrium systems*, arXiv:cond-mat/0412296 (2004).

[100] A. Kamenev, *Field theory of non-equilibrium systems*, Cambridge University Press, 2011.

[101] J. Rammer and H. Smith, *Quantum field-theoretical methods in transport theory of metals*, Rev. Mod. Phys. **58** (1986), 323.

[102] F. Cooper, *Nonequilibrium problems in quantum field theory and Schwinger's closed time path formalism*, arXiv:hep-th/9504073 (1995).

[103] E. Calzetta and B. L. Hu, *Nonequilibrium quantum fields: Closed-time-path effective action, Wigner function, and Boltzmann equation*, Phys. Rev. D **37** (1988), 2878.

[104] J. L. Cardy, *Boundary conformal field theory*, arXiv:hep-th/0411189v2 (2008).

[105] A. A. Belavin, A. M. Polyakov, and A. B. Zamolodchikov, *Infinite conformal symmetry in two-dimensional quantum field theory*, Nucl. Phys. B **241** (1984), 333.

[106] J. L. Cardy, *Conformal invariance and surface critical behaviour*, Nucl. Phys. B **240** (1984), 514.

[107] L. D. Landau and E. M. Lifshits, *Quantum mechanics: non-relativistic theory*, New York: Pergamon Press, 1977.

[108] B. Simon, *Schrödinger semigroups*, Bull. Am. Math. Soc. **7** (1982), 447.

[109] Spyros Sotiriadis and John L. Cardy, *Quantum quench in interacting field theory: A self-consistent approximation*, Phys. Rev. B **81** (2010), 134305.

[110] L. Foini, L. F. Cugliandolo, and A. Gambassi, *Fluctuation-dissipation relations and critical quenches in the transverse field Ising chain*, Phys. Rev. B **84** (2011), 212404.

[111] R. P. Feynman, *Space-time approach to non-relativistic quantum mechanics*, Rev. Mod. Phys. **20** (1948), 367.

[112] M. Moeckel and S. Kehrein, *Interaction quench in the Hubbard model*, Phys. Rev. Lett. **100** (2008), 175702.

[113] M. Moeckel and S. Kehrein, *Real-time evolution for weak interaction quenches in quantum systems*, Ann. Phys. **324** (2009), 2146.

[114] A. Mitra, *Correlation functions in the prethermalized regime after a quantum quench of a spin chain*, Phys. Rev. B **87** (2013), 205109.

[115] J. Marino and A. Silva, *Relaxation, prethermalization, and diffusion in a noisy quantum Ising chain*, Phys. Rev. B **86** (2012), 060408.

[116] P. Calabrese, F. H. L. Essler, and M. Fagotti, *Quantum quench in the transverse-field Ising chain*, Phys. Rev. Lett. **106** (2011), 227203.

[117] P. Calabrese, F. H. L. Essler, and M. Fagotti, *Quantum quench in the transverse field Ising chain: I. time evolution of order parameter correlators*, J. Stat. Mech. (2012), P07016.

[118] P. Calabrese, F. H. L. Essler, and M. Fagotti, *Quantum quenches in the transverse field Ising chain: II. stationary state properties*, J. Stat. Mech. (2012), P07022.

[119] D. Rossini, S. Suzuki, G. Mussardo, G. E. Santoro, and A. Silva, *Long time dynamics following a quench in an integrable quantum spin chain: Local versus nonlocal operators and effective thermal behavior*, Phys. Rev. B **82** (2010), 144302.

[120] D. Rossini, A. Silva, G. Mussardo, and G. E. Santoro, *Effective thermal dynamics following a quantum quench in an spin chain*, Phys. Rev. Lett. **102** (2009), 127204.

[121] M. Fagotti, *Finite-size corrections versus relaxation after a sudden quench*, Phys. Rev. B **87** (2013), 165106.

[122] D. Patanè, A. Silva, L. Amico, R. Fazio, and G. E. Santoro, *Adiabatic dynamics in open quantum critical many-body systems*, Phys. Rev. Lett. **101** (2008), 175701.

[123] T. Holstein and H. Primakoff, *Field dependence of the intrinsic domain magnetization of a ferromagnet*, Phys. Rev. **58** (1940), 1098.

[124] E. Barouch, B. M. McCoy, and M. Dresden, *Statistical mechanics of the* XY *model. I*, Phys. Rev. A **2** (1970), 1075.

[125] E. Lieb, T. Schultz, and D. Mattis, *Two soluble models of an antiferromagnetic chain*, Ann. Phys. **16** (1961), 407.

[126] P. Jordan and E. Wigner, *Über das Paulische äquivalenzverbot (on the Pauli exclusion principle)*, Z. Phys. **47** (1928), 631.

[127] C. D. Batista and G. Ortiz, *Generalized Jordan-Wigner transformations*, Phys. Rev. Lett. **86** (2001), 1082.

[128] J. Williamson, *On the algebraic problem concerning the normal forms of linear dynamical systems*, Am. J. Math. **58** (1936), 141.